The use of Novel Poly(allylamine) Based

Amphiphilic Polymers for Drug Delivery

Clare Hoskins

A thesis submitted in partial fulfilment of the
requirements of

The Robert Gordon University

for the degree of Doctor of Philosophy

April 2010

Contents

List of Tables

List of Figures

Abstract

Fourteen novel comb shaped amphiphilic polymers were successfully synthesised to determine the effect of polymer architecture on the potential of these amphiphilic polymers for hydrophobic drug delivery. Polyallylamine (PAA) was grafted with four different types of hydrophobic pendant groups (Cholesteryl (Ch), (Fmoc), (Dansyl) and (Naphth)). Some amphiphilic polymers were further reacted with methyl orange to form quaternary ammonium moieties. The polymers were characterised by elemental analysis and nuclear magnetic resonance spectroscopy (NMR). In the aqueous environment the amphiphilic polymers formed nano self assemblies with particle size from 99 to 284 nm. The critical aggregation concentration (CAC) of the self assemblies was successfully determined by surface tension measurement. The CAC ranged from the lowest value of 0.093 to the highest 1.5 mgmL^{-1} (Ch$_5$ and Fmoc$_5$ respectively). The Fmoc and Naphth grafted polymers showed the presence of two CMC values, this phenomenon was due to stacking of the planar hydrophobic ring structures resulting in excimer formation. The theory of excimer formation was confirmed by the observation of peak shifting on the emission spectra of the compounds in water over a large concentration range (0.023 – 3 mgmL^{-1}).

The drug loading potential of the polymers was investigated using five model hydrophobic drugs, propofol, prednisolone griseofulvin, etoposide and novel anticancer agent BNIPDaoct. The Ch$_5$ and Dansyl$_{10}$ showed excellent drug solubilisation capacities. At 6 mgmL^{-1} the Ch$_5$ achieved propofol solubility 70-fold greater than its aqueous solubility, prednisolone, griseofulvin and etoposide solubility's were increased 20-fold, 30-fold and 7-fold respectively. Similarly at 6 mgmL^{-1} the Dansyl$_{10}$ achieved a 200-fold increase on the aqueous solubility of propofol and increased the solubility of prednisolone, griseofulvin and etoposide by 100-fold and 400-fold and 12-fold respectively. The Ch$_5$ (at 1 mgmL^{-1}) was also used to solubilise the novel anticancer agent Bisnaphthalimidopropyl diaminooctane (BNIPDaoct) which was otherwise insoluble achieving a solubilisation of 0.3 mgmL^{-1}. The sizes of the optimal formulations differed greatly for both modified polymers. This was possibly due to the varying architectures of both the drug and the modified polymers and their ability to expand the hydrophobic core and shield the drugs from the 'hostile' aqueous environment.

The *in vitro* drug release profiles, showed controlled release of the hydrophobic drugs from the core of the nano aggregates (Ch$_5$ and Dansyl$_{10}$), the time span for 100% of the drugs to be released ranged from 48- 96 h. Biological characterisation of the polymers found that most of the polymers showed negligible haemolytic activity over the concentrations tested (0.05 – 1 mgmL^{-1}), the IC$_{50}$ values for the cytotoxicity assay ranged from 0.01740 - 0.05585 mgmL^{-1} on Caco-2 cells (Fmoc$_5$ to QCh$_5$ respectively). The quaternized polymers showed a slightly better safety profile than their unquaternized counterparts, despite exhibiting low drug solubilisation capacities. The optimal

formulations of Ch_5 and $Dansyl_{10}$ loaded with etoposide and BNIPDaoct were tested for their cytotoxicity *in vitro* on Caco-2 and HEK293 cells. All formulations were capable of lowering the IC_{50} values when compared with the free anticancer drugs, thus increasing their therapeutic effect. The Ch_5 decreased the solubility of etoposide 2.2-fold and BNIPDaoct 1.3-fold on Caco-2 cells, with $Dansyl_{10}$ achieving a 14 -fold and 16–fold reduction respectively. *In vivo* oral administration of Ch_5 and $Dansyl_{10}$, griseofulvin formulations demonstrated significantly enhanced the absorption of griseofulvin absorption in rats compared with griseofulvin in water (8.89-fold and 5.20-fold increase respectively on total concentration of griseofulvin solubilised over 24 h study). A formulation of Ch_5, BNIPDaoct was also shown to significantly decrease the tumour growth when treated on tumour bearing nude mice over a 4 week period. This is the first time these novel PAA's grafted with cholesteryl and dansyl have shown promising potential in hydrophobic drug delivery.

Chapter One

Introduction

Drug delivery describes the delivery of a pharmaceutical compound into humans or animals. Traditionally inert excipients were used as carriers for the active ingredient and as bulking agents for formulations enabling convenient and accurate dosage. However, modern excipients can increase the bioavailability of the therapeutic agent and control its release site and rate [1].

The mode of drug delivery is usually chosen by investigation into the physiochemical properties of the drug, the desired site of action, the duration of action and the biological barriers (e.g. degradation) [1]. The most common forms of drug delivery available at present are oral, nasal, rectal, parenteral, transdermal and aerosol administration [2].

Approximately 40% of all new drugs in the developmental stage are hydrophobic [3]. As a result a large number of potentially beneficial compounds do not reach clinical trials due to their poor bioavailability [4]. Therefore formulation technologies are required in order to effectively administer hydrophobic drugs.

1.1. Hydrophobic Drugs

Hydrophobic drugs do not dissolve in water. The British Pharmacopoeia classes drugs as sparingly soluble and practically insoluble if they possess an aqueous solubility below 1 and 0.1 mgmL^{-1} at 25 °C respectively [5]. These drugs cannot be formulated as aqueous based injections. In order for a drug to be delivered via the parenteral route, the drug must be in solution (or suspension). Hydrophobic drugs are unable to form hydrogen bonds with the polar water molecules and therefore they cannot be readily absorbed by the body. In order for a drug to be administered orally, it must have good aqueous solubility to dissolve in the gastrointestinal (GI) fluid facilitating crossing through the GI tract [6].

1.1.1. Physiochemical properties of drugs
1.1.1.1. Solubility of drugs

The degree of drug solubility can be influenced by a number of factors. Firstly, the size and shape of the drug molecule is important. In order for a drug to become solvated within a given solvent, its molecules must be able to be accommodated within the cavities between the solvent molecules [2]. This is more accurately explained using the Noyes–Whitney equation (1).

$$\frac{dw}{dt} = k(c_s - c) \qquad (1)$$

where

$$k = DA / \delta$$

2

The Noyes-Whitney equation relates the rate of dissolution of solid particles in the dissolution medium [2]. The rate of dissolution of the solid is dw/dt, A is the surface area, c indicates the concentration in the bulk of the medium, c_s is the saturation solubility of the solid in the dissolution layer. The diffusion coefficient is denoted by D, k is representative of the rate constant of dissolution and δ is the thickness of the diffusion layer. The relevance of this equation is due to the influence of A (particle size). A reduction in particle size results in larger surface area which increases the solubility in solution c_s. If the rate limiting factor in bioavailability is the dissolution properties of the drug, then a change in c_s will result in a change in bioavailability [2]. Thus, the smaller the drug molecule, usually the higher solubility exhibited. This may be true for non-polar compounds, however polar compounds behave in a different manner. Polar compounds are compound which possess inherent charges due the presence of electronegative functional groups or ions within their structure. Polar compounds are notably more water soluble [2]. Their ionic charge enables the formation of electrostatic and hydrogen bonds with the water molecules facilitating solubilisation.

1.1.1.2. *Partition coefficient*

In solution drug molecules can partition (P) between the phases of two immiscible solvents relative to their concentration and affinity for each phase. *In vivo*, drugs can move from the hydrophilic gut lumen into the lipid gut epithelial cells depending on their ability to partition between the two phases. The partition coefficient is the measure of hydrophobicity of a molecule and hence are useful for example in estimating distribution of drugs within the body. The partition coefficient, P, (2) is usually quoted as log P whereby, C_0 is the concentration of a drug in the hydrophobic organic phase and C_w is the concentration of drug in the hydrophilic water phase.

$$P = C_0 / C_w \qquad (2)$$

Hence drugs with a high log P value mainly dissolve in the lipophilic phase whilst drugs with a low log P value have higher affinity for the hydrophilic phase. Log P offers an estimation of bioavailability where drugs with high log P in theory achieve higher bioavailability as they can easily partition across the intestinal epithelium. However, *in vivo* this is not always the case, as drugs which exhibit a high degree of hydrophobicity are unable to initially dissolve in the aqueous GI fluid and therefore cannot cross the GI tract.

Delivery systems are required to increase the solubility and bioavailability of these therapeutic compounds. To overcome this problem, traditional formulation technologies such as surfactants, liposomes, microemulsions and others have been used.

1.2. Existing Technologies for the Delivery of Hydrophobic Drugs

1.2.1. *Surfactants*

In recent years the most common form of excipient for the delivery of hydrophobic drugs was surfactants [7]. Surfactants are low molecular weight amphiphilic compounds which possess one hydrophobic moiety and one hydrophilic moiety (Fig. 1) [8]. The hydrophobic region usually consists of saturated or unsaturated hydrocarbon chains, heterocyclic or aromatic ring systems [2].

Hydrophobic Tail
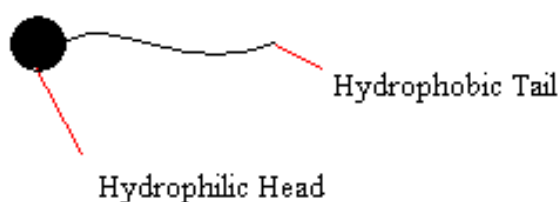
Hydrophilic Head

Figure 1. Schematic diagram of a surfactant molecule.

Surfactants are classified based upon the hydrophilic group present in their structure, for example, anionic (sodium dodecyl sulphate (SDS)) [9], cationic (cetyl pyridinium chloride (CPC)) [10], zwitterionic (cocamidopropyl betaine (CAPB)) [11] or non-ionic (oleyl alcohol) [12] (Fig. 2).

In aqueous environments the surfactants spontaneously aggregate to form micelles [8,13]. Micellar structure is described as a core/shell arrangement whereby a hydrophobic core is surrounded by a hydrophilic shell (Fig. 3). The driving force for micelle formation is the desire of the hydrophobic segment of the surfactant to shield itself from the 'hostile' aqueous environment. Micelles are dynamic structures, possessing stability ranging from milliseconds to seconds [14].

ANIONIC
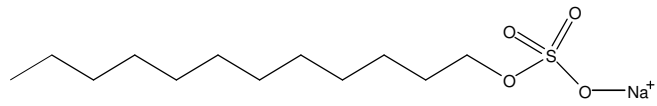
Sodium Dodecyl Sulphate (SDS)

CATIONIC
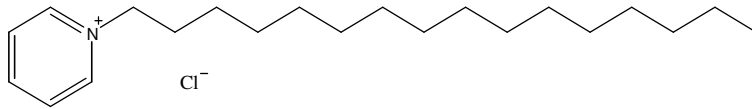
Cetylpyridinium Chloride (CPC)

ZWITTERIONIC
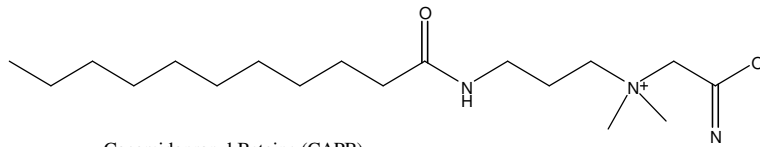
Cocamidopropyl Betaine (CAPB)

NONIONIC
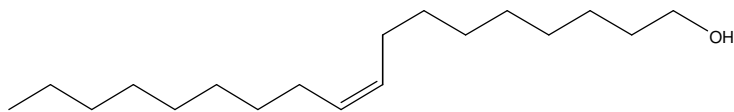
Oleyl Alcohol

Figure 2. Examples of each of the classifications of surfactants.
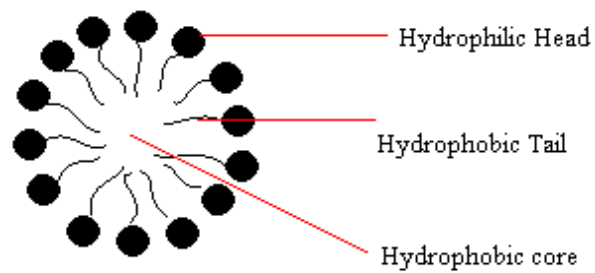
Figure 3. Schematic diagram of a micelle.

5

The stereochemistry of the surfactant has a direct impact on the shape of the micelles being formed [2]. For a surfactant which consists of a hydrophobic chain and a hydrophilic head, the micelles formed will be spherical (Fig.4a). If a secondary alkyl chain (hydrophobic) is present, a bilayer is produced (Fig 4b). Another possible scenario is where a reverse micelle is formed. This occurs when the surfactant is in a non-aqueous medium (Fig. 4c).

a) Micelles

b) Bilayers

c) Reverse Micelles
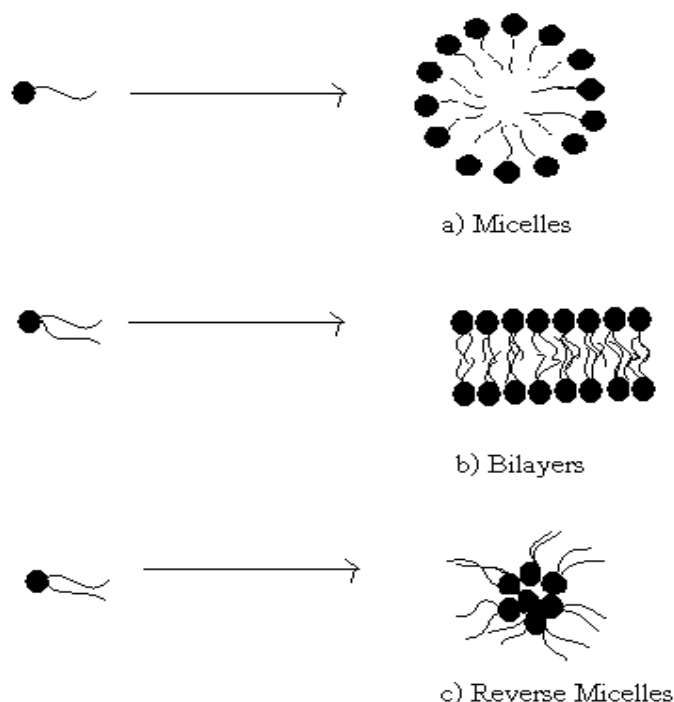
Figure 4. Types of aggregation formed by surfactants in solution.

The spherical structures achieved by ionic surfactants in aqueous environments gradually change in shape as the surfactant concentration in solution is increased [13]. The micelles elongate at higher concentrations and form cylinder like aggregates which have a rod-like structure (Fig. 5) [15].

Increased Concentration

Sphere   Rod
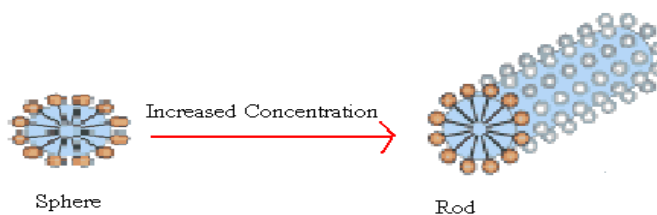
Figure 5. Change in shape of Ionic surfactant micelles at high concentrations.

6

Micellar systems only form above the critical micellar concentration (CMC). This is the lowest surfactant concentration required for aggregation to occur. The lower the CMC of the micelle, the more stable it shall be [16]. The CMC can be effected by a number of factors including the structure and nature of the hydrophobic group, the addition of electrolytes, temperature etc. [2,17,18,19].

The hydrophobic core of the micelle acts as a non-aqueous reservoir for hydrophobic drugs whilst the shell reacts with the biological milieu allowing absorption into the body and enabling transport to the target area [8]. The ability to encapsulate hydrophobic molecules such as drugs and increase their aqueous solubility is called solubilisation. The solubilisation process only occurs if the surfactant is present above its CMC value [8]. The hydrophobic drug is also referred to as the solubilisate. The chain length of the hydrophobic moiety on the surfactant has a direct effect on solubility [20]. In general, a decrease in CMC is experienced when the alkyl chain length of the surfactant is increased [2]. The solubility also decreases with increase of alkyl chain length of the solubilisate [2]. In most cases the solubilisation capacity increases with increasing temperature [21].

To date the commercial surfactants available for human consumption include SDS [22], Tween [23] and Cremophor EL [24].

The major problem with surfactants is that they possess a relatively high CMC making their micelles relatively unstable [25]. Once administered *in vivo*, they become highly diluted in the blood and disruption of the micelle occurs resulting in premature release of the drug [7]. This lowers the efficiency of the desired drug delivery. Another disadvantage is the extremely high excipient/drug ratios (15:1 - 1000:1) drug. A high excipient:drug ratio indicates that the delivery system is inefficient [3]. The use of surfactants can cause pain on administration as some form viscous oily solutions [26]. The high levels of excipient required for drug solubilisation also poses safety concerns, often causing unnecessary side effects.

1.2.2. *Microemulsions*

Traditionally emulsions were used as conventional pharmaceutical excipients. Emulsions are liquid dispersions consisting of a oil phase and a water phase. Oil in water emulsions (o / w) enable hydrophobic drug solubilisation into the oil phase and being dispersed into the bulk aqueous solution. Water in oil (w / o) emulsions solubilise hydrophilic drugs into water droplets dispersed into the hydrophobic oil phase. However, these systems did not possess long stability periods.

Modern advances in pharmaceutical technology have led to the development of microemulsions. Microemulsions are liquid mixtures of oil, water and surfactants (or

cosurfactants) [27]. They are usually clear and are thermodynamically stable [18,27]. Microemulsions are essentially swollen micellar systems [2]. It is difficult to make clear a distinction between emulsification and solubilisation as there is a very gradual transition from one process to the other [28]. At the transition the swollen micelles (also known as microemulsions) occur [28]. The microdroplet size formed is usually less than 100 nm.

Microemulsions are used to enhance solubilisation and bioavailability of hydrophobic compounds [7,29,30]. They possess high solubilisation capacities and offer increased stability, however addition of drug can compromise the stability [14]. They assemble spontaneously in short preparation times, without the use of mechanical force [7]. Two immiscible phases such as oil and water can only mix if a surfactant is present. The surfactant forms a monolayer at the interface of the oil and water. The hydrophobic tail of the surfactant has affinity for the oil layer whilst the hydrophobic head resides in the aqueous phase [31]. The three phases of oil water and surfactant aggregate to form the swollen micelles where the internal phase is the hydrophobic moiety (Fig. 6) [32].
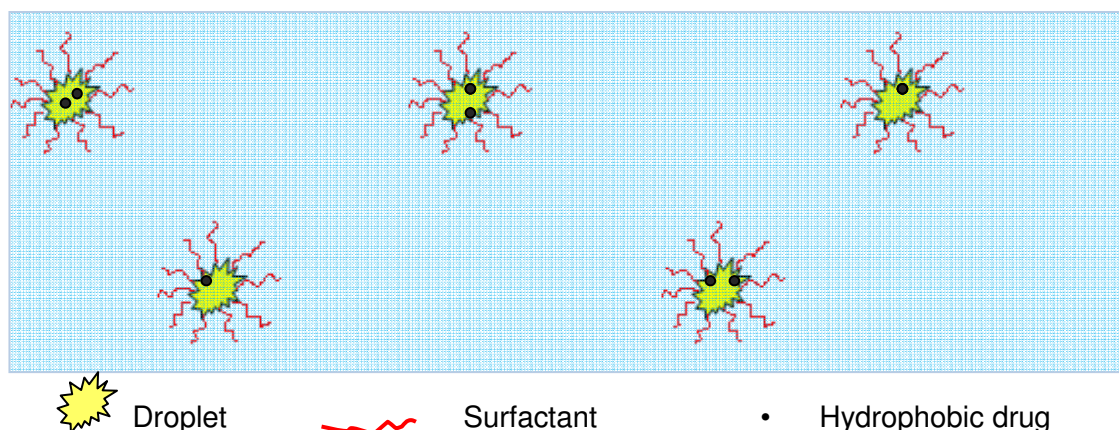
Figure 6. Schematic representation of oil in water microemulsion where drug is solubilised within the micro droplet.

Microemulsions are a complex mix of solute, solution, reversed micelles and normal micelles, and microemulsion droplets [2]. As a result changes in temperature, concentration or pressure can have an effect on equilibrium and stability of the system. Microemulsions of water in oil (w / o), the water is dissolved the tiny water droplets known as nano-scale pools [33]. These pools can be used to solubilise hydrophilic molecules such as proteins, amino acids etc. [34,35,36,37]. In oil in water (o / w) microemulsions, oil is dissolved in the nano-scale pools into which hydrophobic moieties are dissolved [38].

Many commercial microemulsions are commercially available including Neoral® for delivery of immunosuppressant drug cyclosporin A, Fortovase®, Norvir® and Agenerase® for the delivery of antiretroviral drugs saquinavir, ritonavir and amprenavir respectively [39]. However, despite commercial success, large amounts of surfactant are required to make a microemulsion, this results in a high excipient:drug ratio due to the water oil

interface has a very large surface area [7]. This makes them inefficient systems which are not cost effective.

1.2.3. *Liposomes*

Liposomes are spherical structures composed of a phospholipid bilayer surrounding an aqueous reservoir (Fig. 7) [32,40] Liposome vesicles are composed of unilamellar or multilamellar lipid bilayers which have alternative aqueous layers sandwiched between the bilayers [31]. Upon aggregation multilayered liposomes are formed however, these are easily converted to unilamellar entities by sonication [2].
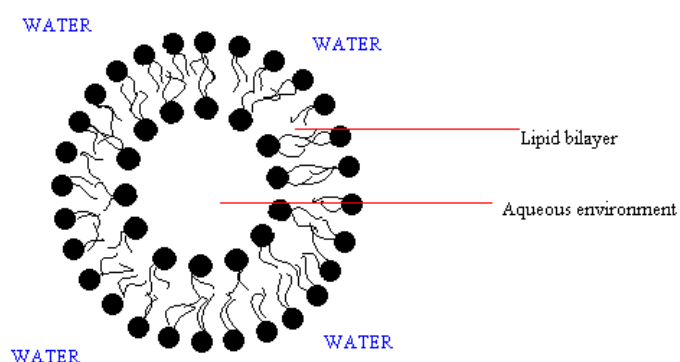
Figure 7. Schematic of a unilamellar liposome.

Hydrophilic or hydrophobic drugs can become encapsulated inside the aqueous or lipid phase of the liposomes respectively [40,41]. Liposomes have been shown to improve the therapeutic efficacy of pharmaceutical drugs including ibuprofen, amphotericin B and doxorubicin [40,42,43,44,45].

A number of liposomes are commercially available for drug solubilisation including VesicALL®, for the delivery of anticancer agents [46], Doxil™ for doxorubicin [47] and AmBisome to deliver amphotericin B [47].

The net charge of a liposome can be varied by incorporation of different molecules onto the structure [48]. Positively charged liposomes are commonly used for gene delivery and DNA vaccines [43,49,50]. Gregoriadis fabricated ImuXen®, which is a commercially available liposomal vaccine delivery system used for the delivery of proteins, polysaccharides and DNA [46].

In general hydrophilic compounds are not well entrapped in liposomes compared to lipophilic compounds which are well retained in these drug carriers [41]. Their major disadvantage as drug carriers is their instability on drug entrapment [44]. The inclusion of

drug into the lipid bilayer causes penetration and results in premature drug release [44,51]. To combat this problem cholesterol is incorporated into the phospholipid bilayer, consequently the liposome possess higher rigidity leading to more stable vesicles [50,52]. Furthermore, poor stability is experienced on storing in aqueous phase.

However, lyophilisation and cryoprotection of the liposomal formulation have been reported to minimise this problem [44,53]. Saccahrides such as sucrose, trehalose and lactose are the most commonly used cryoprotectant for the freeze drying process, however, these are required at high concentrations of up to 30:1 cryoprotectant:liposome which can compromise the liposomal viscosity and induce adverse side effects in patients [44].

Mohammed and colleagues reported that amino acids could be used as successful cryoprotectants during the freeze drying process. They prepared a liposomal formulation consisting of phosphatidylcholine (PC) and cholesterol and ibuprofen [44]. They concluded that lysine offered an alternative cryoprotectant to the traditional saccharides as it offered comparable cryoprotection to trehalose at only 4:1 cryoprotectant: liposome [44]. This work shows great potential enabling increased stability of liposomal formulation stability without compromising the integrity of the preparation.

1.2.4. *Cyclodextrins*

Cyclodextrins are cyclic oligosaccharides that possess a rigid conical structure (Fig. 8) [54,55,56]. They consist of a hydrophilic exterior and a hydrophobic inner core [54,55]. The hydroxyl groups on the exterior of the cyclodextrin structure form hydrogen bonds with water resulting in the formation of inclusion complexes [57,58,59].
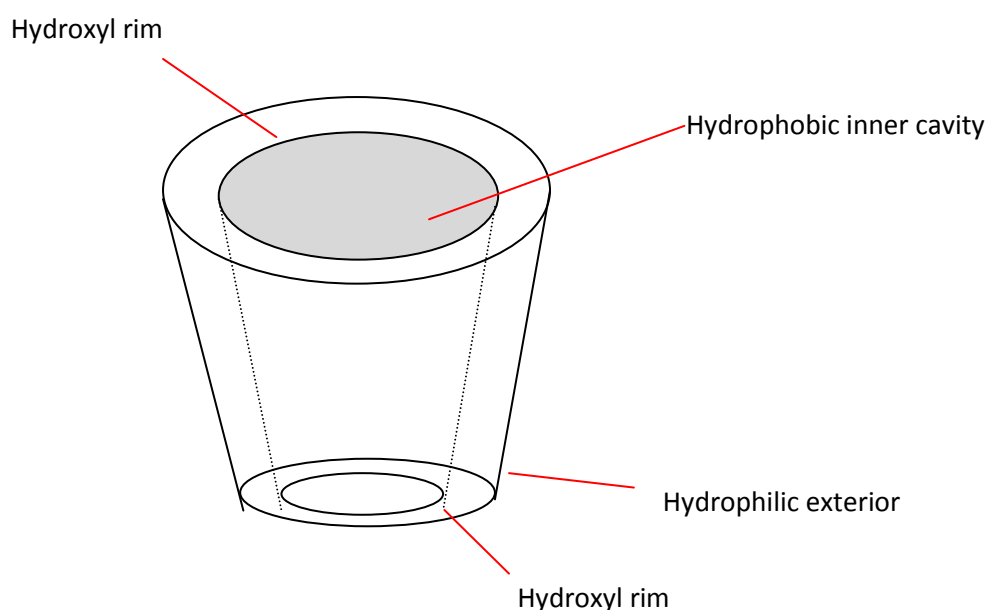
Figure 8. Schematic representation of the conical structure of cyclodextrins.

An inclusion complex is formed when a water molecule located in the lipophilic central cavity of the cyclodextrin is removed and is replaced by a lipophilic guest (i.e. a hydrophobic drug) (Fig. 9) [54,58]. The central cavity plays host to hydrophobic moieties of suitable size through non covalent hydrophobic interactions [55,59]. This forms an alternative to micellar solubilisation.
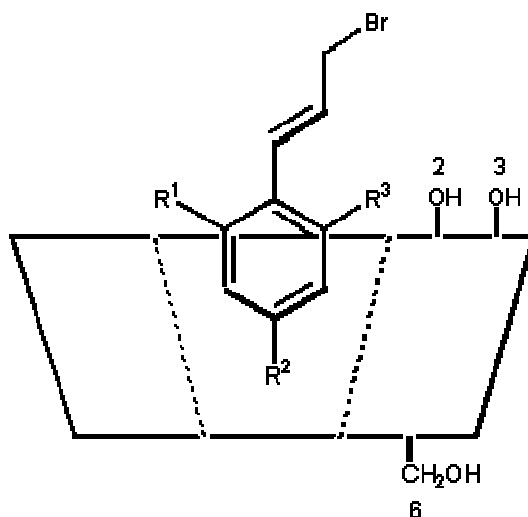
Figure 9. Schematic representation of complexation of alkyl reagent with cyclodextrin [60].

The solubility of hydrophobic drug is enhanced by physical entrapment inside the central cavity of the cyclodextrin. Cyclodextrins have been reported to increase solubility, enhance bioavailability and protect drugs throughout their journey *in vivo* [54]. Worldwide 35 drugs are commercially marketed as solid dosage or liquid based cyclodextrin formulations [59]. However, cyclodextrins are not a generic solubilising agent to hydrophobic drugs. Their solubilising capacity is drug dependant on size and steric structure. In order for the hydrophobic drug to reside within the central core, it must physically fit into the well structured environment of the cyclodextrin [61].

1.2.5. *Calixarenes*

Calixarenes are a family of cyclic oligomers which possess three-dimensional structures [62]. They are commonly used as starting materials or building blocks in the design of supramolecular systems [63]. Calixarenes form 3D cup-like structures with well defined upper and lower rims containing a central cavity in both the solid state and in solution (Fig. 10) [62,64,65].

11
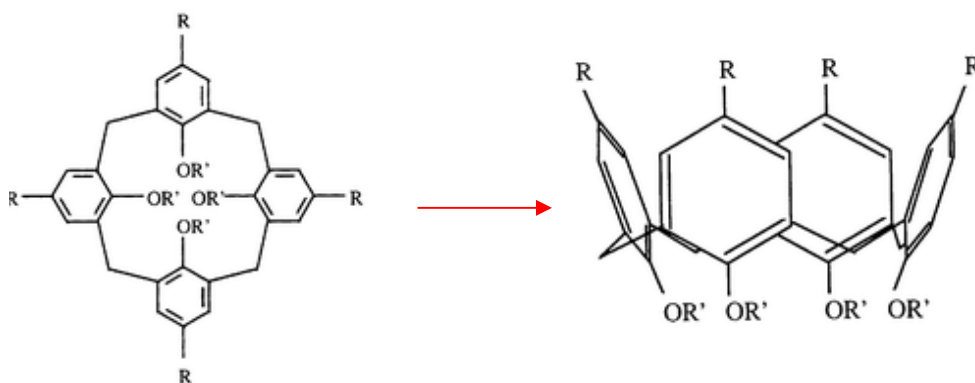
Figure 10 . General structure of a calixarene showing stereochemistry of cup like structure, where R can be replaced by functional groups [66].

They possess a metal binding site and a hydrophobic pocket for host guest interaction with organic molecules [67]. Calixarenes enhance the solubility of hydrophobic drugs via hydrophobic interaction. Yang and de Villers investigated the solubilising effect of 4-sulphonic calix[n]arenes on poorly soluble antianginal drug nifedipine [62]. The maximum solubilisation of nifedipine was achieved using 4-sulphonic calix[8]arene resulting in a 3 fold increase on the aqueous drug solubility [62].

Calixarenes are not completely rigid molecules as their shape can be varied with different solvents, functional groups and temperature [67]. They possess a number of advantages over cyclodextrins, they can be chemically modified easily using low toxicity chemical reactions. Functional groups can easily incorporated via the upper or lower rim of the structure to enable targeted delivery or to further enhance aqueous solubility [62]. They have relatively low production costs and are less toxic than the cyclodextrins [68]. However like cyclodextrins, calixarenes exhibit drug specificity, whereby the drugs need to be physically small enough and sterically able to reside within the central cavity. Therefore calixarenes do not form generic drug solubilisers.

1.2.6. *Cosolvents*

Cosolvents such as propylene glycol, glycerine or ethanol mixed with water are also used to enhance the solubility of hydrophobic drugs [69]. Cosolvents are usually required where drug solubility in one solvent is limited, the presence of two solvents increases the drug solubility [2,31]. In 2002 Millard and colleagues reported that cosolvents made up 13 % of all Food and Drug Administration agency (FDA) approved parenteral products [69].Two miscible solvents are mixed, where one solvents is the desired media (e.g. water), the second solvent is usually an organic solvent in which the drug candidate is readily soluble. This method allows solvation of the drug. However, it is not a preferred method as

residual organic solvents remaining in the formulation may be toxic to the patient which is a major disadvantage.

There is a growing need to design novel delivery systems due to the growing number of hydrophobic drugs discarded in the development stage. It is essential to create a delivery system which is not only capable of encapsulating high levels of active ingredient but is also able to achieve site specific delivery. Furthermore, it is of utmost importance that the delivery system developed exhibits an excellent safety profile. Currently one of the promising strategies is the use of different types of amphiphilic polymers to deliver hydrophobic drugs.

1.3. Amphiphilic Polymers

Amphiphilic polymers have been widely investigated in recent times [70,71,72,73]. The amphiphilic polymers consist of hydrophobic and hydrophilic domains [74]. In the aqueous environments, the amphiphilic molecules associate through weak non-covalent hydrophobic-hydrophobic interactions whereby, the hydrophilic moiety will remain in contact with the aqueous phase whilst the hydrophobic moiety will 'shield' themselves, thus forming a polymeric micelle [74,75]. Amphiphilic polymers have been reported to form a wide range of structures in aqueous environments including polymeric micelles, vesicles and nano-particles [72,76,77,78].

Their ability to form spontaneous self-assembled polymeric micelles and nano-particles in aqueous environments demonstrated great potential for drug solubilisation [72]. Like traditional micelles the hydrophobic core of the micelles can encapsulate hydrophobic drugs and thus increase the water solubility [72,79]. The lowest concentration required for a polymeric micelle to form in an aqueous environment is called the critical aggregation concentration (CAC). The CAC is affected by a number of factors including the structure and nature of the hydrophobic group and the addition of electrolytes [76].

Polymeric micelles have several advantages compared to traditional surfactant micelles. They possess lower CAC values (approximately 1000 times lower) than traditional micelles [72,80,81]. This makes their aggregates more stable in aqueous solution and hence reduce the risk of disruption upon dilution *in vivo* [16]. The size of the self-assemblies formed in aqueous environments are usually between 30 - 100 nm, this size can increase or decrease on drug loading depending on the molecular architecture of the polymer and of the drug [79].

Drugs, including those which cannot enter the cell passively by diffusion, may enter cells by endocytosis when the drugs are entrapped inside the polymeric micelles (Fig. 11) [82,83]. The polymeric micelles' core-shell structure can also mimic naturally occurring transport systems such as plasma lipoproteins and viruses [73].
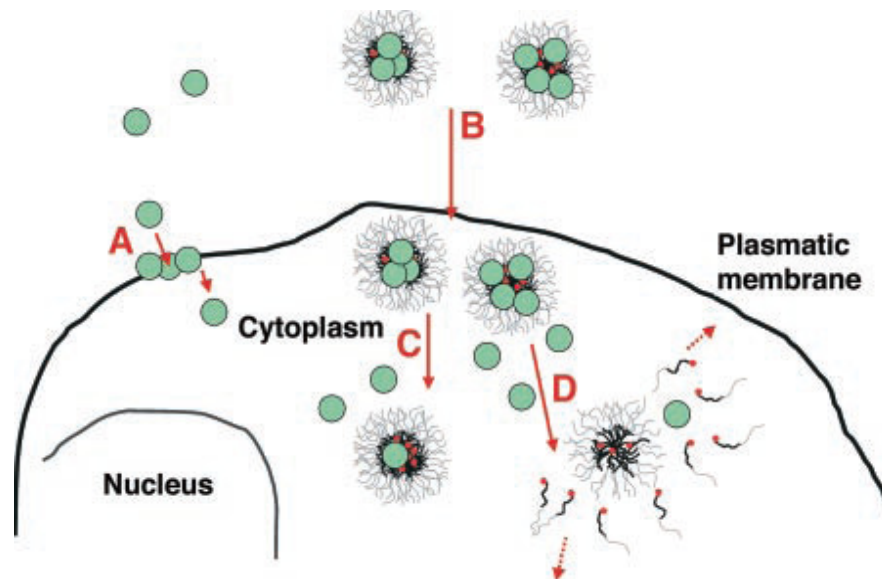
Figure 11. Schematic representation of the cellular internalisation of free drugs and drug loaded micelles. (**A**) Drug diffuses through the cell membrane and slowly in the cytoplasm, (**B**) micelle loaded drug enters the cytoplasm by endocytosis, (**C**) in the cell, drug molecules from micelle diffuse out and distribute through cytoplasm and (**D**) some micelles disassemble into single chains and act locally to internalise into the cellular organelles (dotted arrows) [83].

The micelle protects the drug from chemical degradation or being metabolised during its journey to the desired target area, therefore making the delivery more efficient [73]. The nanoscopic size of micelles enables quick and easy sterilisation by simple filtration [73]. The major advantage of polymeric micelles is that the required polymer/drug ratio can be as little as 5:1 which significantly increases the efficiency and decreases the toxicity of the delivery system [3].

An amphiphilic polymer can be formed from diverse architectures, these are usually classified into four main groups. Block copolymers [72,75,84,85,86], graft polymers [76], star shaped polymers [87,88] and dendrimers [89.90].

1.3.1. *Block copolymers*

Block copolymers are fabricated from the polymerization of two or more types of monomer unit (Fig. 13) [74]. Typically one hydrophobic moiety and one hydrophilic moiety is polymerized together giving an amphiphilic diblock copolymer e.g. poly(ethylene oxide)-block-poly(lactic acid) (PEO-b-PLA) [79]. Triblocks, tetrablocks, pentablocks etc. can also be synthesised using the same reaction. In aqueous solution amphiphilic block copolymers form polymeric micelles (Fig. 12).
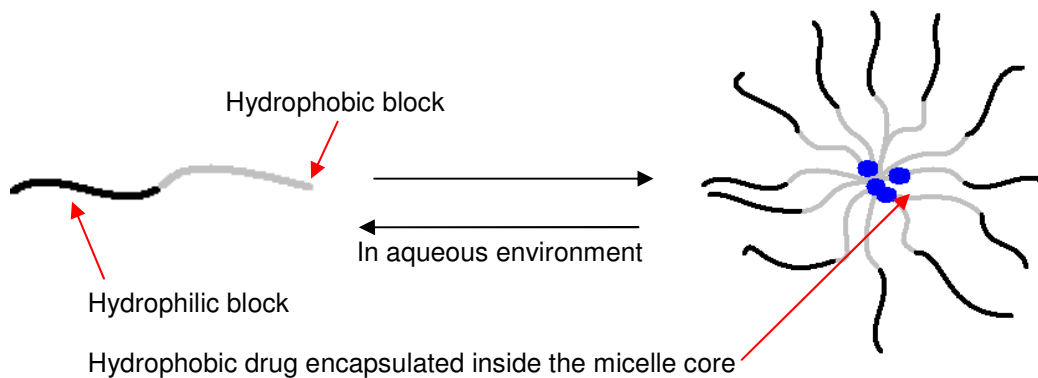
Figure 12. Schematic representation of dynamic micellation of diblock copolymers in aqueous environment.

As drug delivery vehicles, the hydrophobic moiety of block copolymers is usually composed of biodegradable and biocompatible monomers such as polyesters e.g. poly(caprolactone) (PCL) and poly(lactic aid) (PLA) or poly(amino acids) e.g. poly(aspartic acid) (Fig. 13) [74,75,91].
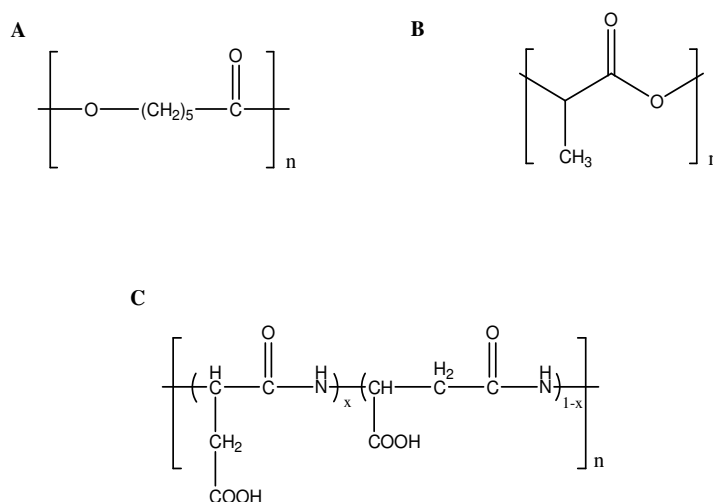
Figure 13. Chemical structure of hydrophobic monomers commonly used in block copolymers A) poly(caprolactone), B) poly(lactic acid) and C) poly(aspartic acid).

The most common hydrophilic segment for block copolymers is poly(ethylene glycol) (PEG), however other hydrophilic monomers have also been reported e.g. poly(ethylene oxide) (PEO), and poly(N-isopropylacrylamide) (PNIPAAm) (Fig. 14) [72,92,93].
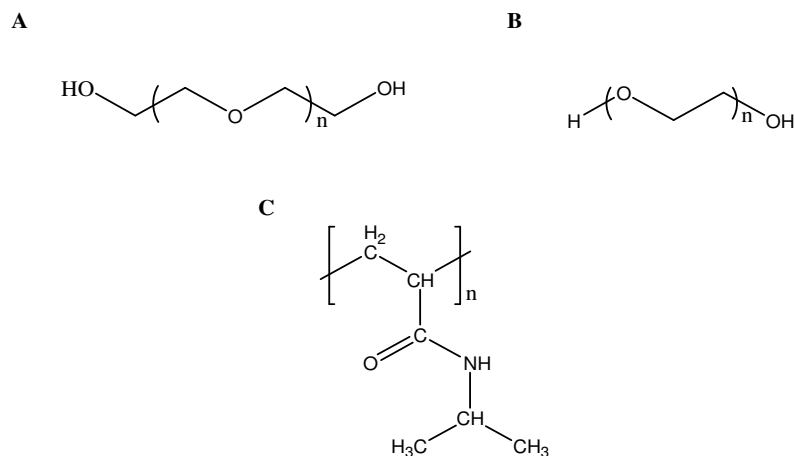
Figure 14. Chemical structure of hydrophilic monomers commonly used in block copolymers A) poly(ethylene glycol), B) poly(ethylene oxide) and C) poly(N-isopropyl acrylamide).

PEG is an FDA approved polymer for intravenous administration [75]. It is highly biocompatible and resistant to protein adsorption and cellular adhesion due to its steric repulsion effect [72,75]. PEG is commonly used due to its highly soluble, non toxic nature [85,91]. It has been reported that PEG can be excreted through renal filtration out of the body [85,91].

Block copolymers have been extensively investigated as potential delivery vehicles for many hydrophobic drugs. Formulation of hydrophobic drugs range from simple drugs such as propofol [94] through to anticancer drugs such as doxorubicin [95,96], etoposide [97], paxlitaxel [98,99,100] and camptothecin [101,102].

Polymer chains have a much wider range of physiochemical properties than the low molecular weight surfactants [2]. Varying the molecular weight or hydrophobicity of the polymer allows a degree of control of the properties of the subsequent nano aggregates [2]. Polymeric micelles formed from block copolymers possess greater kinetic stability upon dilution, the length of hydrophobic segment of the block copolymer influences the stability of the nano aggregates formed whereby increased hydrophobic content results in increased stability [103]. The length of the hydrophobic chain also effects drug loading capacity of the nano aggregates [103,104]. Lee and colleagues investigated polymeric micelles of poly(2-ethyl-2-oxazoline)-block-poly(ε-carprolactone) as potential drug delivery systems for a hydrophobic anticancer drug, paclitaxel. The studies showed that the higher the content of the hydrophobic block in the copolymer, the higher the loading efficiency for the drug [100].

Higher hydrophilic content in a block copolymer results in a higher degree of solubility in aqueous environments. The hydrophilic monomer forms weak hydrogen interactions with the water molecules. Gaucher reported that increasing the hydrophilic chain of the block copolymer resulted in longer circulation times and greater 'stealth' effect whereby the

blood protein adsorption of the polymeric micelles was hindered [103]. However, increasing the hydrophilic content excessively will result in unstable micellation or even no micellation occurring. This is due to the hydrophobic interaction driving forces becoming too weak for self-assemblies to occur. The weaker hydrophobic forces present in higher hydrophilic content amphiphiles also result in lower levels of drug loading efficiency and greater instability.

The level of compatibility between hydrophobic drug and amphiphilic block copolymer has an influence on self-assembly stability, drug loading capacity and release rate [103,104,105]. Shaui loaded monomethoxy poly(ethylene glycol)-b- poly(ε-caproclactone) (MPEG-B-PCL) micelles with doxorubicin and concluded the drug loading capacity was dependant on both hydrophobic associations and hydrogen bonding between the drug and block copolymer [95].

The solubility of amphiphilic polymers is determined using the same considerations that apply to low molecular weight surfactants e.g. chain length, nature of solubilisate, effect of temperature etc. [2]. However, due to the extensive size of polymers, their interactions with water are a lot more complex than for the smaller molecules, as a result some polymers do not possess a saturation point [2]. Water soluble polymers increase the intrinsic viscosities of their solvents when they are present in low concentrations [106].

Cross-linking of block copolymers is a technique frequently used to enhance structural integrity of their nanostructures in aqueous environments [107,108]. Crosslinking is achieved at either the core or the corona of the micelle, and results in a decrease in hydrodynamic radius [105,107]. Crosslinking efficiency of polymeric micelles is dependent on molecular weight of the polymer [105]. By crosslinking the core of the micellar structure, the outer shell structure is unaffected, giving rise to functional group attachment for the design of smart polymers [107].

1.3.2. *Graft Polymers*

Amphiphilic graft polymers consists of a homo polymer as the backbone to which hydrophobic pendant groups are 'grafted' to form a comb like structure. The hydrophobic pendant groups of a comb shaped polymer may consist of homopolymers, copolymers or small molecular weight hydrophobic molecules. In the aqueous environment, self-assemblies are formed with a hydrophobic core stabilised by a hydrophilic corona (Fig. 15) [76,109,110].
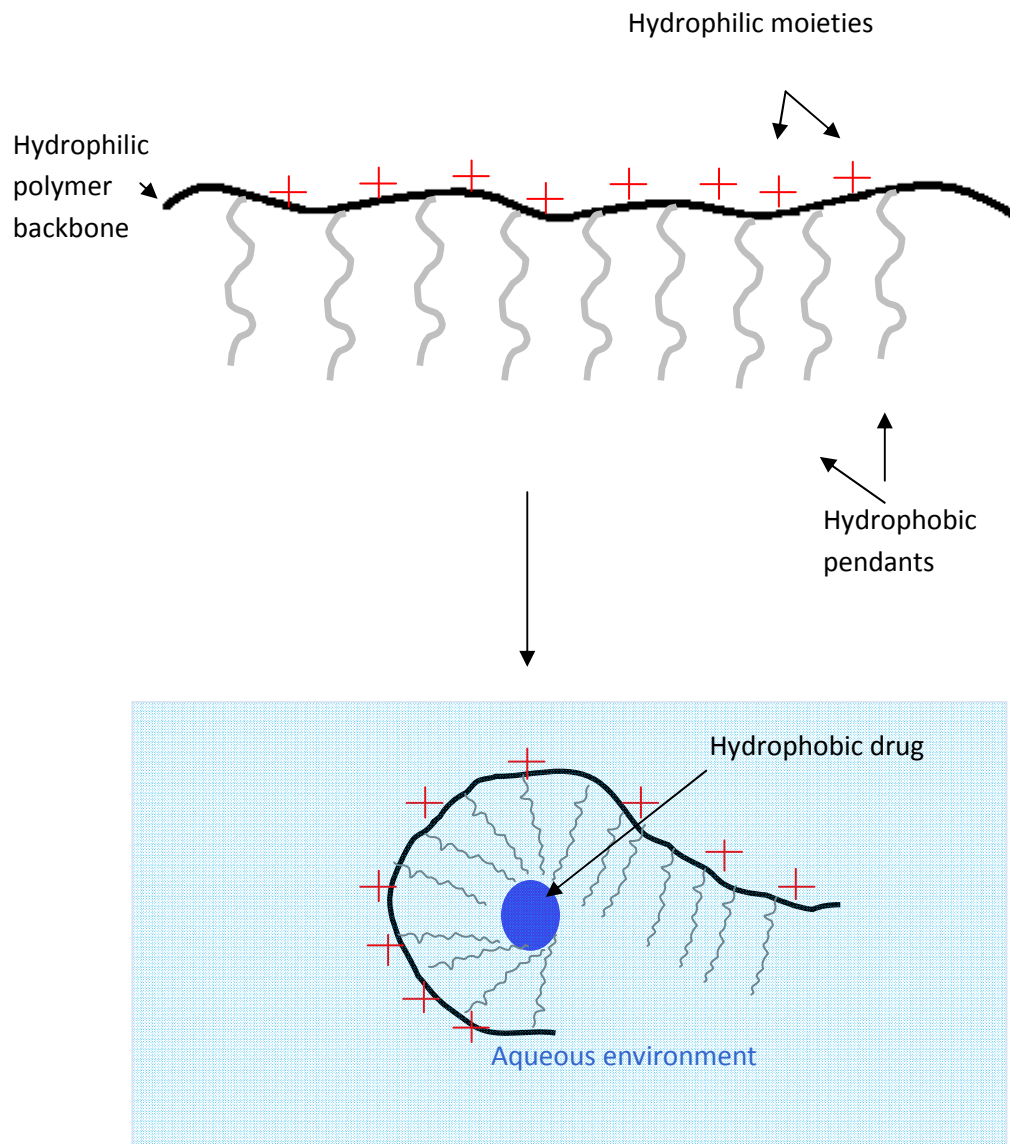
Figure 15. Schematic representation of self-assembly formation of comb shaped polymers in aqueous environment.

Graft polymers are a relatively new area of interest in drug delivery. In 1998 Chiu developed amphiphilic graft copolymers consisting of stearyl methacrylate, methyl acrylate (Fig. 16), acrylic acid and PEG acrylate [111].
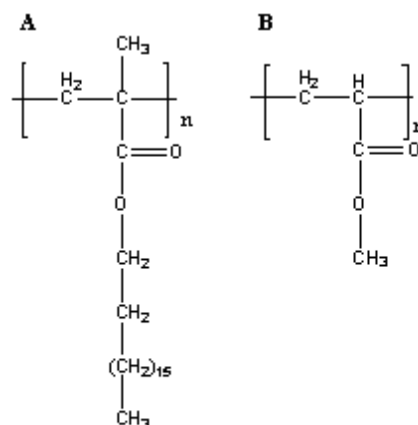
Figure 16. Chemical structure of the amphiphilic graft copolymers A) stearyl methacrylate and B) methyl acrylate [111].

They reported the amphiphilic graft copolymers formed polymeric micelles in aqueous environments, these aggregates showed a bimodal size distribution whereby two size populations of 50 and 389 nm were observed [111]. The rationale behind such aggregation was proposed due to loose aggregates and large association complexes being formed which were in dynamic equilibrium with smaller more compact micelles [111]. The aggregate formed showed potential for encapsulation of hydrophobic drugs. However, they concluded that more work needed to be carried out in this area to further investigate the properties of these systems i.e. biocompatibility, bioavailability, cytotoxicity etc [111]. Sugimoto fabricated poly(*N*-hydroxyethyl L-glutamine)-*graft*-poly(L-tryptophan) (PHEG-*graft*-poly(Trp)) and successfully incorporated hydrophobic azobenzene into hydrophobic region of the polymeric micelles showing their potential for hydrophobic drug solubilisation [112].

The type of aggregates formed in the aqueous environments include polymeric micelles, nano-particles and vesicles [76,77,78]. The physical properties of the amphiphilic comb shaped polymers can be controlled by adjustment of structural components, e.g. type of hydrophobic pendant group and level of grafting [76,113]. Hydrophilic moieties such as quaternary ammonium ions or poly(ethylene glycol) (PEG) can also be attached to the homopolymer backbone to improve the safety profile and determine the *in vivo* fate of the self assemblies [114,115]. Zhu and colleagues attached PEG monomers onto a chitosan-N- trimethylaminoethylmethacrylate (CS-TM-PEG) graft polymer [115]. They investigated the haemolytic activity when red blood cells were exposed to 250 – 2000 µgmL-1 polymer solutions [115]. The CS-TM-PEG polymer showed a reduction in haemolytic activity when compared to its un-pegylated counterpart, the percentage haemolysis was reduced from 10 – 13 % (CS-TM) to 5 – 7 % (CS-TM-PEG) [115]. This reduction in haemolytic effect results in higher biocompatibility of the polymer. Recently Thompson and colleagues

reported that addition of hydrophilic quaternary ammonium ions onto the polymer backbone of modified poly(allylamine) (PAA) polymers not only increased the aqueous solubility of the polymers but also made the polymers less cytotoxic against human epithelial colorectal adenocarcinoma (Caco-2) cells [76,116].

Lin and colleagues investigated the aggregation of poly(ß-benzyl-L-aspartate)-graft-poly(ethylene glycol) (PBLG-g-PEG) [113]. They concluded that lower CMC values were observed at higher grafting levels of hydrophobic PBLG [113]. This perhaps due to the increased hydrophobicity driving aggregation into the core – shell formation [113]. The polymeric micelles formed were spherical at lower concentrations, however they found that as the concentration was increased the conformation of the aggregates changed to rhombic and further increase of the polypeptide content and backbone length resulted in aggregates with a spindle-like morphology [113].

Polymeric micelles formed by comb shaped polymers are generally smaller in size than those formed by block copolymers. This can be attributed to the phenomenon known as intramolecular aggregation whereby, a single polymeric chain has the ability to aggregate with itself forming the self-assembly [117,118]. However, a number of groups have reported larger particles formation, possibly due to the hydrophobic pendant groups in the self-assemblies being in close proximity to the water, hence multiple micelle aggregation occurs [117,119].

Amphiphilic graft polymers are commonly synthesised from soluble polyamine backbones such as poly(allylamine) (PAA) [76,120,121], poly(ethylenimine) (PEI) [3,122,123], poly(L-lysine) (PL) [78,124]. Carbohydrate polymers have also been reported using glycol chitosan [125,126] and dextran [127]. The hydrophobic pendant groups grafted onto the homopolymer backbone are usually alkyl chains [3,76,123], acyl groups [128,129] or cholesterol moieties [76,121,130].

The hydrophobic core of the amphiphilic comb shaped polymer is capable of encapsulating hydrophobic drug through hydrophobic or electrostatic interactions [103]. When the drugs are encapsulated inside the core, their fate is dependent on the micellar properties instead of their own intrinsic properties [131]. Cheng and colleagues showed that varying concentrations of cyclosporine A were absorbed orally *in vivo* into the bloodstream of male Wistar rats when encapsulated inside a range of poly(ethylenimine) amphiphilies [3]. Graft polymers have previously been reported to achieve solubilisation of hydrophobic drugs such as cyclosporine A [3], doxorubicin [131] and paclitaxel [132]. They have also been reported to be good solubilising agents for other therapeutic agents such as proteins and genes [120,133].

McPhail and colleagues studied the combination of liposomes and graft polymers for drug delivery. They developed a vesicle in vesicle system whereby polymeric vesicles were encapsulated inside liposomes to yield a more advanced excipient for enhanced controlled release of drugs, enzymes, vaccines or proteins from the polymeric nano-carrier [134]. They fabricated the vesicle in vesicle system using palmitoyl glycol chitosan polymers and cholesterol polymers and egg phosphatidylcholine (egg PC) and cholesterol liposomes [134]. The structural formation was confirmed using freeze fracture electron microscopy. The polymeric vesicle was loaded with 5(6)-carboxyfluorescein (CF) [134]. Drug release studies concluded that the vesicle in vesicle structure slowed down the release of the drug compared to a normal polymeric micelle [134]. This system has huge implications not only for controlled release of therapeutic agents but also for the possibility of administering more than one active ingredient in combination therapy etc.

1.3.3. *Star shaped polymers*

Star shaped amphiphilic polymers are made up of 3 or more linear polymer chains linked to a central polymeric core (Fig. 17) [87,135]. The arms are of comparable lengths and consist of homo-, co- or terpolymers [87].

Polymeric central core

Polymer arms
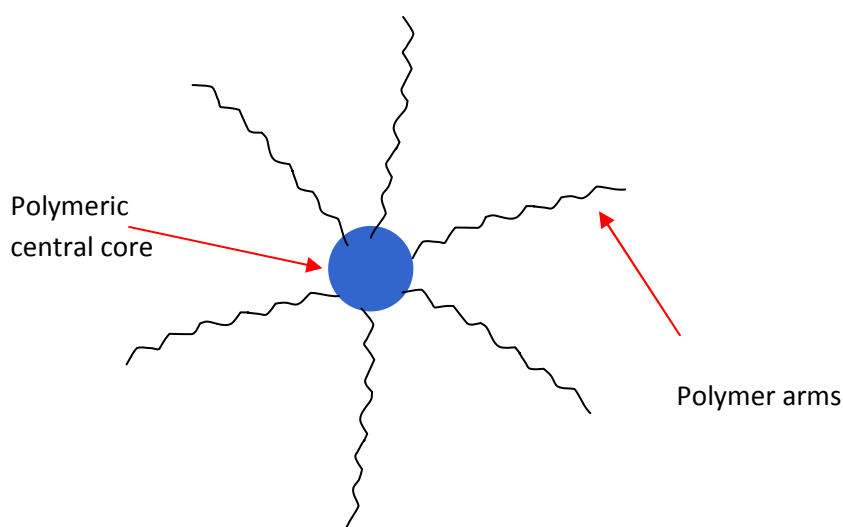
Figure 17. Schematic representation of star shaped polymer.

The nano aggregates formed in aqueous solutions possess a lower hydrodynamic radius and viscosity in solution when compared to linear polymers of the same molecular weight and composition [136,137,138]. The star shaped polymers form unimolecular micelles with increased stability compared to block copolymers [136,137]. The physical properties of the polymer can be altered by changing the chemical structure and composition of the arm chains [87,137]. Star shaped polymers have been reported to enhance the aqueous solubility of hydrophobic drugs such as paclitaxel [88,138,139] and prednisolone acetate [140].

21

Ooya and colleagues reported that 5 armed poly(oligo(ethylene glycol) methacrylate) (poly(OEGMA)) star polymers increased the aqueous solubility of paclitaxel 130 fold and achieved sustained release over long time periods with only 50 % of drug release after 96 h [88].

Wei fabricated a star shaped polymer consisting of hydrophobic poly(methyl methacrylate (PMMA) arm and 4 hydrophilic poly(N-isopropylacrylamine PNIPAAm arms [140]. These self-assembled into polymeric micelles in aqueous environments with the PMMA as the core and the PNIPAAm as the hydrophilic corona. The self assemblies produced from the star shaped amphiphilic polymers were reported to enhance the aqueous solubility of prednisolone acetate with 55 % encapsulation efficiency [140]. Previously Wei had reported an 11 % encapsulation efficiency using the same drug but with the block copolymer, poly(methyl methacrylate-block-poly(N-isopropylacrylamide) PMMA-b-PNIPAAm [141]. They speculated the reason for the marked increase was due to repulsions forces existing between the large hydrophilic PNIPAAm blocks preventing tight contraction of the hydrophobic core [140]. The resultant core would be 'looser' in size thus enabling larger drug loading capacities and improved encapsulation efficiencies [140].

Investigation into star shaped polymers is still relatively novel, however as growing interest arises new research is emerging. The use of star polymer as thermo responsive delivery vehicles is at the forefront of today's research [136,140].

1.3.4. *Dendrimers*

Dendrimers are highly branched 3 dimensional macromolecules [142,143,144]. Their structure consists of a central root core from which regular layered branching occurs, their surface is made up of abundance of terminal groups to which funtional groups such as targeting moeities, bioresponsive moeities, solubilising groups or drug molecules can be attached (Fig. 18) [89,137,142]. Repeated layers of branching can be well defined due to sophisticated layer by layer chemical synthesis, each layer is called a generation [137,145].
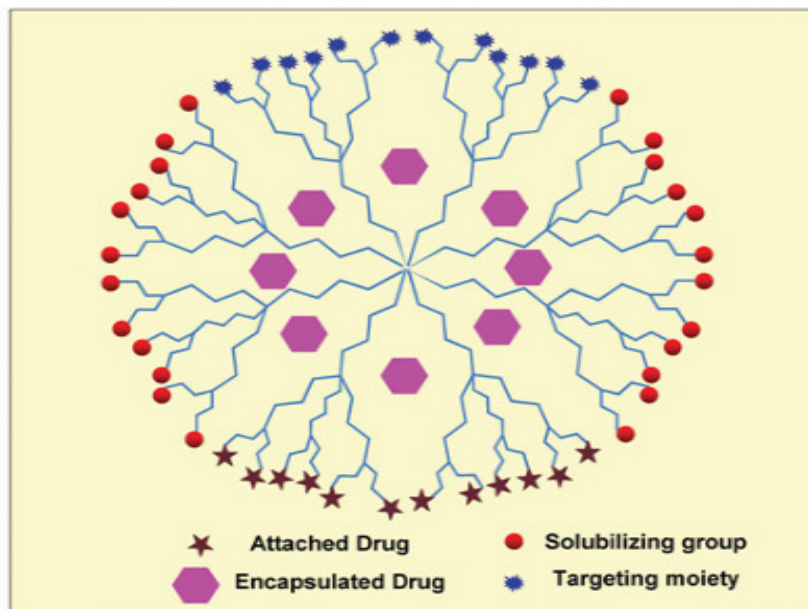
Figure 18. Schematic representation of dendrimer structure [146].

Amphiphilic dendrimers form intramolecular aggregates (unimolecular micelles) in aqueous environments. Aggregation can involve hydrophobic or electrostatic interactions or hydrogen bonding [147]. The aggregates formed possess increased stability at lower concentrations in comparison with block copolymers as the micelles do not disrupt upon dilution [137]. The aggregates are more uniform in size (i.e. monodisperse) than the formation of micelles from block copolymers, due to the nature of the chemistry used in the addition of generations [137,142,148]. The intramolecular hydrophobic core of the dendrimer is capable of encapsulation and controlled release of hydrophobic moeities such as drugs, genes and imaging agents [144,145]. Morgan and colleagues reported solubilisation of hydrophobic anticancer agent 10-hydroxycamptothecin inside poly(glycerol-succinic acid) dendrimers (PGLSA) of generation 4.5. They reported by non-covalent interaction inside the dendrimer core which increased the aqueous solubility of the drug by 20 fold [90,149,150].

Entrapment is also achieved within the multivalent branching network or through adsorption onto the outer shell [145,151]. When a drug is covalently attached to the outer shell of a dendrimer, it will exhibit a decreased release rate when compared to drug encapsulation by hydrophobic or electrostatic interactions [149]. Dendrimers with high drug conjugation can swiftly enter the cell and localise in the nucleus [149]. Kohle and colleagues conjugated ibruprofen onto a generation 4 poly(amidoamine) dendrimer PAMAM via an ester bond [152]. Approximately 58 drug molecules were successfully attached to the 64 functional terminal [152]. They found that this high drug payload system was capable of enhaced cellular delivery which could produce a faster pharmacological response time leading to improved drug efficacy [152]. Further *in vivo* investigation is currently been carried out by Kohle and coleagues.

Dendrimers hold great potential as carriers of hydrophobic compounds as they can be tailor made by adapting their surface groups and branches [89,143,144]. Generation and nature of packing of the dendrimer effects aggregation size, physiochemical properties, stability and drug loading capacity of the intramolecular aggregates formed [137,143,148].

Ooga and colleagues synthesised polyglycerol dendrimers (PGD's) with 3 - 5 generations [153]. The drug loading potential of the dendrimers were investigated. Ooga reported that the PGD's were capable of enhancing aqueous solubility of paclitaxel by 3 orders of magnitude [153]. They concluded that as the generation number increased paclitaxel solubility also increased [153]. This indicated that the drug was not solubilised inside the dendritic core, instead the high concentrations of ethylene glycol provided a hydrotropic environment whereby the hydrophobic drugs would enter the hydrophilic layers of the dendrimers stabilising the layered structure [153,154].

1.3.5. *Smart Polymers for cancer therapy*

Over the past decade polymer science has gone from strength to strength. As new research groups establish, scientists strive to achieve more controlled delivery of therapeutics with increased efficacy and reduced side effects [72,92]. Stimuli responsive or 'smart polymers' as they have affectionately been named have emerged as new front runners in the race for the perfect delivery system. Stimuli responsive polymers undergo active responses to environmental signals or external change, making them ideal candidates for active targeting [92,155]. The stimuli include physical (temperature, ultrasound, light), chemical (pH, ionic strength) and biological (biomolecules) [92,156,157]. The major application for this technology is in the delivery of anti cancer therapeutics.

Temperature responsive polymeric micelles are the most extensively studied to date [92,157,158]. Cancerous tissues posses increased metabolic rate compared to normal healthy tissues [155,159]. As a result they exist at higher temperatures of 40 – 44 ºC [155,159]. This condition makes thermoresponsive polymeric micelles ideal carrier vehicles as once inside the cell, the temperature increase will cause the polymeric micelle to release its payload into the surrounding cytoplasm.

Thermoresponsive poly(2-(N,N-dimethylamino) ethyl methacrylate)-b-poly (caprolactone)-b-poly(2-N,N-dimethylamino) ethyl acrylate (PDMAEMA-b-PCL-b- PDMAEMA) polymers were synthesised by San Miguel and colleagues [160]. The polymer showed a reversible dispersion/aggregation pattern in response to temperature change [160]. The lower critical solution temperature (LCST) was 54ºC. Slight changes in the temperature below or above the LCST can activate disruption of micelle structure and result in drug release [158]. They reported that the polymer possessed lower CMCs and better drug loading capacity for anti cancer drug chlorambucil compared to PDMAEMA non-responsive polymers [160].

The *in vitro* release results suggest that the thermoresponsive polymers would be suitable for transport of anticancer therapeutics, however no *in vivo* data has been reported to date [160].

However many thermoresponsive polymers created possessed poor biocompatibility and were not approved for *in vivo* use [161]. Recently mixed micellar systems consisting of simple block copolymer methoxy poly(ethylene glycol)-b-poly(D,L-lactide) (mPEG-b-PLA) and temperature sensitive polymer methoxypoly(ethylene glycol)-b-poly(N-n-propylacrylamide-co-vinylimidazone) (mPEG-b-P(NnPAAm-co-VIm) have been synthesised [161]. It was reported that the mixed micellar systems successfully encapsulated the anticancer agent doxorubicin. *In vitro* cytotoxicity was reduced when exposing human cervical epithoidal carcinoma (HeLa) cells to the formulation, this indicated increased biocompatibility [161]. Confocal microscopy was used for cellular visualisation of the mixed micelle fate *in vitro*. The mixed micellar system showed increased drug in the cytoplasm after 1 h in comparison with the free drug [161]. Lo and colleagues concluded that this system showed great potential for intravenous delivery of hydrophobic drugs [161].

pH responsive micelles are also useful in cancer treatment. The external pH of tumour tissue cells have been reported to have a lower pH (6.75) than normal healthy tissue cells (pH 7.4) [155,156]. pH sensitive micelles are formed by conjugation of drugs into the monomer blocks of polymeric micelles (Fig. 19) [91].
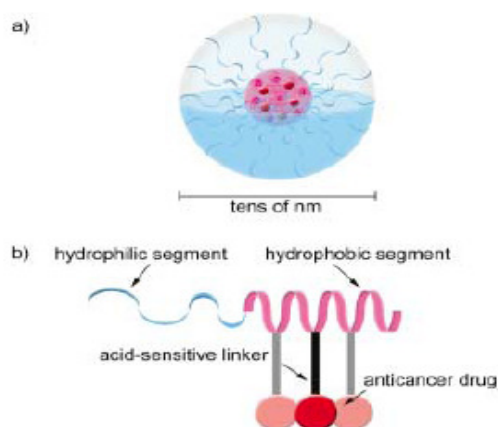
Figure 19. Representation of A) pH responsive polymeric micelle showing B) drug conjugation through acid sensitive linker to amphiphilic polymer [162].

The drug is attached via an acid cleavable bond [163]. These micelles disrupt upon acidic pH ranges hence releasing their payload [163]. Furthermore, if the polymeric nanostructures enter the cell by endocytosis, the micelles will become localised within the endosomes or lysosomes which have pH 5 - 5.5 [156,163]. The release of drugs from the

endosomes and lysosomes into the cytosol is important to achieve high therapeutic effect and thus killing the cancer cells [155].

pH sensitive micelles of poly(ethylene glycol)-pol(aspartate hydrazide) (PEG-p(Asp-Hyd) were synthesised [91,162]. It was reported that 75 – 80 % hydrazide substitution onto the polymer gave the optimal drug release when loaded with anticancer agent Adriamycin [162]. The micelles were shown to undergo disruption at lower pH's [162]. Confocal microscopy was used to determine cellular localisation, the micelles were trapped inside the lysosomes where they were 'programmed' to disrupt through hydrolysis of the hydrazone linker [162]. The results indicated that PEG-p(Asp-Hyd) had great potential for the transport and targeting of cancer therapies.

Gu and colleagues fabricated comb shaped polymers with hydrophobic cholic acid groups grafted onto a poly(L-lysine) backbone [164]. They then grafted hydrophilic poly(ethylene glycol) groups onto the comb shaped polymer via benzoic imine bonds to form poly(ethylene glycol)-g-poly(L-lysine)-g-cholic acid [164]. Benzoic imine bonds are known for their pH responsive nature [164]. The membrane disruptive ability of the nano self-assemblies was investigated using a haemolysis assay at the extracellular pH of solid tumours (pH 6.0) and physiological pH (pH 7.4) [164]. Gu found that at pH 6 the self-assemblies exhibited a large increase in haemolytic activity towards the red blood cells in comparison with pH 7.4, from 37.5 % to 90 % haemolysis at 0.75 mgmL^{-1} respectively [164]. Gu concluded that the micelles showed a pH responsive nature with a higher degree of membrane disruption occurring at extracellular pH's hence showing potential for drug delivery to tumours with intracellular transport [164].

Thus far all the amphiphilic polymers mentioned have been used to passively target cancerous tumours through the phenomenon known as the enhanced permeability and retention effect (EPR) (Fig. 20). Cancerous tissue multiplies at an increased metabolic rate in comparison with normal tissues resulting in the formation of tumours. As a result of the rapid growth rate the blood capillaries in the tumours are under developed forming defective, dilated or 'leaky capillaries' [165]. The tumour tissues also experience poor lymphatic drainage [165]. Polymeric nano-particles from 10 – 500 nm are capable of entering the highly permeable blood capillaries which supply the rapidly growing cancerous site [156,165,166]. Once inside the capillaries they accumulate and are retained in the tumour as a result of the poor lymphatic drainage [166]. The accumulation of drug loaded nano particles in tumour tissue allows for successful passive targeting of anticancer drugs [165]. This however does not occur in normal tissue as the blood vessels are well formed and non porous.
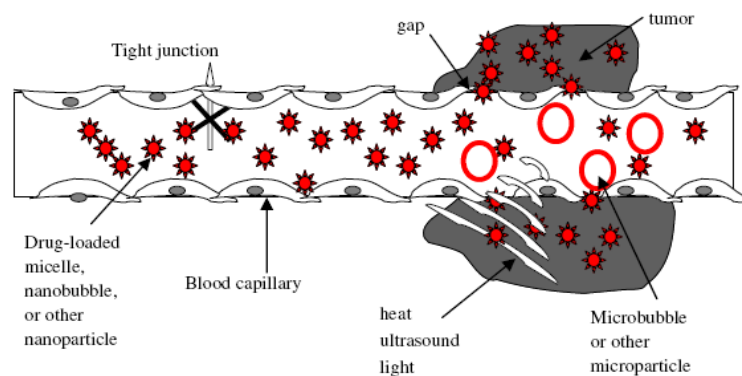
Figure 20. Schematic diagram of passive tumour targeting of drug loaded nano-particles through the permeable tumour vasculature. Heat and pH are used to trigger destabilisation of micelle and drug release into tumour [156].

Amphiphilic polymers can be actively targeted to specific sites by conjugating recognition moieties for receptors or components which are upregulated in the cancerous cells [167]. Ligands specific to receptor sites that are over expressed in cancer cells can be attached to amphiphilic polymers e.g. folate, galactose [156,167]. Folate receptors are often used for active targeting of cancerous tumour sites [156,168,169]. Prabaharan and colleagues synthesised a folate conjugated amphiphilic polymer based on Boltorn®H40 a hyperbranched aliphatic polyester called Boltorn – poly(L-lactide)-b-methoxy poly(ethylene glycol) / folate conjugated poly(ethylene glycol) (H40-PLA-b-MPEG/PEG-FA) [170]. They incorporated anticancer therapeutic doxorubicin into the polymeric micelle which showed prolonged release of up to 40 h. *In vitro* analysis was carried out on 4T1 mice mammalian carcinoma cell lines [170]. The results showed that the folate conjugated polymer exhibited a greater cytotoxic effect on the cells than the non-targeted polymer [170]. They suggested that this was perhaps due to folate receptor - mediated endocytosis improving uptake into the cells [170].

1.3.6. *Fluorescent polymers*

Fluorescent polymers have emerged in recent years as a new class of multifunctional smart delivery systems. Incorporation of fluorophores such as pyrene or naphthalene into monomer units of amphiphilic polymers results in the nano aggregates formed possessing inherent fluorescence [171,172]. Fluorescent polymers have a range of potential applications in medicine, e.g. fluorescent probes for cell labelling and visualisation of cell localisation, bacteria detection, *in vivo* tracer for brain research [171,173]. Previously, fluorescent dyes were used to tag well established polymeric delivery systems for *in vitro* and *in vivo* visualisation [173]. However, the presence of these dyes could affect the physical and chemical properties of the self assemblies altering tissue interactions and cytotoxicity [173]. To avoid such issues inherently fluorescent amphiphilic polymers have been developed.

Recently, Suchao-in and colleagues have reported the synthesis of a novel amphiphilic thermoresponsive, pH responsive and inherently fluorescent graft polymer [174]. The polymer consists of thermosensitive poly(N-isopropyl-acrylamide-co-N-vinyl carbazole) monomers conjugated to pH responsive poly(dimethylamino) ethyl acryate (PNIPPAm-co-PNVC)-b-PDMAEA) (Fig. 21) [174]. Carbazole compounds have been investigated and shown to possess intrinsic fluorescent properties [174,175]. Suchao-in concluded that the successful fabrication of the fluorescent, pH thermo responsive nature of the polymer will be of great importance for the successful imaging of therapeutics [174]. This could be an important stepping stone to fully understand the *in vivo* fate of drug targeted molecules.
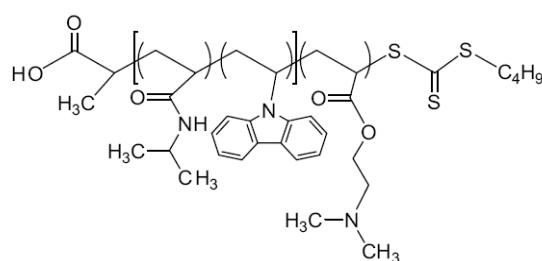
Figure 21. Chemical structure of (PNIPPAm-co-PNVC)-b-PDMAEA) [174].

Wu developed a fluorescent galactosylated polymer for targeted drug delivery to liver cells. The polymer consisted of galactose-polycaprolactone-g-dextran-fluorescein isothiocyanate (Gal-PCL-g-Dex-FTIC) [176]. Galactose is a common recognition moiety for liver cells. Galactose selectively binds onto the ASGPr on HEPG2 cell surfaces allowing active targeting of cells (Fig. 22) [176].
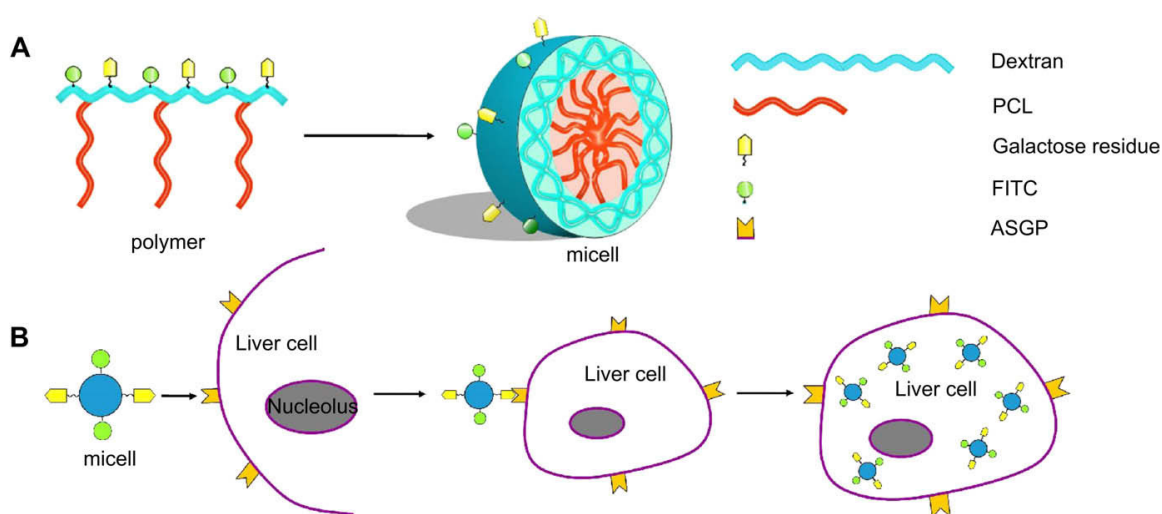
Figure 22. Schematic diagram of A) Gal-PCL-g-Dex-FTIC nano aggregates and B) mechanism of liver tissue targeting via receptor mediated transport [176].

The polymers were found to form stable self assemblies in aqueous environments both *in vitro* and *in vivo* systems [176]. Confocal microscopy enabled cellular localisation through fluorescent imaging of the FTIC moiety. The aggregates were found to accumulate within the liver cells of mice, which was demonstrated using fluorescence imaging of the liver tissue. It was concluded that the polymeric nano aggregates showed great potential for liver targeting drug carriers [176].

1.3.7. *Commercial Success of Polymeric Micelles*

The major frontrunner in the field of polymeric micelles to date is the discovery of poloxamer also known as Pluronic®. Pluronic is the brand name of a triblock copolymer used as an excipient for the delivery of hydrophobic drugs. The Pluronic structure comprises of hydrophilic poly(ethylene oxide) (PEO) and hydrophobic poly(propylene oxide) (PPO) monomers, usually in the PEO-PPO-PEO form. The Pluronic polymer forms unimers below the critical aggregation concentration and forms polymeric micelles in the aqueous environment above this concentration [177]. The micellar structure protects the active ingredient from degradation *in vivo* enabling successful journey to its target destination. Pluronics has attracted a lot of attention because of their low toxicity in the body and the ability to solubilise biologically active lipophilic substances [178,179].

Pluronics are available in many forms, with different ratios of the hydrophobic to hydrophilic monomers and molecular weight. Each variation possesses slightly different characteristic properties. Pluronic polymers have a unique nomenclature whereby the name starts with an F (solid),P (paste) or L (liquid) depending on their physical properties. The letter is followed by three numbers, the first two numbers when multiplied by 100 give the estimated molecular weight of the poly(propylene oxide) polymer, the final digit when multiplied by 10 gives the % poly(ethylene oxide) content for example P105 equates to poly(propylene oxide) mass of 1,000 gmoL^{-1} with 50% poly(ethylene oxide) content.

Husseini used an ultrasonic chamber with real time fluorescence detection to measure acoustic release of doxorubicin (DOX) and its paramagnetic analogue ruboxyl (Rb) from Pluronic P-105 in aqueous solution [180]. The ultimate goal was to produce a formulation which could enhance drug release at the tumour sites. The use of ultrasound to enhance the drug permeability of cell membranes had been previously reported [181,182]. Husseini observed that the released drug was re-encapsulated in between the pulses of the ultrasound by the dynamic equilibrium theory [180]. This led to the hypothesis that upon separation of the sonicated volume, the non-extravasated drug would re-encapsulate in the polymeric micelles and circulate in its encapsulated form, preventing drug interaction with healthy tissues and cells [177,178,180]. This work showed Pluronic's ability to control the release of the encapsulated drug.

Pluronics have helped to overcome the phenomenon known as multidrug resistance (MDR) in tumour cells. This phenomenon arises when tumour cells have the ability to develop a resistance to the cytotoxic drugs which are designed to destroy them. They also develop cross-resistance to other compounds which are structurally and functionally unrelated [183]. Cells treated with the anticancer agent paclitaxel often develop MDR [184]. Paclitaxel is an anticancer agent which requires site specific delivery using an excipient or vehicle due to its cytotoxic nature causing adverse side effects. Wang and colleagues loaded the paclitaxel drug into Pluronic P-105 and L-101 polymeric micelles, the polymers were modified with folic acid to enable binding to the folate receptors on the tumour cells [184]. From the results it was concluded that the combined mechanisms of folate-mediated active internalization and Pluronic-mediated overcoming MDR may be beneficial in the treatment of MDR solid tumours [184].

The major problem encountered with Pluronic polymers is the significantly high CMC value. This has resulted in the polymeric micelles dissociating at low concentrations and the therapeutic agent which they encapsulated being prematurely released [185]. Cross-linking of the Pluronic structure has led to further advancement within the drug delivery area.

Yang and colleagues, carried out research into the possibility of forming cross linkages within the polymer structure which would decrease the CMC [186]. They successfully cross linked the outer shells, by converting the two terminal alcohols on the Pluronic-L121 to aldehydes. Diamines were then used to form a bridge between the aldehyde terminals [186]. The micelles formed were spherical, they were found to possess a much lower CMC value (5.0×10^{-4} % wt) than that of the unmodified L121 polymer (5.0×10^{-3} % wt) enhancing the stability of the micelles [186,187]. The cross-linked micelles were found to be less cytotoxic than their unmodified counterparts when treated on human foreskin fibroblast (Hs68) cells [186]. The unmodified micelles also appeared to be taken up quicker and in greater abundance than the cross-linked micelles when viewed using a fluorescent microscope, however the CMC for the unmodified micelles was much higher resulting in dissociation upon dilution [186].

1.4. Aims and Objectives

The aim of this project was to fabricate novel amphiphilic comb shaped polymers which form polymeric self assemblies capable of encapsulating hydrophobic drugs. Fourteen amphiphilic PAA polymers were synthesised to determine the effect of hydrophobic pendant group, level of molar grafting and hydrophilic modification on physiochemical and biological properties of these polymers. The hydrophobic pendant groups used were aromatic structure which possess inherent fluorescent properties. Structural characterisation of the modified polymers was carried out using elemental analysis,

nuclear magnetic resonance (NMR) and fourier transform infrared spectroscopy (FTIR). The nano aggregates formed in aqueous environments were characterised by using methyl orange as a hydrophobic probe and surface tension measurement. Photon correlation spectrometry (PCS) was used to determine hydrodynamic radius of the nano aggregates. Drug solubilisation capacity was investigated using five model hydrophobic drugs: propofol, prednisolone, griseofulvin, etoposide and a novel anti cancer agent BNIPDaoct. The optimal formulations were imaged using transmission electron microscopy (TEM) and sized using PCS. *In vitro* drug release studies and stability studies were carried out and analysed by high performance liquid chromatography (HPLC). Biological characterisation was carried out *in vitro* to determine the haemolytic and cytotoxic effect of the polymers. Confocal microscopy allowed visualisation of the cellular localisation of the formulations. *In vivo* studies were also carried out to determine the ability of the formulations to enhance bioavailability of hydrophobic drugs.

Chapter Two

Synthesis and Characterisation of
polymer and modified polymers

2.1.Introduction

Amphiphilic polymers have been explored in recent years as one of the promising delivery systems for hydrophobic drugs [72]. Comb shaped amphiphilic polymers are formed by grafting a 'pendant' group onto a homopolymer backbone, whereby one group is hydrophilic and the other is hydrophobic [188,189]. Here a comb shaped amphiphilic polymer was synthesised by introducing hydrophobic group onto a water soluble poly(allylamine) (PAA) backbone.

$$\left[\begin{array}{c} CH_2 - \underset{\underset{NH_2}{|}}{\underset{\underset{|}{CH_2}}{CH}} \end{array}\right]_n$$
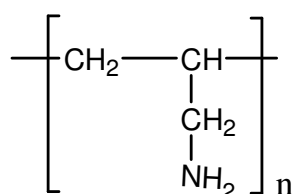
Figure 23. Chemical Structure of poly(allylamine) (PAA).

Poly(allylamine) (PAA) (Fig. 23) is a cationic polymer which is relatively non toxic, making it an ideal biomaterial to be explored in drug delivery [176,190] The cross-linked PAA is available clinically as an oral phosphate binder [176,190]. However, modification of PAA to form amphiphilic polymers to date has not been explored for biomedical application [121,176]. Poly(allylamine) can undergo chemical modification via its primary amine functional groups enabling grafting of various hydrophobic moieties by a simple nucleophilic substitution reaction. Thompson and colleagues have reported that varying the hydrophobic groups on the PAA backbone has a significant impact on the polymer properties and the self-assemblies formed in the aqueous environment [76]. To date no reports of aromatic hydrophobic groups attached to comb shaped PAA polymers have been reported.

In this study cholesteryl, 9-fluorenylmethoxy (Fmoc), dimethylamino-1-naphthalenesulfonyl (Dansyl) and naphthalene moieties will be grafted onto the PAA backbone. Cholesterol is a commonly occurring sterol within the body which regulates membrane fluidity. It plays an important part in the spontaneous association of molecules within biological pathways [191]. Yusa and colleagues reported the copolymerization of sodium 2-(acrylamido)-2-methylpropanesulfonate with cholesteryl methacrylate (CholMA) and cholesteryl 6-methacryloyloxyhexanoate (Chol-C5-MA). They found that even at low cholesteryl grafting ratios, the polymers still possessed a strong tendency for self assembly [192]. Xu and colleagues also reported that the use of cholesterol as a hydrophobic cap on poly(2-methacryloyloxyethyl phosphorylcholine) acted as a biomimetic and improved cytotoxicity of the polymer alone [191]. Fmoc, Dansyl and Naphthalene are common aromatic moieties with similar planar architectures. These

compounds possess inherent fluorescent properties due to the presence of the conjugated aromatic ring systems. The attachment of aromatic groups with fluorescent properties eliminates the need to attach fluorescent tags in later biological characterisation, thus giving a more accurate representation of its *in vivo* fate. However, the presence of the fluorescent tag may alter the physical properties and cytotoxicity of the polymer [173].

Wang previously found that the molar grafting level of hydrophobic pendant groups significantly influenced the physical properties of the polymer [78]. Cholesterol-PAA (Ch-PAA), 9-Fluorenylmethoxy-PAA (Fmoc-PAA), Dimethylamino-1-naphthalenesulfonyl-PAA (Dansyl-PAA) and Naphthalene-PAA (Naphth-PAA) amphiphilic graft polymers of 5 % and 10 % molar ratio (monomer: hydrophobic group) were synthesised as described below. The structure of purified PAA (15 kDa) is shown in Fig.23.

It has been previously reported that hydrophilic substitution such as addition of poly(ethylene glycol) (PEG) or quaternary ammonium moieties onto amphiphilic polymers increases their solubility, bioavailability and safety profile [122,125]. Hence all the hydrophobic modified polymers were subsequently quaternized as described below (2.2.2.1.4). Characterisation of the novel polymers was carried out using a number of analytical techniques including elemental analysis, nuclear magnetic resonance (NMR) and fourier transform infrared spectroscopy (FTIR).

2.1.1. *Elemental Analysis*

Elemental analysis is a useful tool in analytical chemistry. It allows the quantitative measurement of elements in a sample [193]. A schematic diagram of an Elemental Analyser can be seen in Fig.24.
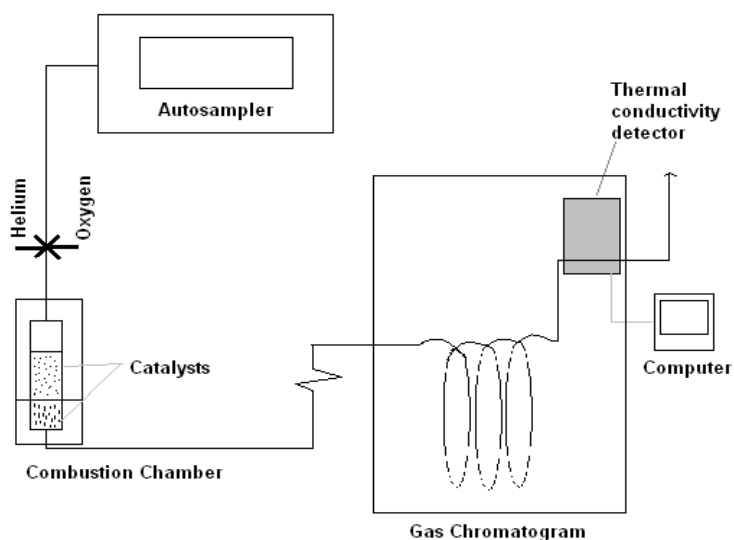
Figure 24.Schematic diagram of an Elemental Analyser.

The analysis can be carried out on solid, liquid or gas samples [194]. The most common type of elemental analysis is C, H, N analysis, where the composition by the mass of carbon, hydrogen and nitrogen in a sample is determined [194]. The analysis is carried out by the combustion (up to 1000 ºC) of the sample in oxygen under controlled conditions in the presence of a catalyst [194,195]. The gases formed (CO_2, H_2O, N_2) are separated by gas chromatography and measured by thermal analysis [195]. The composition of halogen (X, such as Cl^- or I^-) is measured as HX and the sulphur content is measured as SO_2. For the purposes of this study C, H, N, X and S analysis was carried out.

2.1.2. *Nuclear Magnetic Resonance*

Nuclear magnetic resonance is one of the most powerful analytical tools used to elucidate the structure and dynamics of unknown organic compounds (Fig.25) [194,196,197].

When the protons within the nucleus of a particular molecule is placed inside a magnetic field, the nucleus vibrates in which is characteristic to the atom. The frequency of the resonance occurring is proportional to the strength of the magnetic field [198]. Protons in a molecule resonate at slightly different frequencies when they exist in different environments resulting in distinct chemical shifts on the NMR spectra [194,196]. The chemical shift is measured in parts per million (ppm, or δ) and is used to determine structural information about the molecules in a sample [194].
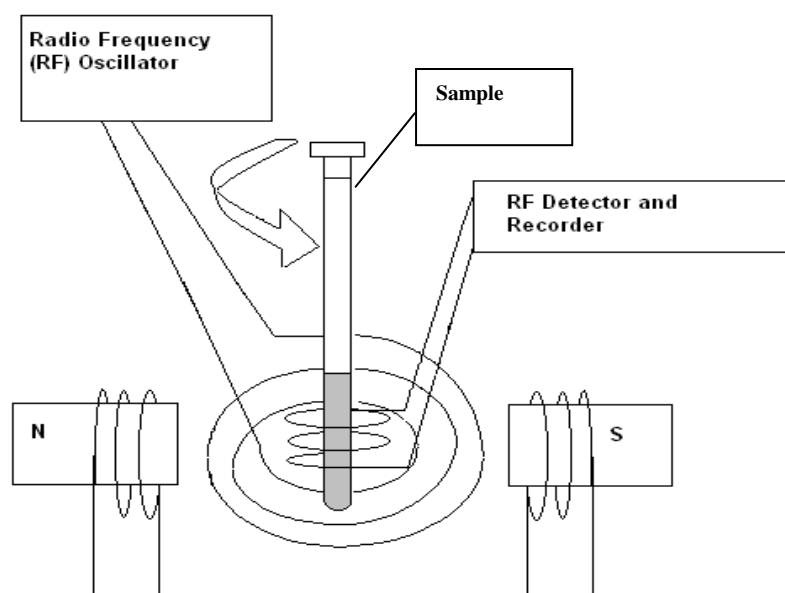
Figure 25.Schematic diagram of NMR spectrometer.

Chemical shift arises due to electronegative atoms (e.g. O, Cl) within the molecule having the ability to de-shield the nucleus from the magnetic field, thus influencing their nuclear resonance frequencies. Deshielded protons appear downfield in the spectra when compared to shielded protons as they require less applied magnetic field to change their

spin state. This phenomena is due to the removal of the electron 'cloud' from the nucleus allowing direct impact of the magnetic field on the protons. The chemical shift allows the NMR signals to be distinguished by functional group [194,198].

An additional effect on the spectral appearance is observed if neighbouring atoms within the molecule also possess spin. The spin of nearby atoms can affect the magnetic environment of the nucleus in question. This is called spin-spin coupling [199]. Typically a singlet signal is observed in the spectra if there is no influence from the nearby atoms. However, if spin-spin coupling occurs a duplet, triplet or multiplet will be present (depending on the surrounding environment) [199].

2.1.3. *Fourier Transform Infrared Spectroscopy (FTIR)*

Fourier Transform Infrared Spectroscopy (FTIR) is a more advanced form of IR spectroscopy. Traditionally Infrared spectroscopy (IR) was used to identify the functional groups in a chemical compound hence aiding with the elucidation of its molecular structure. The samples used in FTIR spectroscopy can be in solid, liquid or gas form [194]. IR spectroscopy works on the basis that molecules possess specific frequencies arising from the internal vibrations in the bonds of the functional groups they possess [194,198,200]. When a beam of IR radiation (200-4000 cm^{-1}) is passed through a compound, it absorbs radiation at frequencies associated to its vibrational frequency and the remaining frequencies are transmitted [194,201]. Each chemical structure has different characteristic vibration and hence its identification is possible through examination of its unique IR spectrum [194].

In FTIR however the radiation applied to the sample is passed through an interferometer instead of a monochromator [194]. In this case the spectrum is indirectly measured using its interferogram. An interferometer combines two waves together and as a result of their combination and amplification, the data can be digitalised to produce a spectrum [201]. This results in an improved resolution of the peaks and a higher energy flow [200]. The signal/noise ratio is also increased and the measurement times are reduced making it a very powerful and sensitive method [194].

2.1.4. *Aims and Objectives*

The polymers were characterised to ensure the correct structures were synthesised. Structural characterisation was carried out by elemental analysis, nuclear magnetic resonance (NMR) and fourier transform infrared (FTIR) spectroscopy. These techniques were used to confirm the hydrophobic groups attachment onto the PAA backbone and the presence of the quaternary ammonium ions.

2.2. Materials and Methods

2.2.1. *Materials used*

Material	Supplier
Poly(allylamine) Hydrochloride (ave.Mw=15 kDa)	Sigma-Aldrich Co., UK
Cholesterol Chloroformate	Sigma-Aldrich Co., UK
5-Dimethylamino-1-naphthalenesulfonyl chloride	Sigma-Aldrich Co., UK
1-Naphtholyl chloride	Sigma-Aldrich Co., UK
9-Fluorenylmethoxy carbonyl chloride	AlfaAesar, UK
Triethylamine	Sigma-Aldrich Co., UK
Methyl iodide	Sigma-Aldrich Co., UK
Sodium iodide	Sigma-Aldrich Co., UK
Sodium hydroxide	Fisher Scientific, UK
Organic solvents	Fisher Scientific, UK
Amberlite - 96 resin	Fluka, UK
Dialysis tubing membranes	Medicell International Ltd, UK
Deuterated Methanol	Cambridge Isotope Laboratories Inc., USA

2.2.2. *Methods*

2.2.2.1. *Synthesis of modified polymers*

2.2.2.1.1. *Conversion of PAA to free base*

PAA-HCl (10 g) salt was dissolved in doubly distilled water. Sodium hydroxide pellets (8 g) were added slowly until pH 13 was achieved. The mixture was stirred for 1 h. The polymer was exhaustively dialysed against water using 7000 Dalton visking tubing membrane for 24 h with at least 6 changes of 5 L distilled water (at 2 h intervals for the first 8 h) in this time. The dialysate was freeze-dried on a 48 h cycle to obtain a cotton like white solid (4.8 g, 78 % yield) [76].

2.2.2.1.2. *Synthesis of 5 % Cholesterol-PAA (Fig. 26)*

Synthesis was carried out as described by Thompson and colleagues [76]. Purified PAA (2 g) was dissolved in 100 mL chloroform:methanol (1:1 v/v). Triethylamine (2 mL) was added and the mixture was stirred for 0.5 h. Cholesteryl chloroformate (0.6678 g) was dissolved in 20 mL chloroform:methanol (1:1 v/v), and then added drop wise to the polymer solution over 2 h at 37 °C. The mixture was then left stirring for 24 h at 37 °C.

After 24 h the solvent was removed using a rotary film evaporator, and the residue washed with diethyl ether (3 x 100 mL). The viscous liquid residue was dissolved in doubly distilled water (50 mL) and the solution was exhaustively dialysed (molar weight cut-off = 7 kDa) against 5 L doubly distilled water for 24 h (6 water changes). The solution was freeze-dried for 48 h and the product was recovered as white cotton like solid (2.2 g , 79 % yield).
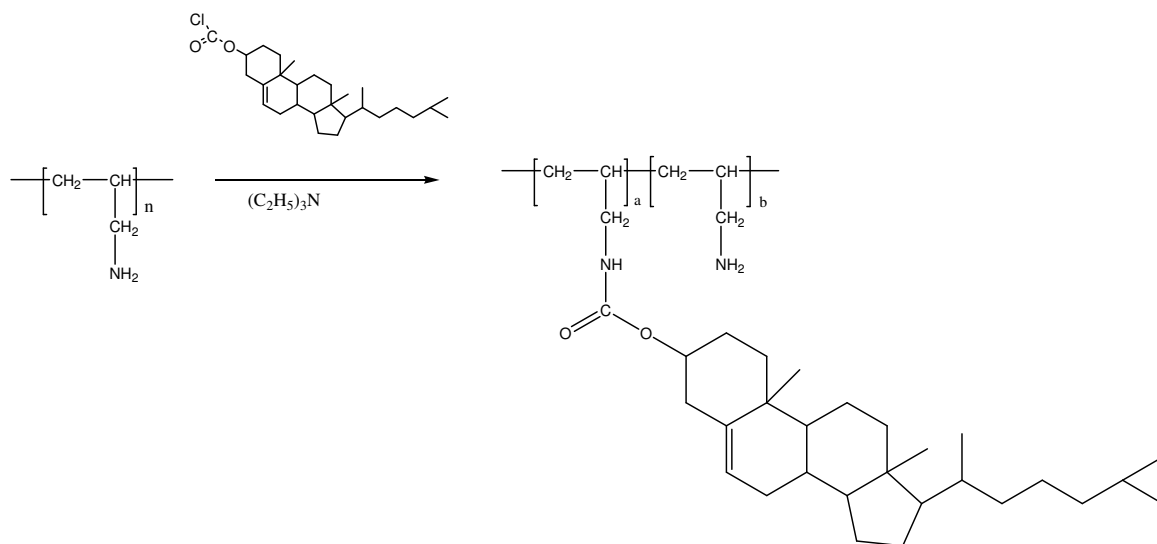
Figure 26. Chemical synthesis of Cholesterol-PAA (Ch-PAA).

2.2.2.1.3. *Synthesis of Fmoc-PAA, Dansyl-PAA and Naphth-PAA*

Purified PAA (2 g) was dissolved in 150 mL dioxane:water (1:1 v/v) with stirring, sodium carbonate was added (in 5% or 10% mole ratio with the hydrophobic moiety). The appropriate mass (0.1855 g for 5 %, 0.371 g for 10 %) based on the molar ratio of 9-Fluorenylmethoxy carbonyl chloride (Fmoc chloride) was dissolved in 20 mL dioxane. The mixture was then added drop wise to the polymer solution over 2 h at 0 °C. The final solution was left stirring for 4 h at 0 °C followed by 8 h at room temperature. After evaporation of solvents, the viscous liquid residue was washed three times with 100 mL diethyl ether and subsequently dissolved in doubly distilled water and exhaustively dialysed (molar weight cut-off = 12 - 14 kDa) against water (5 L) for 24 h (with 6 water changes). The solution was freeze-dried for 48 h and the product was recovered (Fig. 27 a).

38

The above method was repeated with 5-Dimethylamino-1-naphthalenesulfonyl chloride (Dansyl chloride - 0.472 g, 5 % and 0.847 g, 10 %) and 1-Naphthoyl chloride (239 µL, 5 % and 477 µL, 10 %) (Fig. 27 b & c). The Fmoc-PAA (2.0 g, 79 % yield) and the Naphth-PAA (1.8 g, 81 %) had a white cotton like solid appearance while the Dansyl-PAA (1.9 g, 76 %) had a yellow cotton like fluffy appearance.
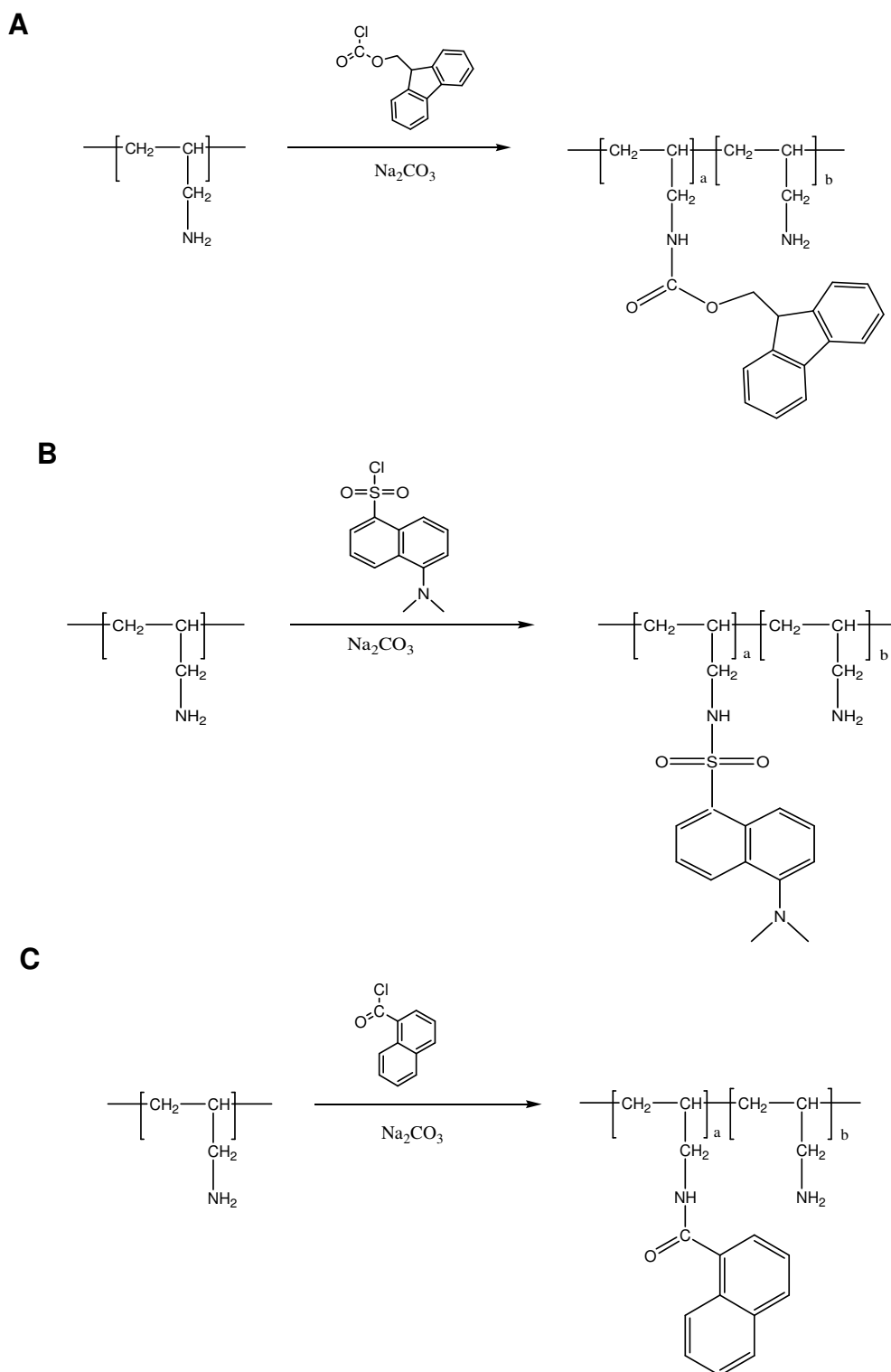
Figure 27. Chemical synthesis of A) Fmoc-PAA, B) Dansyl-PAA and C) Naphthalene-PAA (Naphth-PAA).

2.2.2.1.4. *Quaternization of Modified Polymers*

This method was an adaptation of Domard and colleagues work [202] and had been previously reported [3,76].

The modified polymer (0.6 g) was dissolved in methanol (100 mL) with stirring. Sodium hydroxide (0.58 g) and sodium iodide (0.25 g) were added to the solution, followed by methyl iodide solution (3.5 mL). The mixture was left stirring under nitrogen at 36 ºC for 3 h. The product was precipitated out by the addition of diethyl ether (400 mL) and left overnight. The ether was then decanted off. The precipitates were dissolved in 40 mL ethanol:water (1:1 (v/v)) and the solution was dialysed (molecular weight cut-off = 12 – 14kDa) against water for 24 h with 6 water changes. A column of Amberlite 176 resin was washed with 2 M hydrochloric acid solution followed by deionised water until a neutral pH was established. The dialysate was then passed through the column and the eluant was collected and freeze-dried. The general reaction for the quaternization reaction is shown in Fig. 28. The 1º amine groups left on the PAA backbone are converted to quaternary ammonium ions in a nucleophilic substitution reaction.
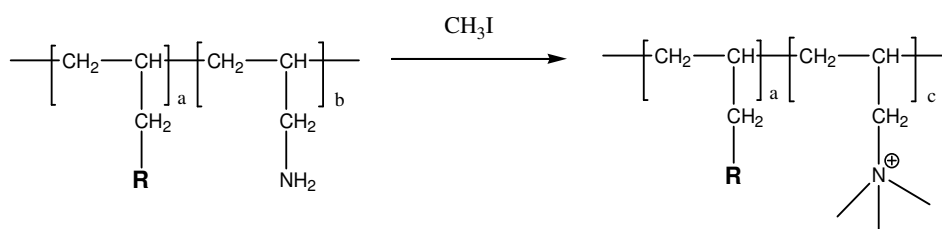
Figure 28. Quaterisation of hydrophobic modified PAA where R= Cholesterol, 9-Fluorenylmethoxy carbonyl, 5-Dimethylamino-1-naphthalenesulfonyl or Naphthalene.

Table 1. Molar feeds of modified polymers.

Polymer	Initial monomer: hydrophobic pendant group molar feed ratio	Type of hydrophobic pendant group	Quaternization (Q)
Ch_5	1:0.05	Cholesterol	No
QCh_5	1:0.05	Cholesterol	Yes
$Fmoc_5$	1:0.05	Fmoc	No
$QFmoc_5$	1:0.05	Fmoc	Yes
$Fmoc_{10}$	1:0.10	Fmoc	No
$QFmoc_{10}$	1:0.10	Fmoc	Yes
$Dansyl_5$	1:0.05	Dansyl	No
$QDansyl_5$	1:0.05	Dansyl	Yes
$Dansyl_{10}$	1:0.10	Dansyl	No
$QDansyl_{10}$	1:0.10	Dansyl	Yes
$Naphth_5$	1:0.05	Naphthalene	No
$QNaphth_5$	1:0.05	Naphthalene	Yes
$Naphth_{10}$	1:0.10	Naphthalene	No
$QNaphth_{10}$	1:0.10	Naphthalene	Yes

*Nomenclature based on molar grafting level of PAA for example Ch_5 = 5 % cholesteryl grafting

2.2.2.2. *Characterisation of Polymers*

2.2.2.2.1. *Elemental Analysis*

2.2.2.2.1.1. *Simultaneous determination of carbon, hydrogen and nitrogen content of polymers*

Modified polymer samples were analysed for their abundance of carbon, hydrogen, nitrogen and halogen. Dansyl grafted polymers were also analysed for the abundance of sulphur. Samples (1 mg) were analysed using a Perkin Elmer series 2 elemental analyser (Perkin Elmer, UK). Sample absorbance values were compared to a standard of acetanilide for determination of elemental abundance.

2.2.2.2.1.2. *Determination of halogen content of polymers*

The polymer (20 mg) was combusted in a flask containing pure O_2, H_2O_2 and KOH for 0.5 h. The flask was then filled with distilled water and cooled back down to room temperature. Ethanol was added before acidified with HNO_3. The final solution was titrated against mercuric nitrate with diphenyl carbazone indicator. The percentage of halogen was determined relative to sample weight. The sulphur content was analysed using similar techniques with the level of sulphur dioxide quantified by measurement relative to sample weight,

2.2.2.2.2. *Nuclear magnetic resonance spectroscopy (NMR)*

^{1}H NMR was carried out on all modified polymers in deuterated methanol (MeOD) (15 mgmL^{-1}) at 25 ºC, using a Bruker 400MHz Ultrashield NMR spectrometer (Bruker BioSpin, Germany). Sonication of samples using a Soniprep 150 (MSE Ltd, UK) was undertaken for 10 mins to ensure that the polymers were completely dissolved in the deuterated methanol before analysis.

2.2.2.2.3. *Fourier transform infrared spectroscopy (FTIR)*

FTIR analysis of all the polymers was carried out with a Perkin Elmer (Spectrum BX, UK), fitted with a diamond powder tip. The polymers (5 mg) were placed under the diamond tip and 20 scans were run following a background correction.

2.3. Results

Polymer synthesis was performed in accordance to Table 1 (pg. 48). Table 2 (pg. 51) shows the percentage yield of each modified polymer. The yield was calculated as follows:

For hydrophobic substitutions:

% Yield = Product weight / Weight of reactants X 100 %

E.g. For Ch_5

= [Weight of Ch_5 / Weight of PAA + Cholesterol Chloroformate] X 100 %

For hydrophilic substitutions:

% Yield = Product weight / Weight of reactants X 100 %

E.g. For QCh_5

= [Weight of QCh_5 / Weight of Ch_5 and CH_3I] X 100 %

The percentage yield was high for all the hydrophobic modified polymers ranging from 60 – 89 %. The percentage yield much lower however for the quaternized polymers, this was due to the methyl iodide being added in excess.

Table 2. Percentage yield of modified polymers showing mean and standard deviation.

Polymer	% Yield (mean ±SD (n≥3) or individual values (n ≤2))	Number of batches synthesised
PAA	78.26 (8.896)	11
Ch_5	79.2 (10.376)	4
QCh_5	17.6 (2.859)	3
$Fmoc_5$	79.2 (6.554)	4
$QFmoc_5$	15.4/16.4	2
$Fmoc_{10}$	74 (72/86)	2
$QFmoc_{10}$	16.7/17.2	2
$Dansyl_5$	76/76	2
$QDansyl_5$	17.6	1
$Dansyl_{10}$	71.5 (3.811)	3
$QDansyl_{10}$	82.5	1
$Naphth_5$	81/89	2
$QNaphth_5$	16	1
$Naphth_{10}$	60/73	2
$QNaphth_{10}$	14.3	1

2.3.1. *Elemental analysis*

The PAA polymer backbone and the novel modified polymers synthesised were analysed to determine their constituent elements. The main objective when looking at the elemental analysis results for the PAA and modified polymers was to determine if correct structure had been synthesised. However, it was also useful to look at the halogen content of the samples. This would establish whether any unreacted materials were still present in the sample and hence confirming its purity. (Elemental analysis is unable to distinguish between specific halogen atoms, however only Cl^- ions were present in the hydrophobic modifications and Cl^- and I^- ions were present in the hydrophilic modifications.

Table 3 (pg. 55) shows the total halogen content in the hydrophobic grafted polymers (and PAA backbone) to be less than 5 %. It was therefore assumed that the majority of Cl⁻ ions had been successfully converted to NaCl and that the salt molecules had been removed during the dialysis step of the synthesis. The quaternized polymers showed higher chloride ion content, this was due to the final step in the synthesis where the dialysate was passed through an ion exchange resin to exchange iodide with chloride ions.The degree of hydrophobic and hydrophilic modification were determined using simple calculations as follows:

PAA

Divide the % element obtained in elemental analysis (Table 3) by its molecular weight.

	C	:	H	:	N
	57.07/12	:	12.27/1	:	21.77/14
=	4.76	:	12.27	:	1.56
=	3.05	:	7.87	:	1

The above results from the elemental analysis confirm the predicted structure of the monomer unit with 3 C's, 7 H's and 1 N atom (Fig. 23, pg. 38).

Ch_5

	C	:	H	:	N
	63.35/12	:	13.80/1	:	16.57/14
=	5.28	:	13.80	:	1.18
=	4.46	:	11.66	:	1

Deduct PAA values

=	1.41	:	3.79	:	0

For every 1 mole of nitrogen present there are 1.41 extra moles of Carbon from PAA

Chemical formula of Cholesteryl formate = $C_{28}H_{45}O_2$

Every mole of nitrogen has 1.41/28 = 0.050 moles of cholesteryl group. Cholesteryl attachment occurs at the 1 º amine of the PAA monomer.

Therefore:

0.05 X 100 % = 5.0 % mole of PAA monomer unit has been modified with cholesteryl group.

The following calculation was based on the assumption that the remaining primary amines on the PAA backbone after quaternization were fully methylated and that no secondary or tertiary intermediates were formed, as these are the energetically favourable intermediates before complete methylation will occur [3]. However, intermediates are unlikely as methyl iodide was added in excess in the reaction.

QCh$_5$

C	:	H	:	N
46.42/12	:	10.20/1	:	8.70/14
= 3.87	:	10.20	:	0.62
= 4.23	:	16.43	:	1

Deduct Ch$_5$ values

= 1.77	:	4.76	:	0

For every 1 mole nitrogen there is 1.77 moles extra carbon.

Since every nitrogen requires 3 carbon for quaternization to occur:

1.77/3 X 100 % = 59 % mole per PAA monomer has been quaternized.

Table 3.Elemental analysis results for hydrophobic and hydrophilic modification of PAA. Showing % C,H,N,Cl and S present with mean and standard deviation.

Polymer	Carbon (mean ±SD (n≥3) or range (n ≤2))	Hydrogen (mean ±SD (n≥3) or range (n ≤2))	Nitrogen (mean ±SD (n≥3) or range (n ≤2))	Chlorine (mean ±SD (n≥3) or range (n ≤2))	Sulphur (mean ±SD (n≥3) or range (n ≤2))	% mole grafting per PAA monomer (mean ±SD (n≥3) or range (n ≤2))
PAA	57.21 (3.439)	12.16 (0.818)	22.52 (1.725)	0.73 (0.280)	-	-
Ch_5	59.58 (2.758)	12.12 (0.824)	15.71 (1.606)	1.53 (0.280)	-	4.7 (1.251)
QCh_5	45.21 (1.049)	10.64 (0.391)	8.68 (0.245)	16.07 (5.260)	-	66.2(10.843)
$Fmoc_5$	51.53 (9.174)	10.25 (1.336)	16.34 (3.189)	4.70 (4.925)	-	4.3 (1.002)
$QFmoc_5$	44.86(43.5/46.2)	10.96(10.8/11.1)	9.56 (9.7/9.4)	20.76(24.5/17.0)	-	64 (66/62)
$Fmoc_{10}$	57.60(57.1/58.1)	9.49 (8.9/10.1)	15.02(13.9/16.2)	0.30 (0.5/0.1)	-	9.3(11.0/7.6)
$QFmoc_{10}$	45.42(45.6/45.2)	10.52(10.4/10.6)	8.99 (8.8/19.2)	20.81(10.2/31.5)	-	61.5 (60/63)
$Dansyl_5$	53.19(52.8/53.5)	10.79(10.7/10.8)	17.14(17.6/16.7)	0.86 (0.7/1.0)	1.4 (1.0/1.8)	4.3 (3.0/5.6)
$QDansyl_5$	47.56	1.040	9.87	15.56	1.00	63
$Dansyl_{10}$	54.91 (0.142)	10.12 (0.127)	8.99 (0.113)	0.70 (0.021)	2.98 (0.140)	9.3 (0.416)
$QDansyl_{10}$	55.84	11.52	17.37	20.81	2.94	63
$Naphth_5$	54.52(55.7/53.4)	11.42(12.3/10.6)	18.64(20.5/16.8)	0.63 (0.5/0.7)	-	7.1 (8.7/5.5)
$QNaphth_5$	42.83	10.50	9.03	20.75	-	61
$Naphth_{10}$	55.64(55.3/56.0)	10.63 (9.6/11.6)	15.96(16.5/15.3)	0.39 (1.49/0.29)	-	7.55(7.1/8.0)
$QNaphth_{10}$	43.01	9.42	8.60	0.31	-	60

2.3.2. *Nuclear Magnetic Resonance of PAA amphiphiles*

2.3.2.1. *^1H NMR spectra of PAA*

The ^1H NMR data showed the protons on the PAA backbone (Fig. 29) were as follows: $\delta_{1.0} = CH_2$, $\delta_{1.5} = CH$, $\delta_{2.5} = CH_2$.
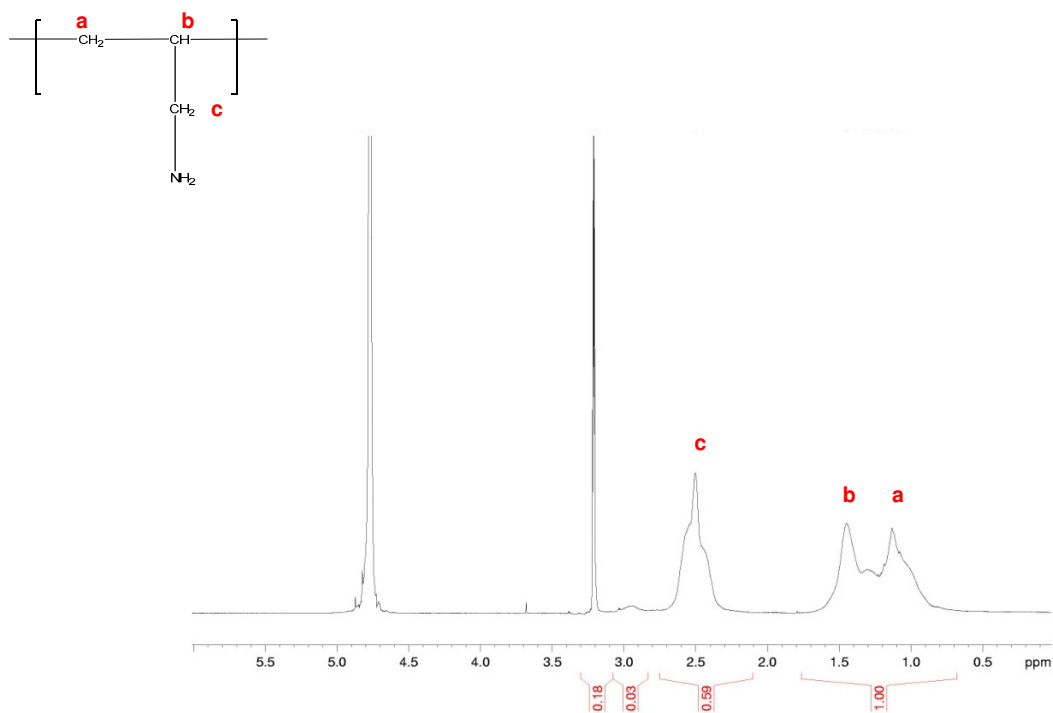
Figure 29. ^1H NMR spectra of PAA in MeOD carried out using 400MHz NMR at 25 ºC.

Peak assignments on the ^1H NMR spectra of the PAA backbone were as follows: $\delta_{1.0} = CH_2$ (Fig. 29a), $\delta_{1.5} = CH$ (Fig. 29b) and $\delta_{2.5} = CH_2$ (Fig. 29c). The peaks at $\delta_{3.25}$ and $\delta_{4.75}$ were due to water and MeOD respectively. Water peaks are commonly broad when observed on the NMR spectra, however the sharp peak suggests hydrogen bonding occurring between the water molecules and the polymer.

2.3.2.2. ^{1}H NMR spectra of Ch$_5$
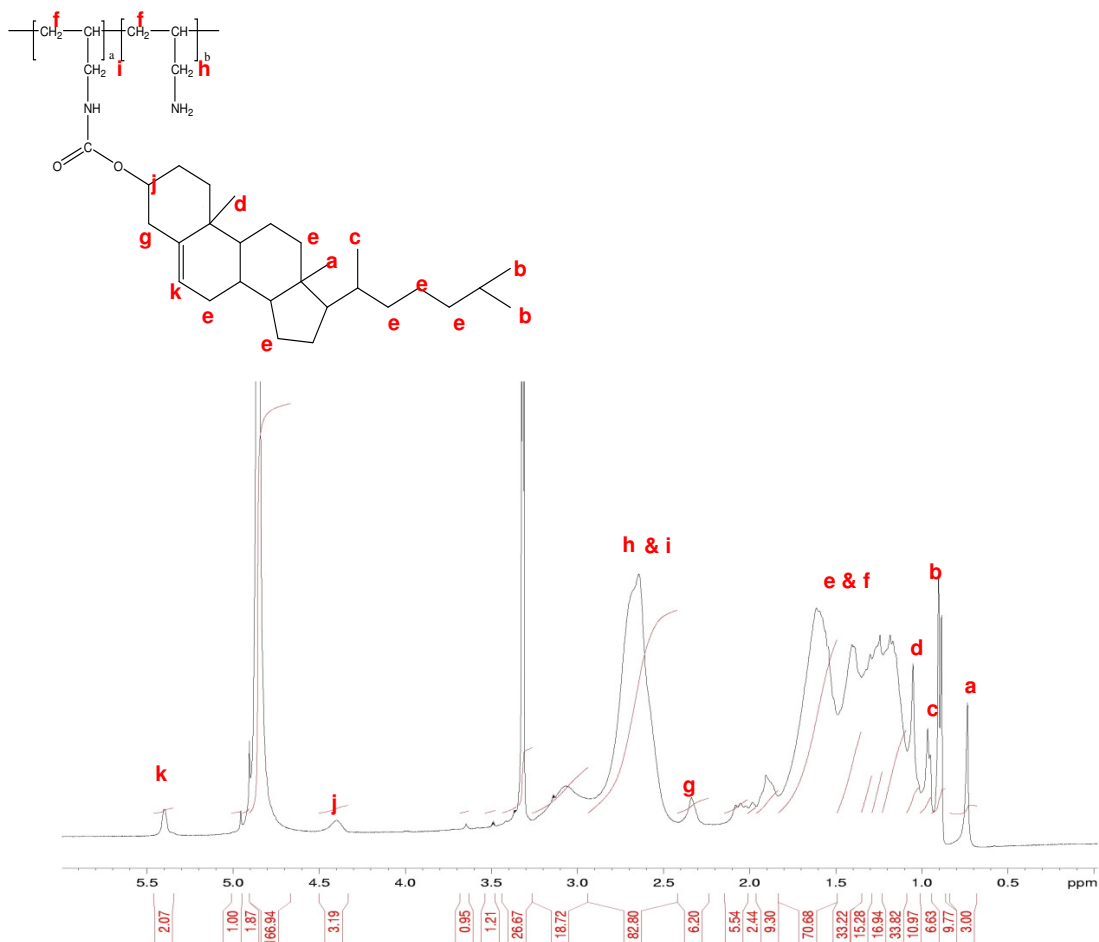
Figure 30. ^{1}H NMR spectra of Ch$_5$ in MeOD carried out using 400MHz NMR at 25 ºC.

The Ch$_5$ spectra (Fig. 30) had peak assignments at: $\delta_{0.75}$, $\delta_{1.10}$, $\delta_{1.15}$ and $\delta_{1.25}$ = CH$_3$ (Cholesteryl), $\delta_{1.4-2.0}$ = CH$_2$ (Cholesteryl, PAA), $\delta_{2.60}$ = CH$_2$ (Cholesteryl), $\delta_{2.75-3.00}$= CH$_2$ (attached to –NH and –NH$_2$ groups on PAA), $\delta_{4.5}$= CH=O (Carbonyl bond), $\delta_{5.5}$ = C=CH (Cholesteryl). The peaks at $\delta_{3.25}$ and $\delta_{4.75}$ were due to water and MEOD respectively.

The degree of hydrophobic modification could be calculated by comparing the peak at $\delta_{0.75}$ (cholesteryl) with the peaks at $\delta_{2.75-3.20}$ (-CH$_2$ attached to –NH and –NH$_2$ groups) on PAA backbone as follows:

(Integration at $\delta_{0.75}$ / 3) / (Integration at $\delta_{2.75-3.00}$ / 2) x 100 %

= 3.6 % hydrophobic substitution.

49

2.3.2.3. ^{1}H NMR spectra of Fmoc$_5$
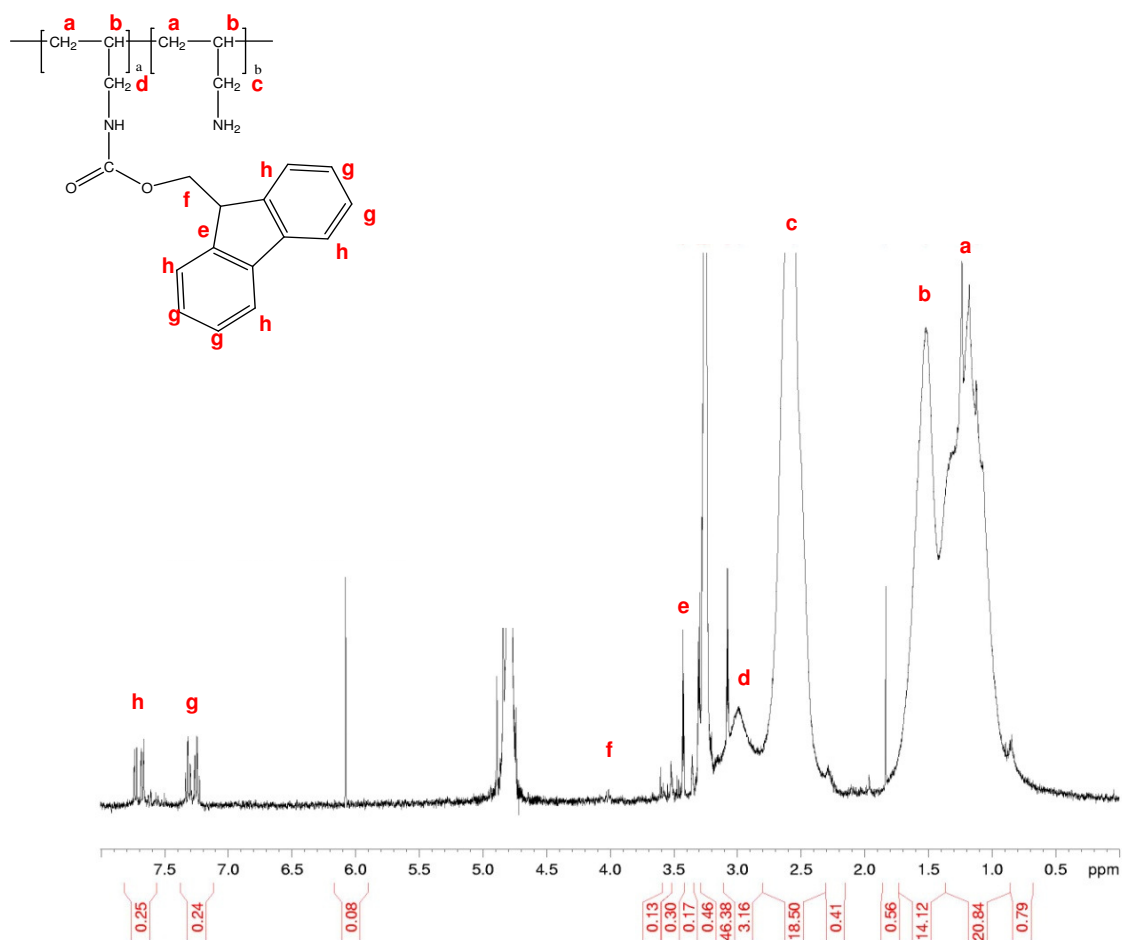
Figure 31.^{1}H NMR spectra of Fmoc$_5$ in MeOD carried out using 400MHz NMR at 25 ºC.

The peak assignments for Fmoc were as follows (Fig. 31): $\delta_{1.3}$ = CH$_2$ (PAA), $\delta_{1.6}$ = CH (PAA), $\delta_{2.5}$ = CH$_2$ (attached to -NH$_2$ of PAA), $\delta_{3.0}$ = CH$_2$ (PAA), $\delta_{3.4}$ = CH (Fmoc), $\delta_{4.0}$ = CH$_2$ (Fmoc), $\delta_{6.0}$ = N-H and N-H$_2$ (PAA) and $\delta_{7.2-7.8}$ = aromatic H's (i.e. g and h) (Fmoc). The peaks at $\delta_{3.3}$ and $\delta_{4.8}$ were due to water and MEOD respectively.

2.3.2.4. *^{1}H NMR spectra of Dansyl$_5$*
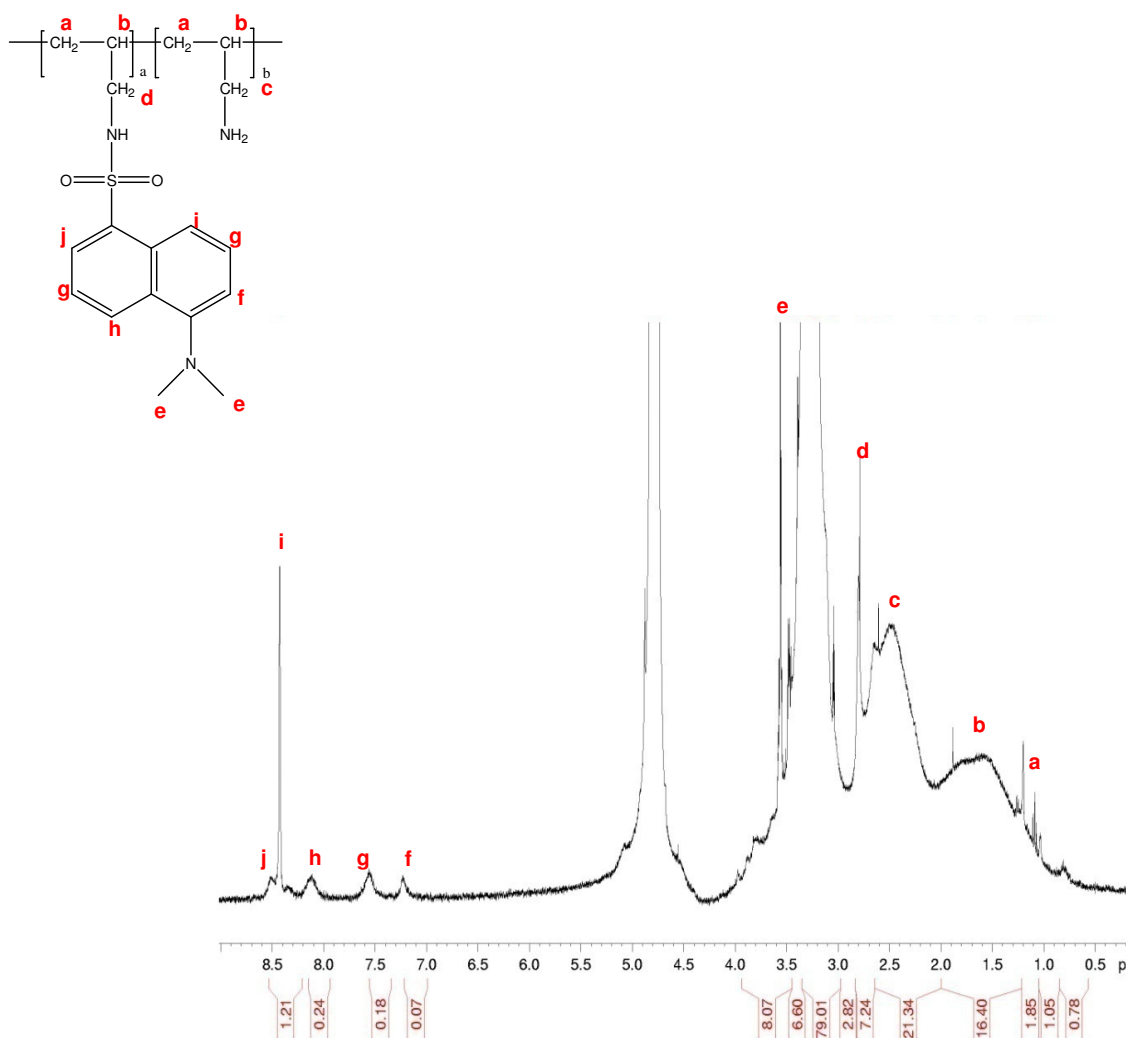
Figure 32.^{1}H NMR spectra of Dansyl$_5$ in MeOD carried out using 400MHz NMR at 25 ºC.

The Dansyl peak assignments were as follows (Fig. 32): $\delta_{1.0}$ = CH$_2$ (PAA), $\delta_{1.5}$ = CH (PAA), $\delta_{2.5}$ = CH$_2$ (PAA), $\delta_{2.8}$ = CH$_2$ (PAA), $\delta_{3.6}$ = CH$_3$ (Dansyl), $\delta_{7.3-8.5}$ = aromatic H's of naphthalene ring (i.e. f, g, h, I and j) (Dansyl). The peaks at $\delta_{3.3}$ and $\delta_{4.8}$ were due to water and MeOD respectively.

51

2.3.2.5. *^{1}H NMR spectra of Naphth$_5$*
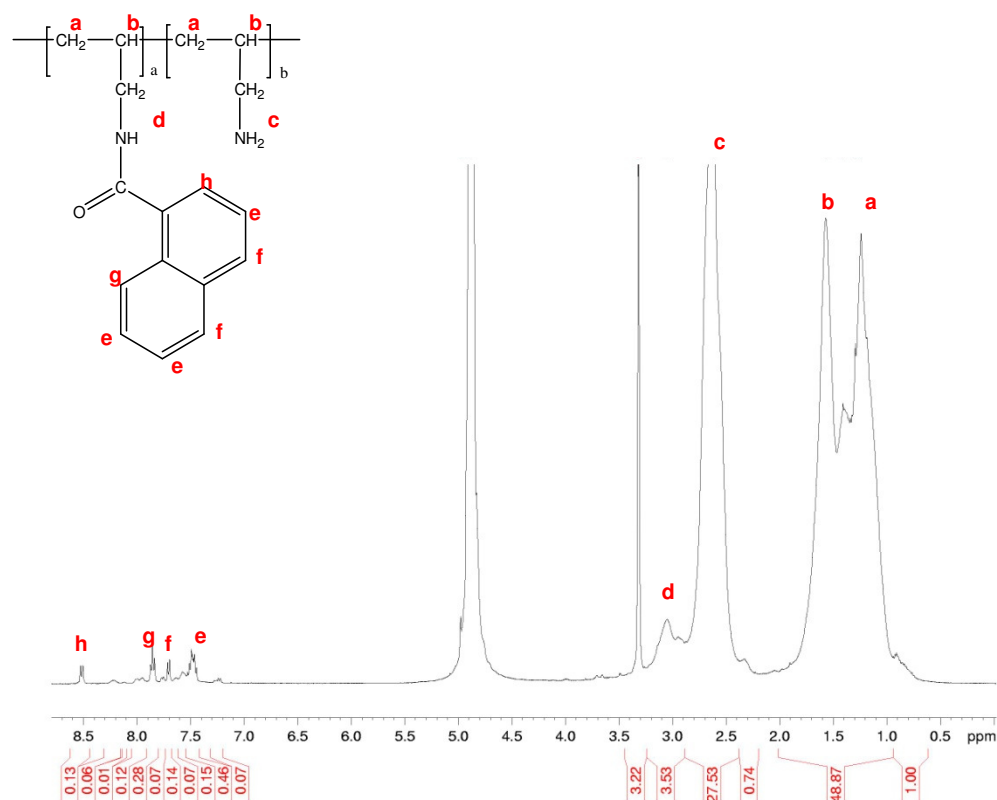
Figure 33.^{1}H NMR spectra of Naphth$_5$ in MeOD carried out using 400MHz NMR at 25 ºC.

The Naphth ^{1}H NMR spectra (Fig. 33) has peak assignments as follows: $\delta_{1.0}$ = CH$_2$ (PAA), $\delta_{1.5}$ = CH (PAA), $\delta_{2.5}$ and $\delta_{3.1}$ = CH$_2$ (attached to –NH$_2$ and –NH on PAA respectively), $\delta_{7.5-8.5}$ = aromatic H's of naphthalene ring (i.e. e, f, g and h) (Naphth).

The ^{1}H NMR spectra for Fmoc$_{10}$, Dansyl$_{10}$ and Naphth$_{10}$ can be seen in Appendix 1.0

2.3.2.6. ^1H NMR spectra of QCh_5

For the quaternary ammonium compound (QCh_5) (Fig. 34) the proton assignments were as follows:- $\delta_{0.5-2.0}$ CH_2's and CH_3's (PAA backbone and cholesteryl moiety Ch_5), $\delta_{3.3-3.6}$ = CH_2's and CH_3's (on quaternary ammonium ion), $\delta_{4.3}$ = CH-O, and $\delta_{5.4}$ due to CH (cholesteryl moiety)
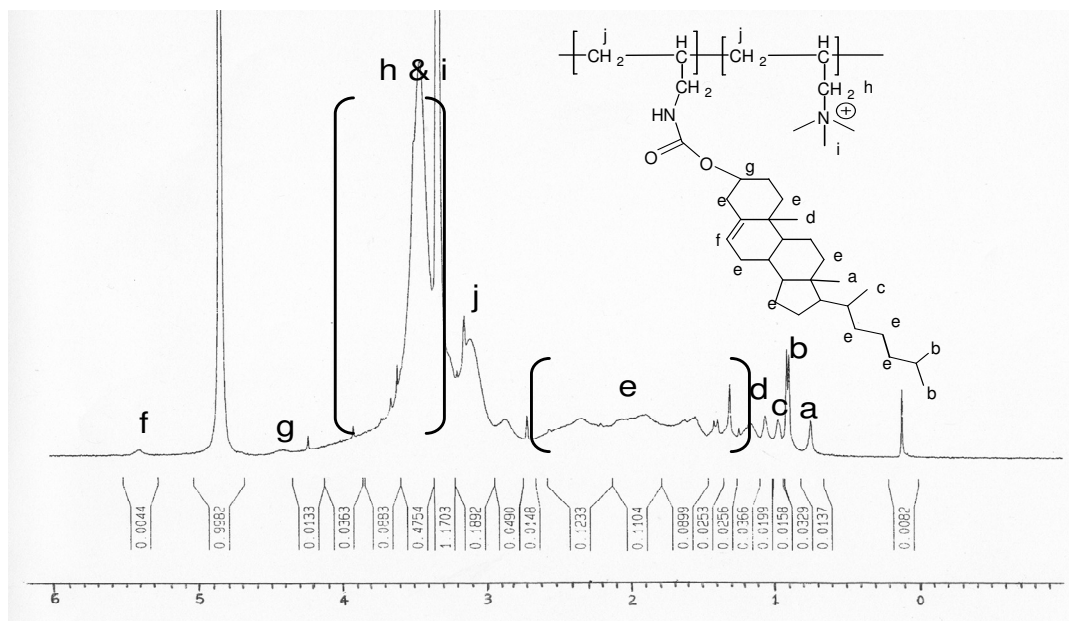
Figure 34. ^1H NMR spectra of QCh_5 carried out in MeOD on 400MHz NMR at 25 °C.

The corresponding quaternized polymers for the Fmoc, Dansyl and Naphth can be seen In Appendix 1.0

53

2.3.3. *Fourier Transform Infrared Spectroscopy (FTIR)*

The FTIR spectra of PAA and modified PAA polymers were run between $4000 - 650$ cm^{-1} to identify the characteristic functional groups present.
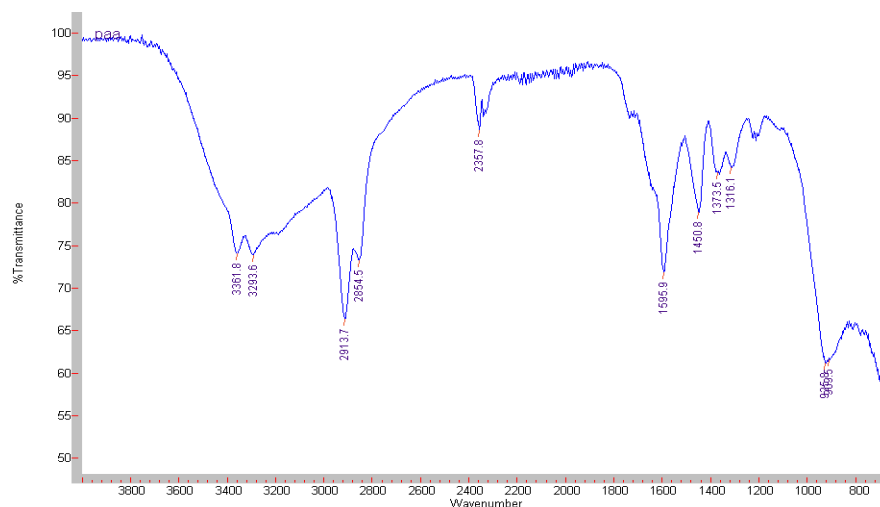
Figure 35.FTIR spectrum of PAA carried out using a diamond powder tip (64 scans).

The FTIR spectrum for PAA (Fig. 35) shows the presence of absorbance for the bonds present within the polymer (Table 4). The peak at 2357 cm^{-1} is due to C-O arising from background CO_2 and the broad peak at 3293 cm^{-1} is due to O-H of water which has been absorbed by the hygroscopic polymer.

Table 4. Peak bandwidth assignment occurring on FTIR spectrum of PAA using diamond powder tip (64 scans).

Polymer / Formulation	Bandwidth (cm^{-1})	Bond type	Functional Group
PAA	3361	N-H Stretch	1 ˚ Amine
	1595		
	2913	C-H Stretch	Alkyl
	2854		
	1373		
	1316		
	1450	C-C Bend	Alkyl
	925	C-N Bend	
	909		

54

The FTIR spectra of all the modified polymers looked identical to that of PAA between $4000 - 1800$ cm^{-1}, but showed significant difference in the region between $1600 - 700$ cm^{-1}. In order to accurately assign and identify the peaks, the modified polymers were therefore run in their fingerprint region ($1600 - 700$ cm^{-1}).
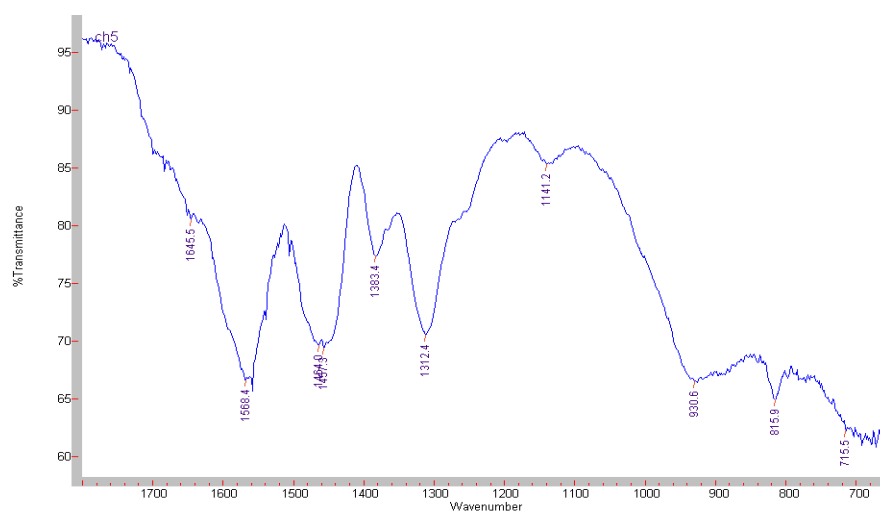
Figure 36. FTIR spectrum of Ch$_5$ carried out using a diamond powder tip (64 scans).

The spectrum of Ch$_5$ (Fig. 36), showed the presence of C=O and C-O peaks due to absorbance at 1464 cm^{-1} and 1141 cm^{-1} respectively indicating the presence of the carbonyl group between the backbone and the cholesteryl moiety.

Table 5. Peak bandwidth assignment occurring on FTIR spectrum of Ch$_5$ using diamond powder tip (64 scans).

Polymer / Formulation	Bandwidth (cm^{-1})	Bond type	Functional Group
Ch$_5$	1645	C=O Stretch	Carbonyl
	1568	N-H Bend	1 º Amine
	1464	C=C Bend	Aromatic
	815		
	1457	C-C Bend	Alkyl
	1383	C-H Bend	Alkyl
	1312		
	1141	C-O Bend	Carbonyl
	930		
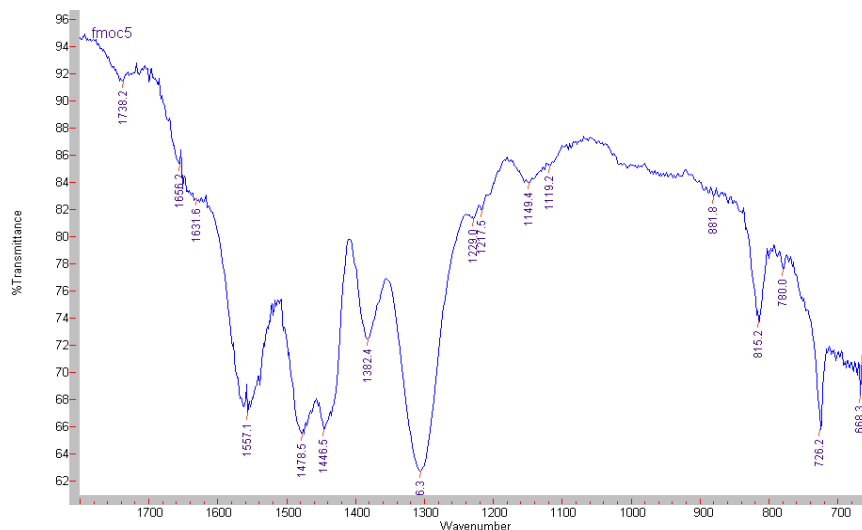
Figure 37. FTIR spectrum of Fmoc$_5$ carried out using a diamond powder tip (64 scans).

The IR spectrum confirms the presence of the fmoc attachment via an oxycarbonyl bond. Peaks where observed at 1306 and 1738 cm^{-1} due to the C-O and C=O respectively. Further peaks were also present between 1557 – 668 cm^{-1}, these peaks were due to the C=C bonds within the aromatic ring systems of the fmoc moiety.

Table 6. Peak bandwidth assignment occurring on FTIR spectrum of Fmoc$_5$ using diamond powder tip (64 scans).

Polymer / Formulation	Bandwidth (cm^{-1})	Bond type	Functional Group
Fmoc$_5$	1738	C=O Stretch	Carbonyl
	1229		
	1656	N-H Stretch	1 ° Amine
	1557	C=C Bend	Aromatic
	1446		Substituted benzene
	780		
	726		
	815		
	668		
	1478	C-C Bend	Alkyl
	1382	C-H Bend	Alkyl
	1306	C-O Bend	Oxyarbonyl
	1149		
	1119		
	1217	C-N Bend	
	881		
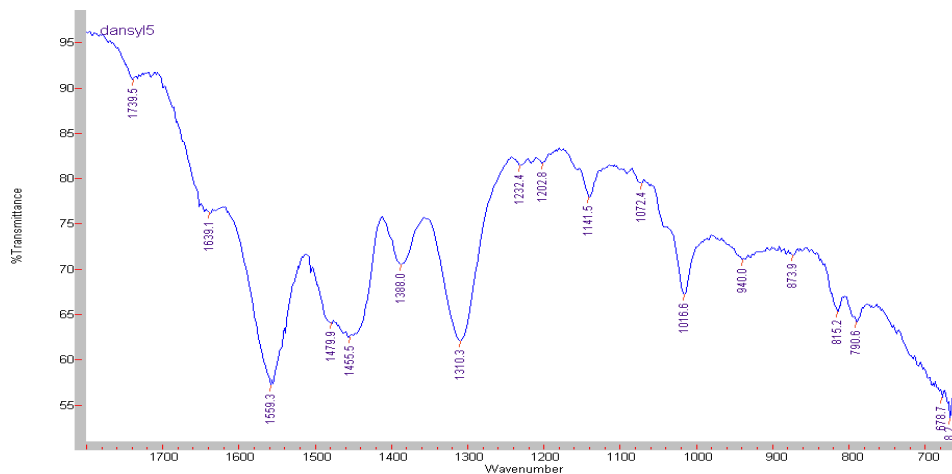
Figure 38. FTIR spectrum of Dansyl$_5$ carried out using a diamond powder tip (64 scans).

The FTIR spectrum of Dansyl$_5$ (Fig. 38) showed absorbance responsible for the dansyl moiety. The presence of methyl peaks (1232 and 1202 cm^{-1}) were attributed to the methyl groups attached to the amine of the dansyl moiety. The peak present at 790 cm^{-1} suggested the presence of aromatic substituted benzene and the most relevant peak at 1739 cm^{-1} showed the prescence of a sulfonyl group (from dansyl) to the PAA backbone.

Table 7. Peak bandwidth assignment occurring on FTIR spectrum of Dansyl$_5$ using diamond powder tip (64 scans).

Polymer / Formulation	Bandwidth (cm^{-1})	Bond type	Functional Group
Dansyl$_5$	1739	S=O Stretch	Sulfonyl
	1639	N-H Stretch	1º Amine
	1559	C=C Bend	Aromatic
	1455		Mono Substituted Benzene
	790		
	678		
	1479	C-C Bend	Alkyl
	1382	C-H Bend	Alkyl
	1310		
	1232	C-H Bend	Methyl
	1202		
	1141	C-N Bend	
	1072		
	1016		
	873		
	815		
	940		
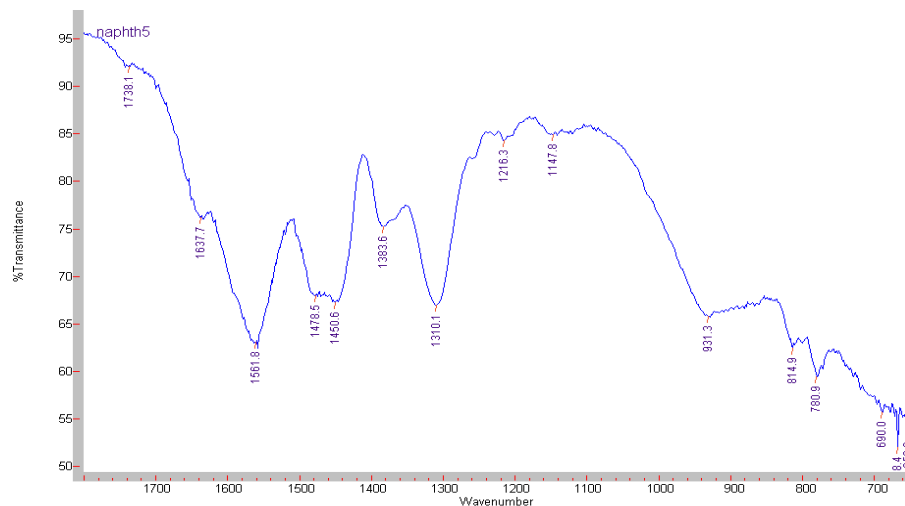
Figure 39. FTIR spectrum of Naphth$_5$ carried out using a diamond powder tip (64 scans).

The presence of aromatic alkene protons (1561 cm^{-1}) on the FTIR of Naphth$_5$ (Fig. 39) suggested the attachment of the naphthalene moiety had been successful. This was further confirmed by carbonyl peaks (1738 cm^{-1}) arising from the carbonyl bond between the PAA and the naphthalene moiety.

Table 8. Peak bandwidth assignment occurring on FTIR spectrum of Naphth$_5$ using diamond powder tip (64 scans).

Polymer / Formulation	Bandwidth (cm^{-1})	Bond type	Functional Group
Naphth$_5$	1738	C=O Stretch	Carbonyl
	1637		
	1216		
	1561	C=C Bend	Aromatic
	1450		Mono Substituted Benzene
	780		
	690		
	1478	C-C Bend	Alkyl
	1383	C-H Bend	Alkyl
	1310		
	1147	C-N Bend	
	931		
	814		

58

The FTIR spectrum for QCh$_5$ (Fig. 40) and all the quaternary compounds were run from 4000 – 650 cm^{-1}, this was due to vital peaks present at the higher region of the spectrum.
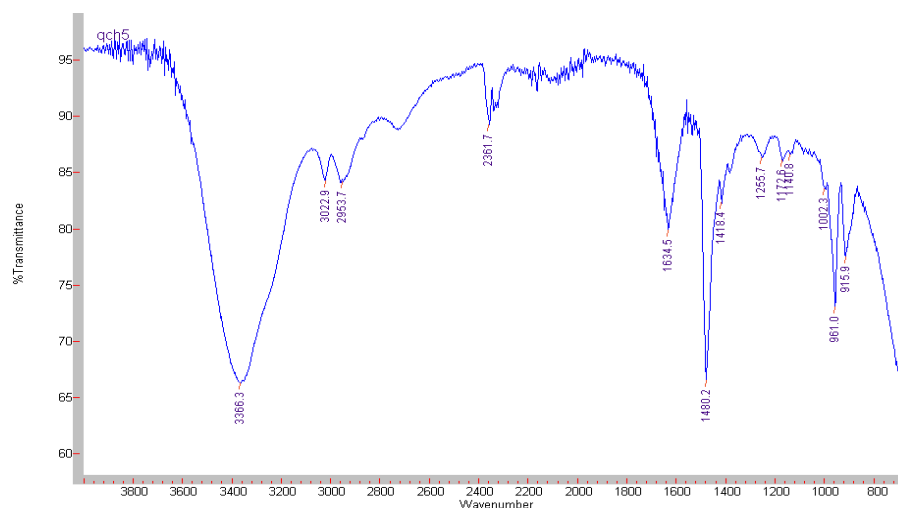
Figure 40.FTIR spectrum of QCh$_5$ carried out using a diamond powder tip (64 scans).

The peak assignment for the FTIR spectra of QCh$_5$ (Fig. 40) showed the presence of the broad band between 3600 – 3000 cm^{-1}. These peaks indicated quaternization had occurred, this was further confirmed by the prescence of CH$_3$ peaks at 1249 cm^{-1}, that resulted from the methyl groups from the ammonium ion.

Table 9. Peak bandwidth assignment occurring on FTIR spectrum of QCh$_5$ using diamond powder tip (64 scans).

Polymer / Formulation	Bandwidth (cm^{-1})	Bond type	Functional Group
QCh$_5$	3600 - 3000	N-H Stretch	Ammonium Ion
	3022	C=O Stretch	Carbonyl
	1634		
	2953	C-H Stretch	Alkyl
	1538	N-H Bend	1 º Amine
	1480	C=C Bend	Aromatic
	815		
	1418	C-C Bend	Alkyl
	1249	C-H Bend	Methyl
	1170	C-O Bend	Carbonyl
	961		

The FTIR spectra for Fmoc$_{10}$, Dansyl$_{10}$, Naphth$_{10}$ and all their corresponding quaternized derivatives can be viewed in appendix 2.0.

59

2.4. Discussion

Grafted polymers were successfully synthesised. The percentage of grafted values calculated using elemental analysis results were in good agreement with the theoretical values (Table 3). The hydrophobicity of a polymer may be altered by changing its initial molar feed ratios in the reactions. However excessive grafting of hydrophobic groups can lead to precipitation [203]. This phenomenon was witnessed for Ch-PAA. Ch-PAA could not be synthesised above 5 % grafting level as the highly hydrophobic nature of the cholesterol facilitate the polymer to precipitate out of solution rendering the modified polymer insoluble.

Hydrophilic modification of amphiphilic polymers can be achieved by quaternization of the primary amines on the polymer backbone [125]. The degree of hydrophilic grafting after quaternization ranged from 52-63 %. Elemental analysis is a commonly used technique for characterisation of block and graft polymers [123,132,204,205]. The percentage hydrophobic modification achieved were close to the theoretical values for the level of grafting based on the initial molar feed ratios (Table 1). Further characterisation was carried out by two qualitative methods (^{1}H NMR and FTIR). For Ch_5, the level of hydrophobic grafting was estimated using the NMR spectra by comparison of the cholesteryl CH_3 peak at $\delta_{0.75}$ with the CH_2 multiplet of the PAA at $\delta_{2.75-3.2}$ [76]. The level of modification was 4.4 mol% for Ch_5, showing close agreement between the cholesteryl levels estimated using ^{1}H NMR and elemental analysis (Table 1). Previously the use of this technique for quantitative analysis of polymer structures has been published [3,125,206].

For Fmoc, Dansyl and Naphth polymers ^{1}H NMR could only be used to qualitatively show the presence of the hydrophobic and hydrophilic groups with respect to PAA alone. This was due to the extensive overlapping of peaks making this type of analysis very difficult.

The NMR spectra of the PAA backbone shown in Fig. 29 shows the presence of peaks at $\delta_{1.0}$ and $\delta_{1.5}$, these peaks arise from the presence of the CH_2 and CH groups of the polymer backbone. At $\delta_{2.5}$ the peak wasdue to the CH_2 attached to the amine group. The amino groups adjacent to the CH_2 deshield the protons resulting in a downfield shift in their NMR spectra.

The Ch_5 spectrum (Fig. 30) shows additional peaks at $\delta_{4.5}$, assigned as the H attached to the carbonyl bond of the cholesteryl moiety (CH=O). Further peaks at $\delta_{0.75}$ - $\delta_{1.25}$, were due to the –CH_3 groups on the cholesteryl structure. At $\delta_{5.5}$ the peak can be attributed to the alkene protons (C=C-H) in the B ring of the cholesteryl group (Fig. 41). The presence of these additional peaks strongly suggests the attachment of the cholesteryl moiety on the polymer backbone.

60
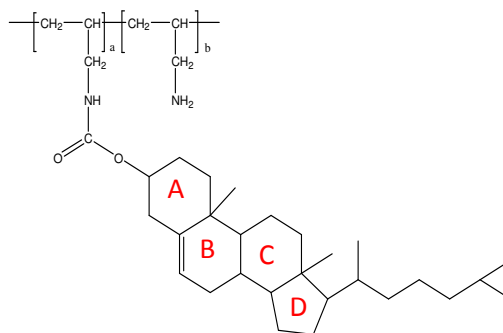
Figure 41. Chemical structure of Ch-PAA.

The NMR spectra for Fmoc$_5$ and Naphth$_5$ (Fig. 31 & 33) both showed the presence of further peaks occurring between $\delta_{7.0-8.0}$. These peaks arise from the hydrogen atoms on the aromatic rings of fmoc and naphthalene structures. Aromatic protons characteristically occur between $\delta_{7.0-8.0}$ on the ^{1}H NMR spectra [193]. However on closer inspection, peak splitting characteristic properties for each group can be assigned. Peak splitting arises from a proton existing in a magnetic field environment which is shared with neighbouring protons. The sharing of environments effect the total magnetic field strength experienced by the proton and thus peak splitting occurs [207].

In the Fmoc$_5$ spectrum (Fig. 31) two sets of triplets are observed between $\delta_{7.2-7.4}$, these were due to the C-H's on the aromatic rings with two neighbouring protons (indicated by 'g'), therefore forming a triplet (Fig. 42).
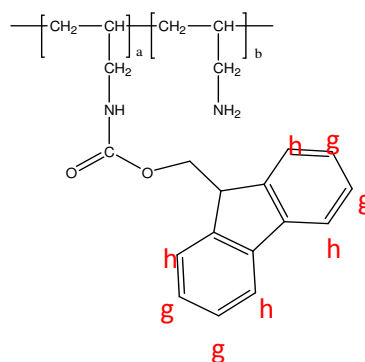
Figure 42. Chemical structure of Fmoc-PAA.

The two sets of triplets were observed because there were two equivalent environments existing. The two doublets observed $\delta_{7.6-7.8}$ were attributed to the C-H's in the aromatic ring systems of the fmoc group where only one neighbouring proton was present indicated by 'h' (Fig.42). Again two equivalent environments existed for this scenario hence producing two sets of doublets on the spectra.

In the NMR spectrum of the Naphth$_5$ polymer (Fig. 33), the aromatic region showed different spectral patterns than the fmoc polymer. This is due to the aromatic hydrogen on the Naphth$_5$ having a larger number of hydrogen in different environments. A triplet was

observed at $\delta 7.5$, this was due to the C-H's with two neighbouring protons on the aromatic ring indicated by 'e' (Fig. 43).
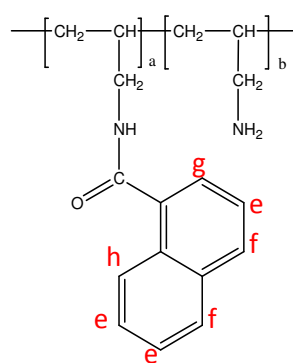
Figure 43. Chemical structure of Naphth-PAA.

Interestingly two sets of doublets were observed on the spectra, however they were quite separate ($\delta_{7.7}$ and $\delta_{8.5}$). These peaks were due to C-H's in the rings with only one neighbouring proton indicated by 'f' and 'h' respectively. However, the doublet at $\delta_{7.8}$ was shifted downfield on the spectra. This was because of the proximity of this proton to the electromagnetic O atom, thus causing deshielding. A triplet was present at $\delta_{7.9}$ denoted by 'g', this was expected to be a duplet due to the C-H with one neighbouring protons indicated by 'e', perhaps slight impurities where present within the polymer causing this irregularity.

The addition of dansyl to the polymer backbone produced extra peaks at $\delta_{3.6}$ (Fig. 32), due to the hydrogen's attached to the nitrogen on the dansyl moiety. More importantly peaks are present between $\delta_{7.3-8.5}$, these peaks are due to the aromatic rings on the dansyl moiety. However, it was more difficult to distinguish the peak splitting patterns on the Dansyl$_5$ spectra. Perhaps this was due to abundant equivalent protons causing peak overlap in the spectra or due to poor spectral resolution. However the presence of these peaks did indicate the presence of aromatic groups and when considered alongside the aforementioned peaks at $\delta_{3.6,}$ it strongly indicated that the dansyl moiety had successfully attached to the PAA backbone.

In the NMR spectra for the QCh$_5$, the presence of peak at $\delta_{3.3-3.6}$ confirms the presence of the CH$_3$ of the quaternary ammonium ion (Fig. 34), suggesting quaternization was successful [76,208]. This peak was present in all quaternized polymer spectra.

Fourier transform infrared spectroscopy was carried out for all the modified polymers. The FTIR spectra positively identified the grafting of each of the hydrophobic and hydrophilic groups. Although it is not a quantitative technique, it is still widely used for the confirmation of chemical structure within the amphiphilic polymer field [109,110,131,132, 209].

Further characterisation could be carried out using gel permeation chromatography (GPC). GPC separates its analytes on the basis of its molecular size and not its chemical structure like other analytical techniques [210]. GPC is carried out by passing a mobile phase through a column packed with hydrophobic porous beads. The sample is injected, its retention is determined by its molecular size (using the principle of steric size exclusion) [211]. Smaller molecules are capable of penetrating the porous beads of the stationary phase and thus are retained longer on the column [211]. This method has been extensively used for the quantitative analysis of polymers [100,136,212,213]. GPC is useful in the characterisation of block copolymers as they are synthesised from monomers which may result in a range of molecular weight products being formed. GPC is used to measure the molecular weight distribution of the monomers within the polymer structure [214]. However it is not used frequently within the comb shaped polymer field. This is because a homopolymer backbone is grafted with small hydrophobic pendant groups, and the synthesis is a lot easier to control. For graft polymers GPC can only be used to give a rough value for the grafting level which is not accurate for this application.

2.5. Conclusion

Polymers were successfully grafted in good agreement with predicted molar feed ratios in initial reactions. Full characterisation indicated that the correct polymer structures where produced.

Chapter Three

Characterisation of polymeric self-assemblies in aqueous environment

3.1. Introduction

In aqueous environments amphiphilic polymers spontaneously self assemble to form polymeric self-assemblies [75]. These self-assemblies formed can be polymeric micelles, nano-particles or vesicles [74]. The driving force behind aggregate formation is due to non-polar and hydrophobic-hydrophobic interactions between the amphiphilic polymer and the aqueous media [103]. Amphiphilic polymers have an equivalent value to the CMC known as the critical aggregation concentration (CAC) [215,216]. The ability of the nano aggregates to encapsulate hydrophobic drug molecules has been extensively investigated [72,217,218].

3.1.1. *Photon correlation spectroscopy*

Photon correlation spectroscopy (PCS) or dynamic light scattering (DLS) is a powerful technique used for estimating hydrodynamic size of particles or macromolecules in solution [194,197]. The size is measured by passing a beam of light through the desired sample. Upon collision with the macromolecular structures in the sample the beam scatters. These structures randomly move and vibrate by the phenomenon known as Brownian motion. The scattering of the light beam will result in changes in intensity, which led to the formation of a moving pattern. The moving pattern is used to deduce particle size as smaller particles move at a faster rate than larger heavier ones and scatter less light. The rate of change of light fluctuation is used to determine size distribution of the particles in the sample scattering light. The size measured by PCS is a representation of the hydrodynamic radius. The size is fractionally larger than that of the sample particle. This is due to the presence of a hydration layer surrounding the particles from the solvent [194]. This technique is very useful for macromolecules as it is capable of measuring sample sizes from only a few nanometres up to as large as five micrometers [194].

The distribution of particle size in solution indicates the degree of monodipersity or polydispersity. The polydispersity index (PDI) indicates the variation of size distribution within the sample. The PDI is measured on a scale of 0 to 1. A PDI of 0 indicates the size of self assemblies in the sample are uniform whereas a PDI of 1 indicates non-uniformity where numerous size distributions are present.

3.1.2. *UV Visible spectroscopy*

UV-Visible spectroscopy is a useful technique for identification and quantification of chemical and biological samples [219]. The basic principle is the measurement of the intensity of radiation at specific spectral wavelengths which are characteristic to the samples involved [219].

Atoms or molecules absorb radiation with a specific photon energy (matching to the difference in energy between their ground state and excited state); the wavelength at

which this occurs depends upon the bonding of the atom or molecules' electrons [195]. The electrons involved in single bonds are held tightly, making them difficult to excite. Whereas, the electrons are held less tightly in double and triple bonds and are a lot more excitable and therefore producing well defined absorption spectra [195]. When UV/Visible light is passed through a liquid or gaseous sample, the light emerging from the sample is then analysed by a spectrometer producing an absorption spectra [195].

3.1.3. *Surface tension*

Water molecules in the bulk solution will be surrounded by other molecules in all directions which possess equal attractive forces [28]. However, at the liquid air interface this is not the case. Molecules at the surface of the liquid have fewer neighbouring molecules and therefore cohesive forces can only form with the limited number of molecules which are directly situated below or beside them [2, 28,31]. As a result a net inward force is experienced by the molecules at the interface towards the bulk of solution [28,31]. The net inward attraction described results in the molecules being pulled together, contracting the surface [31]. The surface is now said to be in a state of lateral tension, this is also known as surface tension [28]. A minimum free energy state is achieved. In order to expand the newly contracted surface an increase in free energy is required [2].

When amphiphilic molecules such as surfactants or amphiphilic polymers accumulate at the surface of a liquid interface, their hydrophobic moiety protrudes from the surface layer into the gaseous phase above (here we assume that the surfactant amphiphiles are soluble in the aqueous phase). The intrusion of the surface layer results in the replacement of some water molecules with non-polar groups such as hydrocarbons [2]. The attractive forces between water molecules and non-polar groups are considerably less than that of water-water interactions and a reduction in surface tension is experienced [28,31]. The surface tension is decreased with the addition of very low concentrations of amphiphile, and continues to decrease as the concentration of the amphiphile is increased [2]. When the interface of the aqueous environment is 'saturated' with amphiphilic molecules addition of further amphiphile does not result in the decline of surface tension [79]. The remaining molecules in solution find other means of shielding their hydrophobic groups from the aqueous environment. They self assemble into aggregates known as micelles. A graph of surfactant concentration is plotted against surface tension, the point at which the gradient plateau is determined as the critical micellar concentration or critical aggregation concentration.

3.1.4. *UV hydrophobic probes*

UV hydrophobic probes such as methyl orange and N-phenyl-1-naphthylamine (PNA) have been used to investigate the self-assembly formation of surfactant micelles and polymeric nano-particles in aqueous media [76,220,221].

In the aqueous environment methyl orange favours the hydrophobic domains in surfactant or polymeric self assemblies. The hydrophobic interaction of the methyl orange inside the self-assemblies results in a hypsochromic shift in the λ_{max} on the methyl orange absorption spectra over varying polymer concentrations. The hypsochromic shift can be identified using a UV spectrometer (Fig. 44) [3,123,222]. UV probes can be used to deduce the CAC of amphiphilic polymers as the hypsochromic shift is experienced when the self-assembly formation occurs.
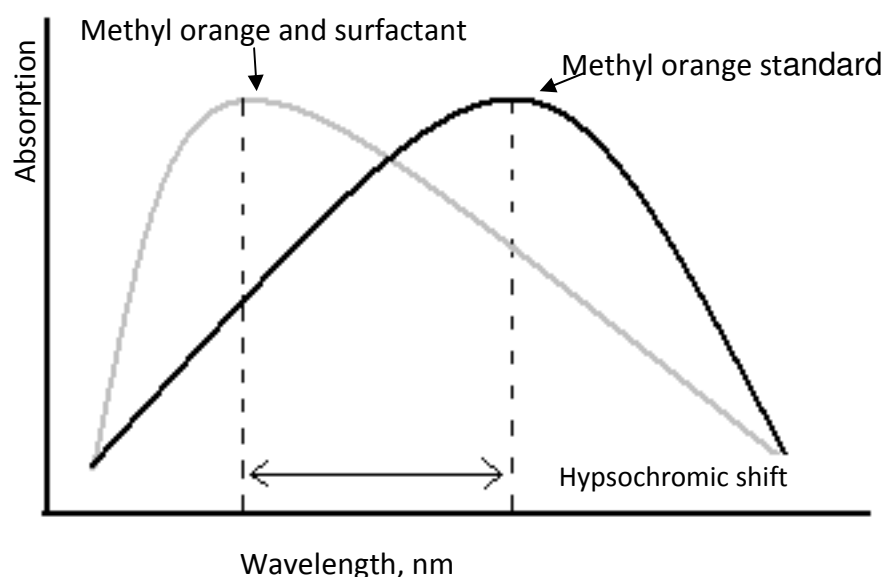
Figure 44.Hypsochromic shift occurring when methyl orange is partitioned inside the hydrophobic core of a micelle.

3.1.5.*Fluorescence spectroscopy*

Fluorescence spectroscopy is a very sensitive analytical method for quantification of fluorescent compounds. Compounds which possess fluorescent properties are usually those with rigid molecular structures like aromatic ring systems, double and triple bonds [200].

When an atom or molecule absorbs a photon of energy due to UV radiation, the resultant excited electronic state causes a change in the energy of that molecule. However as the molecule returns to its ground state the excess electronic energy is emitted as a photon of light giving rise to the phenomenon known as fluorescence [223,224].

Fluorescent excitation can lead to the formation of diatomic molecules between atoms or molecules which would not bond if they were in their unexcited ground states. This phenomenon is known as excimer formation. An excimer is a short-lived dimeric molecule formed from two species, at least one of which is in an excited electronic state. They are often diatomic and are formed between two atoms or molecules that would not bond if

they were both in their ground states [225]. Excimer formation causes a shift in the emission wavelength of a fluorophore [225].

3.1.6. *Transmission electron microscopy*

The transmission electron microscope is an extremely useful piece of equipment which can be used to study the aggregation structure of a sample [194]. The instrument passes a beam of electrons through a thin layer of sample causing interactions [194]. The interactions allow a high resolution image of the aggregation architecture to be produced. Samples less than 1 µm can be imaged using this technology [194].

3.1.7. *Aims and Objectives*

The modified polymers were characterised using surface tension measurements, a UV hydrophobic probe and PCS to determine whether they formed self-assemblies in aqueous solution. To fully understand their physical properties in aqueous solution, fluorescent studies were also carried out for $Fmoc_5$ to investigate whether excimer formation was occurring upon spontaneous aggregation. The properties of nano aggregates (e.g. CAC, size) can give indication to their drug loading potential and hence their success as vehicles for drug delivery.

3.2. Materials and Methods

3.2.1. *Materials used*

Material	Supplier
Modified PAA polymers	Synthesised in Chapter Two
Methyl orange	Sigma-Aldrich Co., UK
Sodium Tetraborate	Sigma-Aldrich Co., UK
Acetone	Fisher Scientific, UK
0.45µm GDX PVDF filters	Whatman, UK
Highly purified water	MillexQ system (UK)

3.2.2. *Methods*

3.2.2.1. *Photon correlation spectroscopy*

Polymeric self-assemblies were formed by probe sonication of the polymers (1 mgmL^{-1}) in doubly distilled water before filtering with 0.45 µm syringe filter. Hydrodynamic diameters and polydispersity index measurements were carried out using a photon correlation spectrometer (Zetasizer Nano-ZS, Malvern Instruments, UK). All measurements were conducted in triplicate at 25 °C and an average value was determined. A simple t-test was carried out in excel to determine the statistical significance of results, whereby p≤0.01 was significant.

3.2.2.2. *CAC determination*

3.2.2.2.1. *UV Hydrophobic probe*

This method was an adaptation of Uchegbu's method [125]. A stock solution of methyl orange (25 µM) was prepared with sodium tetraborate buffer (0.02 M, pH 9.4) in deionised water. The solution was placed in a sonic bath for 3h. Twenty two concentrations of modified polymers (0.00145 - 3 mgmL^{-1}) were made up using the methyl orange solution as the diluent. Each sample was probe sonicated for 5 min and allowed to cool to room temperature. The polymer solutions were placed in a UV-visible spectrophotometer (Agilent 8453) and their maximum absorbance was recorded (350-600 nm). The methyl orange stock solution was used as the control. The presence of hypsochromic shift was determined by comparing the polymer solution wavelength maxima with the λ_{max} of methyl orange stock solution.

3.2.2.2.2. *Surface tension*

The polymers were made up in aqueous solution (twenty two solutions, 0.00145 - 3 mgmL^{-1}) and sonicated for 5 min before cooling to room temperature. The surface tension of polymer solutions were measured at 25 °C using a torsion balance (OS, White Electrical Instrument Co, London). The platinum ring and platform were cleaned with ethanol and doubly distilled water prior to analysis of each sample. The measurement was conducted in triplicate for each polymer solution to obtain an average value. The surface tension of deionised water was determined between each concentration to ensure no cross contamination of samples had occurred.

3.2.2.2.3. *Fluorescent spectra of Fmoc$_5$*

Fmoc$_5$ was dissolved in doubly distilled water and sonicated for 10 min. After cooling to room temperature eight samples of 0.023 - 3 mgmL^{-1} concentration were run on the Luminescence Spectrometer (Perkin Elmer LS55, USA) with excitation wavelength set at

259 nm. The samples were scanned between 200 - 500 nm at 400 nmsec^{-1}, excitation slit width of 15 nm and emission slit width of 3 nm. Emission spectra were collected and analysed using the supplied software.

3.2.2.3. *Transition electron microscopy*

All samples were visualised at The University of Glasgow, Division of Infection & Immunity, IBLS, Integrated Microscopy Facility. Formvar/carbon-coated 200 mesh nickel grids were glow discharged. Polymer solutions made up in doubly distilled water were dried onto the hydrophilic support film. 1 % aqueous methylamine vanadate (20 µL) (Nanovan; Nanoprobes , Stony Brook, NY, USA) stain solution was applied and the mixture dried down immediately with filter paper to remove excess liquid. The dried samples were imaged with a LEO 912 energy filtering transmission electron microscope at 120 kV. Contrast enhanced, zero-loss energy filtered digital images were recorded with a 14 bit /2 K Proscan CCD camera.

3.3. Results

3.3.1. *Photon correlation spectroscopy*

Characterisation was carried out on the nano aggregates in aqueous solution. The hydrodynamic size of 5 % mole grafted polymer aggregates (1 $mgmL^{-1}$) formed in aqueous solution ranged from 99 nm ($QDansyl_{10}$) to 284 nm ($QFmoc_5$) (Table 10). The low polydispersity index indicated that fairly uniform single sized populations were produced [226].

Table 10. Size analysis for 1 $mgmL^{-1}$ aqueous polymer solutions n=3, ave (SD).

Modified Polymer	Size (nm)	P.D.I
Ch_5	183 (2)	0.167 (0.101)
QCh_5	272 (33)	0.303 (0.025)
$Fmoc_5$	199 (2)	0.140 (0.053)
$QFmoc_5$	284 (2)	0.142 (0.001)
$Fmoc_{10}$	128 (3)	0.163 (0.015)
$QFmoc_{10}$	169 (15)	0.136 (0.102)
$Dansyl_5$	120 (6)	0.285 (0.025)
$QDansyl_5$	215 (29)	0.337 (0.041)
$Dansyl_{10}$	99 (29)	0.367 (0.153)
$QDansyl_{10}$	138 (22)	0.125 (0.102)
$Naphth_5$	188 (3)	0.127 (0.001)
$QNaphth_5$	128 (4)	0.268 (0.201)
$Naphth_{10}$	156 (5)	0.258 (0.002)
$QNaphth_{10}$	172 (12)	0.135 (0.013)

On increasing the molar grafting level from 5 % to 10 %, a trend was witnessed whereby the size of the self assemblies formed decrease from 199 to 128 nm (Fmoc), 120 to 99 nm (Dansyl) and 188 to 156 nm (Naphth) (Table 10). This suggests that increased hydrophobicity of the amphiphile resulted in stronger hydrophobic interactions with the aqueous environment forming more compact aggregates, however these were not

statistically significant. The PDI values increased slightly with higher hydrophobic grafting, perhaps due to the random nature of the grafting allowing the formation of both intra and intermolecular aggregates.

Figure 45 shows the size distribution report for Dansyl$_5$. The chart shows that all the aggregates formed are within the size range of 50 - 300nm. Although this is a relatively large range, only one type of aggregation is present as only one peak is observed.
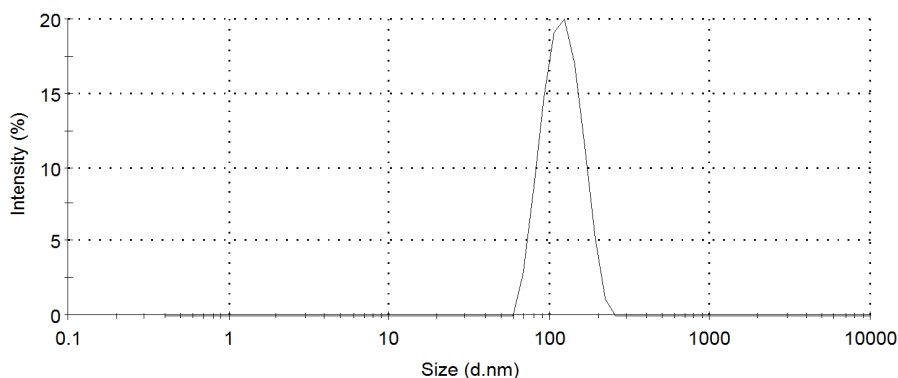
Figure 45. Photon correlation spectroscopy size correlation chart for 1 mgmL^{-1} Dansyl$_5$ in doubly distilled water (n=3, ave).

The size correlation chart for Dansyl$_{10}$ (Fig. 46) shows the self assemblies formed are not all of uniform size and that two size populations are present in solution. The larger peak between 45 - 150 nm indicates that the majority of the aggregates in solution exist within this size range. This peak can be attributed to intermolecular aggregation whereby more than one polymer strand comes together to form the self-assembly. The smaller peak at 5 – 15 nm perhaps is due to intramolecular aggregation, whereby one lone polymer strand can spontaneously self aggregate forming a self-assembly. The presence of these two peaks means the aggregates formed are poly disperse.
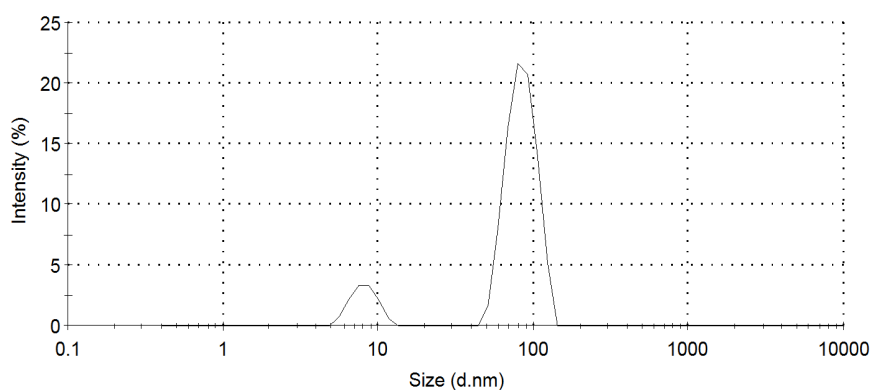
Figure 46. Photon correlation spectroscopy size correlation chart for 1 mgmL^{-1} Dansyl$_{10}$ in doubly distilled water (n=3, ave).

72

Addition of hydrophilic moieties generally increased the self-assembly size was witnessed for all quaternized polymers with exception to QNaphth$_5$ (however this was not statistically significant)(Table 10). Upon quaternization Ch$_5$ (183 nm) increased to 272 nm (QCh$_5$). The increase in hydrodynamic size is possibly due to a higher level of solvation with the presence of the quaternary ammonium ions on the shell of the polymeric self-assemblies.

In general all the 5 % modified polymers experienced a higher degree of polydispersity upon quaternization while for the 10 % quaternized polymers, although their size did increase, the polydispersity index decreased slightly (Table 10).

Size correlation charts for all the polymers can be viewed in Appendix 3.0

3.3.2. *Determination of CAC*

3.3.2.1. *Surface Tension*

Surface tension measurements were used to estimate the CAC values of the self-assemblies formed. The CAC values for the modified polymers were measured at the point in the graph where the surface tension comes to a plateau. The appearance of the surface tension graphs changed dramatically depending on the hydrophobic group. From the surface tension graph (Fig. 47) the CAC values for Ch$_5$ and Dansyl$_5$ were determined as 0.093 and 0.5 mgmL^{-1} respectively. The appearance of the Fmoc$_5$ and Naphth$_5$ surface tension graphs differed greatly from the Ch$_5$ and Dansyl$_5$. Both these polymer solutions showed two areas of plateau in the graph suggesting the presence of two CAC values at 0.4 and 1.5 mgmL^{-1} (Fmoc$_5$) and 0.187 and 0.5 mgmL^{-1} (Naphth$_5$).
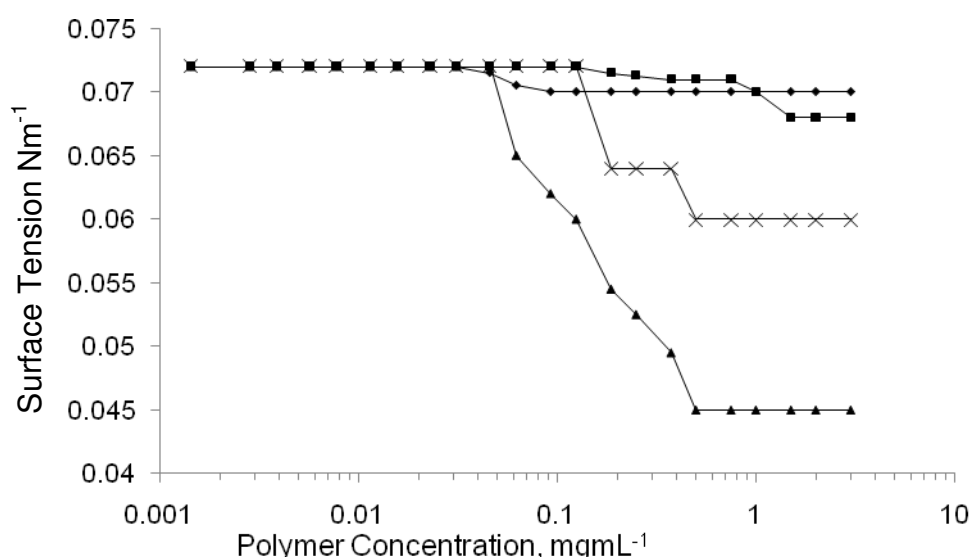
Figure 47.Surface Tension results for ♦ Ch$_5$, ■ Fmoc$_5$, ▲ Dansyl$_5$ and X Naphth$_5$ carried out on a torsion balance at 25 ºC, (n=3, ave ± SD).

The Fmoc$_5$, Dansyl$_5$ and Naphth$_5$ had much lower surface tension values than the Ch$_5$, this can be attributed to the presence of aromatic rings within the pendant groups. The

aromatic rings are more hydrophobic than the alkyl chain or ring system present in the cholesteryl moiety of Ch_5 [227]. $Dansyl_5$ showed the greatest decrease in surface tension from 0.072 Nm^{-1} of water to 0.045 Nm^{-1}. This indicted that the dansyl moiety was the most hydrophobic, with stronger aggregation interactions in aqueous phase [227].

Fig. 48 shows that addition of a hydrophilic moiety decreases the CAC value from 0.25 and 1 $mgmL^{-1}$ ($Fmoc_5$) to 0.125 and 0.5 $mgmL^{-1}$ ($QFmoc_5$). This reduction was also observed for the Ch_5 (0.093 $mgmL^{-1}$) and QCh_5 (0.023 $mgmL^{-1}$) (Table 11). However addition of hydrophilic moieties to all other polymers resulted in the presence of no CAC value. At higher hydrophobic grafting levels the CAC appeared to be lowered. The CAC value of the Fmoc self-assemblies decreased from 0.4 and 1.5 $mgmL^{-1}$ ($Fmoc_5$) to 0.187 and 0.75 $mgmL^{-1}$ ($Fmoc_{10}$) (Fig. 48).
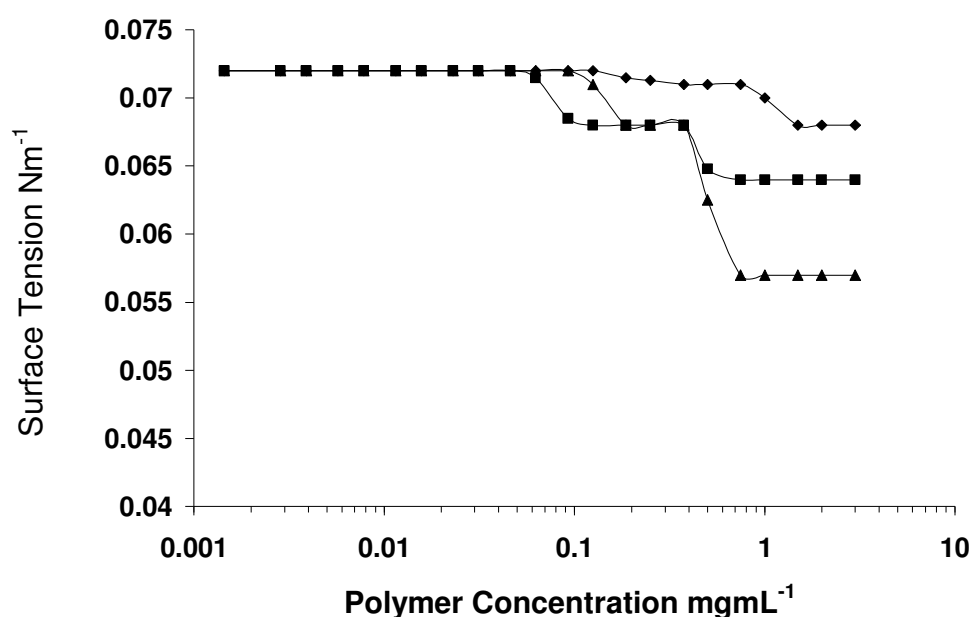
Figure 48.Surface Tension results for ♦ $Fmoc_5$, ■ $QFmoc_5$ and ▲ $Fmoc_{10}$ carried out on a torsion balance at 25 °C (n=3, ave).

For the quaternized polymers excluding QCh_5 and $QFmoc_5$, no CAC was observed over the concentration range tested (0.0145 – 3 $mgmL^{-1}$). The surface tension for $QDansyl_5$ (Fig. 49) shows the surface tension remained at the surface tension value for water (0.072 Nm^{-1}). The surface tension plots for all other modified polymers are in Appendix 4.0. Table 11 shows the CAC values for all the modified polymers determined using surface tension measurements.
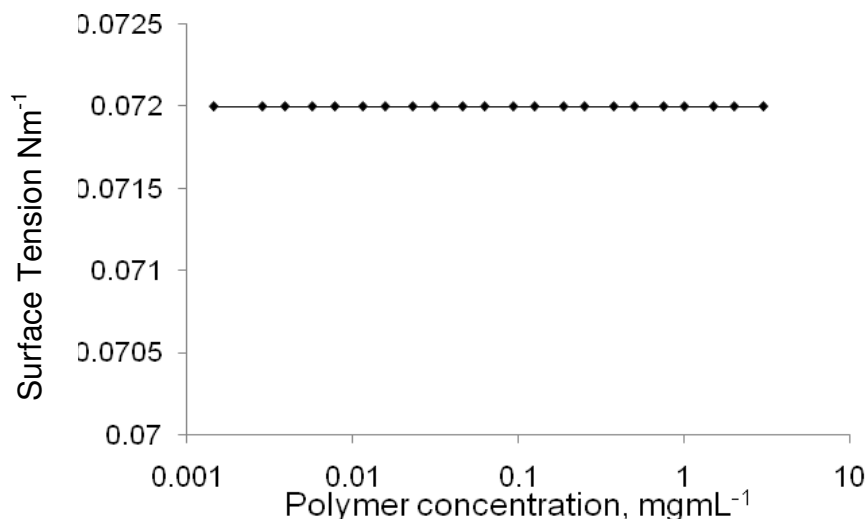
Figure 49.Surface Tension results for QDansyl$_5$ carried out on a torsion balance at 25 °C (n=3, ave).

Table 11.CAC values for modified polymers in aqueous solutions and appearance in solution above CAC value (n=3, ave).

Modified Polymer	CAC value (mgmL^{-1})	Appearance in solution above CAC
Ch$_5$	0.093	White cloudy solution
QCh$_5$	0.023	Colourless clear solution
Fmoc$_5$	0.4 and 1.5	Colourless clear solution
QFmoc$_5$	0.125 and 0.75	Colourless clear solution
Fmoc$_{10}$	0.187 and 0.75	Colourless clear solution
QFmoc$_{10}$	No CAC observed	Colourless clear solution
Dansyl$_5$	0.5	Yellow clear solution
QDansyl$_5$	No CAC observed	Yellow clear solution
Dansyl$_{10}$	0.25	Yellow clear solution
QDansyl$_{10}$	No CAC observed	Yellow clear solution
Naphth$_5$	0.187 and 0.5	Colourless clear solution
QNaphth$_5$	No CAC observed	Colourless clear solution
Naphth$_{10}$	0.125 and 0.75	Colourless clear solution
QNaphth$_{10}$	No CAC observed	Colourless clear solution

3.3.2.2. *UV hydrophobic probe*

Methyl orange studies were carried out in order to observe a hypsochromic shift allowing determination of the CAC value of the modified polymer. Methyl orange has a λ_{max} of 464 nm. When an amphiphile is diluted in a methyl orange solution, a hypsochromic shift occurs in the UV spectra [76]. This is due to the methyl orange favouring the hydrophobic core of the surfactant micelles. The CAC is identified as the point where the wavelength remains constant and a plateau is observed on the graph.

For Ch$_5$ (Fig. 50) the shift occurred at 0.0313 mgmL^{-1}. After this concentration the wavelength, (and thus the gradient of the graph) reached a plateau indicating the occurance of complete aggregation [3]. After the plateau the values started to rise up to 450 nm, this may be due to the high polymer concentration (0.5 mgmL^{-1}) making the solution cloudy, thus giving inaccurate UV reading. A hypsochromic shift was observed at 2 mgmL^{-1} for Fmoc$_5$ (Fig. 51).
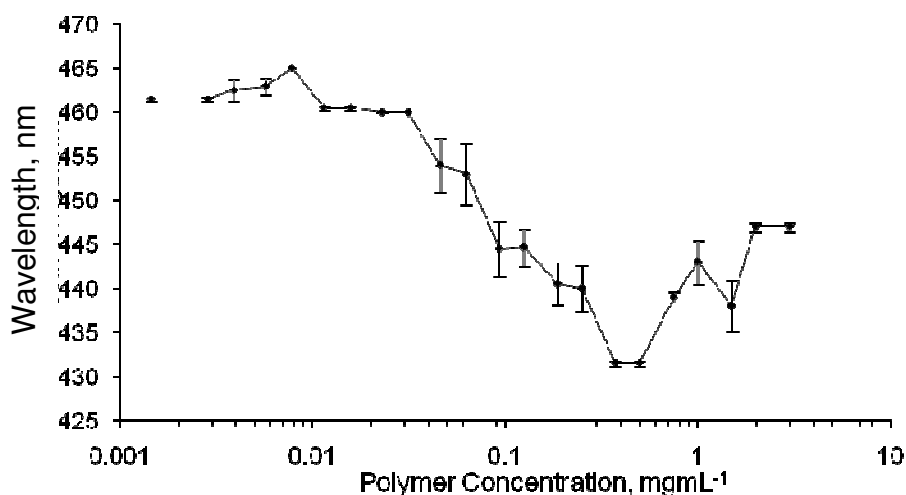
Figure 50. Effect of Ch$_5$ on the peak absorbance of methyl orange at 464 nm (n=3, ave ± SD).
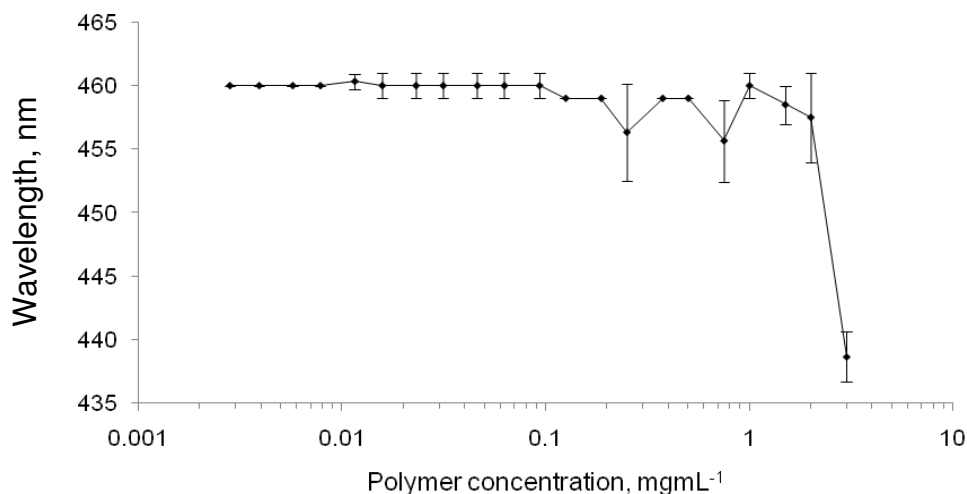
Figure 51. Effect of Fmoc$_5$ on the peak absorbance of methyl orange at 464 nm (n=3, ave ± SD).

The formation of aggregates at lower concentrations of Fmoc$_5$ were not detectable in the methyl orange study indicating surface tension measurements were more sensitive in determining CAC values. All the other polymers tested did not show any noticeable shift in λ_{max} (Fig. 52) perhaps due to the method being insensitive or the aromatic nature of the hydrophobic groups, fmoc, dansyl and naphthalene groups (normally used as fluorophores) interfering with or quenching the methyl orange readings [228].
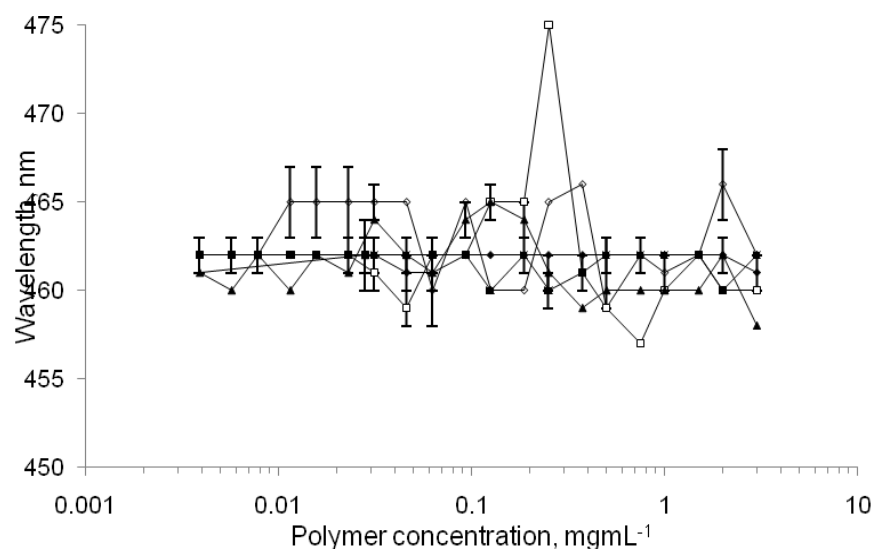
Figure 52. Effect of ◊ Dansyl$_5$, □ Naphth$_5$, ▲ Fmoc$_{10}$, ♦ Dansyl$_{10}$ and ■ Naphth$_{10}$ on the peak absorbance of methyl orange at 464 nm (n=3, ave ± SD).

Consistent with the unquaternized results, the QCh$_5$ showed hypsochromic shifts upon aggregation of methyl orange (Fig. 53). The CAC value for QCh$_5$ (0.0313 mgmL^{-1}) was identical to its corresponding unquaternized polymer. QFmoc$_5$ (Fig. 53) together with the rest of the quaternized polymers showed no hypsochromic shift, resulting in no CAC value.
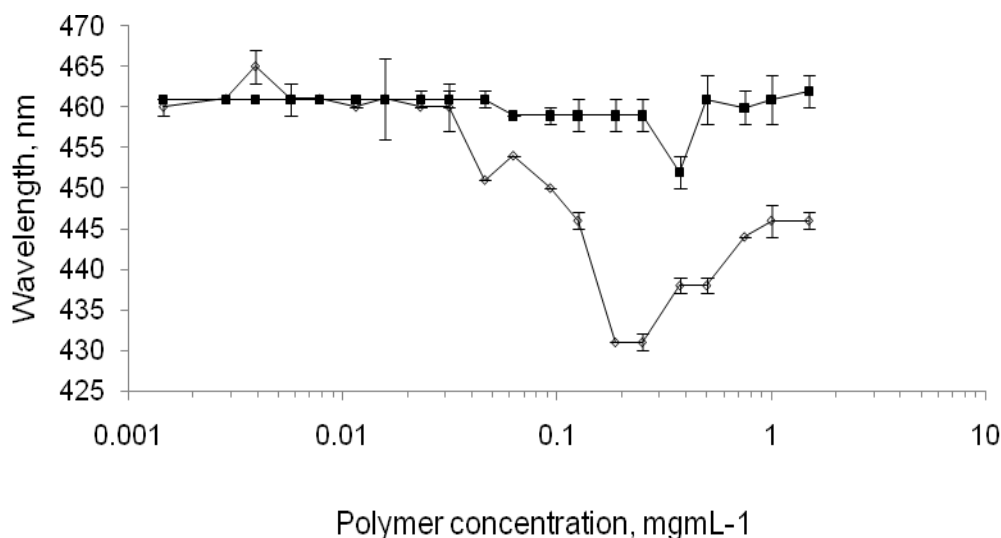
Figure 53. Effect of ◊ QCh$_5$ and ■ QFmoc$_5$ on the peak absorbance of methyl orange at 464 nm (n=3, ave ± SD).

3.3.2.3. *Fluorescent spectra of Fmoc₅*

A possible explanation for the two CAC values obtained by surface tension measurement of Fmoc and Naphth modified polymers could be due the formation of excimers. To further investigate the theory of excimer formation at higher concentrations of Fmoc$_5$, its fluorescent emission spectra was studied (Fig. 54).
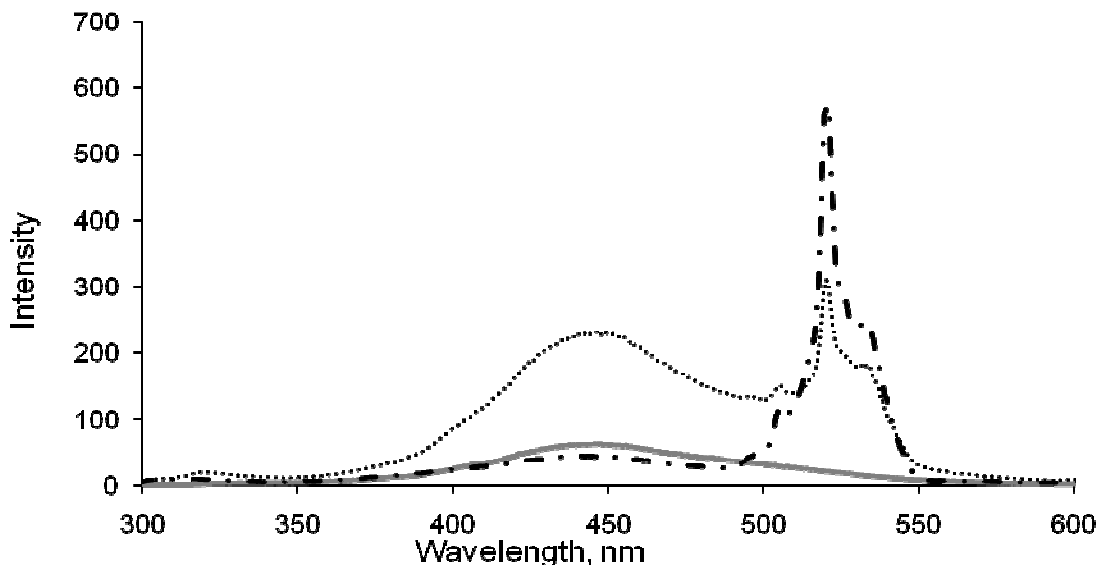
Figure 54. Fluorescent emission spectra of Fmoc$_5$ ——0.02 mgmL^{-1},·········0.4 mgmL^{-1} and _._.._ 1.5mgmL^{-1}, excited at 315 nm.

As the concentration increases (0.02 – 1.5 mgmL^{-1}), the emission peak shifts from 440 nm across the range of wavelengths to 525 nm. At 1.5 mgmL^{-1} a large peak is observed at 525 nm, however as the concentration decreases to 0.4 mgmL^{-1} this peak diminishes until it completely disappears at 0.02 mgmL^{-1}. The spectra produced gives a good indication that excimer formation has occurred as peak shift is a common occurrence [229,230,231]. It was therefore also assumed that excimer formation was occurring with Naphth-PAA polymers since they have similar structures and also exhibited two CAC values when surface tension measurements were carried out.

3.3.3. *Transition electron microscopy*

The Ch$_5$ micrograph (Fig. 55) showed the nano particles to be less than 100 nm in size. Traditionally at this size it would be expected to see polymeric micelles, however the particles appeared to be much more dense in structure suggesting the formation of nano-particles.
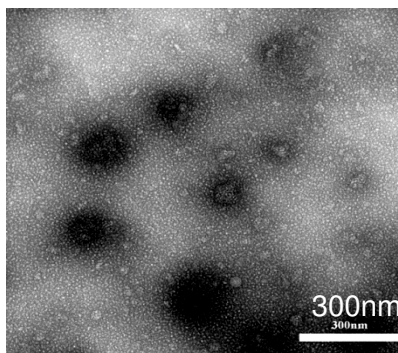
Figure 55.TEM analysis of Ch$_5$ in doubly distilled water (1 mgmL^{-1}).

The Fmoc$_5$-PAA TEM showed that self assemblies formed both at the lower (0.3 mgmL^{-1}) (Fig. 56 a) and the higher (2 mgmL^{-1}) concentrations (Fig. 56 b). The concentrations tested were significant due to the two CAC values observed from the surface tension measurement (0.4 and 1.5 mgmL^{-1}). The self-assemblies at the higher concentration appear to be of larger size (50 nm) than that of the lower concentration sample (25 nm). The TEM of the 0.3 mgmL^{-1} sample suggests that self assemblies are formed at this lower concentration and therefore the first CAC value obtained from the surface tension measurement is a true CAC measurement.
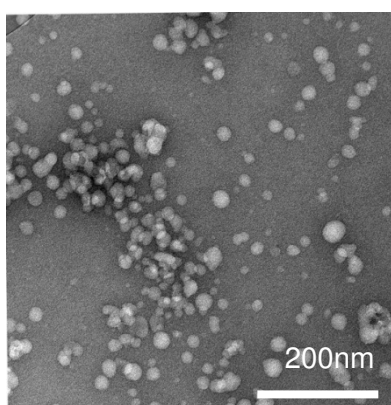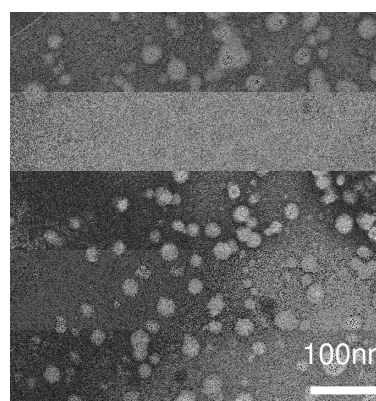
a)   *b)*

Figure 56.TEM analysis of Fmoc$_5$ in doubly distilled water a) 0.3 mgmL^{-1}, b) 2 mgmL^{-1}.

Photon correlation spectroscopy of the Fmoc$_5$ at varied concentration was carried out (Table 12). Table 12 shows that at 0.3 mgmL^{-1} the self-assemblies formed were 247 nm which was much bigger than the TEM result. Perhaps, the large difference in size could be due to the aggregated formed clustering together resulting in a large hydrodynamic radius when analysed by photon correlation spectroscopy.

Table 12. Photon correlation spectroscopy results for increasing polymer concentrations of $Fmoc_5$ in aqueous solution n=3, ave (SD).

Polymer concentration $mgmL^{-1}$	Size (nm) (n=3, ave± SD).	PDI
0.3	247 (1)	0.142 (0.018)
1.0	199 (2)	0.140 (0.053)
2.0	295 (4)	0.169 (0.013)

The self-assemblies decrease in size at higher concentration of 1 $mgmL^{-1}$ (199 nm), the reason for the size decrease can be attributed to the higher hydrophobic content in solution forming stronger hydrophobic interactions with the water thus resulting in more compact aggregation. However at further polymer concentration increase up to 2 $mgmL^{-1}$ the self-assemblies increased in size up to 295 nm. This size increase indicates that as more polymer strands aggregate together at higher concentrations, larger self-assemblies are formed.

3.4. Discussion

The formation of self-assemblies of modified polymers in aqueous environments were characterised and their critical aggregation concentration (CAC) determined.

The hydrophobic pendant group had a direct impact on self-assembly size. This may be due to pendant group exhibiting differing level of hydrophobic interactions [76]. Thus, the higher the level of hydrophobic grafting encourages stronger hydrophobic interaction and hence the formation of smaller self-assemblies occurred [76]. This trend was observed for the 10 % mole grafted polymers in comparison with the 5 % mole grafted (Table 10). Addition of hydrophilic moieties onto the polymer backbone also affected the self-assembly size (Table 10). Apart from $QNaphth_5$, quaternization of the polymers led to larger self-assemblies formed in aqueous environments (however no statistical significance was observed). Perhaps this could be attributed to the permanent positive charge on the polymer backbone decreasing the hydrophobic interaction between the hydrophobic pendant groups and thus forming less compact self-assemblies [76].

Appearance of a hypsochromic shift in the UV absorption of methyl orange allows successful CAC determination. Methyl orange is a well established hydrophobic probe for CAC measurement [3,123,125,203]. However in this case accurate determination was not possible for all the polymers. This was due to the method not being sensitive enough to detect the CAC values or to the aromatic pendant groups possessing an inherent fluorescent nature and therefore masking of the hypsochromic shift occurred [228]. It was

therefore necessary to find a more appropriate method for determination of CAC value for those polymers.

Surface tension measurement is a commonly used technique for the determination of surfactant CMC [117,232,233,234]. PAA substituted with 5% mole hydrophobic groups exhibit different trends in the surface tension confirming the choice of hydrophobic group had a major impact on aggregate formation. Both Fmoc and Naphth polymers appeared to have two CAC values according to the surface tension data (Fig. 47). This is unusual and to the best of my knowledge has not been reported before. The first CAC value observed may be a attributed to intermolecular aggregation as the polymer strands come together to shield the hydrophobic groups from the aqueous environment. The second CAC value observed is thought to be due to excimer formation occurring as more polymer strands come closer together resulting in the stacking of the molecules.

To further investigate the theory of excimer formation at higher concentrations of $Fmoc_5$-PAA, a fluorescent spectrum was run on (Fig. 54). The resultant spectrum showed clearly that as the polymer concentration is increased, the emission peak shifts from 440 nm to 525 nm with increased intensity [235]. The spectral changes resulting upon excimer formation showed the appearance of a new, broader and strongly shifted band to higher wavelengths in the emission spectra. This is due to the charge transfer interaction and stabilisation occurring especially in polar solvents [236].

This phenomenon was unique to these two polymers as they possess a flat stereochemistry, thus tight stacking could occur at higher concentrations. However the cholesterol moiety lacking planarity was too bulky for such stacking to occur. The dansyl group looks similar to the fmoc and naphthalene moieties. However, the sulphur – oxygen double bonds (sulphoxide) give a 3D structure, thus preventing any stacking.

The addition of the hydrophilic groups onto the PAA backbone enhances the solubility of the modified polymer due to the presence of a permanent charge. This phenomenon has previously been reported for both PAA and chitosan quaternary derivatives [76,237]. This helps to increase the aggregation of the modified polymers at lower concentrations due to an increased solvation layer, thus lowering the CAC value.

Measurement of surface tension of $QDansyl_5$, $QNaphth_5$, $QFmoc_{10}$, $QDansyl_{10}$ and $QNaphth_{10}$ yielded unexpected results. Upon quaternization, the compounds showed no change in surface tension from water (0.072 Nm^{-1}). Thus no CAC occurred within the range of concentrations tested (0.0145 - 3 $mgmL^{-1}$). The CAC could either be lower than 0.0145 $mgmL^{-1}$ or the phenomenon was due to the formation of intramolecular aggregates (Fig. 57) [238,239,240].
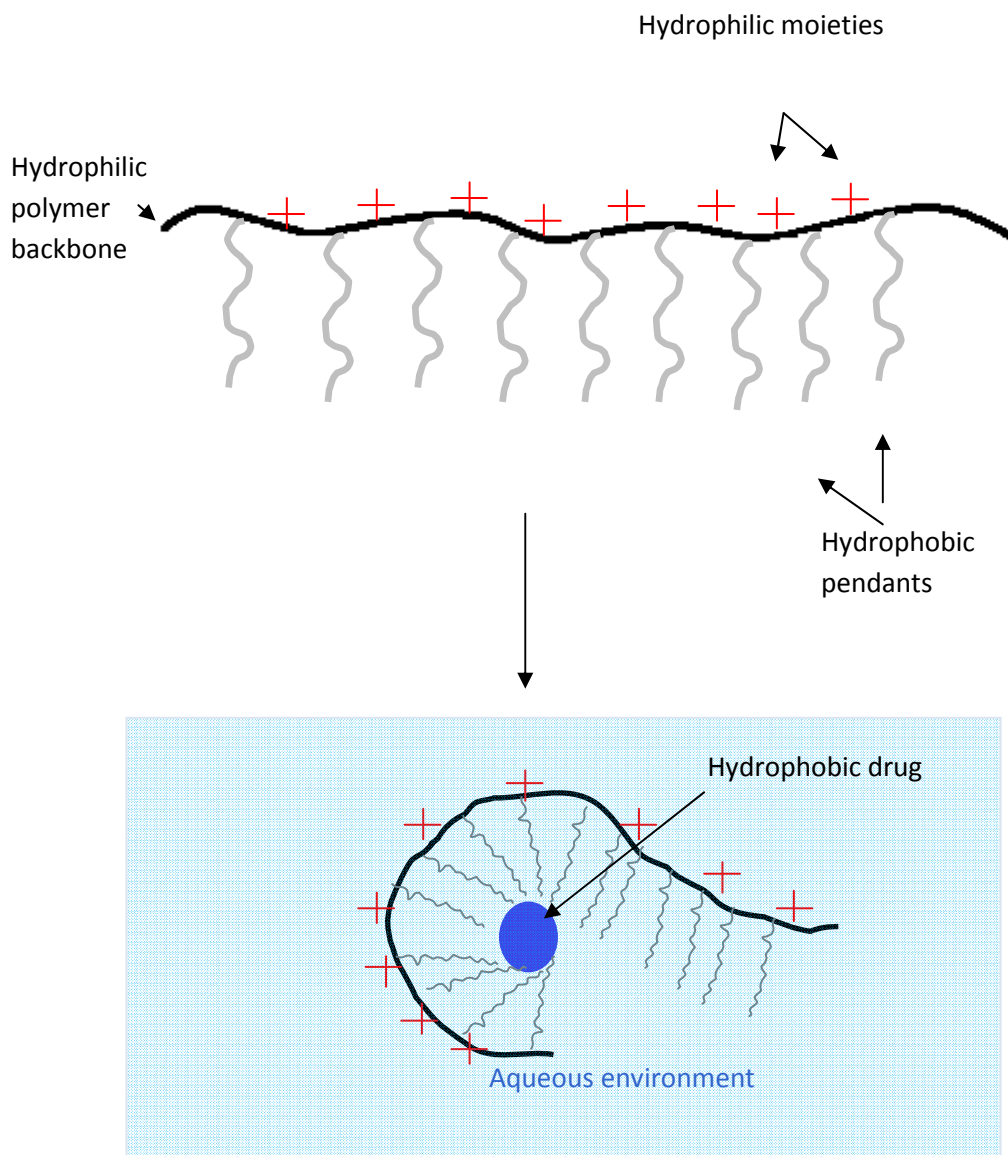
Figure 57. Schematic representation of intramolecular formation of quaternized polymers in aqueous solution.

Intramolecular aggregates are formed when one lone polymer strand aggregates with itself to form a self-assembly. The positive charge of the quaternary ammonium moiety could be enough to initiate intramolecular aggregation at very low polymer concentrations therefore the surface tension of the solutions are unaffected (Fig. 49). Interestingly, the addition of the quaternary ammonium ion, eliminated the two types of aggregation formation observed between the Ch and Dansyl and the Fmoc and Naphth polymers. The aggregation differed due to the formation of excimers within the self-assemblies of the Fmoc and Naphth polymers due to the planar nature of the hydrophobic pendant groups. However with formation of intramolecular aggregates in the quaternary polymers no CAC values were observed and it was assumed the aggregation formation was consistent for all quaternized10 % grafted polymers whereby no excimer formation occurred.

In general the CAC values achieved in this work were higher than others quoted in the literature for polymeric micelles [215, 241,242, 243]. This may be attributed to charge repulsion forces due to the ammonium ion preventing the polymer strands coming

together. In addition, this could be due to increased steric repulsion forces between the bulky nature of the hydrophobic pendant groups compared to the straight chain alkyl molecules traditionally used [244].

The electron micrograph of Ch_5 TEM (Fig. 55) and $Fmoc_5$ (Fig. 56) both show that the self assemblies formed in aqueous solution are nano aggregates. The size estimation from the TEM micrographs (Ch_5, <100 nm) were lower than the size found using PCS (Ch_5, 183 nm). This is due to the fact that PCS measures the hydration layer around the particles giving rise to the larger size. Therefore PCS may give more accurate size estimation.

Overall, the size varied little between the modified polymers formed. However the greatest factor affected was the CAC value. This was particularly apparent when conducting the surface tension measurements. The polymers with planar aromatic groups (Fmoc and Naphth), showed two CAC values, whereas the polymers with cholesteryl and Dansyl group only showed one. Interestingly this indicated that the planar aromatic pendant groups and the bulkier pendant groups resulted in the formation of self-assemblies in two very different manners in the aqueous environment.

The surface tension graph for the Ch_5 and for the $Dansyl_5$ showed the presence of only one CAC value (0.093 and 0.5 mgmL^{-1}, respectively) (Fig. 47). Below the CAC values, no self-assemblies formed, while above the CAC values, the surface tension measurement remained constant, even at concentrations of up to 3 mgmL^{-1}. This suggested that only one aggregation mechanism was present, i.e. intermolecular aggregation. The surface tension value varied with hydrophobic pendant group, Ch_5 exhibited a much lower CAC value than the $Dansyl_5$. Lower CAC values often indicated a higher degree of hydrophobicity of the pendant groups, however as previously discussed the dansyl moiety was more hydrophobic than the cholesteryl resulting in greater decrease in surface tension values [227]. Therefore the reason Ch_5 had lowered CAC value can perhaps be attributed to the larger bulky groups coming in closer contact at lower concentrations in solution driving aggregation formation. This aggregation phenomenon was consistent with low molecular weight surfactants which assemble via intermolecular aggregation which possess one CAC value. Intermolecular aggregation, where more than one polymer strand was coming together to shield their hydrophobic groups in a larger self-assembly (Fig. 58).
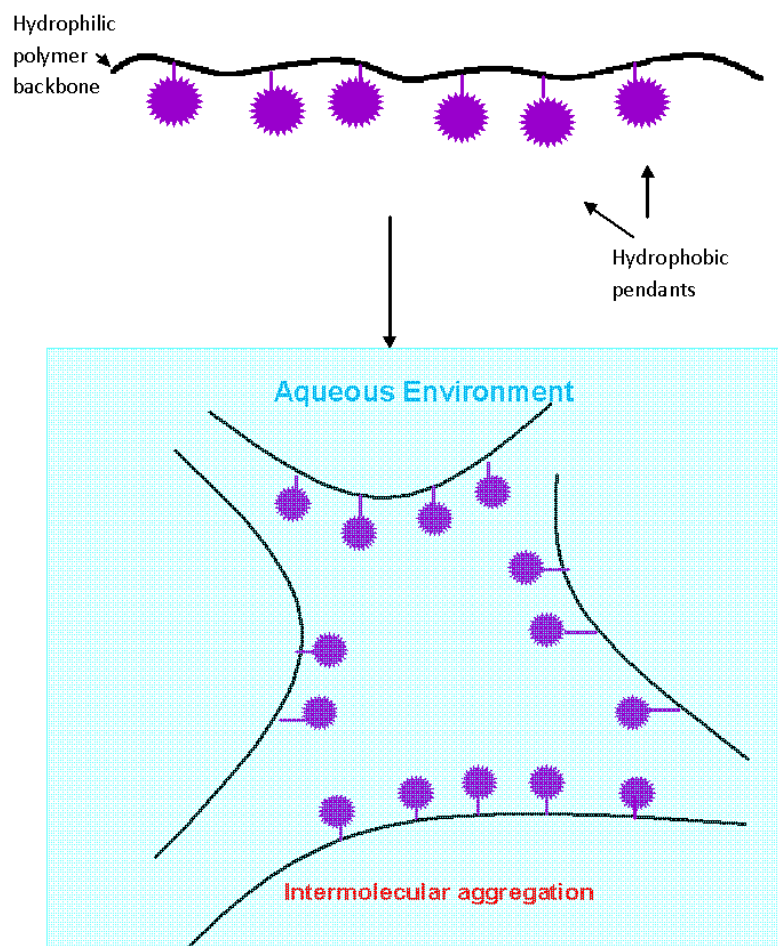
Figure 58. Polymer aggregation model for Ch-PAA and Dansyl-PAA.

The TEM of the Fmoc$_5$ (Fig. 56) showed that at polymer concentrations of 0.3 mgmL^{-1} self assemblies formed, which corresponded with the CAC determination from the surface tension measurement (Fig. 47). Self-assemblies produced at this concentration may be due to intermolecular aggregation of the polymer (Fig. 59). At higher concentrations of Fmoc$_5$ (1 mgmL^{-1}), the self assemblies had decreased in size from 247 nm to 199 nm respectively. This was due to polymer intermolecular aggregation forming excimer stacking of the hydrophobic pendants, making the self assemblies more compact and stable, this was confirmed with the shift of emission on the fluorescent spectra (Fig. 54). The larger size observed at 2 mgmL^{-1} (295 nm) using photon correlation spectroscopy can be attributed to a higher number of polymer strands aggregating together with excimer formation forming more layered and larger self assemblies.
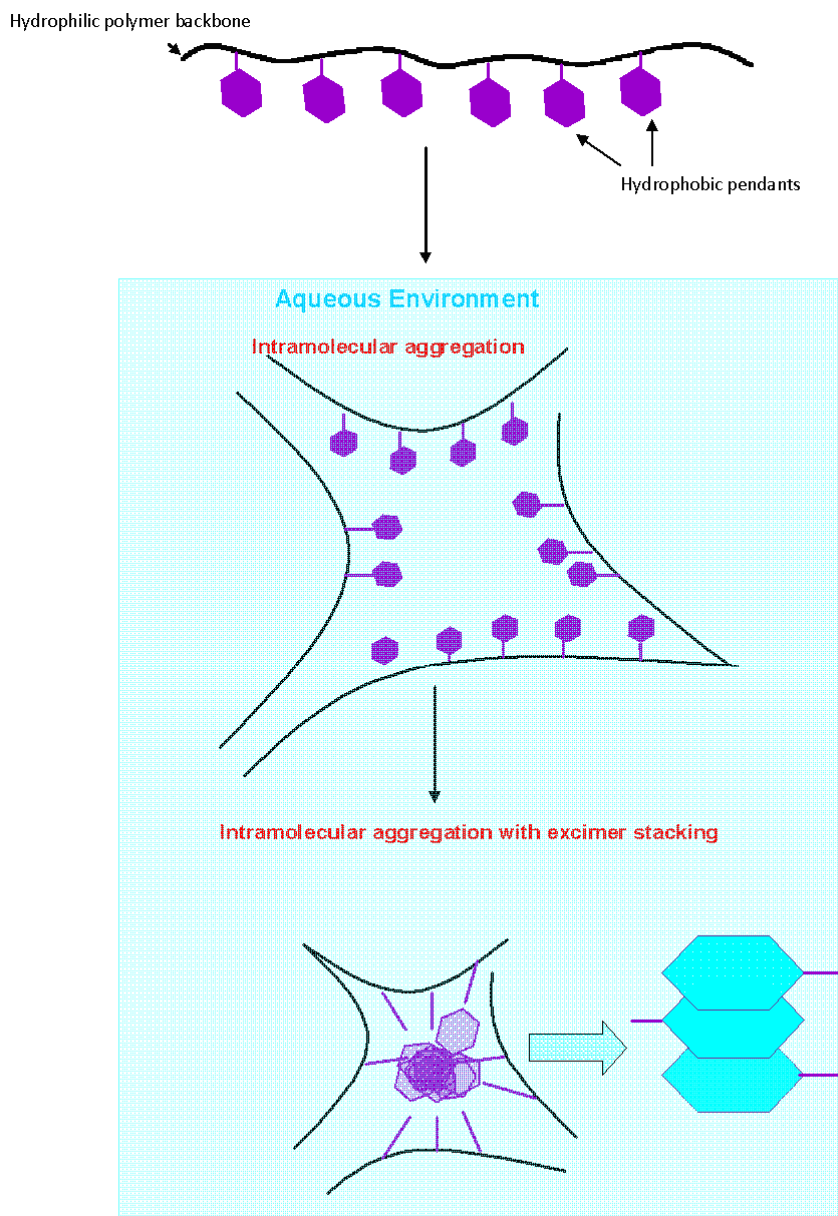
Figure 59. Polymer aggregation model for Fmoc-PAA and Naphth-PAA.

3.5. Conclusion

Novel comb shaped amphiphilic polymers have been successfully synthesised which are able to form nano self-assemblies in aqueous solution. The results showed that the presence of different hydrophobic groups gave rise to significant differences in properties both with the polymer and their self-assemblies. The presence of a permanent positive charge on the polymer backbone due to quaternization also had an impact on the self-assemblies and their properties in the aqueous solution. Further work needs to be carried out to determine the solubilisation capacities of all the modified polymers synthesised.

Chapter Four

Drug Loading of Polymeric self-assemblies

4.1. Introduction

In aqueous environments amphiphilic polymers form polymeric self-assemblies. It has been well documented that hydrophobic drugs can become physically encapsulated inside the lipophilic core of these self-assemblies [70,75,91,158]. The driving force behind such encapsulation can be attributed to hydrophobic interaction forces, whereby the hydrophobic drug favours the lipophilic core of the polymeric self-assemblies.

Traditionally two methods of drug loading in self-assemblies were employed. The first method used was called solvent evaporation [245,246], were both the polymer and drug were dissolved in organic solvents [245]. The solvents were then removed and the resulting residue was reconstituted with water. On the addition of water, self-assembly formation was initiated. The second method involves dialysis [218,247]. The polymer and drug were again both dissolved in organic solvents and placed inside a dialysis membrane and exhaustively dialysed against water [218]. The diffusion of the solvent out of the membrane and water into the membrane drives the formation of self-assemblies. The excess free drug was also removed via diffusion gradient out of the dialysis membrane. However, the self-assemblies were too large and remained inside the dialysis tubing. These methods were effective. However, the use of organic solvents in drug loading is not favourable. This is due to the possibility that residual organic solvents could remain inside the formulation. Organic solvents are toxic and this would lead to problems on administration *in vivo*.

More recently a much simpler and safer technique has been reported using probe sonication [3,76]. Sonication of the amphiphilic polymers in aqueous phase encourages aggregation formation. Upon sonication of the nano-aggregates with the desired hydrophobic drug, easy and efficient drug loading of the self-assemblies occurs. The lack of organic solvents in this drug loading method eliminates the safety concerns associated with the previous methods.

The release of drug from any delivery system is extremely important as it gives an estimation of the *in vivo* fate of the drug [245]. The desired drug release profile is dependent upon both the route of delivery and the therapeutic effect required. In oral delivery of drugs, it is imperative that the drug is not prematurely released in the upper gastrointestinal regions however, it is also essential that the drug is quickly and effectively released and not retained in the carrier vehicle [248].

Polymeric nano-particles have been extensively investigated for their ability to deliver anticancer agents to tumour sites [70,156,249]. Their ability to accumulate in tumour tissues due to the enhanced permeability and retention effect (EPR) gives rise to their huge popularity in this field. Generally drug release from polymeric self-assemblies occurs quicker than from larger micro sized systems [250]. This is due to the increased surface

area of the nano-particles giving rise to higher diffusion rates [250]. These polymeric systems needs to be stable in the blood and should not release the drug prematurely before it reaches its target site. Also it is desirable to achieve controlled release for anticancer drug delivery. This would decrease the likelihood of under or over dosing and the number of administrations and hence increase patient compliance [251]. In order to determine the time taken to release a drug from its carrier system an *in vitro* release study is often performed.

Consistency of drug release and administration dose depends upon the stability of the initial formulation [252]. Every formulation has its unique stability, this is determined by assessing the quality of the formulation under various conditions over periods of time i.e. temperature, light etc [253]. Although nano-particulate formulations have shown widespread potential in drug and gene delivery, their major disadvantage is their poor stability in aqueous form [252,253,254]. These systems may exhibit good short term stability, however particle aggregation and loss of payload may occur over longer periods [254].

Freeze drying has been considered a good technique to improve stability of nano particulate formulations [253]. Freeze drying (or lyophilisation) is a process which removes water from the formulations by deep freezing them followed by sublimation of the ice crystals under lowered pressure [18]. The freeze dried formulations can then be reconstituted with exact amounts of water before administration.

4.1.1. *Model Hydrophobic Drugs*

The model hydrophobic drugs propofol (2,6-diisopropylphenol), prednisolone (1-dehydrocortisone), griseofulvin ((2S)-trans-7-chloro-2',4,6-trimethoxy 6'-methylspiro(benzofuran-2[3H],1'-[2] cyclohexene)3,4'-dione), etoposide (VP-16-213, 4′-Demethylepipodophyllotoxin 9-(4,6-O-ethylidene-β-D-glucopyranoside) and BNIPDaoct (Bisnahthalimidopropyldiamino octane) were used in drug solubilisation studies.

Propofol (Fig. 60) is a commonly used short acting anaesthetic agent with favourable pharmacokinetic abilities [255, 256,257,258]. Propofol has an aqueous solubility of 100 μgmL^{-1} at 25 ºC. Due to its low water solubility it is formulated as oil in water emulsion for intravenous administration (10 mgmL^{-1}). However, intravenous administration of the emulsion proves very painful to patients and often has to be preceded by an initial injection of painkillers [259]. Another problem associated with this formulation is its high number of infections within patients [256,258]. It is therefore desirable to develop an aqueous based formulation for intravenous administration.
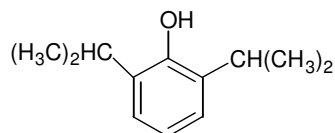
Figure 60.Chemical structure of propofol, molecular weight (MW) = 178 gmol^{-1}, log P = 4.16 [260].

Prednisolone (Fig. 61) is a steroid drug prescribed for the treatment of inflammatory conditions for example arthritis, asthma etc. Prednisolone is slightly soluble in water (215 µgmL^{-1} at 25 °C), which results in reduced oral bioavailability [4,261,262]. In order for a drug to be administered orally, it must first dissolve in the aqueous GI fluid before drug absorption can occur. Prednisolone is currently administered as coated tablets or more commonly in a suspension formulation (3 mgmL^{-1}) [263]. The large dose concentration needed for therapeutic effect leaves an undesirable taste and many side effects resulting in poor patient compliance [263,264]. A formulation is required to increase aqueous solubility and oral bioavailability, thereby reducing administration dosage and unfavourable taste.
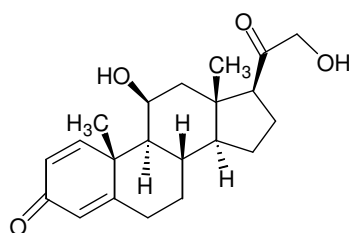
Figure 61.Chemical structure of prednisolone, MW = 360 gmol^{-1}, log P = 1.8 [265].

Griseofulvin (Fig. 62) is a lipophilic drug with an aqueous solubility of 30 µgmL^{-1} at 25 °C [266]. The antifungal properties of griseofulvin are used in both animals and humans for the treatment of dermatophyte infections [267,268,269].
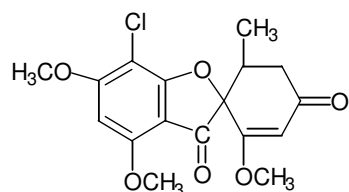
Figure 62.Chemical structure of griseofulvin, MW = 353 gmol^{-1}, log P = 2.2 [272].

The hydrophobic nature of the drug results in low solubility in GI tract resulting in poor oral bioavailability [265,270]. Currently griseofulvin is administered orally in microcrystalline preparations with 500-1000 mgday^{-1} doses prescribed [269]. However, a great deal of intersubject and intrasubject variation is experienced, perhaps due to erratic and incomplete absorption of the drug in the GI tract [271]. This results in poor patient dosing which may lead to some patients being under dosed while others may be over dosed. A formulation used to improve the aqueous solubility of griseofulvin could potentially

increase its bioavailability [271]. This would result in lower dosages and a higher dose consistency compared to the current market formulations.

Etoposide (Fig. 63) is one of the most efficient antineoplastic chemotherapeutics used today [273,274]. The drug acts as a topoisomerase II inhibitor [274]. DNA topoisomerases are enzymes found in the cell nucleus which allow rearrangement of its DNA by making transient breaks in the DNA strand [274]. The inhibition of topoisomerase II results in the death of cancerous cells [274]. Clinically etoposide is used for treatment of lung, ovarian and testicular cancer [273,275,276]. Etoposide has a low aqueous solubility of 148-153 μgmL^{-1} [276]. The drug is currently formulated in a cosolvent formulation for parenteral routes. However, its poor aqueous solubility has led to precipitation upon dilution *in vivo* [274,276].
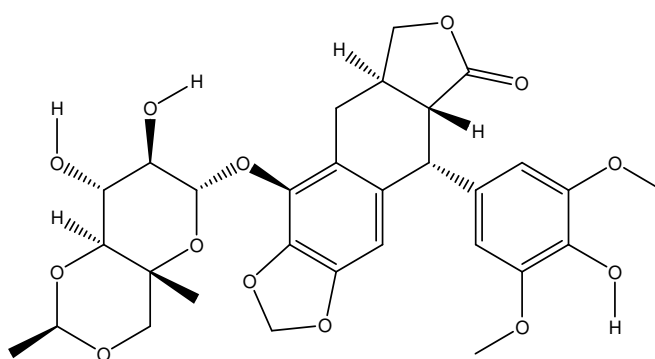
Figure 63.Chemical structure of etoposide, MW = 589 $gmol^{-1}$, log P = 0.698 [277].

BNIPDaoct (Fig. 64) is a novel anticancer agent from the bisnaphthalamidopropyl series designed by Oliveira and colleagues [278]. Bis-naphthalimide derivatives have been reported to possess great potential as cytotoxic drugs for treatment of cancer [278,279,280,281,282]. However the compounds exhibited poor solubility in aqueous solutions [282]. BNIPDaoct showed negligible aqueous solubility and as a result harsh solvents such as DMSO have been needed in order to get the drug into solution [278]. A formulation is required to enhance aqueous solubility of BNIPDaoct thus improving its antitumor activity and making it more efficient. BNIPDaoct had to be synthesised for this study as the novel nature of the drug means it is not commercially available (Appendix 5.0).
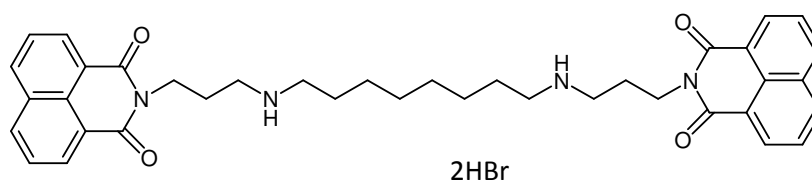
Figure 64.Chemical structure of BNIPDaoct, MW= 780.58.

4.1.2. *High performance Liquid Chromatography*

High performance liquid chromatography (HPLC) is perhaps one of the most important analytical tools used in the pharmaceutical industry today. Its uses span across a range of applications from drug discovery to formulation development and beyond. HPLC allows the separation of compounds on the basis of transport of molecules by a mobile phase through a stationary phase known as a column [283].

Reverse phased (RP) HPLC employs a non polar stationary phase such as carbon or silica and a polar mobile phase. Separation of compounds occurs dependant on the hydrophobicity of the molecules [283]. Hydrophobicity is governed by polarity and size of the molecule. The larger and less polar compounds are retained on the column for longer with the smaller polar molecules being eluted first. The versatility of this technique allows the separation of polar, non-polar and ionisable compounds, whereby increasing the polarity of the mobile phase increases the retention time of non-polar molecules in the column.

4.1.3. *Aims and Objectives*

The aim of this study focuses on the ability of amphiphilic poly(allylamine) (PAA) comb shaped polymers to form polymeric self-assemblies capable of solubilising hydrophobic compounds. HPLC analysis will be carried out to determine the maximum drug loading capacity of the polymers for each of the 5 drugs (propofol, prednisolone, griseofulvin, etoposide and BNIPDaoct). The optimal formulations will be characterised using photon correlation spectroscopy (PCS), fourier transform infrared spectroscopy (FTIR) and transmission electron microscopy (TEM). *In vitro* drug release profiles will be determined by HPLC. The formulations will be freeze dried. A stability study over one month will be carried out to determine optimal storage conditions for the freeze dried and solution formulations.

4.2. Materials and Methods

4.2.1. *Materials used*

Material	Supplier
Modified PAA polymers	Synthesised in Chapter Two
Propofol	Sigma-Aldrich Co., UK
Prednisolone	Sigma-Aldrich Co., UK
Griseofulvin	Sigma-Aldrich Co., UK
Etoposide	Sigma-Aldrich Co., UK
BNIPDaoct	Synthesised in section 4.3.1
0.45µm GDX PVDF filters	Whatman, UK
HPLC grade methanol	Fisher Scientific, UK
HPLC Grade acetonitrile	Fisher Scientific, UK
Highly purified water	MillexQ system (UK)
Orthophosphoric acid	Sigma-Aldrich Co., UK
Potassium dihydrogen phosphate	Sigma-Aldrich Co., UK
Octane sulfonic acid	Sigma-Aldrich Co., UK
Anhydrous sodium acetate	Sigma-Aldrich Co., UK
Phosphate buffered saline	Fisher Scientific, UK

4.2.2. *Methods*

4.2.2.1. *Synthesis and Characterisation of BNIPDaoct (Bisnaphthalimido propyl diaminooctane)*

Fig. 65 shows the reaction pathway for the synthesis of BNIPDaoct. The reactions were carried out stepwise with the product from each step being fully characterised to ensure completion of the reactions and the purity of the compound. For synthesis method see Appendix 5.0.
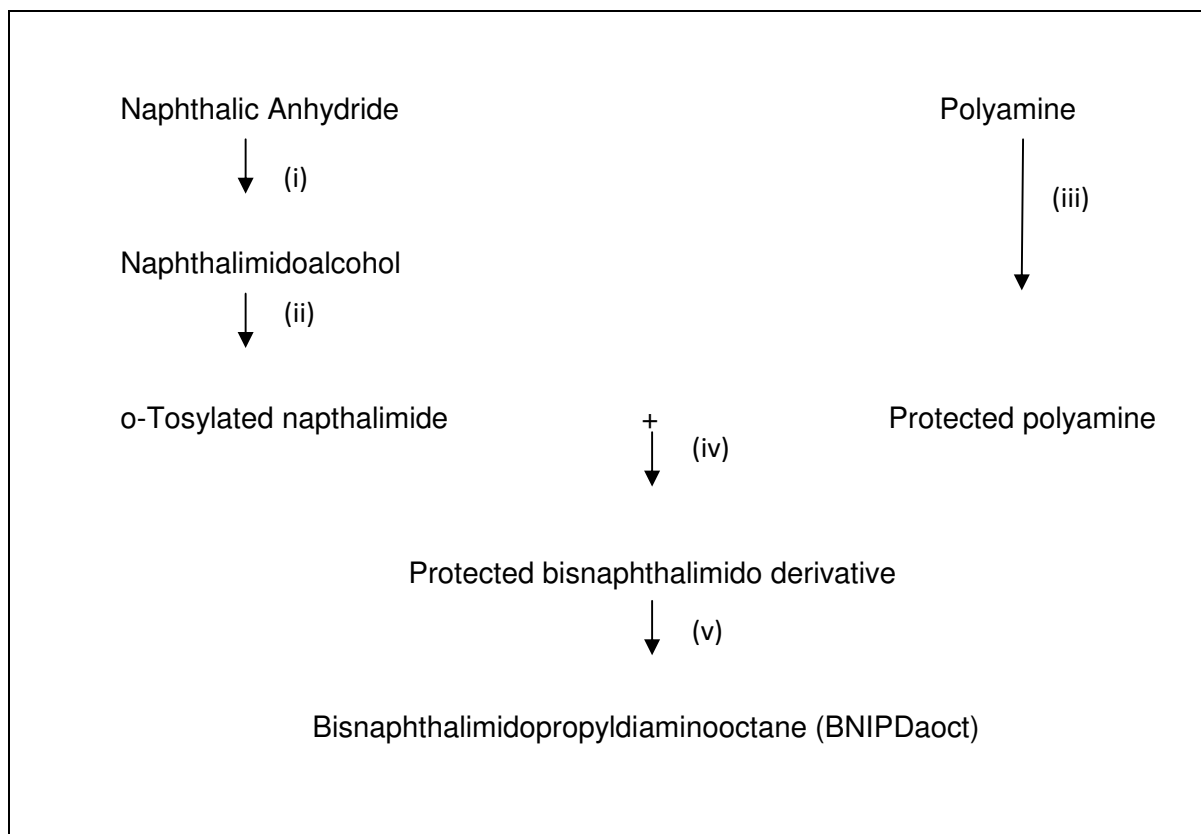
Figure 65. Synthetic pathway for BNIPDaoct.

4.2.2.2. *Drug Loading of Nano-particles*

Polymer solutions of 1 mgmL^{-1}, 3 mgmL^{-1} and 6mgmL^{-1} were made up in deionised water and probe sonicated for 10 min to ensure aggregation of the self-assemblies was achieved. The hydrophobic drug was added in 1:1, 5:1 and 10:1 initial drug:excipient weight ratios and the drug-polymer solutions were probe sonicated for a further 10 min to ensure maximum encapsulation was achieved. After cooling to room temperature, the solutions were filtered using 0.45 μm syringe filters (with prefilters) to ensure any excess unencapsulated drugs were removed.

4.2.2.3. *Determination of Drug Loading Capacity*

4.2.2.3.1. *Solubilisation of Propofol*

The drug loading capacity of the self-assemblies was determined using high performance liquid chromatography (HPLC) (Shimadzu prominence UFLC, UK), as previously reported by Qu and colleagues [203]. A RP Zorbax ODS 250 mm x 46 mm x 5 μm HPLC column (Hichrom, UK) was used with flow rate of 1 mLmin^{-1} (80:20 v/v methanol:water) in an isocratic mode. The samples were diluted with mobile phase and 20 μL was injected onto the column. The resultant peak at 7 min was analysed at 229 nm (Shimadzu prominence UFLC, UK). The amount of propofol present in the samples was determined by comparing to a standard calibration carried out previously with propofol dissolved in methanol (4 μgmL^{-1} – 250 μgmL^{-1}), R^2 = 0.999.

4.2.2.3.2. *Solubilisation of Prednisolone*

The content analysis of prednisolone in the formulation was carried out using an HPLC consisting of a RP Phenomenex C_{18} 150 mm x 4.6 mm x 3.5 µm column with the mobile phase at 1 mLmin^{-1} in an isocratic mode. A UV detector (Shimadzu prominence UFLC, UK) was set at 243 nm. A mobile phase of 36:64 (v/v) acetonitrile:water was run through the column and 20 µL of sample was injected each time. The retention of the peak was 3 min. Prednisolone content in the samples was quantified by comparing to a standard calibration of prednisolone dissolved in acetonitrile:water 36:64 (v/v) (6 µgmL^{-1} – 25 µgmL^{-1}), R^2 = 0.999.

4.2.2.3.3. *Solubilisation of Griseofulvin*

This method was an adaptation of Trimaille's method [284]. The samples were passed through a RP Phenomenex C_{18} 250 mm x 46 mm x 5 µm HPLC column and detected at 293 nm (Shimadzu prominence UFLC, UK). The mobile phase (45:55 v/v) acetonitrile:45 mM potassium dihydrogen phosphate made up in water and pH adjusted to pH3 with orthophosphoric acid) ran at a rate of 1 mLmin^{-1}. The samples were diluted with mobile phase and 20 µL was injected onto the column, the resultant peak at 9.5 min was analysed. The quantification of griseofulvin present in the samples was determined from a standard calibration of griseofulvin in mobile phase (0.6 µgmL^{-1} – 10 µgmL^{-1}), R^2 = 0.999.

4.2.2.3.4. *Solubilisation of Etoposide*

Etoposide content was carried using an adaptation of Dandaundi's method [285]. The formulations were passed through a RP Zorbax ODS 250 mm x 46 mm x 5 µm HPLC column was used with flow rate of 1 mLmin^{-1} of the mobile phase (40:3:57 v/v/v) methanol:acetonitrile:water). The column eluent was monitored at 229 nm (Shimadzu prominence UFLC, UK). The samples were diluted with mobile phase and 20 µL was injected onto the column, the resultant peak at 20 min was analysed for peak area using the HPLC software (Shimadzu prominence UFLC, UK). The drug content was determined using a calibration graph of etoposide in methanol (31 µgmL^{-1} - 500 µgmL^{-1}), R^2 = 0.999.

4.2.2.3.5. *Solubilisation of BNIPDaoct*

BNIPDaoct concentration in self-assemblies was analysed using a RP Zorbax ODS 250 mm x 46 mm x 5 µm HPLC column. The mobile phase consisted of 55:45 (v/v) buffer:acteonitrile with a flow rate of 1 mLmin^{-1}. The buffer for the mobile phase was made up of octane sulfonic acid (0.432 g) and anhydrous sodium acetate (1.64 g) in 200 mL with deionised water with the pH adjusted to pH 4.5. The column eluent was monitored at 234 nm excitation and 394 nm emission, using a fluorescent detector (Shimadzu prominence UFLC, UK). The samples were diluted with the mobile phase and 20 µL was injected onto the column, the resultant peak at 10 min was analysed. A calibration was

carried out by dissolving BNIPDaoct in DMSO:water (50:50 (v/v)) (39 - 625 μgmL^{-1}), R^2 = 0.999.

4.2.2.4. *Sizing of Nano-aggregates*

Size measurements were determined for drug formulations using photon correlation spectroscopy (PCS). This was carried out as previously reported in section 3.2.2.1.

4.2.2.5. *Transition Electron Microscopy*

The optimal formulations were viewed under the transmission electron microscope (TEM) as described in section 3.2.2.3.

4.2.2.6. *FTIR analysis of freeze dried Formulations*

The optimal freshly prepared formulations (as described in 2.2.2.2.3) were freeze-dried. The freeze-dried preparation was run on the fourier transform infrared (FTIR) with a diamond tip and the peaks identified and compared to the spectra obtained for the freeze-dried free drug and unloaded polymer separately.

4.2.2.7. *In vitro drug release*

The formulation (2 mL) was pipetted inside dialysis tubing (MW cut off = 12-14 kDa) and dialysed against PBS *in sink* (200 mL, 0.2 M) at 37 ºC with stirring. At various time points 1 mL of the external PBS was extracted and replaced with 1 mL of fresh PBS. The presence of drug in the collected PBS was determined using HPLC (see sections 4.2.2.3.1 - 4.2.2.3.5), according to the method of Lee *et al.* [286].

4.2.2.8. *Stability of Formulations*

The formulation for each drug was prepared as described in 4.2.2.2. were stored in both their freeze dried and solution forms, in air tight desiccators (55 % humidity) at room temperature and in dark conditions. After set time periods, the formulations were examined by HPLC analysis to quantify the amount of drug encapsulated by the polymeric nano-aggregates. The formulation stability testing was carried out both in solution and in freeze-dried formulations which were reconstituted with water before testing.

4.3. Results

4.3.1. *Synthesis of BNIPDaoct*

BNIPDaoct was successfully synthesised. Characterisation confirmed the pure product was produced and its ^{1}H, ^{13}C and Dept NMR data correlated well with the published data (Appendix 5.0) [278].

4.3.2. *Drug Loading of Nano-particles*

4.3.2.1. *Solubilisation of Propofol*

All polymeric nano-aggregates (1, 3 and 6 mgmL^{-1}) were loaded with propofol in 1:1, 5:1 and 10:1 drug:polymer mass ratio. HPLC was used to determine the maximum loading concentration for each polymer. Fig. 66 shows a typical HPLC spectra for propofol. The retention time for this drug was around 7 min.
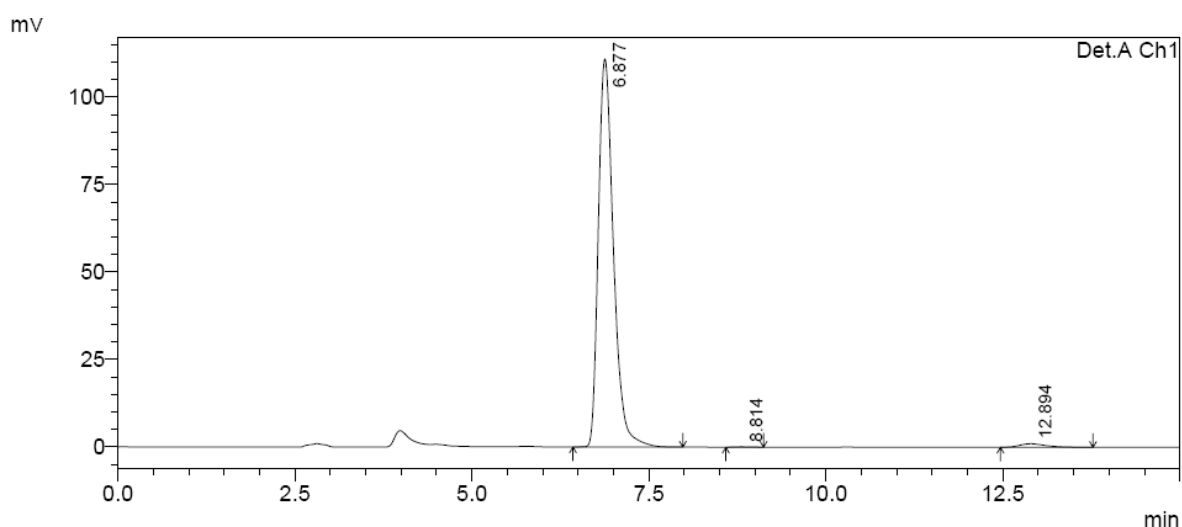
Figure 66. Reverse phase HPLC chromatogram of propofol detected at 229 nm.

The amount of solubilised propofol ranged from 0.19 to 22.4 mgmL^{-1} (QDansyl$_5$ and Dansyl$_{10}$ respectively). The maximum concentration solubilised by each of the amphiphilic polymers is shown in Figure 67. Both Ch$_5$ and Dansyl$_{10}$ (6 mgmL^{-1}, at initial drug:polymer loading ratio of 10:1) proved excellent in the solubilisation of propofol. These polymers improved the aqueous solubility up to 78-fold and 223-fold respectively (Fig. 67). These formulations possessed excipient to drug levels as low as 0.77 and 0.13 respectively. However, the quaternized counterparts of all the modified polymers were not as effective with a maximum of 1.05 mgmL^{-1} propofol solubilised by Ch$_5$.
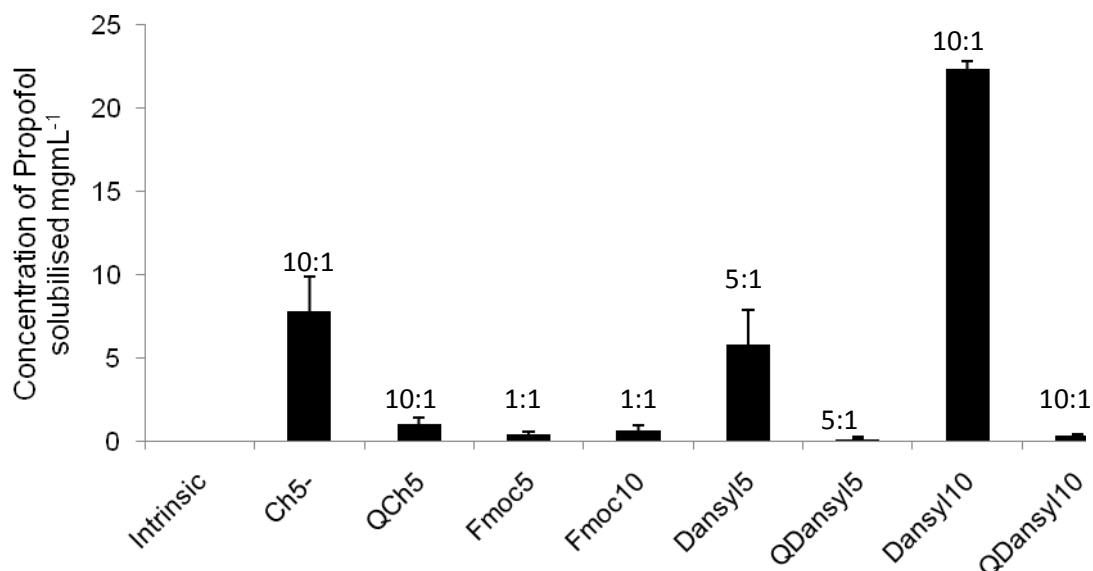
Figure 67. Maximum propofol concentration   solubilised by each modified polymer (6 mgmL^{-1}) at 1:1, 5:1 or 10:1 initial drug:polymer loading ratios determined by HPLC, compared to the intrinsic solubility (n=3, ave ± SD).

Figure 68 shows the relationship between the initial mass feed ratio of drug:polymer. For the cholesteryl self-assemblies (Fig. 68a) a trend is observed whereby the higher the initial drug:polymer loading ratio the greater the concentration of propofol solubilised. Also it is apparent that the higher the polymer concentration, the higher the concentration of propofol in formulation. For Ch$_5$ and QCh$_5$ the optimal level of drug loading was observed with 6 mgmL^{-1} polymer and with 10:1 drug:polymer ratio, however the QCh$_5$ loading was notably poor compared with the Ch$_5$.
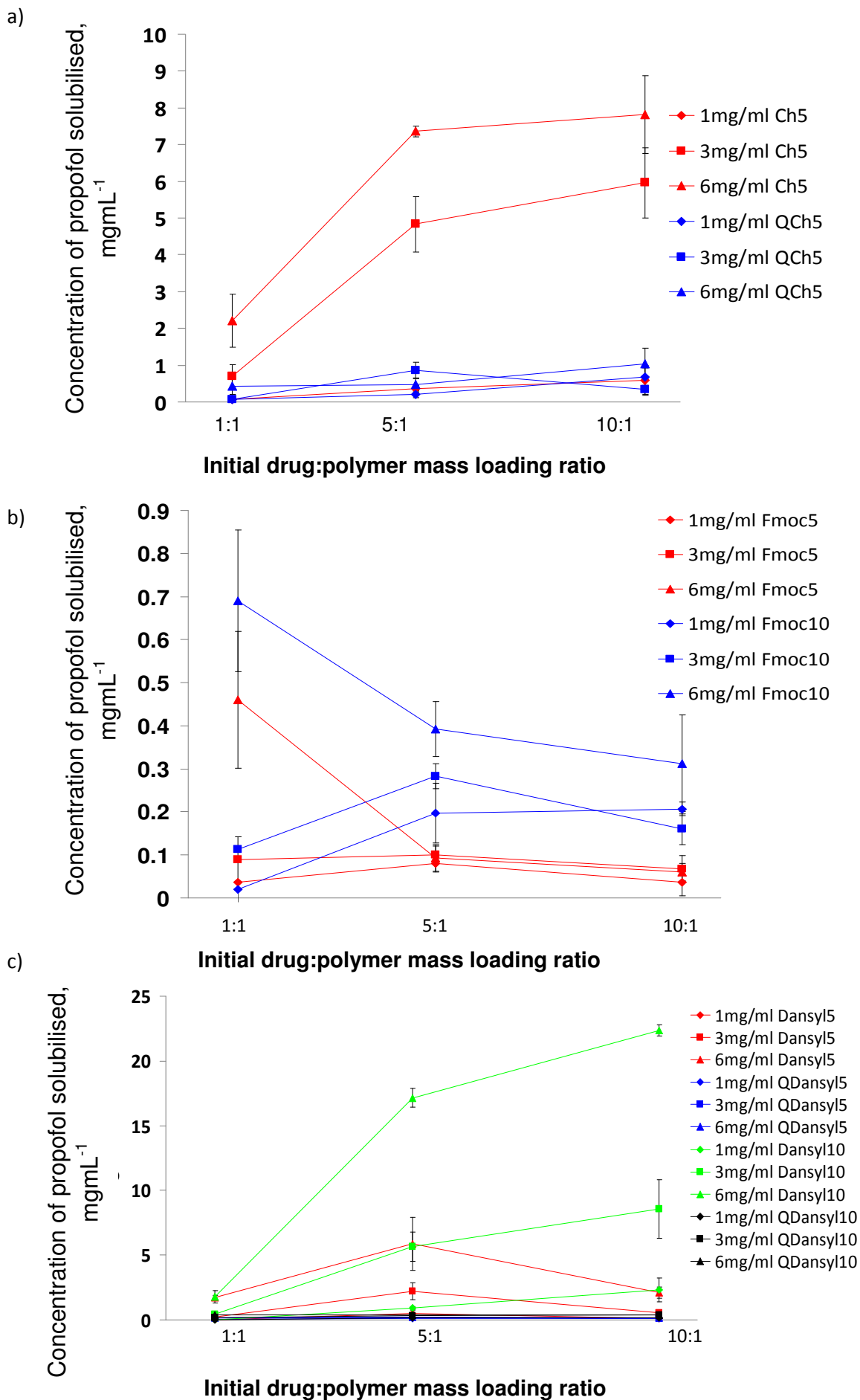
Figure 68. Propofol solubilisation capacity in a) cholesteryl, b) fmoc and c) dansyl self-assemblies in aqueous solution at 1, 3 and 6 mgmL^{-1} with 1:1, 5:1 and 10:1 drug:polymer initial mass loading ratio (n=3, ave ± SD).

Fmoc modified self-assemblies showed a much different trend to the cholesteryl polymers (Fig. 68b). At lower polymer concentrations both the $Fmoc_5$ and $Fmoc_{10}$ appeared to load the maximum concentration of propofol at 5:1 drug:polymer initial feed ratio. However at higher polymer concentration this was not true. At $6mgmL^{-1}$, the optimal propofol loading was achieved at 1:1 drug:polymer ratio. This could be due to a number of reasons. Perhaps this phenomenon was due to the expansion of the self-assembly to accommodate larger quantities of propofol resulting in large aggregates which may have been removed during the filtration process [117]. It was also observed that at higher grafting levels of fmoc, greater propofol solubilisation occurred. This perhaps was due to higher hydrophobic content of polymer allowing greater hydrophobic interaction between the drug and the core without destabilisation of the aggregates. The optimal propofol formulations with $Fmoc_5$ and $Fmoc_{10}$ were at $6mgmL^{-1}$ and 1:1 drug:polymer ratio with 0.46 and 0.69 $mgmL^{-1}$ of drug being solubilised respectively.

The dansyl modified self-assemblies showed an interesting change in drug loading profile with the addition of more hydrophobic content on the polymer (Fig. 68c). At 5 % molar grafting the self-assemblies encapsulated the highest propofol concentration at 5:1 drug:polymer ratio. This was witnessed for all polymer concentrations (1,3 and 6 $mgmL^{-1}$). This could be attributed to the aromatic dansyl groups not being hydrophobic enough to cope with the 'bombardment' of excess drug entering their core causing collapse of their aggregates as witnessed with the fmoc polymers or simply that no more drug could physically fit inside the core. However, at 10 % molar grafting of the dansyl nano-aggregates, the trend observed was similar to that of the cholesteryl polymers. The highest solubilisation of propofol using $Dansyl_{10}$ (22.4 $mgmL^{-1}$) occurred at 6 $mgmL^{-1}$ polymer concentration at 10:1 drug:polymer initial feed ratio. This formulation improved the aqueous solubility of propofol 223-fold.

The excipient:drug ratio is the relative amount of polymer needed to solubilise $1mgmL^{-1}$ of drug. For cholesteryl and dansyl PAA self-assemblies, the excipient:drug ratio decreases with increasing polymer concentration and increasing drug:polymer initial feed ratio of hydrophobic drug (Fig. 69). However, the excipient:drug ratios were independent of the initial drug:polymer loading ratio, whereby the amount of drug initially loaded did not directly affect the actual concentration of drug solubilised. The Fmoc formulations did not seem to follow the solubilisation trend. Whereby, at higher polymer concentrations, lower excipient:drug ratios were observed and increasing the initial drug loading ratio resulted in lower excipient:drug ratios. Higher levels of grafting in fmoc modified self-assemblies show lower excipient:drug ratios due to more drug being encapsulated at higher degrees of grafting as previously discussed.

The quaternized counterparts possess higher excipient:drug ratios, confirming that these polymers were less effective than the non-quaternized polymers, therefore more polymer was needed to solubilise a smaller amount of the drug. This relationship is an inverse relation of the solubilisation data (Fig. 68).
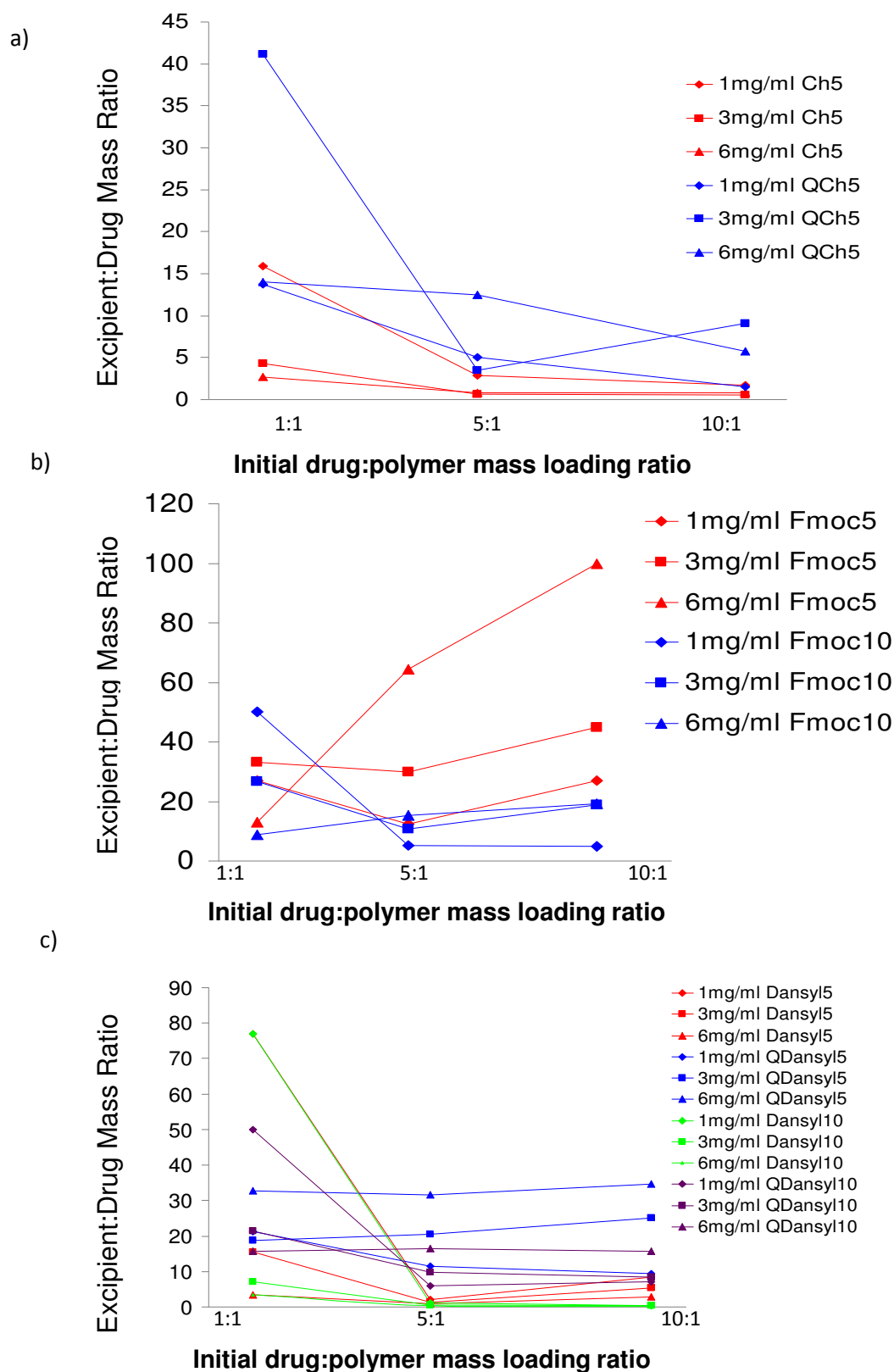
Figure 69. Excipient:drug ratio of propofol formulations in a) cholesteryl, b) fmoc and c) dansyl self-assemblies at increasing drug:polymer loading ratios.

The propofol solubilisation study could not be carried out using the Naphth polymers as their inherent fluorescent excitation was around the same wavelength as the propofol and thus interference was observed on the HPLC spectra (Fig.70). An attempt was made to separate the peaks using a range of techniques including altering the mobile phase and flow rates, however, no peak separation was achieved. Therefore it was decided not to carry out any further solubilisation studies on the Naphth polymers.
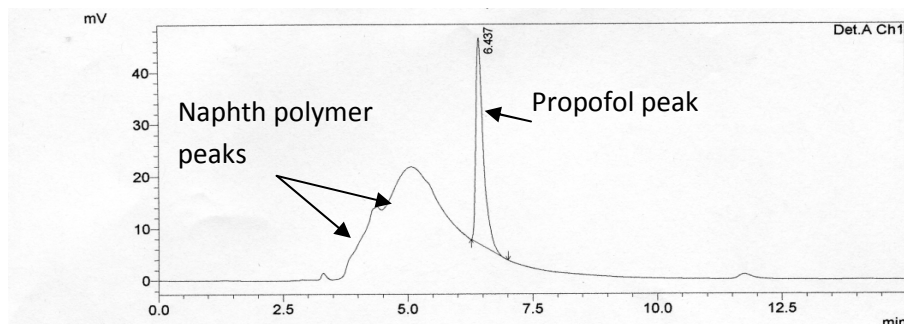
Figure 70. HPLC spectra of Naphth$_5$ and propofol formulation showing overlapping peaks.

4.3.2.2. *Solubilisation of Prednisolone*

The propofol drug loading study helped to deduce which polymers were good at drug loading. This was useful as it helped to narrow the range of polymers used for the prednisolone drug loading. As all the previous quaternized compounds seemed to be inefficient at drug loading, only one quaternized polymer was used for the prednisolone study (QCh$_5$). No Naphth polymers were tested as no previous data could be gained. The polymers were tested at 1, 3 and 6 mgmL^{-1} and using 1:1, 5:1 and 10:1 drug:polymer mass loading ratios.
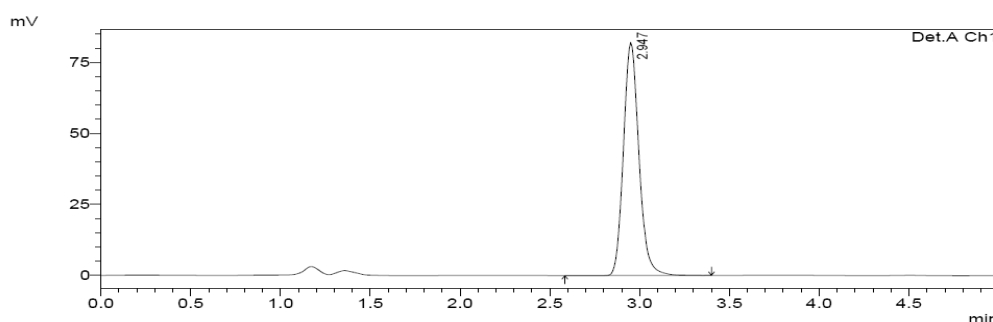
Figure 71. Reverse phase HPLC chromatogram of prednisolone detected at 243 nm.

The retention time for prednisolone was around 3 mins (Fig. 71). Maximum solubilisation achieved ranged from 2.05 to 31.82 mgmL^{-1} (QCh$_5$ and Dansyl$_{10}$ respectively) (Fig. 72). Dansyl$_{10}$ was the most effective system as 31.82 mgmL^{-1} of drug was solubilised which was 100-fold improvement of its aqueous solubility giving and excipient:drug ratio of only 0.19. The solubilisation capacity QCh$_5$ (2.05 mgmL^{-1}) was significantly lower than Ch$_5$ (7.05 mgmL^{-1}) consistent with propofol; therefore no further analysis was carried out on the quaternized compounds.

101
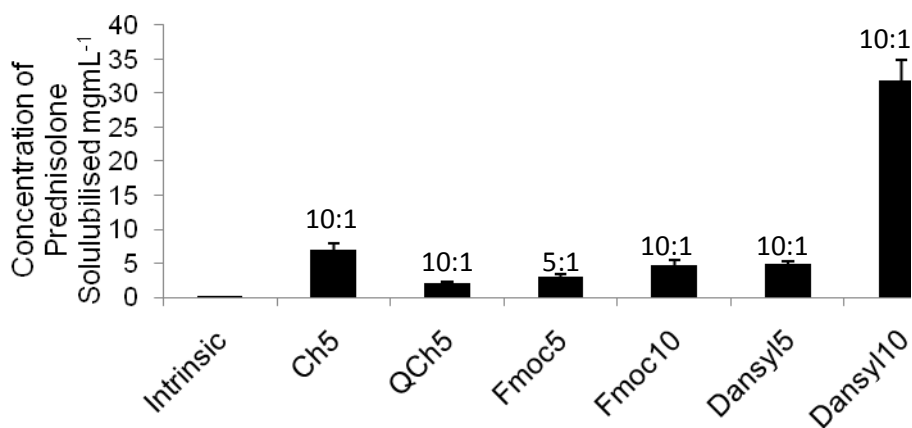
Figure 72. Maximum prednisolone concentration solubilised by each modified polymer (6 mgmL^{-1}) at different 1:1, 5:1 or 10:1 initial drug:polymer loading ratios, determined by HPLC, compared to the intrinsic solubility (n=3, ave ± SD). (Fmoc$_5$ and Dansyl$_5$ polymer concentration 3 mgmL^{-1}).

Figure 73 shows the concentration of prednisolone solubilised at each concentration (1,3 and 6 mgmL^{-1}) and drug:polymer ratio. In general the prednisolone loading of the self-assemblies generally increased with increasing polymer concentration except Fmoc$_5$ and Dansyl$_5$. Increasing initial drug:polymer mass loading ratio, resulted in lower excipient:drug ratio's as total drug encapsulated increased (Fig. 74). This trend correlated well with the trend observed for the propofol solubilisation study. Fmoc$_5$ proved an exception to the trend as its maximum drug loading was at 3 mgmL^{-1} and at 5:1 initial drug:polymer loading ratio. Perhaps as previously discussed for the propofol solubilisation the Fmoc$_5$ hindered drug solubilisation at higher concentrations due to excimer formation or excess drug entering the hydrophobic core resulted in core destabilisation and ultimately collapse of the self-assembly.

The excipient:drug ratios for prednisolone formulations (Fig. 74) formed unique patterns. For Ch$_5$ (Fig. 74a) at the highest polymer concentration of 6 mgmL^{-1} the excipient:drug ratio appeared to be dependent on the initial drug:polymer mass loading ratio. This meant that the higher the initial feed of the hydrophobic drug to the polymer self-assemblies, the more efficient the aggregates became at encapsulating the drug within their lipophilic core. This phenomenon was also witnessed for 1 mgmL^{-1} QCh$_5$. The rationale behind this dependant drug loading is that with increasing drug content a greater driving force for hydrophobic interactions is experienced and ultimately drug encapsulation is increased thus decreasing the excipient:drug ratio. For all other Ch$_5$ and QCh$_5$ polymer concentrations the excipient:drug ratio appeared independent whereby the initial feed of drugs did not influence the encapsulation efficiency of the self-assemblies. This phenomenon is not well understood however it may be due to external forces determining the drug loading ability of the self-assemblies such as steric hindrance, core stability etc.

For all the concentrations of $Fmoc_5$ and $Fmoc_{10}$ the excipient:drug ratio was independent of the initial drug:polymer mass loading ratio (Fig. 74b). However, at 1 $mgmL^{-1}$ $Fmoc_5$ the graph showed an interesting trend. The excipient:drug ratio appeared to be dependant up to 5:1 mass loading ratio. However with further increase of the loading ratio to 10:1 the efficiency of the system remained constant (and the graph plateaued). A similar trend was observed for 6 $mgmL^{-1}$ $Dansyl_5$ however at the increased 10:1 loading ratio the efficiency decreased i.e. Higher excipient:drug ratio. The reason for this trend is unknown, however, it could be attributed to the previously discussed 'limiting factors' in the drug loading of these self-assemblies. Whereby, the formation of excimers by the $Fmoc_{10}$ or steric hindrance of the prednisolone within the self-assemblies or destabilisation of the core occurred at increased drug loading ratio. All other concentrations of $Fmoc_5$ and $Fmoc_{10}$ appeared to be independent.

At 3 $mgmL^{-1}$ $Dansyl_5$ and 6 $mgmL^{-1}$ $Dansyl_{10}$ the excipient:drug ratio for prednisolone loading appeared to be dependant upon concentration and initial loading ratio (Fig. 74c). Interestingly for Ch_5 and $Dansyl_{10}$ the polymer concentrations for which a dependant trend was observed, were the concentrations were maximum drug solubilisation occurred (6 $mgmL^{-1}$). This would suggest in order to achieve an efficient system, it is desirable to have a inverse linear relationship between the excipient:drug ratio and the initial drug:polymer mass loading ratio. Whereby, at higher drug loading concentrations, higher drug encapsulation is achieved, thus, lowering the excipient:drug ratio (QCh_5 is an exception to this theory as all of the solubilisation studies showed low drug encapsulation). Not surprisingly the Ch_5 and $Dansyl_{10}$ achieved the lowest excipient:drug ratio, $Fmoc_5$, $Fmoc_{10}$ and QCh_5 were least efficient, this data correlated well with the drug solubilisation data (Fig. 73).
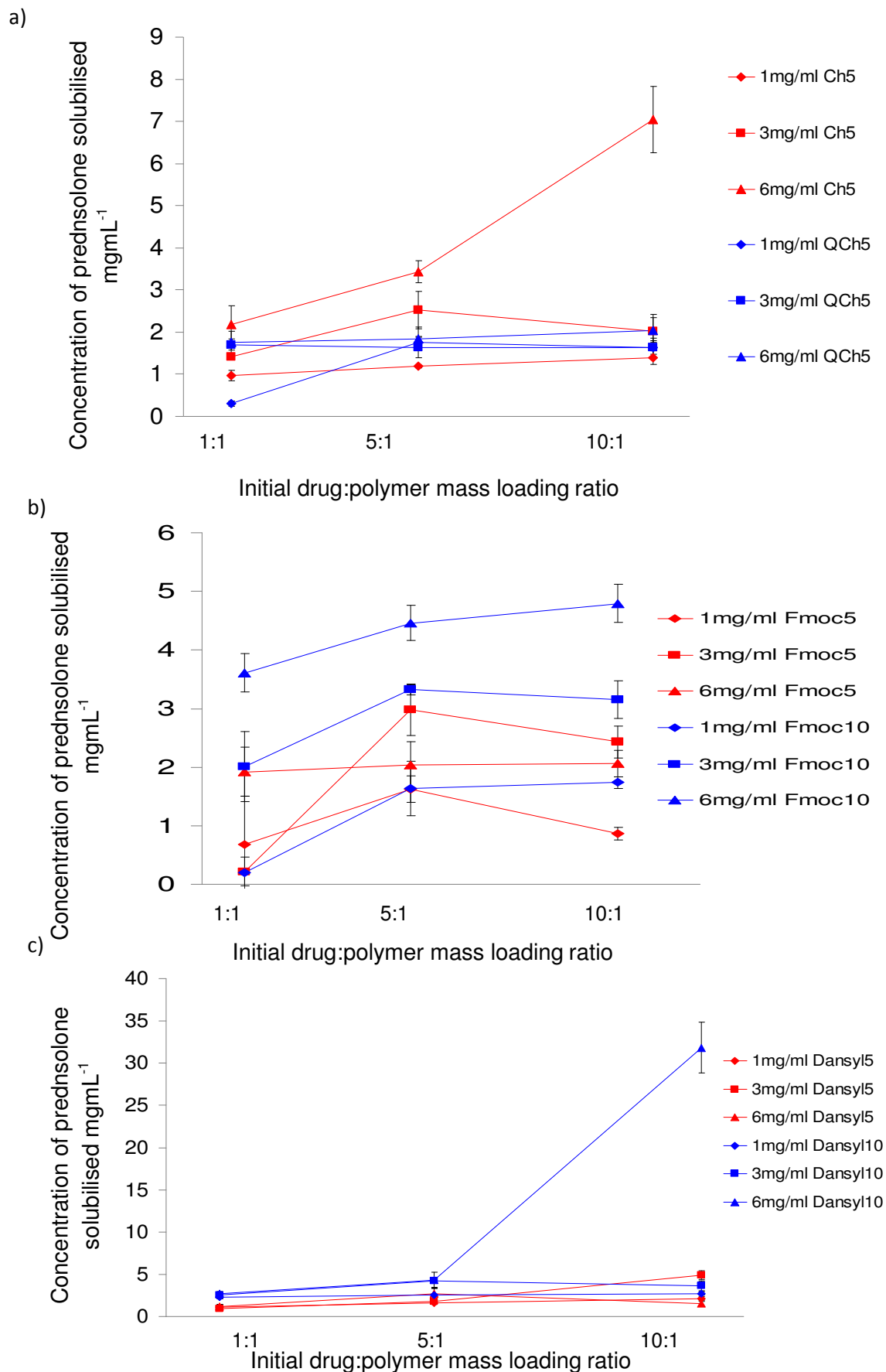
Figure 73. Prednisolone solubilisation capacity in a) cholesteryl, b) fmoc and c) dansyl self-assemblies in aqueous solution at 1, 3 and 6 $mgmL^{-1}$ with 1:1, 5:1 and 10:1 drug:polymer initial mass loading ratio (n=3, ave ± SD).
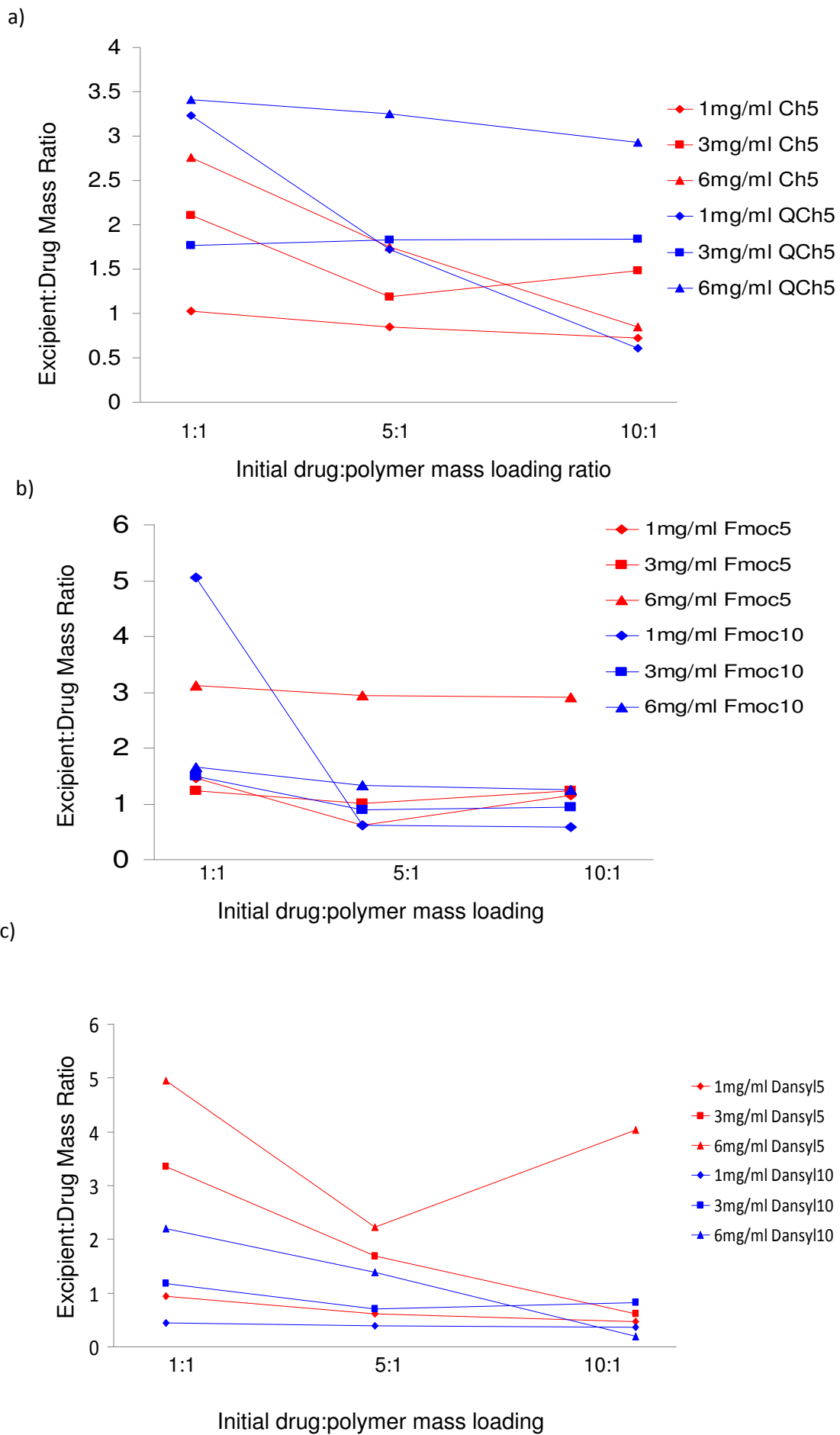
Figure 74. Excipient:drug ratio of prednisolone formulations in a) cholesteryl, b) fmoc and c) dansyl self-assemblies at increasing drug:polymer loading ratios.

4.3.2.3. *Solubilisation of Griseofulvin*

When comparing the solubilisation data for propofol and prednisolone, two polymers consistently stood out as excellent solubilising agents, these were Ch_5 and $Dansyl_{10}$. The optimal initial drug loading ratio and the most effective polymer concentration were chosen based on the previous model hydrophobic drugs. Therefore all subsequent experiments will use these ratios and concentrations for the Ch_5 and $Dansyl_{10}$ polymers.
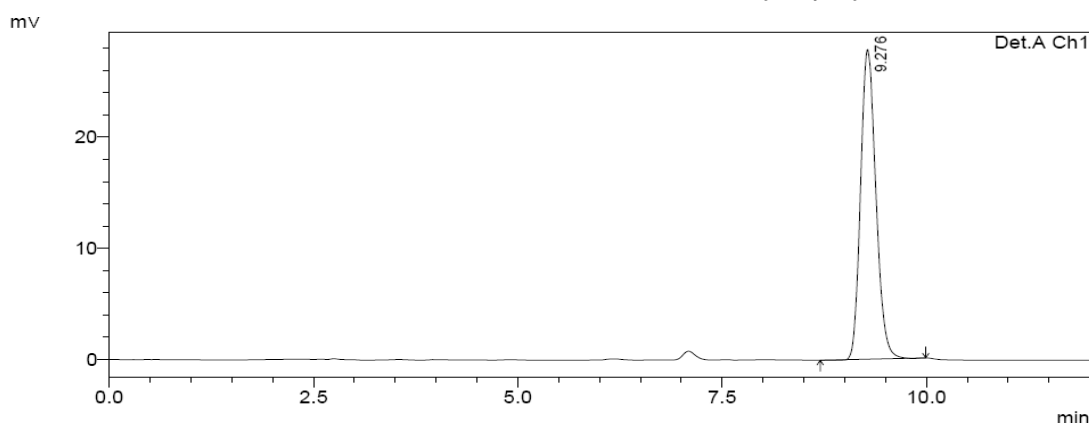
Figure 75. Reverse phase HPLC chromatogram of griseofulvin detected at 293 nm.

The retention time for griseofulvin detection on the HPLC was around 9 min (Fig. 75). Ch_5 and $Dansyl_{10}$ were capable of solubilising 1.2 and 16.7 $mgmL^{-1}$ griseofulvin (Table 13). This was an increase in the aqueous solubility (0.03 $mgmL^{-1}$) by 40-fold and 557-fold respectively. The $Dansyl_{10}$ had an extremely low excipient:drug ratio of 0.34, this result was consistent with the low ratios obtained for the prednisolone and propofol formulations.

Table 13. Griseofulvin loading capacity in modified polymers determined using reverse phase HPLC n=3, ave (SD).

Polymer	Polymer Conc. $(mgmL^{-1})$	Initial Drug:Polymer Mass Ratio	Concentration of Griseofulvin solubilised $(mgmL^{-1})$	Excipient:Drug Ratio after solubilisation	Increment from griseofulvin aqueous solubility
Ch_5	6	10:1	1.200 (0.017)	5.00	40 Fold
$Dansyl_{10}$	6	10:1	16.710 (4.121)	0.34	557 Fold

4.3.2.4. *Solubilisation of Etoposide*
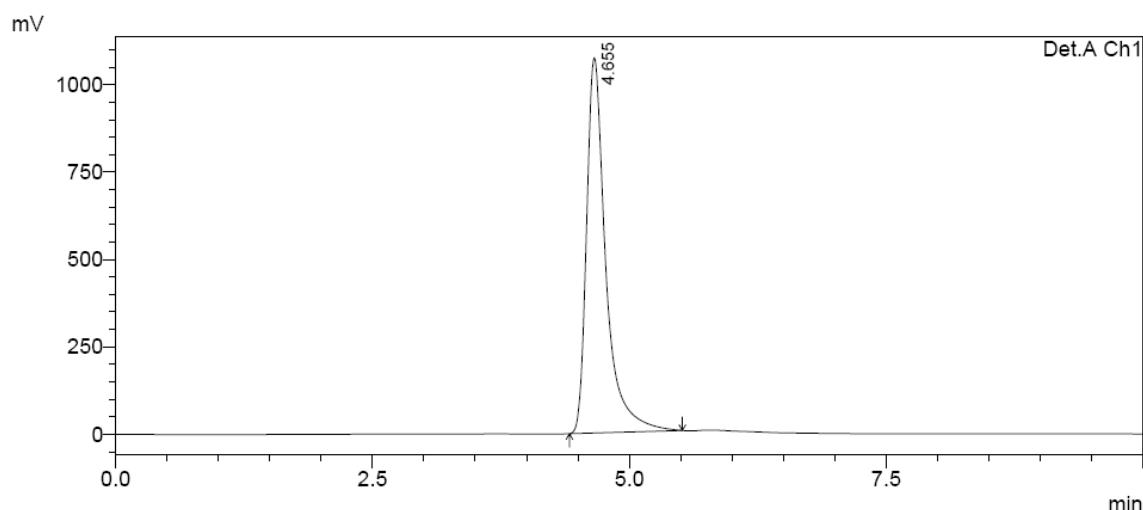
Figure 76. Reverse phase HPLC chromatogram of etoposide detected at 229 nm.

Etoposide was detected at around 5 min (229 nm) (Fig. 76). Table 14 shows that Ch_5 and $Dansyl_{10}$ were capable of solubilising up to 1.0 and 1.9 $mgmL^{-1}$ of etoposide respectively. Consistent with the previous solubilisations studies, $Dansyl_{10}$ was the most efficient with a 13-fold increase from the aqueous solubility of the drug (0.15 $mgmL^{-1}$). However, etoposide solubilisation was relatively lower compared to all the other model drugs (excipient:drug ratio of 3.17 for $Dansyl_{10}$).

Table 14. Etoposide loading capacity in modified polymers determined using reverse phase HPLC for each drug:polymer ratio n=3, ave (SD).

Polymer	Polymer Conc. (mgmL⁻¹)	Initial Drug:Polymer Mass Ratio	Concentration of Etoposide solubilised (mgmL⁻¹)	Excipient:Drug Ratio after solubilisation	Increment from etoposide aqueous solubility
Ch_5	6	10:1	1.020 (0.040)	5.88	7 Fold
$Dansyl_{10}$	6	10:1	1.890 (0.011)	3.17	13 Fold

107

4.3.2.5. *Solubilisation of BNIPDaoct*

The solubilisation study for BNIPDaoct yielded some strange results. Fig. 77 shows an HPLC spectrum for the drug at low concentration (0.039 mgmL^{-1} in DMSO:Water (50:50 v/v)). A signal peak is observed at around 7 min.
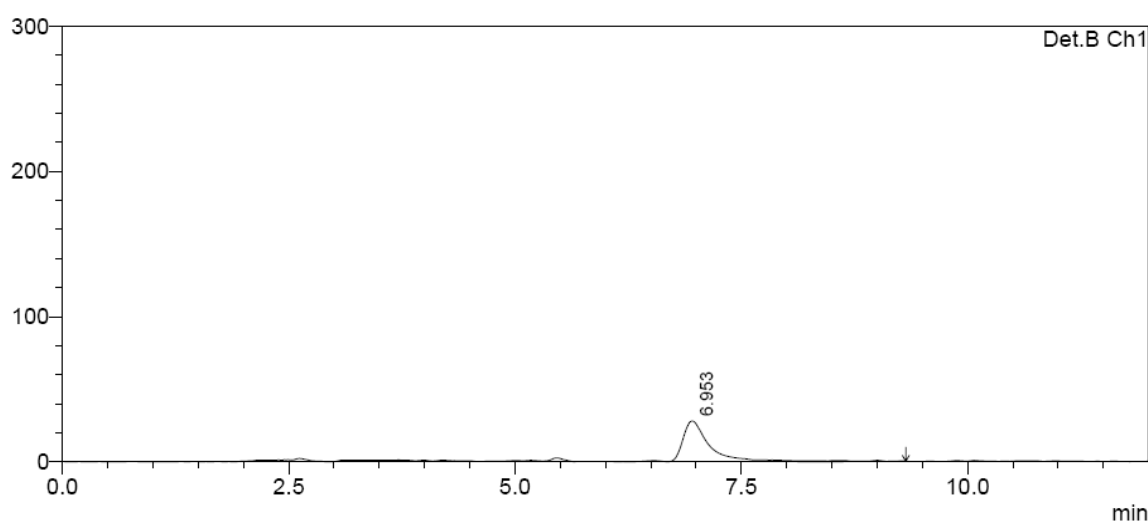
Figure 77. Reverse phase HPLC chromatogram of BNIPDaoct detected at 394 nm emission.

At polymer concentration of 1 mgmL^{-1}, Ch$_5$ was capable of solubilising 0.3 mgmL^{-1} of the drug using 1:1 initial drug:polymer mass ratio (Table 15). Previously all studies to find an aqueous solubility of BNIPDaoct yielded no results as the aqueous solubility was negligible. Therefore the increment increase from aqueous solubility could not be determined. The excipient:drug ratio was 3.33. However on loading the drug at higher polymer concentrations using higher initial drug:polymer mass ratios, the HPLC spectra changed dramatically. Fig. 78 shows the HPLC spectra of 1 mgmL^{-1} Ch$_5$ at 1:1, 5:1 and 10:1 initial drug:polymer mass ratios.

Table 15. BNIPDaoct loading capacity in modified polymers determined using reverse phase HPLC for each drug:polymer ratio n=3, ave (SD).

Polymer	Polymer Conc. (mgmL^{-1})	Initial Drug:Polymer Mass Ratio	Concentration of BNIPDaoct solubilised (mgmL^{-1}) ±SD	Excipient:Drug Ratio after solubilisation	Increase from BNIPDaoct aqueous solubility
Ch$_5$-PAA	1	1:1	0.3 (0.01)	3.33	-

a)

b)

c)
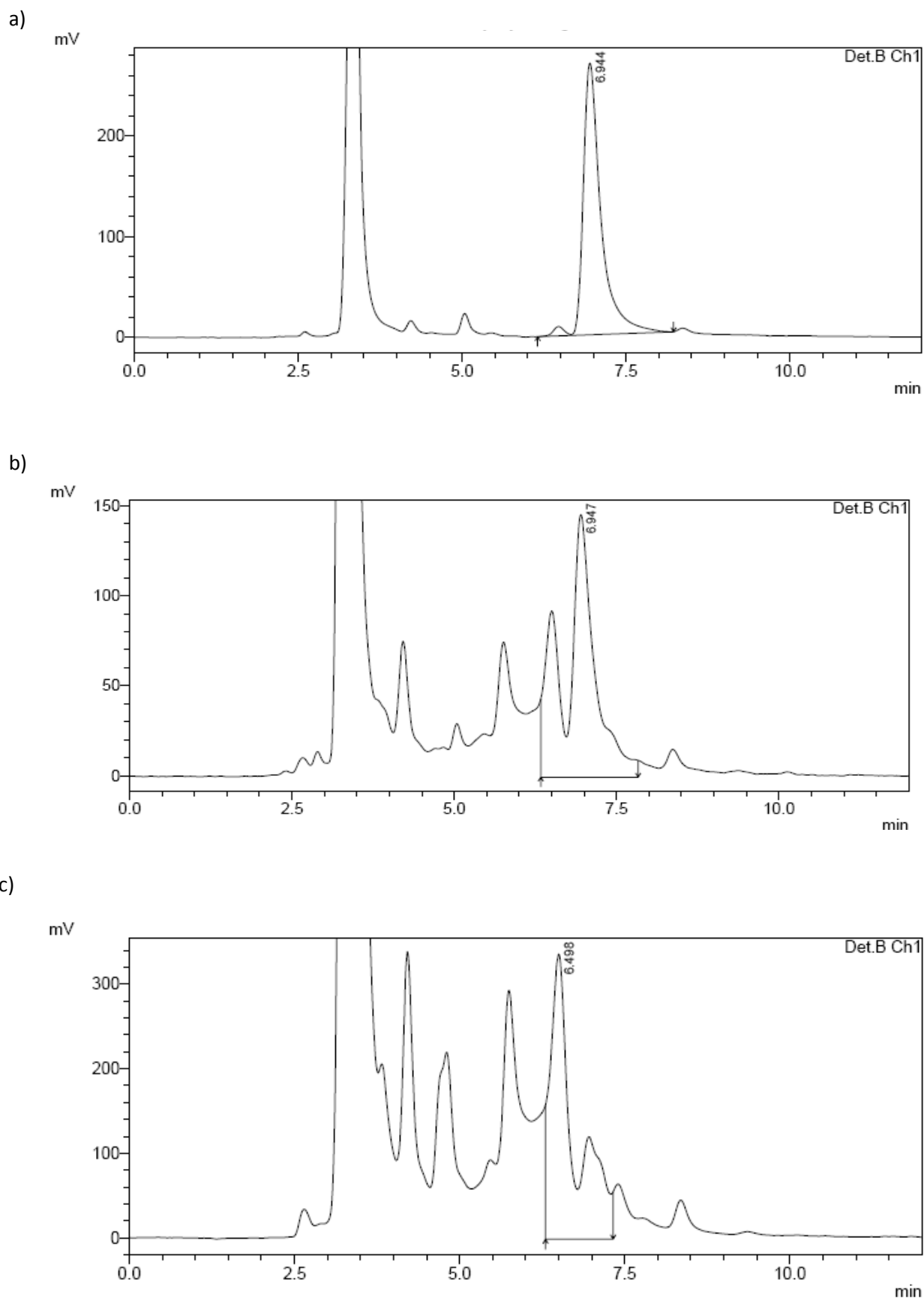
Figure 78.HPLC spectra of BNIPDaoct using 1 mgmL^{-1} of Ch$_5$ at a) 1:1 b) 5:1 c) 10:1 initial drug:polymer mass ratios.

Previous Ch_5 solubilisation studies demonstrated that increased initial drug:polymer mass ratio resulted in increased drug solubilisation capacity. It was therefore assumed that by increasing the initial drug:polymer mass ratio (Fig. 78) of BNIPDaoct, the actual concentration solubilised would also be increased. As the concentration of solubilised drug increased (even upon extensive dilution) additional peaks were observed on the spectra making it inaccurate for determination of drug loading concentration. These extra peaks were observed when using the $Dansyl_{10}$ polymer also. Therefore no further solubilisation data for Ch_5 or $Dansyl_{10}$ could be obtained. However, the assumption made could be visually confirmed as at higher initial drug:polymer mass ratios the formulations appearance changed from translucent white and yellow (Ch_5 and $Dansyl_{10}$ polymer alone respectively) to orange. This change in colour can be attributed to the solubilisation of drug as it was an orange solid compound. The orange colour appeared sequentially darker from 1:1 to 5:1 to 10:1 ratios suggesting more drug had been solubilised.

The reason for this phenomenon is unknown. However, one possible explanation is that higher drug concentrations may result in the formation of drug conformers. Conformers are different structural configurations of the same molecule. These may have been retained at different times on the HPLC column, giving rise to extra peaks. However, since these peaks were not found in the calibration, addition of the peak areas of the hypothesised isomer peaks would be inaccurate.

4.3.3. *Photon correlation spectroscopy*

The hydrodynamic size of optimal formulations for each drug was determined by a photon correlation spectrometer (Table 16).

The Ch_5 alone had a size of 295 nm. Interestingly the pattern of the size measurements seemed to follow the pattern of the drug loading capability. The propofol loaded self-assemblies had the largest amount of propofol solubilised (7.80 $mgmL^{-1}$) and size (666 nm), followed by the prednisolone with solubilisation of 7.05 $mgmL^{-1}$ and a size of 304 nm. The Ch_5 self-assemblies containing griseofulvin were only capable of solubilising 1.2 $mgmL^{-1}$ of drug and the size measurement also followed this trend with a size of only 284 nm. This indicated that the larger the particle size of the loaded self-assemblies, the higher concentration of hydrophobic drug encapsulated. The size of the griseofulvin loaded micelles appeared to be smaller than the unloaded self-assemblies; this possibly suggests a strong interaction was being experienced in the core of the micelle, resulting in a compact formation of the assemblies.

Table 16. Photon correlation spectrometry size analysis of optimal Ch_5 and $Dansyl_{10}$ formulations at 6 $mgmL^{-1}$ with initial drug:polymer mass ratio of 10:1, (n=3, ave).

Polymer / Formulation	Size (nm) mean (SD)	PDI mean ±SD
Ch_5 alone	296 (4)	0.285 (0.004)
Ch_5, propofol	666 (79)	0.376 (0.025)
Ch_5, prednisolone	304 (4)	0.318 (0.014)
Ch_5, griseofulvin	284 (6)	0.209 (0.012)
Ch_5, etoposide	654 (24)	0.392 (0.011)
Ch_5, BNIPDaoct	183 (2)	0.167 (0.001)
$Dansyl_{10}$ alone	126 (8)	0.465 (0.022)
$Dansyl_{10}$, propofol	608 (49)	0.385 (0.009)
$Dansyl_{10}$, prednisolone	350 (4)	0.369 (0.007)
$Dansyl_{10}$, griseofulvin	305 (7)	0.254 (0.007)
$Dansyl_{10}$, etoposide	886 (115)	0.425 (0.012)

The size of the $Dansyl_{10}$ polymer was 126 nm; this was significantly smaller than the drug loaded self-assemblies. The inner hydrophobic core possessed the ability to expand to a higher degree and therefore encapsulate a high drug concentration. The propofol loaded system had the greatest size of 608 nm, followed by the prednisolone loaded system with 350 nm, and with griseofulvin having the smallest size of 305 nm. The size trend observed for the $Dansyl_{10}$ formulations were similar to the trends for the size of the Ch_5 formulations. The formulations loaded with griseofulvin were consistently smaller than for the propofol and prednisolone formulations; however the $Dansyl_{10}$, griseofulvin still has a larger size compared to $Dansyl_{10}$ unloaded self-assemblies which is different from the Ch_5, griseofulvin formulation.

On loading the Ch_5 and $Dansyl_{10}$ self-assemblies with etoposide, both the self-assemblies appeared to experience a large increase in size (Table 16). The Ch_5 (296 nm) increased to 654 nm whilst the $Dansyl_{10}$ (126 nm) increased to 886 nm upon encapsulation the drug. This appeared to be a large increase considering the low concentration of etoposide encapsulated within the formulations (1.02 $mgmL^{-1}$ and 1.89 $mgmL^{-1}$ Ch_5, etoposide and

Dansyl$_{10}$, etoposide respectively). However, the large size of the self-assemblies size can be attributed to the large molecular size of the etoposide drug physically expanding the inner core of the aggregates.

4.3.4. *Negative staining transmission electron microscopy*

Optimal formulations were sent for TEM imaging. The TEM micrographs of the Ch$_5$ and Ch$_5$ formulations (Figure 79) show clearly the formation of aggregates. The Ch$_5$ alone and all the Ch$_5$ formulations appear to form solid nano-particles at 6 mgmL^{-1}. The sizes observed on the micrographs follow a similar trend to the PCS, however, the size of the nano-aggregates observed in the TEM micrographs appear smaller than the results obtained by PCS (Table 16). This may be due to the fact that PCS measures the hydrodynamic size around the particle (including its hydration layer) and thus results in a higher size estimation.

The TEM micrographs of Dansyl$_{10}$ and Dansyl$_{10}$ formulations (Fig. 80) show that nano-particles are formed at 6 mgmL^{-1} of the polymer in solution and the resultant formulations. However, the sizes observed on the micrographs do not follow the same trend as the previous PCS results. The Dansyl$_{10}$, propofol and Dansyl$_{10}$, prednisolone formulation appear to be smaller in size when compared with the Dansyl$_{10}$, griseofulvin formulation. The reason for the change in trend is unknown; however, it may be possible that as a result of sample preparation the nanoparticle collapsed appearing to form smaller particles. The Dansyl$_{10}$, etoposide (Fig. 80 e) appears to have formed clusters, which perhaps accounts for its large size on the PCS.
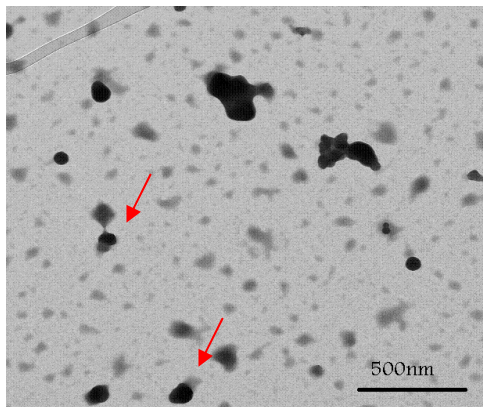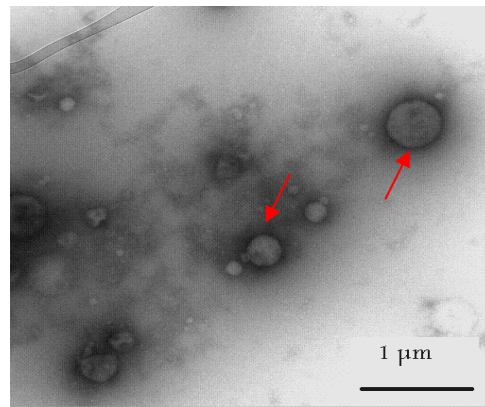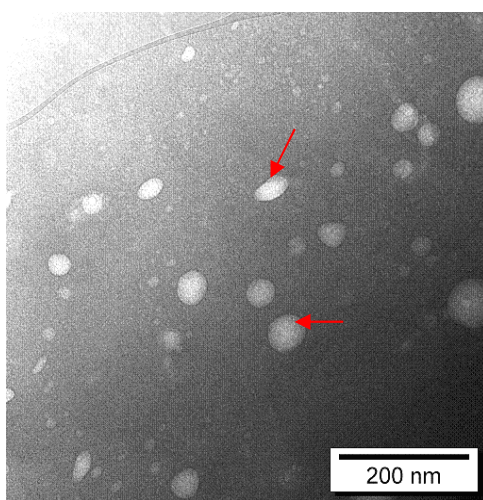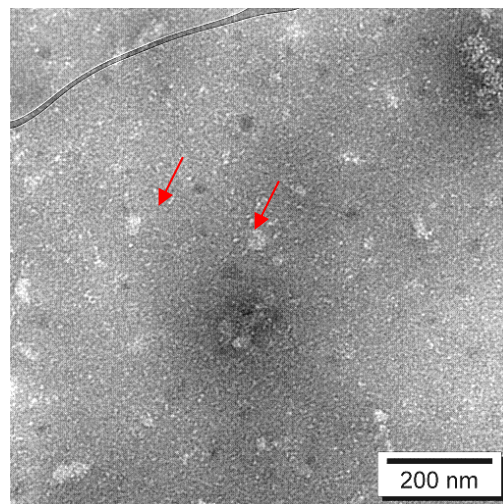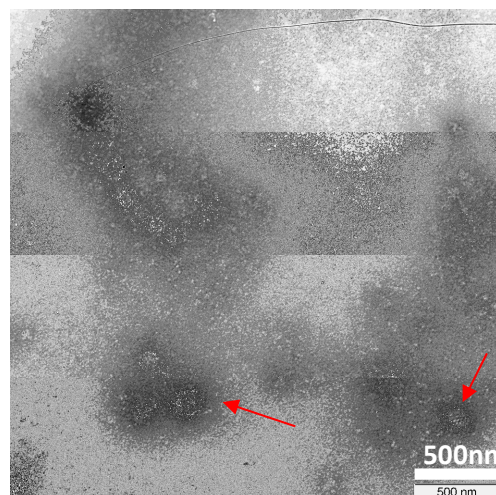
Figure 79. a) Negative-stained TEM of a filtered (0.45 μm) aqueous dispersion of Ch_5 on probe sonication in water (bar=500 nm), b) Ch_5, propofol (bar= 1 μm), c) Ch_5, prednisolone nano-particles, d) Ch_5, griseofulvin (bar=200 nm) and e) Ch_5, etoposide (bar= 500nm). All the formulations consisted of 6 mgmL^{-1} polymer and 10:1 initial drug:polymer mass ratio. Arrows show drug loaded self-assemblies.
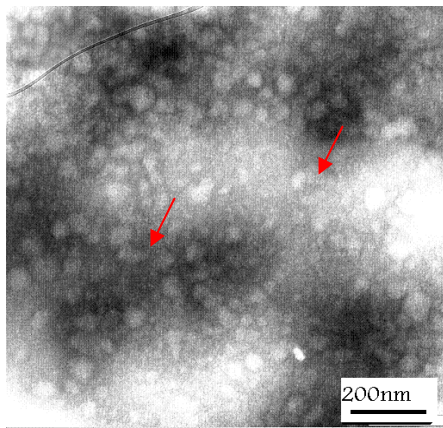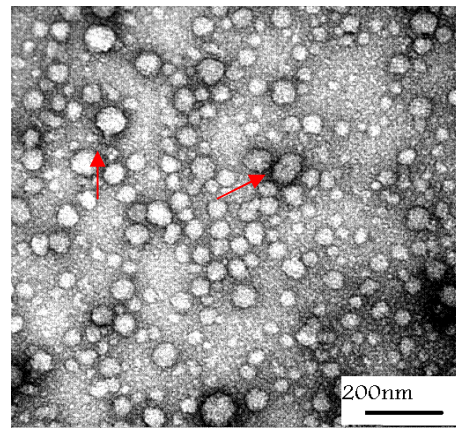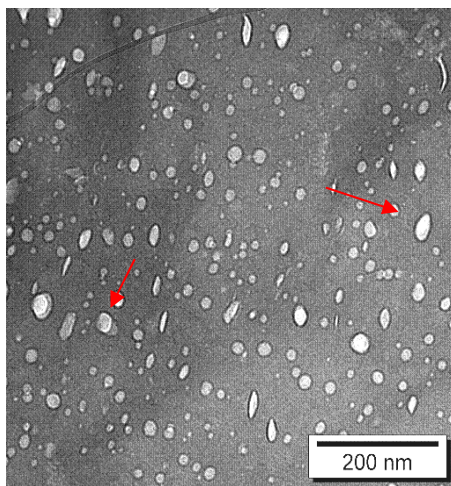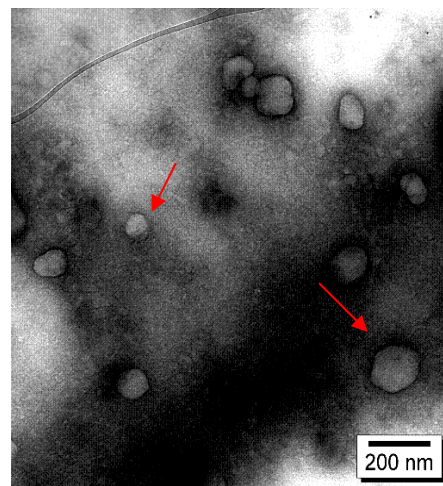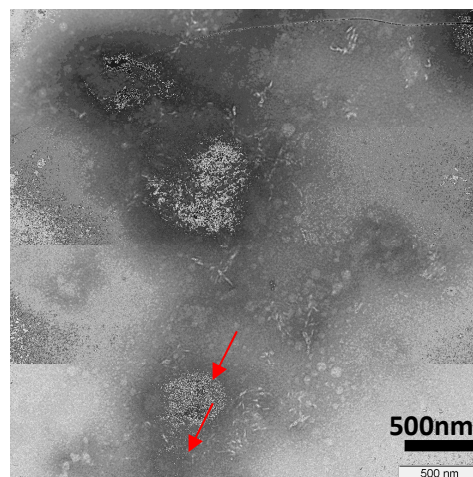
Figure 80. a) Negative-stained TEM of a filtered (0.45 µm) aqueous dispersion of Dansyl$_{10}$ on probe sonication in water (bar=200 nm), b) Dansyl$_{10}$, propofol (bar= 200 nm), c) Dansyl$_{10,}$ prednisolone nano-particles (bar=200 nm), d) Dansyl$_{10}$, griseofulvin (bar=200 nm) and e) Dansyl$_{10}$, etoposide (bar= 500 nm). All the formulations consisted of 6 mgmL^{-1} polymer and 10:1 initial drug:polymer mass ratio. Arros show drug loaded self-assemblies formed.

4.3.5. *FTIR Analysis of freeze dried formulations*

The FTIR spectrum of the freeze dried preparations were obtained in order to confirm the presence of functional groups of the drug and polymer.

4.3.5.1. *FTIR of Ch_5 formulations*

4.3.5.1.1. *FTIR of Ch_5, propofol formulation*

Figure 81 c) shows the FTIR spectra obtained from the Ch_5, propofol formulation. The presence of the O-H peak at 3600 cm^{-1} and the ortho substituted aromatic benzene peaks at 748 cm^{-1} were the functional groups present on the propofol moiety. This indicated that propofol had been successfully encapsulated in the formulation. All peak assignments can be seen in Table 17.

Table 17. Peak bandwidth assignment occurring on FTIR spectra of Ch_5, propofol formulation using diamond powder tip (20scans).

Formulation	Bandwidth (cm^{-1})	Bond type	Functional Group
Ch_5, propofol	3600	O-H Stretch	Hydroxyl (propofol)
	3300	N-H Stretch	2º Amine (Ch_5)
	1640-1560		
	3100	C-H Stretch	Aromatic (propofol)
	748		Ortho subs benzene
	2962	C-H Stretch	Alkyl (Ch_5)
	1460		
	1600	C=O Bend	Carbonyl (Ch_5)
	1311	C-C Bend	Alkyl (Ch_5)
	815	C-O Bend	(Ch_5)
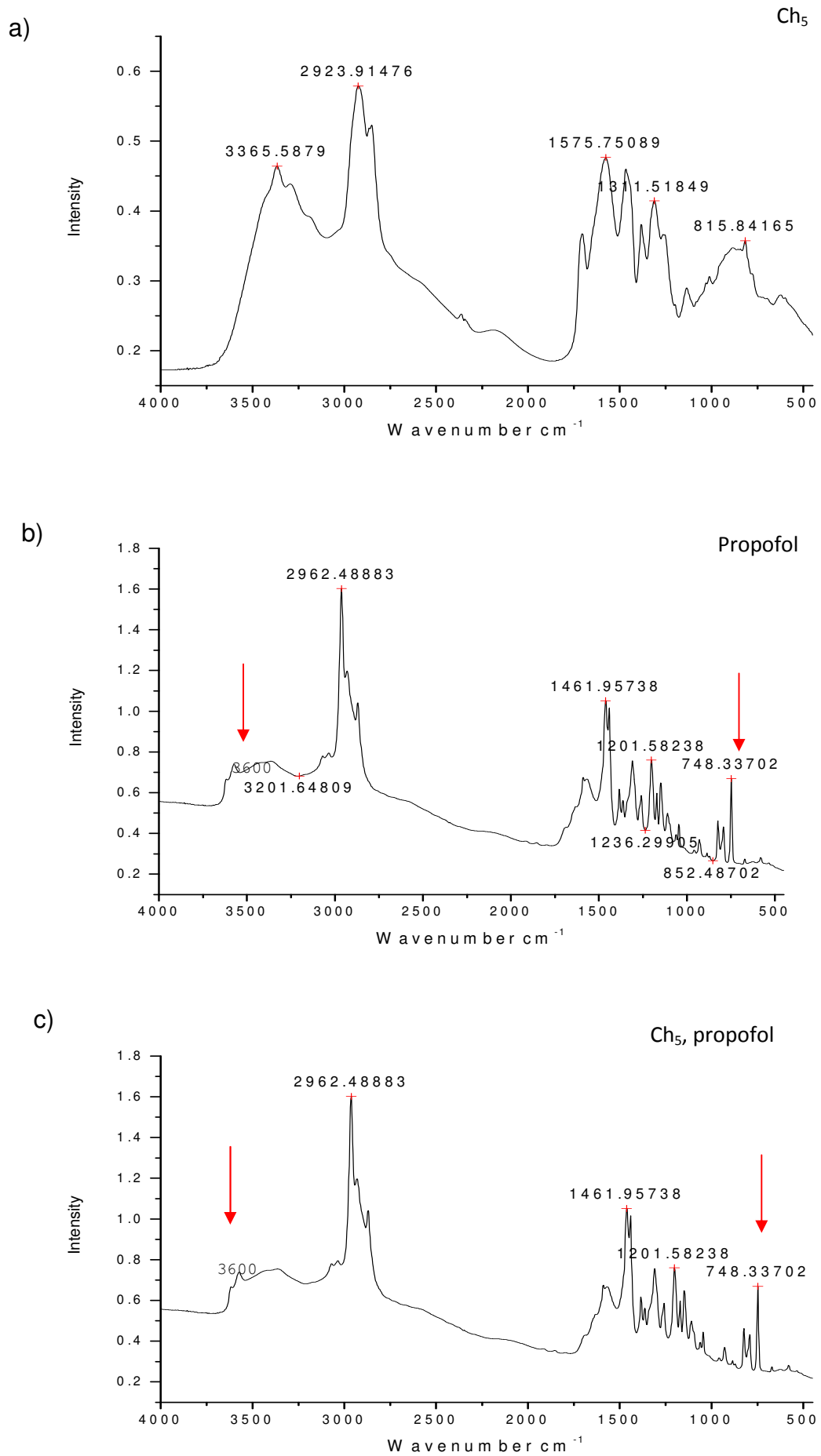
Figure 81. FTIR spectra of a)Ch_5, b) propofol and c) Ch_5, propofol formulation.

4.3.5.1.2. *FTIR of Ch$_5$, prednisolone formulation*

Peak assignment of the FTIR spectra obtained for the Ch$_5$, prednisolone formulation (Fig. 82 c) confirmed the presence of the drug in formulation. This was due to the presence of the hydroxyl band at O-H (3404 cm^{-1}) and the C=O (1720 cm^{-1}) of the 6 membered carbonyl ring, these groups were not present in the spectra for Ch$_5$ alone and therefore can be attributed to the drug molecule. Full peak assignment can be viewed in Table 18. The large negative peak observed at 2350 cm^{-1} was due to changes in the background CO$_2$.

Table 18. Peak bandwidth assignment occurring on FTIR spectra of Ch$_5$, prednisolone formulation using diamond powder tip (20scans).

Formulation	Bandwidth (cm^{-1})	Bond type	Functional Group
Ch$_5$, prednisolone	3404	O-H Stretch	Hydroxyl (prednisolone)
	1656	N-H Stretch	2° Amine (Ch$_5$)
	900-850	C-H Bend	Aromatic (prednisolone) Subs benzene
	2923	C-H Stretch	Alkyl (Ch$_5$)
	1460		
	1720	C=O Bend	Carbonyl 6 membered ring (prednisolone)
	1311	C-C Bend	Alkyl (Ch$_5$)
	950	C-O Bend	(Ch$_5$)

a) Ch₅

b) Prednisolone
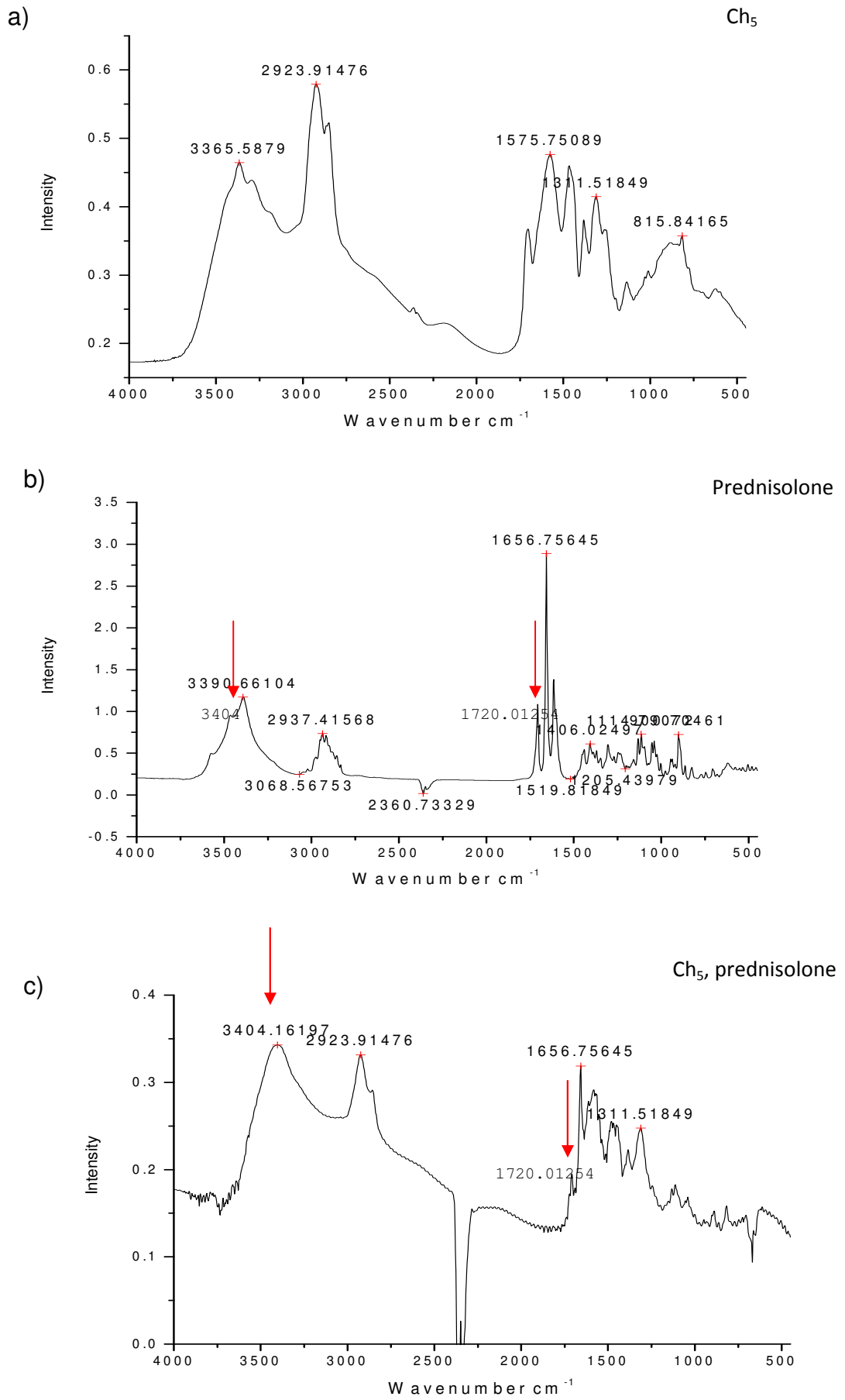
c) Ch₅, prednisolone

Figure 82. FTIR spectra of a) Ch₅, b) prednisolone and c) Ch₅, prednisolone formulation.

4.3.5.1.3. *FTIR of Ch$_5$, griseofulvin formulation*

Fig. 83c) gives confirmation of the successful encapsulation of griseofulvin within the self-assemblies. This can be deduced due to extra peaks being present at 3359 cm^{-1} (O-H), 1750 cm^{-1} (C=O), 800 cm^{-1} (Aromatic substituted benzene) and a weak peak at 550 cm^{-1}. These extra peaks correlate well with the functional groups present on the griseofulvin moiety. For all peak assignments see Table 19. As previously mentioned the peak or trough witnessed at 2350 cm^{-1} was due to changes in background CO$_2$.

Table 19. Peak bandwidth assignment occurring on FTIR spectra of Ch$_5$, griseofulvin formulation using diamond powder tip (20scans).

Formulation	Bandwidth (cm^{-1})	Bond type	Functional Group
Ch$_5$, griseofulvin	3359	O-H Stretch	Hydroxyl (griseofulvin)
	1620	N-H Stretch	2° Amine (Ch$_5$)
	800	C-H Bend	Aromatic (griseofulvin) Subs benzene
	2941	C-H Stretch	Alkyl (Ch$_5$)
	1460		
	1750	C=O Stretch	Carbonyl 5 membered ring (griseofulvin)
	1600	C=O Stretch	Carbonyl (griseofulvin)
	1500	C-C Bend	Alkyl (Ch$_5$)
	950	C-O Bend	(Ch$_5$)
	550	C-Cl Bend	Chloro alkane (griseofulvin)
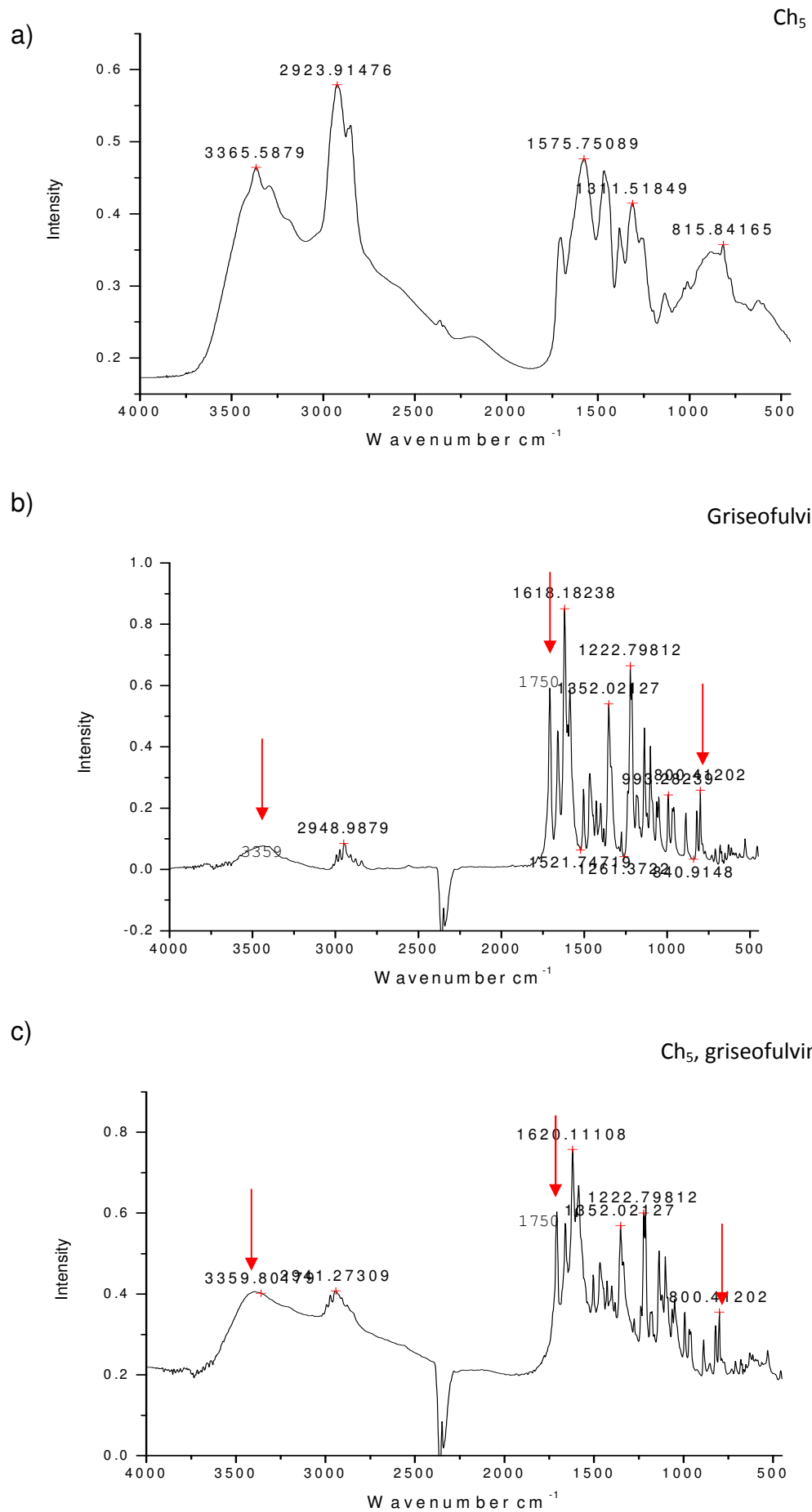
Figure 83. FTIR spectra of a) Ch_5, b) griseofulvin and c) Ch_5, griseofulvin.

120

4.3.5.2. *FTIR of Dansyl$_{10}$ formulations*

4.3.5.2.1. *FTIR of Dansyl$_{10}$, propofol formulation*

Figure 84c) shows the FTIR spectrum obtained from the Dansyl$_{10}$, propofol formulation. As with the Ch$_5$, propofol spectra, the presence of the O-H peak at 3419 cm^{-1} and the ortho substituted aromatic benzene peaks at 750 cm^{-1} were resultant from the functional groups present on the propofol moiety. This indicated that propofol had been successfully encapsulated in the formulation. All peak assignments can be seen in Table 20.

Table 20. Peak bandwidth assignment occurring on FTIR spectra of Dansyl$_{10}$, propofol formulation using diamond powder tip (20scans).

Polymer	Bandwidth (cm^{-1})	Bond type	Functional Group
Dansyl$_{10}$, propofol	3419	O-H Stretch	Hydroxyl (propofol)
	1640-1560	N-H Stretch	1° Amine (Dansyl$_{10}$)
	750	C-H Bend	Aromatic (propofol)
			Ortho Subs. benzene
	2960	C-H Stretch	Alkyl (Dansyl$_{10}$)
	1450	C=C Bend	Aromatic (Dansyl$_{10}$)
	1095	C-N Bend	Aliphatic amine (Dansyl$_{10}$)
	950	C-O Bend	(Dansyl$_{10}$)
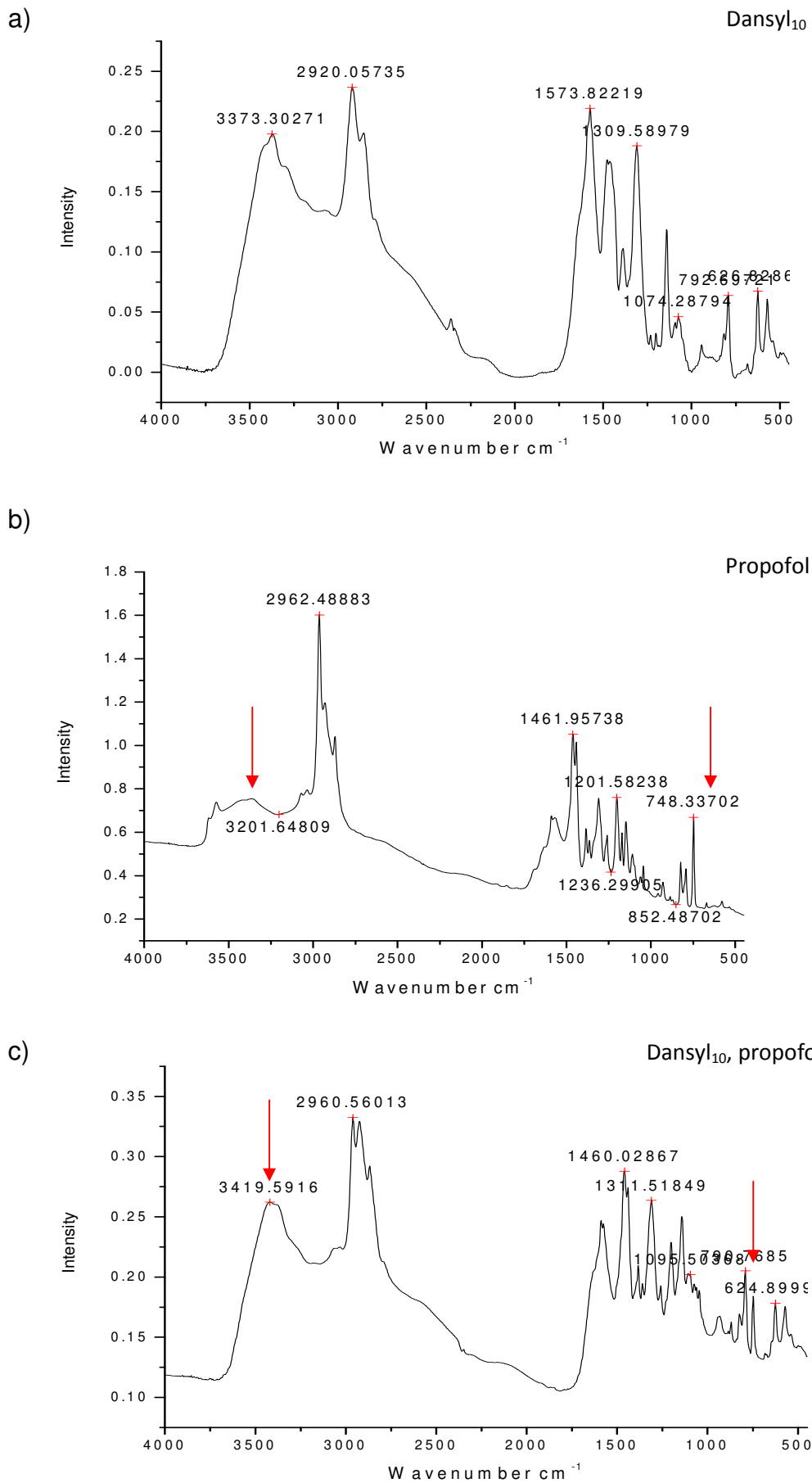
Figure 84. FTIR spectra of a) Dansyl$_{10}$, b) propofol and c) Dansyl$_{10}$, propofol formulation.

4.3.5.2.2. *FTIR of Dansyl$_{10}$, prednisolone formulation*

Peak assignment of the FTIR spectra obtained for the Dansyl$_{10}$, prednisolone formulation (Fig. 85) showed similar peaks to the Ch$_5$, prednisolone spectra indicating the presence of the drug in the formulation. This was due to the presence of the hydroxyl band at O-H (3413 cm^{-1}) and the C=O (1720 cm^{-1}) of the 6 membered carbonyl ring, these groups were not present in the spectra for Dansyl$_{10}$ alone and therefore can be attributed to the drug molecule. Full peak assignment can be viewed in Table 21.

Table 21. Peak bandwidth assignment occurring on FTIR spectra of Dansyl$_{10}$, prednisolone formulation using diamond powder tip (20scans).

Polymer	Bandwidth (cm^{-1})	Bond type	Functional Group
Dansyl$_{10}$, prednisolone	3413	O-H Stretch	Hydroxyl (prednisolone)
	1656	N-H Stretch	1º Amine (Dansyl$_{10}$)
	900-850	C-H Bend	Aromatic (prednisolone) Subs. benzene
	2927	C-H Stretch	Alkyl (Dansyl$_{10}$)
	1720	C=O Stretch	Carbonyl 6 – membered ring (prednisolone)
	1450	C=C Bend	Aromatic (Dansyl$_{10}$)
	950	C-O Bend	(Dansyl$_{10}$)
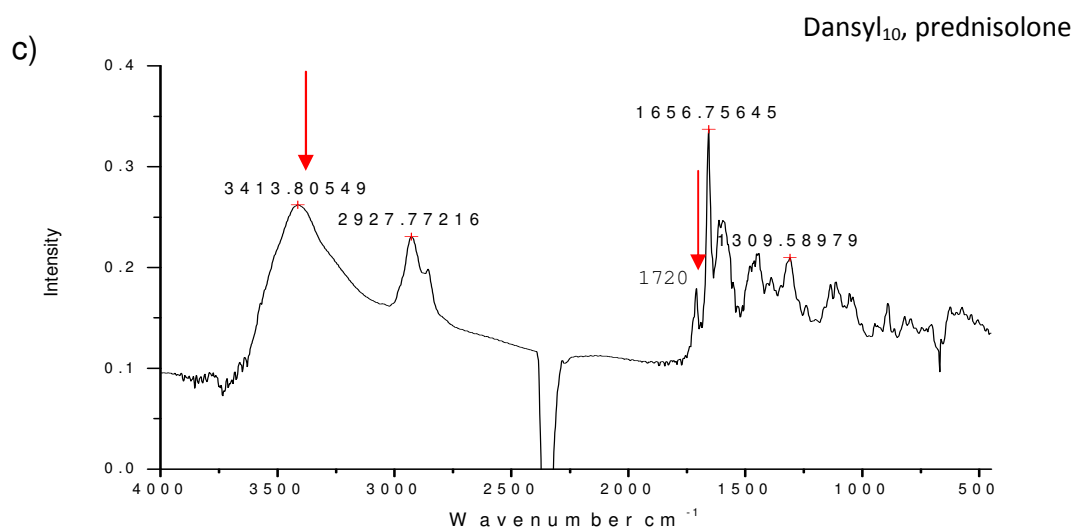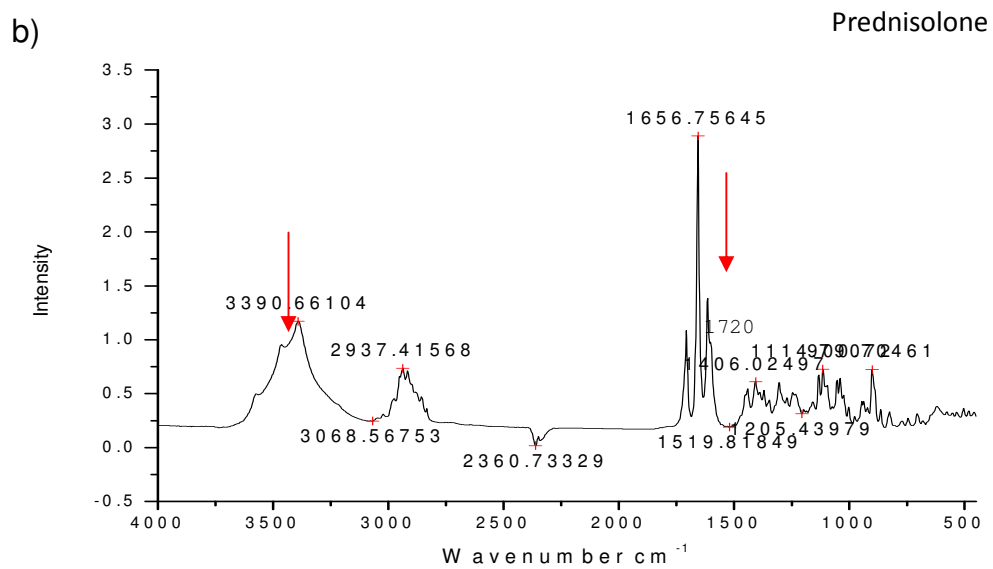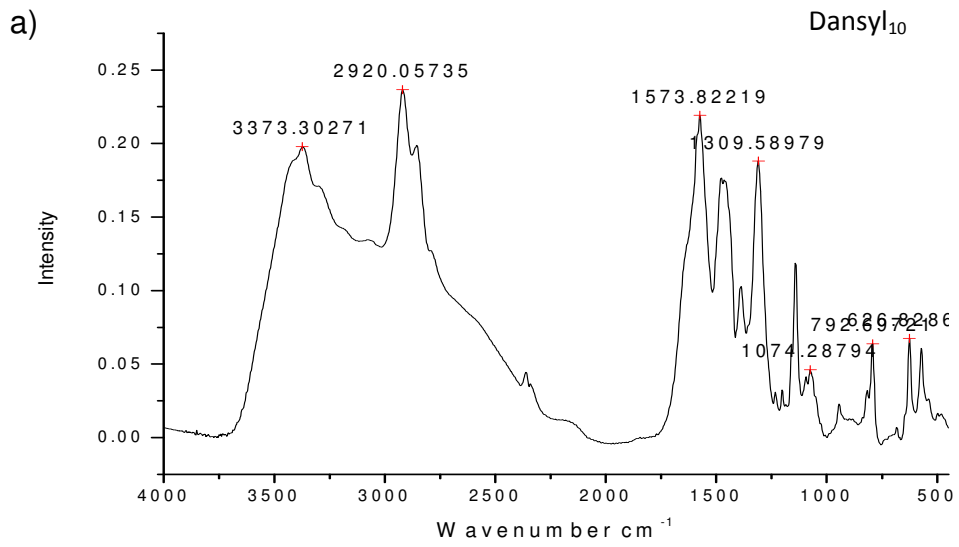
Figure 85. FTIR spectra of a) Dansyl$_{10}$, prednisolone and c) Dansyl$_{10}$, prednisolone formulation.

4.3.5.2.3. *FTIR of Dansyl$_{10}$, griseofulvin formulation*

Fig. 86 gives confirmation of the successful encapsulation of griseofulvin within the self-assemblies. This can be deduced due to extra peaks being present at 3377 cm^{-1} (O-H), 1750 cm^{-1} (C=O of aromatic substituted benzene) and a weak peak at 750 cm^{-1}. These extra peaks correlate well with the functional groups present on the griseofulvin moiety and the Ch$_5$, griseofulvin formulation. For all peak assignments see Table 22.

Table 22. Peak bandwidth assignment occurring on FTIR spectra of Dansyl$_{10}$, griseofulvin formulation using diamond powder tip (20 scans).

Polymer	Bandwidth (cm^{-1})	Bond type	Functional Group
Dansyl$_{10}$, griseofulvin	3377	O-H Stretch	Hydroxyl (griseofulvin)
	1587	N-H Stretch	1º Amine (Dansyl$_{10}$)
	900-850	C-H Bend	Aromatic (griseofulvin) Subs. benzene
	2921	C-H Stretch	Alkyl (Dansyl$_{10}$)
	1585		
	1750	C=O Stretch	Carbonyl 6 – membered ring (griseofulvin)
	1500	C-C Bend	Alkyl (Dansyl$_{10}$)
	1450	C=C Bend	Aromatic (Dansyl$_{10}$)
	1150	C-N Bend	Aliphatic amine (Dansyl$_{10}$)
	750	C-Cl Bend	Chloroalkane (griseofulvin)
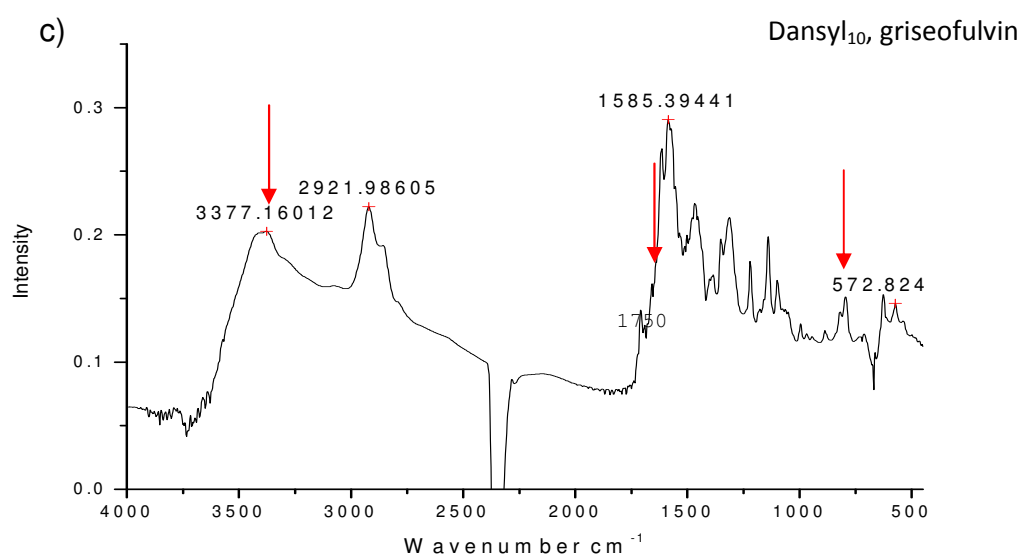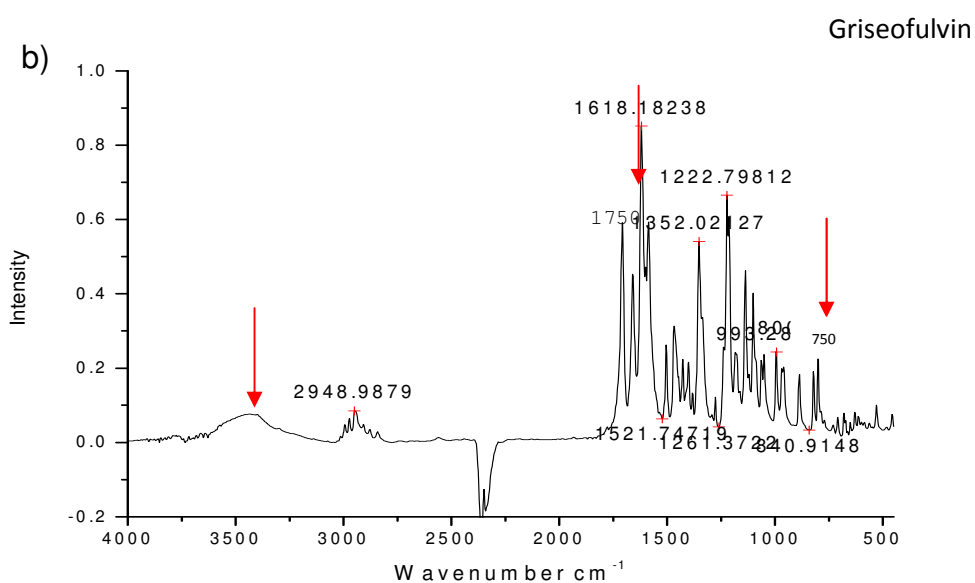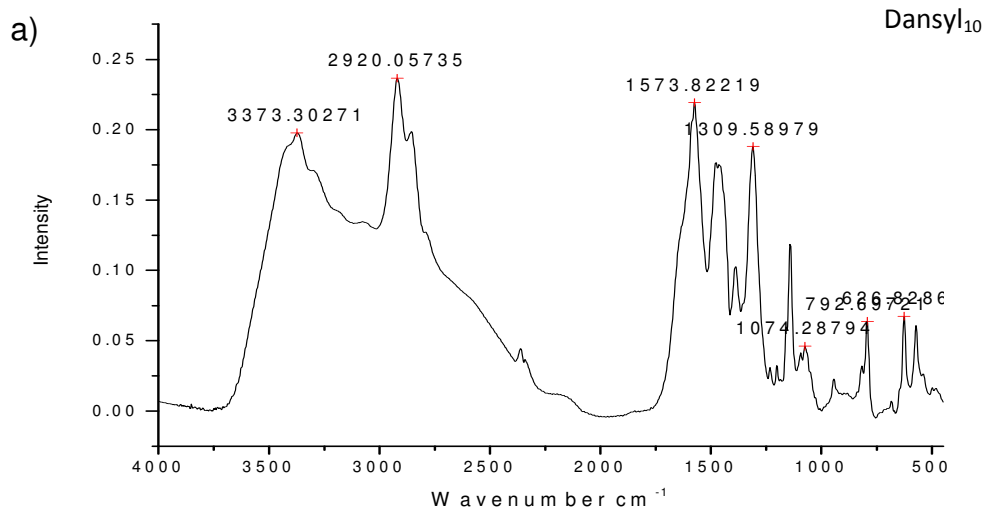
Figure 86. FTIR spectra of a) Dansyl_{10}, b) griseofulvin and c) Dansyl_{10}, griseofulvin formulation.

4.3.6. *In vitro Drug Release*

The release of the drugs from the optimal formulations was carried out in sink conditions over 96 h at 37 °C in phosphate buffer saline (PBS). Fig. 87 and 88 show the drug release from the Ch_5 and $Dansyl_{10}$ formulations. The Ch_5 formulations were able to achieve sustained drug release over 48 to 72 h, whilst the $Dansyl_{10}$ formulations achieved sustained release over 72 to 96 h.
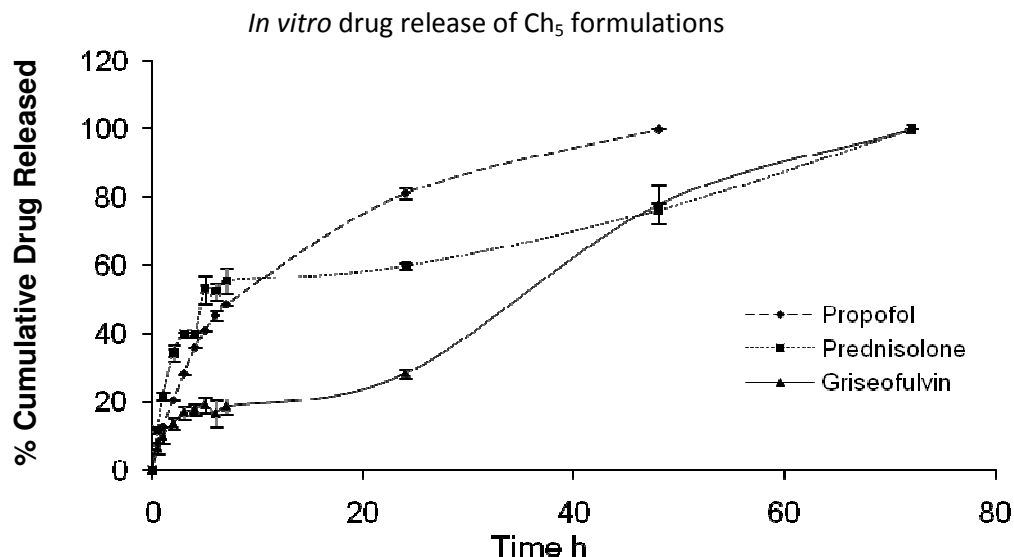
Figure 87. *In vitro* release of propofol, prednisolone and griseofulvin from Ch_5 formulations in PBS at 37 °C (n=3, ave ± SD).
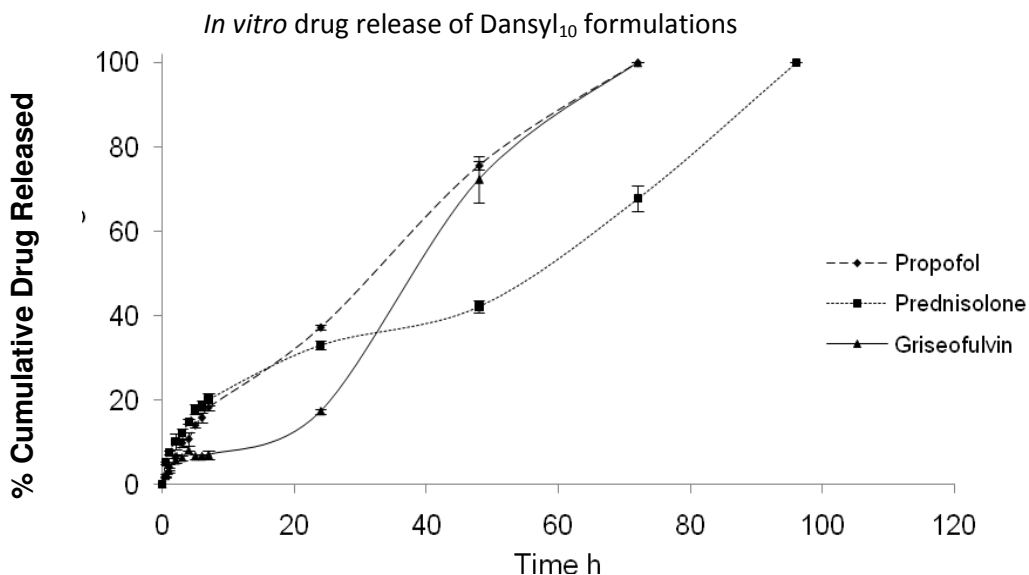
Figure 88. *In vitro* release of propofol, prednisolone and griseofulvin from $Dansyl_{10}$ formulations in PBS at 37 °C (n=3, ave ± SD).

Propofol release from Ch_5 and $Dansyl_{10}$ showed different release profiles over 72 h. The release was almost constant upon initial drug release. For Ch_5 50 % of propofol (7.8 mg)

was released in the first 7 h, after 48 h the drug had been completely released, the release profile showed a consistent release over the 48 h period. The $Dansyl_{10}$ showed a slower release pattern with only 20 % of propofol (8.95 mg) being released after 7 h and after 48 h less than 80 % of the propofol drug content had been released. The release continued steadily until after 72 h the drug was completely released. The release profile for $Dansyl_{10}$ resembled a zero order release profile; however when a linear trend line was fit to the data the R^2 value was 0.9733. This meant the drug release could not be described as perfectly zero order.

Prednisolone release for both formulations measured over 96 h showed a triphasic release profile. This is normally exhibited by biodegradable polymers [287,288]. An initial burst is followed by a lag phase and then a secondary lag phase (Fig. 87 & 88). For Ch_5, the initial burst occurs in the first 6 h and accounts for 53 % of the total drug content (7.47 mg), the after initial lag phase between 6 - 48 h only 60 % of the drug has been released. After 72 h the drug had been completely released. The $Dansyl_{10}$ had only released 20 % (12.73 mg) of prednisolone in its initial burst phase in the first 7 h. After 48 h less than 40 % of the drug was released. In the final lag phase the drug was steadily released until 100 % of the drug (63.64 mg) was released at 96 h. The $Dansyl_{10}$ showed a more sustained release profile for prednisolone.

The release profile of griseofulvin was also triphasic (Fig. 87). 20 % of the Ch_5 was released within the first 7 h, the release appeared to plateau at this time, after 20 h, it appeared that no more griseofulvin was released. After 24 h, the drug was consistently released until after 72 h 100 % release had been achieved. The $Dansyl_{10}$ showed a similar pattern, however after 7 h less than 10 % of the griseofulvin was released. A plateau was also observed but, after 24 h the drug was constantly released up to 100 % at 72 h.

4.3.7. *Stability of formulations*

The formulations were stored in a dark airtight container for 4 weeks. Over this time the formulations were analysed for total drug content and the hydrodynamic size was determined using photon correlation spectroscopy. The formulations were initially stored in two forms; as liquid formulations and as freeze dried 'cakes' (reconstituted with water and sonicated). However, on initial testing of the freeze dried 'cakes', it was deduced using HPLC that all the propofol in the formulations had been lost in the freeze drying process, perhaps due to the volatile nature of this drug [289].

At the commencement of testing it was apparent that prednisolone and griseofulvin liquid preparations were forming viscous gels over time. Those gels were too thick to be analysed. The stability data shown (Fig. 89 & 90, Table 23-24) are therefore of liquid propofol preparations and freeze dried prednisolone and griseofulvin preparations.
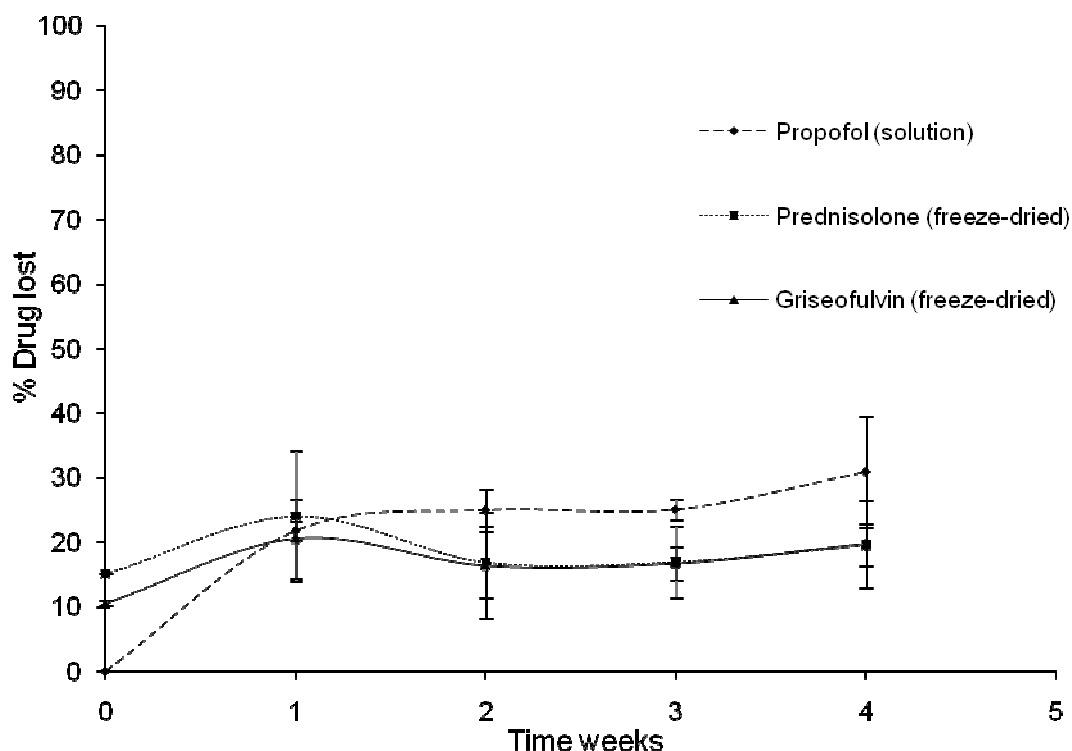
Figure 89. % of drug lost from nano-aggregates of Ch_5 over 4 weeks. Propofol stored in solution, prednisolone and griseofulvin formulations stored as freeze dried 'cakes' and reconstituted with water. The formulations were stored in 55 % humidity, at room temperature and protected from light (n=3, ave ± SD).

Over the 4 week period propofol appeared to be gradually lost from the Ch_5 formulation (Fig. 89) from 0 to 30 % (0 to 4 weeks). The size data for the propofol formulation correlates well with the drug loss. The size of the self-assemblies are reduced from 666 nm to 239 nm as the drug content decreases (0 to 4 weeks) (Table 23). The initial loss of prednisolone and griseofulvin (15 % and 10 % respectively) experienced from the Ch_5 formulation is possibly due to the freeze drying process. However no further notable loss is apparent over the 4 wk period. The self assembly sizes of prednisolone and griseofulvin formulation notably increased after the freeze-drying process. The absorbance wavelength of the freshly prepared Ch_5, prednisolone and Ch_5, griseofulvin liquid formulations had increased from 304 nm and 284 nm to 907 nm and 658 nm respectively after freeze drying and reconstitution. The reason for this is unknown; however it may be due to disruption of the polymer structure during the freeze-drying process resulting in different aggregation formation. Over the 4 week period it appeared that the longer the freeze-dried formulations were stored, the more stable they became as no drug loss had occurred but the size and PDI decreased.

Table 23. Size data for Ch_5 formulations over a 4 week period.

Formulation	Time (wks)	Photon correlation spectroscopy	
		Size (nm)	**PDI**
		mean (SD)	*mean (SD)*
6 mgmL^{-1} Ch_5 1:10 propofol	0	666 (79.418)	0.376 (0.025)
	1	394 (49.048)	0.340 (0.066)
	2	367 (79.811)	0.282 (0.104)
	3	264 (5.356)	0.285 (0.025)
	4	239 (3.804)	0.237 (0.023)
6 mgmL^{-1} Ch_5 1:10 prednisolone	0	907 (37.470)	0.560 (0.044)
	1	881 (52.818)	0.477 (0.069)
	2	1006 (14.962)	0.584 (0.093)
	3	809 (18.540)	0.375 (0.009)
	4	883 (37.906)	0.399 (0.038)
6 mgmL^{-1} Ch_5 1:10 griseofulvin	0	658 (20.932)	0.694 (0.027)
	1	437 (34.453)	0.674 (0.156)
	2	536 (24.278)	0.593 (0.089)
	3	464 (10.313)	0.433 (0.035)
	4	424 (5.352)	0.382 (0.006)

Propofol samples stored as solution, prednisolone and griseofulvin samples stored as freeze dried 'cakes' and reconstituted with water. All samples stored at 55 % humidity, room temperature and protected from light n=3, ave (SD).

The stability profiles from the Dansyl$_{10}$ formulations (Fig. 90) show similar patterns to the Ch_5 formulations. The propofol had a cumulative loss over the 4 week period, however only 10 % was lost (in comparison with Ch_5, propofol formulation, 30 %). The size of the aggregates in the formulations remained consistent across the 4 wk period (Table 24). The initial loss of prednisolone and griseofulvin (10 % and 20 %) from the freeze drying process was also observed and was consistent with the Ch_5 formulations. However the griseofulvin content did decrease over the 4 wk period with 40 % being lost after wk 4. Consistent with the Ch_5 formulations, the freshly prepared Dansyl$_{10}$, prednisolone and

Dansyl$_{10}$, griseofulvin liquid formulations increased from 350 nm and 305 nm to 462 nm and 545 nm after freeze drying. Both the prednisolone and griseofulvin self-assemblies increased in size across the 4 wk period from 462 to 829 nm and from 545 to 1055 nm respectively. The polydispersity index's also varied greatly, this indicated that the Dansyl$_{10}$ formulations were less stable than the Ch$_5$ formulations.
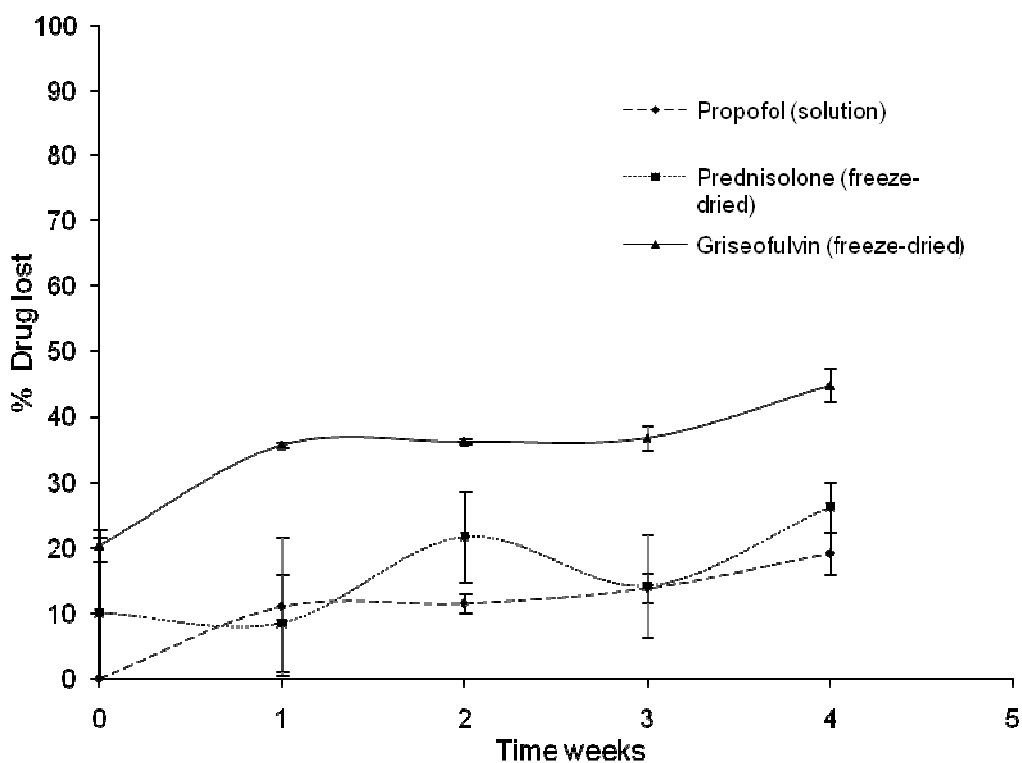
Figure 90. % of drug lost from nano-aggregates of Dansyl$_{10}$ over 4 weeks. Propofol stored in solution, prednisolone and griseofulvin formulations stored as freeze dried 'cakes' and reconstituted with water. The formulations were stored in air tight containers, at room temperature in darkened conditions (n=3, ave ± SD).

Table 24. Size data for Dansyl$_{10}$ formulations over a 4 week period.

Formulation	Time (wks)	Photon correlation spectroscopy	
		Size (nm)	**PDI**
		mean (SD)	*mean (SD)*
6 mgmL^{-1} Dansyl$_{10}$ 1:10 propofol	0	608 (49.37)	0.385 (0.009)
	1	631 (140.922)	0.300 (0.083)
	2	585 (90.113)	0.349 (0.059)
	3	741 (133.671)	0.386 (0.009)
	4	677 (124.107)	0.324 (0.063)
6 mgmL^{-1} Dansyl$_{10}$ 1:10 prednisolone	0	462 (29.441)	0.422 (0.111)
	1	703 (4.561)	0.499 (0.235)
	2	715 (43.736)	0.646 (0.254)
	3	618 (87.825)	0.552 (0.102)
	4	829 (134.476)	0.970 (0.541)
6 mgmL^{-1} Dansyl$_{10}$ 1:10 griseofulvin	0	545 (18.785)	0.586 (0.022)
	1	687 (84.742)	0.131 (0.105)
	2	806 (20.731)	0.247 (0.087)
	3	1090 (83.781)	0.541 (0.101)
	4	1055 (75.434)	0.513 (0.029)

Propofol samples stored as solution, prednisolone and griseofulvin samples stored as freeze dried 'cakes' and reconstituted with water. All samples stored at 55 % humidity, at room temperature and protected from light n=3, ave (SD).

4.4. Discussion

The driving force behind the encapsulation of hydrophobic drugs inside the core of polymeric self-assemblies is a basic energetic principle. It is energetically favourable for hydrophobic drugs to shield themselves from aqueous environments. As the polymeric self-assemblies spontaneously formed the core – shell structures, the smaller lipophilic drug molecules accumulate within the hydrophobic region where they remain physically entrapped. These self-assemblies continuously and spontaneously break and reform in dynamic equilibrium above their critical aggregation concentration (CAC) [72,249,290].

Model hydrophobic drugs were encapsulated inside the modified PAA polymers and their drug content was analysed. In general drug loading capacities of drugs are affected by a number of factors. Previously it has been reported that by changing the polymer architecture and hydrophobic content, the drug loading capacity varied [72,137]. Sezgin and colleagues fabricated block copolymer poly(ethylene glycol)–distearoyl phosphatidyl ethanolamine (PEG$_{2000}$-DPSE) polymers for solubilisation of poorly soluble and insoluble drugs. However they found that the hydrophobic core acted in a drug specific manner, whereby only certain drugs were capable of encapsulation [291]. The polymeric nano-aggregates were loaded with anticancer drugs camptothecin (CPT), octaethylporphine (OEP) and meso-tetraphenyl porphine (mTPP) [291]. Sezgin found that the polymer had very low loading capacities for CPT and OEP (0.15 % and 4.7 % w/v of drug incorporated respectively), whilst the mTPP achieved up to 93.3 % drug loading [291]. Furthermore, they also reported that as the chain length of the PEG group was increased, so too did drug solubilisation, thus concluding that for specific drugs and applications, the self-assemblies could be tailor made by varying polymer structure and hydrophobic block length to allow solubilisation of specific molecules [291]. Zhang reported that by varying the poly(DL-lactide)-block-methoxy polyethylene glycol (PDLLA-MePEG) monomer weight ratio, the concentration of anticancer drug Taxol® was modified [292]. The drug loading concentration of Taxol® was increased with increasing the PDLLA monomer of the block copolymer, thus resulting in higher lipophilic content causing stronger hydrophobic interactions with the drug molecules [292]. Although this principle has been extensively studied using amphiphilic polymers [137], the use of hydrophobic aromatic groups and the differences in drug loading on comb shaped polymers is seldom reported.

The modified PAA's described in this work all possessed the ability to encapsulate practically insoluble drugs within their hydrophobic core. The results confirm that varying the hydrophobic group directly impacts the self-assembly loading capacity. This is perhaps due to the chemical structure of the hydrophobic pendant group. The small planar structure of fmoc enabled excimer formation to occur, where stacking of the molecules occurred. This was also witnessed in the naphthalene modified polymer. The close stacking of these molecules may limit the number of drug molecules entering the

hydrophobic core, thus making them less effective. However, this may differ with differing drug architecture. The more bulky hydrophobic molecules such as cholesterol or dansyl may experience some steric hindrance when in close proximity to each other, and hence small drug molecules may be able to 'slot' into such spaces and maximise their loading concentration (Fig. 67 & 72).

At higher hydrophobic grafting, increased concentrations of drugs were solubilised (Fig. 91). This can be attributed to greater hydrophobicity of the polymer forming polymeric self-assemblies with greater hydrophobic interactions with the lipophilic drug molecules [293]. The higher extent of hydrophobic interactions results in greater driving force for hydrophobic drug solubilisation and hence a higher drug loading capacity is experienced.
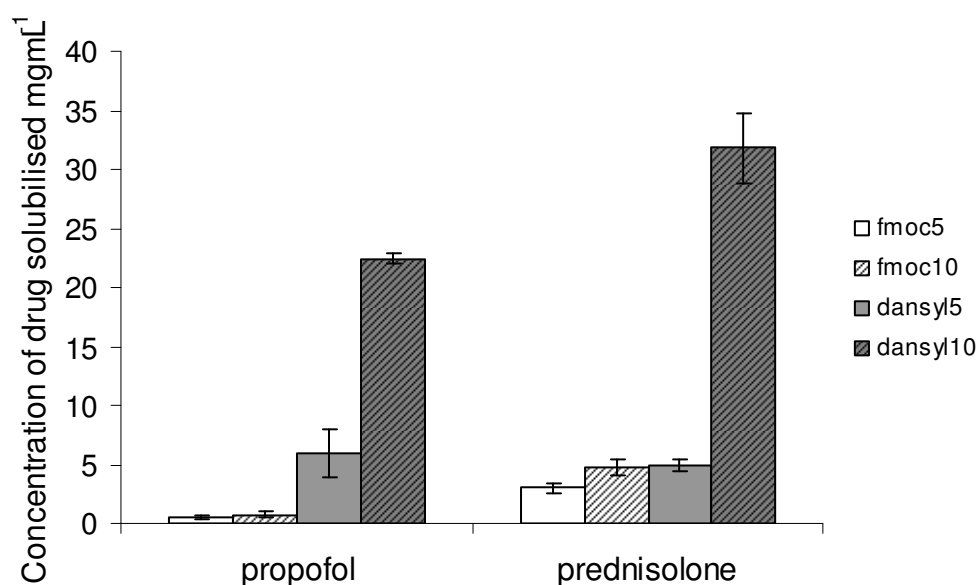
Figure 91. Solubilisation of propofol and prednisolone and 5 % and 10 % molar grafting levels using fmoc and dansyl modified polymers.

Hydrophilic modification of the polymer backbone appeared to decrease the maximum concentration of propofol solubilised. However, visual examination of the formulations before filtration would suggest otherwise. Clear solutions before filtration were formed upon sonication suggesting complete drug solubilisation. This could be due to the positive charge forming less hydrophobic or larger self-assemblies encapsulating the propofol which were removed during the filtration process.

Ch_5 and $Dansyl_{10}$ proved to be the best solubilising polymers across the library of polymers synthesised. The solubilising potential of these amphiphilic polymers was consistent across the range of model drugs used (Fig.92). This indicates that the polymers are non-drug selective i.e. they are capable of solubilising any hydrophobic drug and are not specific to one molecular type. This is an excellent property to possess in a drug

delivery system indicating its potential as a universal solubiliser and can be used across a broad range of applications.
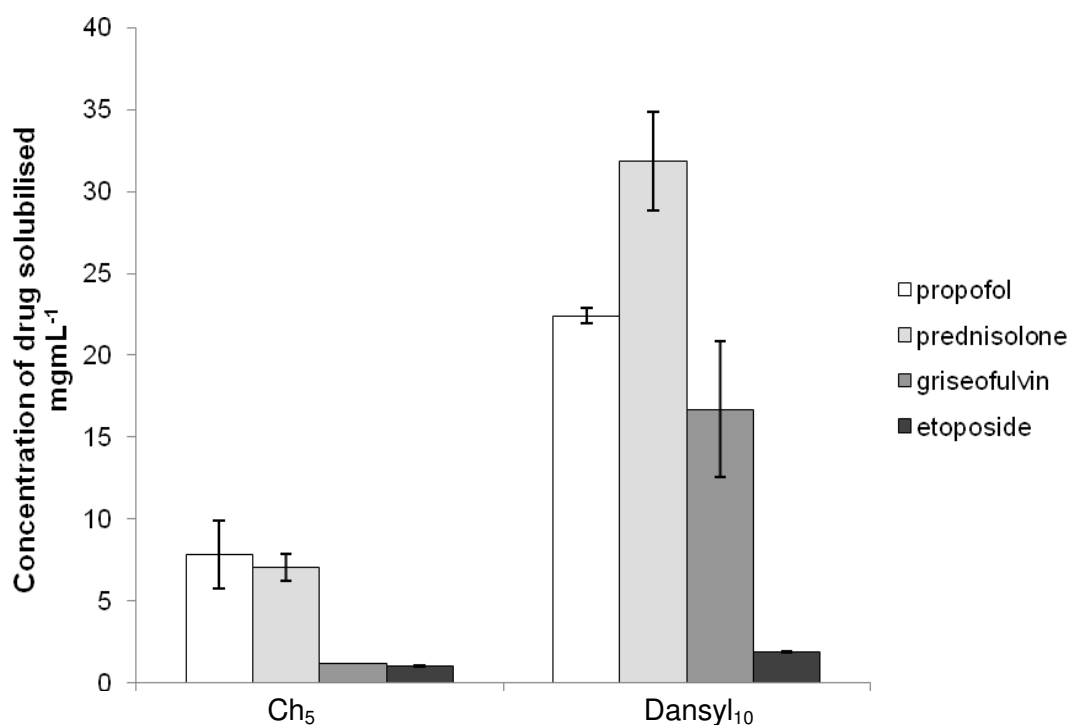
Figure 92. Solubilisation capacities of Ch_5 and $Dansyl_{10}$ polymers of propofol, prednisolone, griseofulvin and etoposide.

Overall it was observed that for the Ch_5 and $Dansyl_{10}$ formulations, higher polymer concentration achieved greatest solubility of the hydrophobic drugs. This was due to the fact that more micelles would have been present in solution, resulting in higher degree of solubilisation. At increased initial drug:polymer mass loading ratios increased solubility was achieved for these polymers (Fig. 68 & 73). With increased drug loading there was a larger driving force for hydrophobic encapsulation within the lipophilic core of the self-assemblies and thus more drug was solubilised [294]. The excipient:drug ratios of the filtered formulations were calculated. Solubilisation was achieved at excipient:drug ratios as small as 0.13 (Fig. 69). These ratios were considerable less than the values needed with traditional low molecular weight surfactants or liposomes which often require excipient:drug ratios ranging from 15:1 to as high as 1000:1 [3]. It is desirable to use low excipient:drug ratios when solubilising a drug, the system is not only more efficient and cost effective, but it also minimises any harmful or uncomfortable side effects to the patient.

The ability of one polymer to load different drugs with differing efficiency was observed. This was also due to a number of factors. The structural properties of drugs being loaded has an impact on drug loading capacity [295]. Planar drugs (consisting of aromatic ring systems) have the ability to stack closely together, allowing higher concentrations to become encapsulated within the hydrophobic core. Bulkier or more rigid molecules with

higher molecular weight (e.g. etoposide) find it more difficult to accumulate together in high concentration as steric hindrance prevents this occurring, meaning the encapsulation efficiency is decreased.

In the case of propofol, its low molecular weight (MW = 178) (Fig. 60), allows the molecules to fit closely together without much steric hindrance thus maximising the concentrations being encapsulated (Fig. 67). The chemical structures of prednisolone and griseofulvin (Fig. 61 & 62), are more bulky and inflexible thus hindering close proximity of the molecules by stacking. Perhaps the low solubilisation capacity for etoposide in both Ch_5 (1.02 mgmL^{-1}) and Dansyl$_{10}$ (1.89 mgmL^{-1}) can be attributed to its large molecular weight and complicated structure (Fig. 63).

The aqueous solubility of lipophilic drugs also impacts on solubility inside self-assembly cores. The more lipophilic the drug molecule, the greater affinity it will have for the hydrophobic core of the polymeric self-assembly. Prednisolone was solubilised by Dansyl$_{10}$ (31.82 mgmL^{-1}) achieving a 100-fold improvement of its aqueous solubility. Griseofulvin was solubilised by Dansyl$_{10}$ (16.71 mgmL^{-1}) 400-fold better than the aqueous solubility (Table 13). Griseofulvin possesses very low aqueous solubility (0.03 mgmL^{-1}). Perhaps the highly lipophilic nature of the drug resulted in a greater driving force for hydrophobic interactions between the griseofulvin and the self-assemblies, thus increasing the amount of drug solubilised. However when griseofulvin is compared with propofol and prednisolone, a much lower concentration of drug was encapsulated (Table 13).

Log P is another parameter which affects the solubility of drugs in solutions. Log P values are often used to compare the hydrophobicity of molecules [295]. Drugs with high log P values indicate that the drugs would rather partition into lipophilic than aqueous media [296]. This phenomenon results in drugs with higher log P values having higher affinity for the hydrophobic core of the polymeric nano-aggregates and thus higher concentrations are solubilised. Looking at the model drug solubilisation, this trend is witnessed. The propofol had the highest log P value of 4.16 and a high degree of drug loading was achieved. Prednisolone and griseofulvin have similar log P values (1.8 and 2.2 respectively) and thus would be expected to have similar drug loading capabilities; however this is not the case. As mentioned previously the griseofulvin loading was notably less than the prednisolone loading, this perhaps due to other factors such as steric hindrance being present. The etoposide has the lowest log P value (0.698) this would indicate that it is the most hydrophilic molecule of all the drugs. In our study, this was not the case, etoposide achieved the lowest drug loading within all the formulations (Table 14). However as previously mentioned etoposide was the largest drug molecule which appears to be the limiting factor as regards to its encapsulation inside Ch_5 and Dansyl$_{10}$.

Propofol has for many years been the focus of solubilisation studies [94, *258,*297,298]. Its highly lipophilic nature makes it an ideal drug for researchers to incorporate within their novel drug delivery systems. Previously propofol has been formulated by complexation with hydroxypropyl and sulfobutyl-β-cyclodextrin [298,258]. Other technologies to improve propofol solubility were the synthesis of water soluble prodrugs and the use of other chemical delivery systems [257,297,299,300,301]. In 1996 Trapani reported achieving a 266 fold increase on the aqueous solubility of propofol using 2-Hydroxypropyl-β-cyclodextrin [258]. In this study he recorded a solubility of 39.73 mgmL^{-1} of propofol. However other solubility studies have failed to reach this concentration [94,203,257]. In this study we reported that Dansyl$_{10}$ achieved a 223-fold increase from the aqueous solubility. Although this is not as high as previously reported by Trapani and colleague's [258], cyclodextrins can be very drug selective, whereas the Dansyl$_{10}$ and Ch$_5$ have demonstrated good solubilising potential across all the drugs tested in this study.

In 2007 Seedher and Sharma reported that combination of prednisolone with other common soluble drugs such as caffeine, paracetamol and ibuprofen could enhance its solubility [302]. They reported that combination of prednisolone with soluble paracetamol enhanced the solubility 2.14-fold [302]. In comparison with previous work, the Ch$_5$ and Dansyl$_{10}$ polymer show excellent results greatly exceeding this data with solubilities up to 7.05 mgmL^{-1} (Ch$_5$) and 31.82 mgmL^{-1} (Dansyl$_{10}$) and without the addition of a secondary drug substance.

Balakrishnan reported a 105-fold increase in the aqueous solubility of griseofulvin using sodium dodecyl sulphate (SDS) [303]. SDS is a commonly used surfactant within the pharmaceutical field, it is frequently used as an excipient to solubilise hydrophobic drugs. Ch$_5$ and Dansyl$_{10}$ achieved 40-fold and 557-fold enhancement of griseofulvin solubility. Although the SDS achieved higher loading than the Ch$_5$ polymer, polymeric nano-aggregates possess lower excipient:drug ratios making them more efficient for drug solubilisation.

Etoposide has previously been used by many research groups for solubility studies [276,285,304,305]. Its anticancer potential has been hindered its by poor aqueous solubility. Recently Shin and colleagues have reported achieving 3.31 mgmL^{-1} solubility of etoposide within poly(ethylene glycol)-block-poly(D,L-lactic acid) (PEG—B-PLA). This is a 22-fold increase from the aqueous solubility of the drug [304]. Ch$_5$ (1.02 mgmL^{-1}) and Dansyl$_{10}$ (1.89 mgmL^{-1}) were capable of increasing the aqueous solubility of etoposide by 7-fold and 13-fold respectively.

The difference in release profiles between polymeric self-assemblies can be attributed to the variation in hydrophobic group attached to the polymer backbone [306]. The higher hydrophobicity of the 10 % molar grafted dansyl self-assemblies made water penetration

of the nano aggregate difficult thus slowing drug release [307]. Therefore higher hydrophobicity of the Dansyl$_{10}$ can lead to a more controlled release of the drugs.

The variation of drug release between the types of drugs can be explained by the aqueous solubility of these drugs. The lower aqueous solubility of the drugs, the higher their affinity for the hydrophobic core of the nano aggregate [296,308]. This high affinity results in the 'reluctance' of the drug to become released into solution [308]. This trend is observed predominantly within the first 7 h for all the drugs. Griseofulvin has the lowest aqueous solubility (0.03 mgmL^{-1}) followed by propofol (0.1 mgmL^{-1}) with prednisolone having the highest solubility (0.2 mgmL^{-1}). Figure 87 shows for the initial 7 h period, the fastest drug is released from the Ch$_5$ self-assemblies was prednisolone followed by the propofol, the griseofulvin releases the lowest concentration over this time period. This trend was also observed in the release from the Dansyl$_{10}$ nano-aggregates in the first 7 h of the study (Fig. 88).

Lin and colleagues reported the *in vitro* release of naproxen from poly(β-benzyl-L-aspartate)-graft-poly(ethylene glycol) (PBLG-g-PEG) [113]. They reported that by varying the polyethylene glycol content of the polymer, varied drug release profiles occurred. After 7 h 25 – 40 % of total naproxen release had occurred (PBLG-g-PEG1 and PBLG-g-PEG2 respectively) [113]. After the initial burst the drug release slowed down, at the end of their 80 h study 40 – 90 % of drug release had occurred (PBLG-g-PEG1 and PBLG-g-PEG2 respectively) [113]. San Miguel and colleagues loaded amphiphilic triblock copolymer poly(2-N,N-dimethylamino) ethyl methacrylate)-block-poly(caprolactone)-block-poly(2-N,N-dimethylamino) ethyl methacrylate) (PDMAEMAco) with anticancer agent chlorambucil [160]. They found that PDMAEMAcoCL$_{20}$ micelles were capable of sustained release of chlorambucil over more than 100 h. In the first 24 h of the study only 22 % of drug release had occurred [160]. Only after 130 h total drug release was achieved [130]. When compared with other amphiphilic polymer formulations the Ch$_5$ and Dansyl$_{10}$ formulations release the drug notably quicker. Perhaps further modification of the polymer backbone such as higher grafting or use of secondary hydrophobic groups could be used to achieve a more sustained drug release *in vitro*.

The stability of a formulation is one of the most important aspects for pharmaceutical application. Liquid and freeze dried formulations were tested for drug content over a 4 week period in dark conditions and at room temperature with 55 % humidity. The results reinforce the fact that different formulations using the same excipient do not all require the same storage conditions, i.e. Propofol could not be freeze-dried due to high level of drug loss and prednisolone and griseofulvin samples could not be stored as liquids as they formed viscous gels. The stability of each formulation differed, the propofol formulations stored as liquids appeared to slowly lose drug content over the 4 week period up to a maximum of 30 % (Ch$_5$) and 10 % (Dansyl$_{10}$) (Fig. 89 & 90). The prednisolone and

griseofulvin formulations on the whole appeared to be stable across the 4 week period. The major drug loss for these formulations occurred at the initial freeze drying process, however with careful optimization and perhaps the use of cryoprotectants could minimise drug loss [253]. Interestingly the sizes of the self-assemblies were larger after freeze drying and reconstitution at week 0, the reason for this is unknown and needs to be further investigated [309].

4.5. Conclusion

The varied size, solubilisation potential of the drug loaded polymers reinforced the theory that the structural features of the hydrophobic drug hugely affects its ability to load within the micelle core. Ch_5 and $Dansyl_{10}$ have shown excellent drug loading capacities over a range of hydrophobic drugs, indicating that they were not drug specific and could be used as universal drug solubilisers. *In vitro* release profiles showed that all the Ch_5 and $Dansyl_{10}$ formulations achieved sustained release between 48 – 96 h. Biological characterisation is necessary for the amphiphiles and formulations to indicate their potential as drug solubilisers *in vitro* and *in vivo*.

Chapter Five

Biological Characterisation of Modified Amphiphilic Polymers and Formulations

5.1. Introduction

Novel drugs and novel drug delivery systems go through rigorous testing both in preclinial and clinical stages before they are mass produced and marketed. After initial characterisation of the compounds, *in vitro* testing is carried out. *In vitro* analysis is an important process, in which mammalian cells are tested outside the body. This is the most accurate estimation of the *in vivo* fate of the compounds. *In vitro* work or tissue culture allows the study of cells without the variations occurring *in vivo* [310]. The physiochemical environment, homogeneity of the sample and scale can be controlled by the user [310]. However, it is important to mention, that although *in vitro* analysis is beneficial, it cannot give a true representative of *in vivo* conditions.

5.1.1. *Bioavailability Investigation*

It is important to determine the biocompatibility of a formulation *in vitro* before it can be used *in vivo*. In order to do so, a number of assays are carried out. There is no set type or number of assays for this type of evaluation. The most common tests used are simple haemolysis assays and cytotoxicity assays. These tests are simple, quick, relatively cheap and most importantly reproducible.

5.1.1.1. *Haemolysis Assay*

Haemolysis assays are carried out on red blood cells to determine whether a compound has a haemolytic effect towards the red blood cells resulting in cell lysis. This is a particularly beneficial assay for formulations which are to be administered via intravenous injection. Intravenously administered formulations are injected directly into the bloodstream and therefore must not cause any haemolytic or adverse effect on blood cells for their safe use. The assay is carried out with a Tween 80 standard. Tween 80 is a low molecular weight surfactant that has been approved in the UK for intravenous administration and oral consumption [311].

5.1.1.2. *Cytotoxicity Assay*

3-[4,5-dimethylthiazol-2-yl]-2,5-diphenyltetrazolium bromide (MTT) assay is a standard assay for determining the cytotoxic effect of a compound or formulation when exposed to cells. The assay is carried out by treating cells in the exponential growth phase to a formulation for a set period of time [288]. The formulation is removed and the cells are allowed a set amount of time to recover or to die from the effect of exposure to the formulation. After this the % cell viability can be determined by referring to the IC_{50} value produced; this is the polymer concentration at which only 50 % of the cells are still viable.

MTT is a soluble tetrazolium dye with a distinctive yellow appearance. However, in the presence of viable cells, the MTT is reduced to an insoluble purple formazan crystal. By

dissolving the formazan crystal in dimethyl sulfoxide (DMSO) the viability of cells can be measured on a microplate reader. The optimal time for cells to be incubated with MTT to achieved accurate viability determination has been reported to be 4 h.

5.1.1.3. *Cellular Localisation of Formulations*

It is essential to track a formulation on its cellular journey in order to fully understand how the formulation enters the cell and to confirm that the target site for payload release is reached. Cellular localisation studies are carried out on successful formulations usually via the attachment of fluorescent tags to the polymer backbone [312]. It is quite common for the drug molecules to fluoresce as many drug molecules consist of aromatic ring systems exhibiting inherent fluorescence. However, in order for distinction between the delivery vehicle and the drug, it is imperative that they emit fluorescence at different wavelengths and in different colours.

Commonly used fluorescent tags include rhodamine and fluoroisothiocyanate (FITC) [152,313]. However, recently advancement in polymer chemistry has led to the fabrication of fluorescent polymers such as poly(N-isopropyl-acrylamide-co-N-vinyl carbazole-block-poly(dimethylamino) ethyl acryate (PNIPPAm-co-PNVC)-b-PDMAEA) and galactose-polycaprolactone-g-dextran-fluorescein isothiocyanate (Gal-PCL-g-Dex-FTIC) where no tag is needed for fluorescent emission [174,176].

5.1.2. *In vivo analysis*

In vivo analysis uses animal models to determine the pharmacokinetic effects of drugs and formulations after administration i.e. the drug plasma levels to determine drug half life ($T_{1/2}$) and the area under the curve (AUC) to determine the bioavailability of a drug. *In vivo* studies are the most effective and valuable method of determining the fate of drugs after administration to the body. Mice and rats are the most common animals used for *in vivo* studies as their immune system is comparable to humans, they are also more economical as they cost less and small amounts of drug are used in the studies compared with larger animals such as rabbits, guinea pigs and dogs [314].

Drugs can be administered through various routes, the most common are through intravenous injection and oral dosage. Analysis can be carried out on healthy or diseased animal models depending on the desired therapeutic effect. The pharmacokinetic properties of the drugs can be analysed using simple assays or HPLC analysis to determine drug concentration in the blood. Other inspection methods can also be carried out, for example the time taken for the animal to fall asleep in the delivery of anaesthetics, or the time taken for loss of reflex in legs [203]. In anticancer therapeutics tumour growth delay is measured in diseased models [315].

5.1.2. *Aims and Objectives*

The modified polymers will be tested *in vitro*. Their safety profile will be characterised using haemolysis assay and their cytotoxic effect on human colorectal carcinoma (Caco-2) and human smooth muscle kidney (HEK) cells will be determined using MTT assay. The cytotoxic effect and cellular localisation of optimal formulations of Ch_5 and $Dansyl_{10}$ using etoposide and BNIPDaoct will be determined. *In vivo* absorption of griseofulvin through oral gavage of sprague dawley rats will be carried out. The effect of a novel anticancer drug Bisnahthalimidopropyldiamino octane (BNIPDaoct) in the presence of Ch_5 on tumour bearing nude mice will also be undertaken to determine the antitumoral activity after repeated dosing.

5.2. Materials and Methods

5.2.1. *Materials used*

Material	Supplier
Modified PAA polymers	Synthesised in Chapter Two
Formulations of modified PAA	Formulated in Chapter Four
BNIPDaoct	Synthesised in section 4.3.1
Etoposide	Sigma-Aldrich Co., UK
Griseofulvin	Sigma-Aldrich Co., UK
Bovine blood samples	McIntosh Abattoir, (UK)
HPLC Grade methanol	Fisher Scientific, UK
HPLC Grade acetonitrile	Fisher Scientific, UK
Highly purified water	MillexQ system (UK)
Phosphate buffered saline	Fisher Scientific, UK
DMSO	Fisher Scientific, UK
Sodium chloride	Fisher Scientific, UK
Hydrochloric acid	Fisher Scientific, UK
Rhodamine B isothiocyanate	Sigma-Aldrich Co., UK
HEK cell lines	Kindly donated by the University of Hertfordshire

Material	Supplier
Caco-2 cell lines	ECCAC
Minimal essential media (MEM)	Sigma-Aldrich Co., UK
Dulbecco's minimal essential media (DMEM)	Sigma-Aldrich Co., UK
Foetal bovine serum	Fisher Scientific, UK
Trypsin in EDTA	Fisher Scientific, UK
Penicillin streptomycin	Fisher Scientific, UK
L-Glutamine	Sigma-Aldrich Co., UK
Non essential amino acids	Sigma-Aldrich Co., UK
Glycerol	Sigma-Aldrich Co., UK
Triton X	Sigma-Aldrich Co., UK
3-[4,5-dimethylthiazol-2-yl]-2,5-diphenyltetrazolium bromide (MTT)	Sigma-Aldrich Co., UK
L-Glycine	Sigma-Aldrich Co., UK
Microvette®CB300	Vet Tech Solutions, UK
Sprague Dawley rats	Charles River, UK
Female NMRI Nu/Nu mice	le Genest-St.-Isle, France
Amphotericin B	Sigma, St. Louis, MO
Gemcitabine	Sigma, St. Louis, MO
RPMI 1640 media	BioWhitaker, Belgium
10 % heat activated foetal bovine serum	BioWhitaker, Belgium
Non-enzymatic cell-dissociation solution	Sigma, St. Louis, MO
Thiopental	Sigma, St. Louis, MO

5.2.2. *Methods*

5.2.2.1. *Haemolysis Assay*

Fresh bovine blood was washed with phosphate buffered saline (PBS buffer) (0.1 M) and centrifuged (2500 rpm) for 10 min at 4 ºC. The supernatant was discarded. This process was repeated until the supernatant was clear. The erythrocyte was isolated and weighed and a 3 % (w / v) dilution in PBS solution was carried out. The red blood cell solution (80 µL) was pipetted into the wells of a 96 well round bottom plate.

A 10 mgmL^{-1} stock solution of polymer was made up in deionised water and pH adjusted to pH 7.4 with NaOH / HCl. Various concentrations (1 - 0.05 mgmL^{-1}) of polymer solution were prepared from the stock solution using PBS as the diluent. The wells of the plate were then treated with 80 µl of increasing polymer concentrations. PBS and Triton X (80 µL each) were used as the negative and positive controls respectively. The plates were incubated at 37 ºC for 4 h before being centrifuged at 2500 rpm for 10 min at 4 ºC. The supernatant (100 µL) was transferred to a flat bottomed 96 well plate for analysis. The absorbance of the plate was read at 570 nm on a microplate reader (Ascend Lab-Systems, UK). The % haemolysis was calculated in relation to the positive and negative controls.

The remaining pellets were viewed under the light microscope (Leica DM3000B, Leica UK) and observations were recorded.

5.2.2.2. *Cytotoxicity Assay*

5.2.2.2.1. *Cytotoxicity of Modified Polymers*

The cytotoxicity of the modified PAA polymers was determined using the MTT assay model. Caco-2 cells were cultured in minimum essential medium (MEM) containing 10 % foetal bovine serum (FBS), 1 % L- glutamine and 1 % non essential amino acids (NEAA).

A 10 mgmL^{-1} polymer solution was prepared using sterile water as the diluent. The solution was further diluted with media to form a 0.5 mgmL^{-1} stock solution. From the stock solution nine dilutions (0.2 - 1x10^{-4} mgmL^{-1}) were made using media as the diluent (Table 25).

Table 25. Polymer dilutions for MTT assay $0.5 - 1 \times 10^{-4}$ mgmL^{-1}.

Polymer concentration (mgmL^{-1})	Volume of 0.5 mgmL^{-1} polymer stock solution (mL)	Volume of media (mL)
0.5	-	-
0.2	1.400	2.100
0.1	0.700	2.800
0.08	0.560	2.910
0.05	0.350	3.150
0.025	0.175	3.325
0.01	0.070	3.430
0.005	0.050	4.950
0.001*	0.700	2.800
0.0001*	0.070	3.430

*Prepared using 0.005 mgmL^{-1} polymer stock solution

Caco-2 cells (200µL, 10000 cells/well) in exponential growth phases were seeded into a 96-well flat bottomed plate and incubated for 24 h at 37 ºC with 5 % CO_2. The media was replaced with increasing polymer concentrations ($0.5 - 1 \times 10^{-4}$ mgmL^{-1}) as prepared above. Media and Triton X (1:5 PBS) were the negative and positive controls respectively. The plate was incubated as before. After 24 h the polymer solutions were removed and replaced with fresh media. The plate was further incubated for 24h before the media was removed and replaced once more. 3-[4,5-dimethylthiazol-2-yl]-2,5-diphenyltetrazolium (MTT) (50 µL, 5 mgmL^{-1}) was added to the wells and the plate was incubated (37 °C with 5 % CO_2) in the dark for 4 h. After this time the MTT solution was removed from the wells. The remaining purple formazan complexes were dissolved in DMSO (200 µL) and L-glycine buffer (25 mL, made up of 3.75 g glycine and 2.93 g NaCl made up in 500 mL and pH adjusted to pH 10.5) and the absorbance of the plates was read at 570 nm using a microplate reader (Ascend Lab-Systems, UK). Percentage cell viability was calculated relative to the positive and negative controls.

5.2.2.2.2. *Cytotoxicity of anticancer drug formulations*

An MTT assay was carried out (5.2.2.2.1.) using Caco-2 and HEK cells. Caco-2 cells were cultured as previously described (5.2.2.2.1.). HEK cells were cultured in Dulbecco's minimum essential medium (DMEM) containing 10 % FBS and 1 % *penicillin streptomycin* (Penstrep). Cytotoxicity assays for anticancer drugs etoposide and BNIPDaoct alone (0.5 $- 1 \times 10^{-6}$ mgmL^{-1}) and formulations of the anticancer drugs using Ch$_5$ and Dansyl$_{10}$

polymers were carried out. The polymers were fixed at a concentration of 0.005 mgmL^{-1} were the cell viability is 90 % (IC$_{90}$) based on the MTT assay.

Polymeric self-assemblies were formed by probe sonicating the polymers in sterile water (5 mgmL^{-1}). The polymer stock solutions were diluted to 0.005 mgmL^{-1} with media. Etoposide and BNIPDaoct stock solution (20 mgmL^{-1}) was prepared by diluting the drug in DMSO. The formulations were prepared by addition of drug into 0.005 mgmL^{-1} polymer solution (Table 26).

Table 26. Preparation of anticancer drug formulations for MTT assay (1 x 10^{-6} – 0.5 mgmL^{-1}).

Drug concentration (mgmL^{-1})	Volume of 20 mgmL^{-1} drug stock solution (µL)	Volume of 0.005 mgmL^{-1} polymer stock solution (mL)
0.5	112.500	4.5
0.2	45.000	4.5
0.1	22.500	4.5
0.05	11.500	4.5
0.025	5.600	4.5
0.01	2.250	4.5
0.005	1.125	4.5
0.001*	90.000	4.5
0.0001*	9.000	4.5
0.000001*	1.000	4.5

*Prepared using 0.05 mgmL^{-1} drug stock solution

5.2.2.3. *Cellular localisation of BNIPDaoct formulations*

In order to visualise the cells using the confocal microscope, a fluorescent tag was attached to the Ch$_5$ polymer. The Dansyl$_{10}$ and BNIPDaoct possessed inherent fluorescence and therefore no tagging was required.

5.2.2.3.1. *Grafting of rhodamine to primary amines of Ch$_5$*

Ch$_5$ (50 mg) was dissolved in 100 mL water with stirring. A solution of rhodamine B isothiocyanate (1 mgmL^{-1}, 10 mL) was prepared in DMSO and added dropwise to the polymer solution over 0.5 h at room temperature. The reaction was stirred for 1 h in dark conditions before exhaustive dialysis against water using dialysis membrane, molecular

cut off 12 – 14 KDa. At least six 5 L water changes were made over a 24 h period until the water turned from pink to colourless to ensure all the free rhodamine was removed. The dialysate was freeze dried and the product recovered. Successful attachment of rhodamine was confirmed by the polymer product displaying a distinctive pink colour.

5.2.2.3.2. *Confocal imaging of cells*

Caco-2 and HEK cells were cultured in exponential growth phase in 6-well plates containing glass cover slips (5 x 10^4 cell/mL). The cells were allowed to grow for 2 days in a CO_2 incubator at 37 ºC. After this time the media was removed and replaced with 3 mL of polymer, drug or polymer-drug formulation over various time intervals. The polymer concentrations were fixed at 0.005 mgmL^{-1} and the BNIPDaoct was tested at 0.0001mgmL^{-1}. Both concentrations were the IC$_{90}$ value determined from the MTT data.

BNIPDaoct stock solution (0.05mgmL^{-1}) was prepared by dissolving the drug in DMSO. The formulations were prepared by the addition of stock BNIPDaoct (40 µL) in polymer solution (20 mL, 0.005 mgmL^{-1}).

The polymers were incubated with the cells for 0.5, 1, 2 and 4 h after which the solutions were removed and the cells were washed with media (X 3) and allowed to recover in 3 mL of media at 37 ºC in a CO_2 incubator.

After 0.5 h the media was removed and the cells were quickly exposed to icy paraformaldehyde (2 %) for a couple of seconds before being washed and allowed to rehydrate in PBS for 10 min. The cover slips were then removed from the wells and air dried before being mounted with glycerol onto slides. The slides were viewed using the confocal microscope (Nikon D-Eclipse C1, Nikon UK) using the appropriate filters (green for Dansyl$_{10}$, red for Ch$_5$ and blue for BNIPDaoct).

5.2.2.4. *In vivo oral absorption of griseofulvin*

5.2.2.4.1. *Preparation of griseofulvin formulations*

All solutions were made immediately prior to *in vivo* administration.

5.2.2.4.1.1. *Preparation of griseofulvin in water*

Griseofulvin (2 mgmL^{-1}) was added to doubly distilled water and sonicated for 10 min to ensure maximum solubilisation of the drug had occurred. The solution was filtered using 0.45 µm syringe filters with prefilters to remove any excess undissolved drug.

5.2.2.4.1.2. *Preparation of Ch$_5$ and Dansyl$_{10}$ griseofulvin formulations*

Ch$_5$ polymer solution (6 mgmL^{-1}) was prepared by dissolving the polymer in water followed by probe sonication (10 min). Griseofulvin (60 mgmL^{-1}) was added to the Ch$_5$ solution and sonicated for a further 10 min to ensure maximum drug solubilisation had occurred. The

solution was filtered using 0.45 µm syringe filters with prefilters to remove any excess undissolved drug. The amount of solubilised griseofulvin was 1.2 mgmL^{-1} (Table 15, pg 108). The Dansyl$_{10}$, griseofulvin formulation was prepared as described above (16.71 mgmL^{-1}) except a 1 in 5 dilution was then performed of the polymer-drug formulation, to adjust the dosage and enable direct comparison of the results with the Ch$_5$, griseofulvin formulation.

5.2.2.4.2. *In vivo oral administration and evaluation of griseofulvin absorption*

18 male sprague dawley rats (280 g) were separated into four groups (n=4 groups or n=3, ave controls) (Table 27) and their food was withdrawn over night (18 h), the rats had free access to water at all times. The rats were orally dosed with a griseofulvin suspension in water and two griseofulvin formulations (11.8 mgKg^{-1}) via oral gavage. The formulations were prepared as previously described (5.2.2.4.1.). The rats were monitored to evaluate their behaviour immediately after administration and throughout the investigation. Blood samples (approximately 100 µL) were collected using 300µL microvettes (Microvette$^®$CB300, Vet Tech Solutions, UK) at various time points (1, 4 and 7 h) via tail vein venesection. After the first time point (1 h) food was given to the rats. After 24 h the rats were sacrificed using a carbon dioxide chamber and an immediate heart puncture was carried out to retrieve the blood. All blood samples were centrifuged at 2000 rpm for 10 min and the plasma was pipetted off into separate eppendorf tubes. The plasma samples were frozen until ready for analysis. Polymers alone were used as the controls.

Plasma (100 µL) was diluted with 250 µL acetonitrile and vortexed for 30 sec. The mixture was then centrifuged at 3000 rpm for 10 min. The supernatant was collected and 50 µL was injected onto the column. The griseofulvin content of the plasma was determined by HPLC analysis reported by Ahmed [271]. A RP Zorbax ODS 250 mm x 46 mm x 5 µm HPLC column (Hichrom, UK) was used with a flow rate of 2 mLmin^{-1} (50:50 v/v acetonitrile:water) in an isocratic mode (Varian LC, Varian UK). The resultant peak at 3 min was analysed at 260 nm (excitation) and 389 nm (emission) using a fluorescent detector (Varian LC, Varian UK). The amount of griseofulvin present in the samples was determined by comparing to a standard calibration carried out previously with griseofulvin spiked blank plasma samples (1.9 µgmL^{-1} – 10 µgmL^{-1}), R^2 = 0.992 .

Table 27. Group labels and numbers of griseofulvin formulations administered to male Sprague dawley rats by oral gavage.

Group label	Number of rats	Formulation
PC	3	Ch_5 alone
PD	3	$Dansyl_{10}$ alone
G	4	Griseofulvin in water
C	4	Ch_5, griseofulvin
D	4	$Dansyl_{10}$, griseofulvin

The statistical significance of the results was assessed using two-way analysis on variance ANOVA and Dunnett multiple comparison t-test via SPSS 13.0 for Windows.

5.2.2.5. *In vivo therapeutic effect of BNIPDaoct*

5.2.2.5.1. *Preparation of Ch₅, BNIPDaoct formulation*

Ch_5 polymer solution (1 $mgmL^{-1}$) was prepared by probe sonicating the polymer in distilled water (10 min). BNIPDaoct (1 $mgmL^{-1}$) was added to the Ch_5 solution and sonicated for a further 10 min to ensure maximum drug solubilisation had occurred. The solution was filtered using 0.45 µm syringe filters with prefilters to remove any excess undissolved drug. The final drug content in the formulation is 0.3 $mgmL^{-1}$ (Table15, pg105).

5.2.2.5.2. In vivo Effect of CH₅, BNIPDaoct formulation on xenograff tumour (BxPC3 cell line implanted)

The method was carried out as described by Aubert and colleagues [316].Female NMRI Nu/Nu mice (24 – 30 g) were kept in pathogen-free conditions. All surgical procedures and animal care were carried out according to accreditation number 04333 given by the French ministry of agriculture. Human pancreatic cancer cells (BxPC-3) were cultured in RPMI 1640 media which was supplemented with 10% heat inactivated fetal bovine serum, L-glutamine (2 mM), penicillin streptomycin and amphotericin B (100 $µgmL^{-1}$ of each).The cells were washed twice with cold PBS followed by cell harvesting with non-enzymatic cell-dissociation solution for 10 min at 37°C. The cells were washed with PBS (X 3) and kept on ice until ready for injection. The mice were transiently anesthetised (<30 s) with a low dose (2.5 mg) of thiopental and placed into a restraining tube. The tumor cell suspension (1.8×10^6 cells in 100 µL of PBS) was injected subcutaneously into the right flank of the mice. When the tumor became palpable (2 weeks), 2 dimensional

measurements were taken using Vernier calipers once a week, the volume of the tumors was calculated using the formula: $(\pi/6) \times (a \times b^2)$, where a is the largest and b the smallest diameter of the tumor.

Two treatments were performed per week over 4 weeks. Four groups of mice were treated with 1 mgKg^{-1} of the Ch$_5$ polymer and Ch$_5$, BNIPDaoct formulation via interperitoneal injection (Table 28). Gemcitabine, one of the current treatments of pancreatic cancer was used as a control (2.5 mgmKg^{-1}) to compare with the novel formulation. The efficacy of the treatment was evaluated by the change in the tumor volume during the 4 week period. The tumour volume was measured twice a week over the 4 week study. The mice were sacrificed after 5 weeks. Statistical analysis was carried out using the Mann Whitney test and the results were considered to be statistically different when $P<0.05$.

Table 28. Groups of BNIPDaoct formulations administered to nude tumour bearing mice via intravenous injection.

Number of mice	Formulation
6	Ch$_5$ alone
11	Gemcitabine
13	Ch$_5$, BNIPDaoct

5.3. Results

5.3.1. *Haemolysis Assay*

The modified PAA polymers were tested for their haemolytic activity against red blood cells. Figure 93 shows the haemolysis results for the 5 and 10 % hydrophobic grafted polymers. Ch$_5$ could not be tested within the $0.5 - 1$ mgmL^{-1} concentration range as the polymer precipitated out of PBS solution, however at below 0.1 mgmL^{-1} the assay could be carried out. At the low concentration range of $0.005 - 0.1$ mgmL^{-1} the Ch$_5$ showed negligible haemolytic activity with the % haemolysis below 0.5 % (Fig. 94).
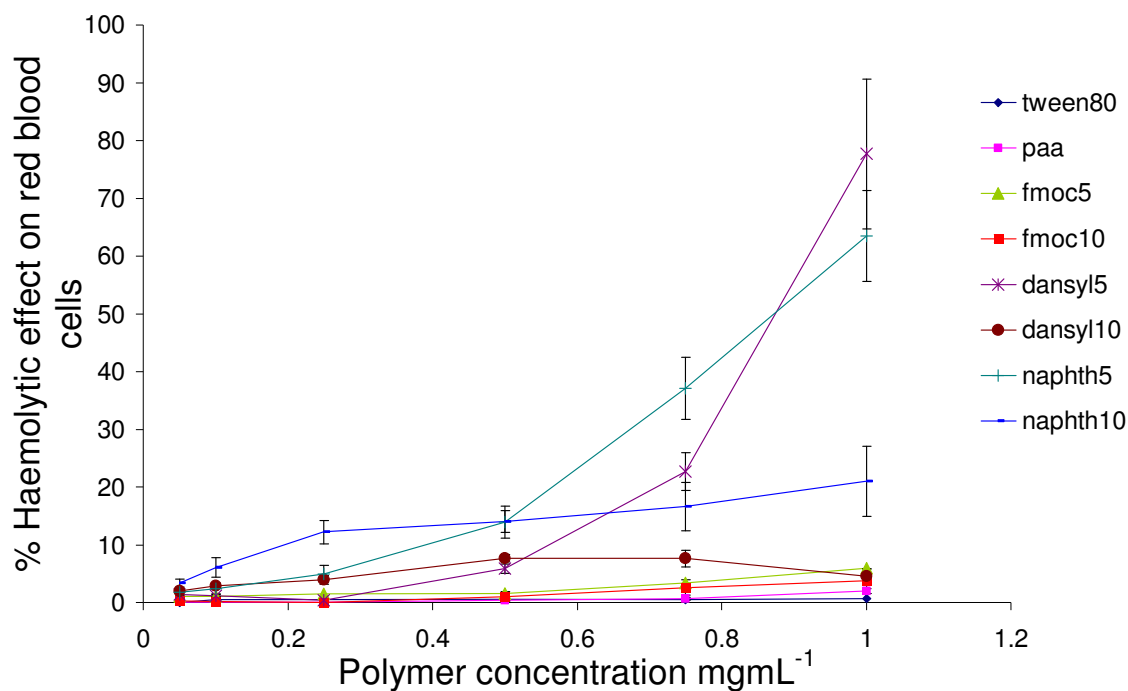
Figure 93. % Haemolytic activity of hydrophobic modified polymers on bovine red blood cells with polymer solutions of 0.5 – 1 mgmL^{-1} (n=3, ave ± SD).
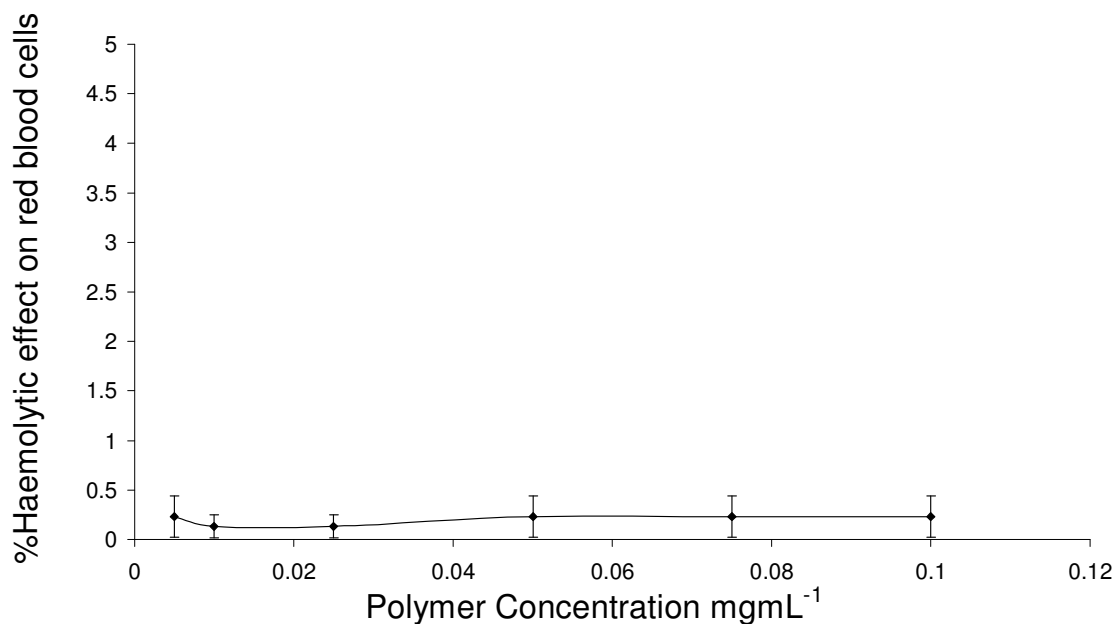
Figure 94. % Haemolytic activity of Ch$_5$ on bovine red blood cells with polymer solutions of 0.1 – 0.005 mgmL^{-1} (n=3, ave ± SD).

Introduction of hydrophobic groups onto the PAA backbone increased the haemolytic effect of the PAA (Fig. 93). However, most of the amphiphiles caused no haemolytic effect on the red blood cells with (% haemolysis ≤ 10 % from polymer concentration from 0.05 to 1 mgmL^{-1}) with exception to Dansyl$_5$, Naphth$_5$ and Naphth$_{10}$. The haemolytic activity varied

with different hydrophobic pendant group on the amphiphiles. The Naphth$_5$ and Dansyl$_{10}$ polymers resulted in notably higher haemolytic activity than the other groups.

As a general trend, higher levels of hydrophobic grafting lowers the haemolytic activity (Fig. 93). Lower levels of haemolytic activity was also experience upon quaternization of the amphiphiles (Fig. 95). The reduction in haemolytic activity results in greater biocompatibility.

Most of the PAA amphiphiles showed an independent haemolytic trend, whereby, increase in polymer concentration did not have an effect on haemolytic activity. However, Dansyl$_5$ and Naphth$_5$ appeared to be concentration dependant (Fig. 95). This possibly explained their unusually high haemolytic activity at the higher concentration ranges.
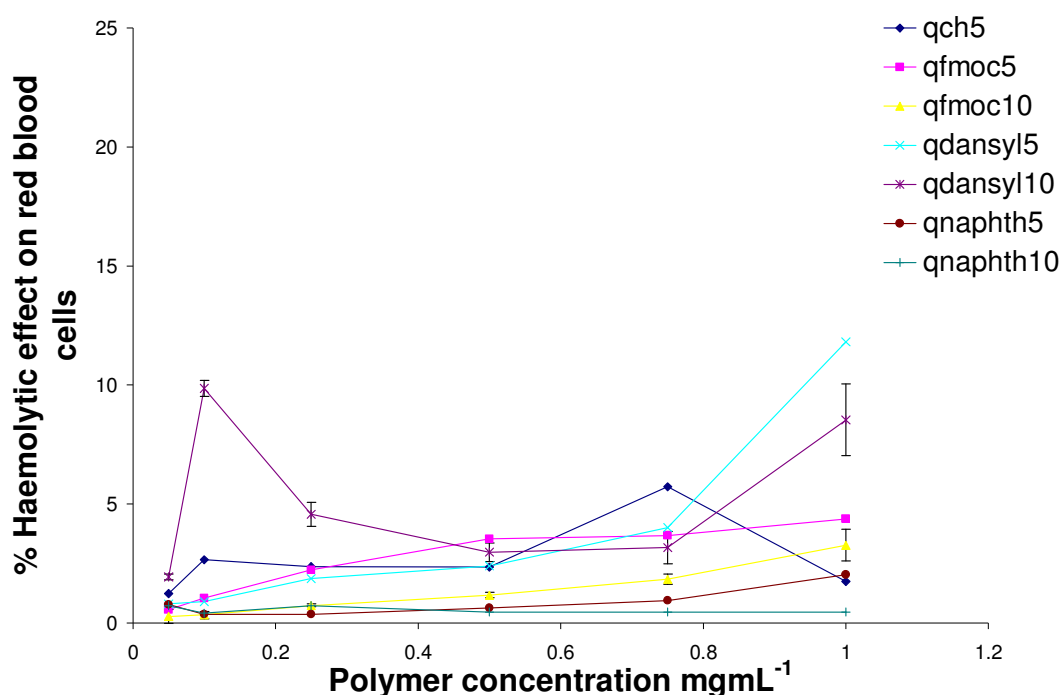
Figure 95. % Haemolytic activity of quaternized polymers on bovine red blood cells with polymer solutions of 0.5 – 1 mgmL^{-1} (n=3, ave ± SD).

The red blood cells where imaged under the light microscope to identify any changes in the appearance of red blood cells. In Figure 96(a) the red blood cells where incubated with PBS which mimics the conditions naturally occurring in the body. The biconcave disc shape can clearly be identified. The cells exist individually and not in clusters. In Fig. 96(b) the cells have been incubated with Triton X, no healthy red blood cells remained, only broken fragments of the cells were visualised. This was due to the surface active Triton X lysing all the cells.

153
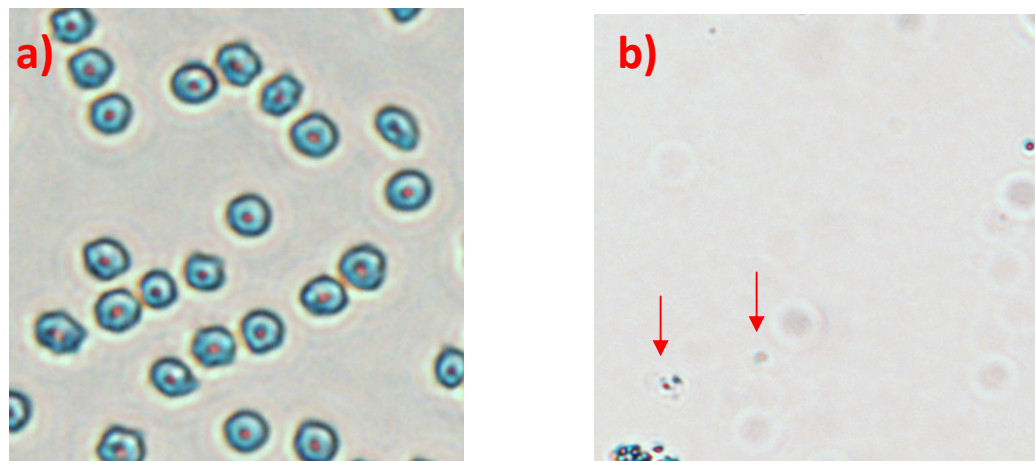
Figure 96. Bovine red blood cells incubated with a) PBS b) Triton X (x 100 magnification).

The morphology of the red blood cells did not change in the presence of the 5 or 10 % hydrophobic grafted polymers (Fig 97 a&b). The type of hydrophobic group and level of grafting did not appear to alter or disrupt the red blood cell structure. However, at higher concentrations of Dansyl$_5$, Naphth$_5$ and Naphth$_{10}$ cell lysis occurred resulting in reduced population of blood cells (Fig. 98).
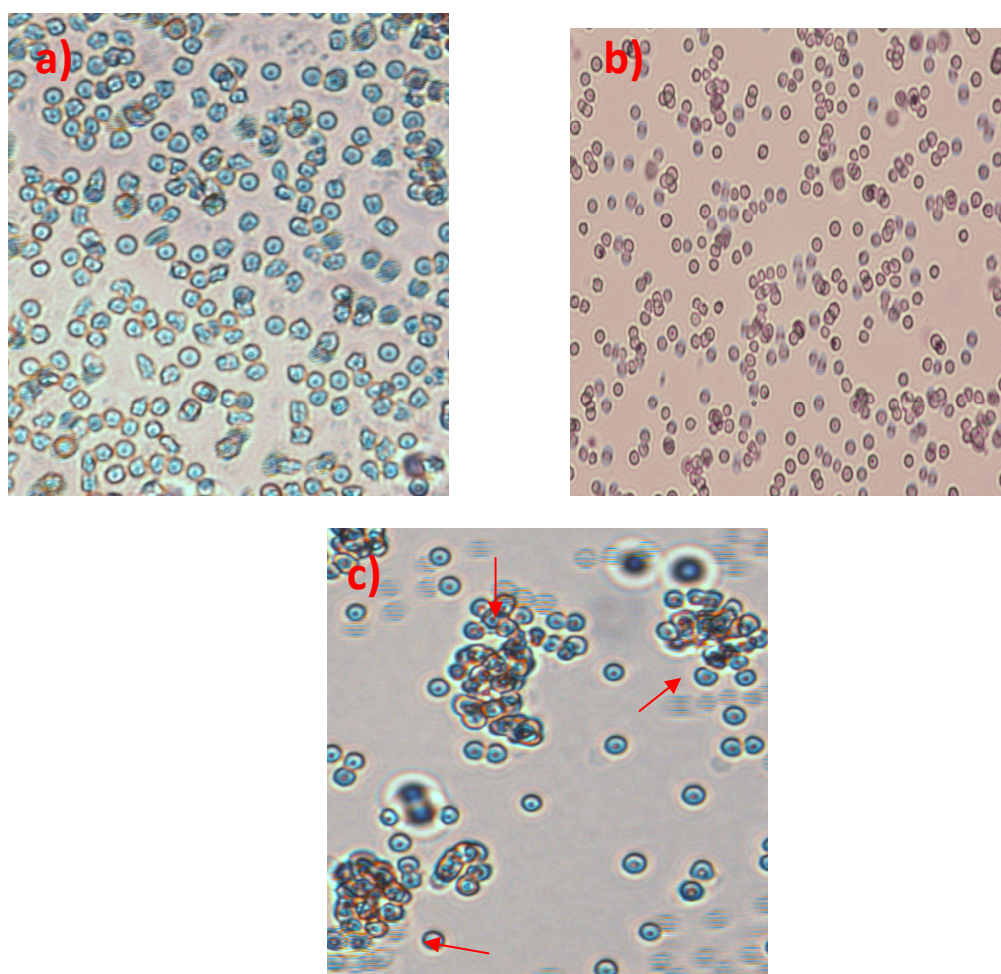
Figure 97. Bovine red blood cells incubated with a) 0.75 mgmL^{-1} Fmoc$_5$ b) 0.75 mgmL^{-1} Fmoc$_{10}$ and c) 0.75 mgmL^{-1} QFmoc$_5$ (x 40 magnification).

154

The red blood cells formed large clusters in the presence of all the quaternized polymers. Fig. 97 c) shows the clumping of red blood cells in the presence of QFmoc$_5$ when compared with Fmoc$_5$. This trend was observed for all the quaternized amphiphiles. Perhaps this phenomenon may be due to the positive charge on the hydrophilic modified polymer causing haemagglutination to occur. However, the shape of the red blood cells was not altered in the presence of the positively charged polymers; they still retained their round appearance until the point when cell lysis occurred.
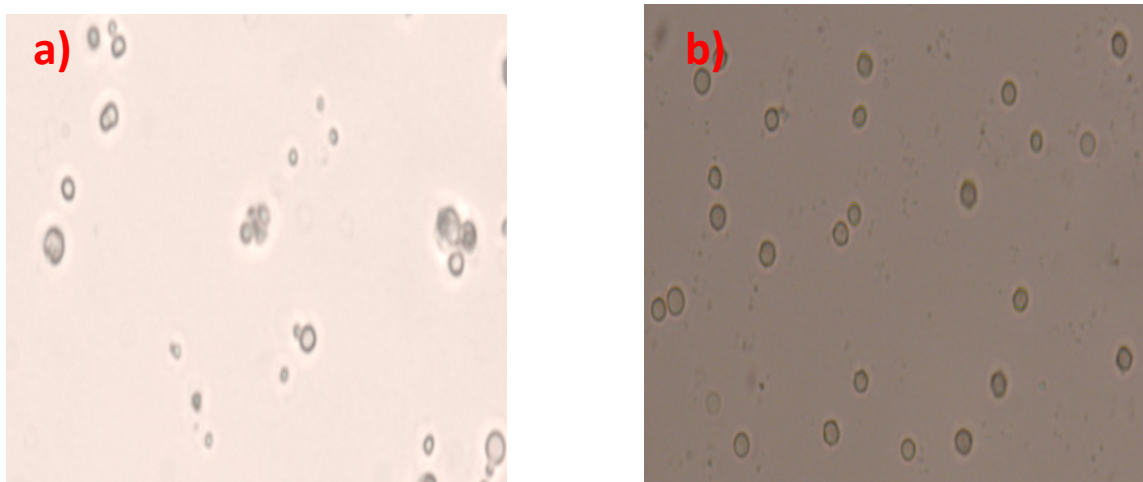
Figure 98. Bovine red blood cells incubated with a) 0.75 mgmL^{-1} Dansyl$_5$ b) 0.75 mgmL^{-1} QNaphth$_5$ (x 40 magnification).

5.3.2. *Cytotoxicity Assay*

5.3.2.1. *Cytotoxicity of modified polymers*

The MTT assay was carried out to determine the polymer concentration at which only 50 % (IC$_{50}$) of the cells population were viable. Polymers with lower IC$_{50}$ values, have a greater cytotoxic effect. No notable difference was observed between the IC$_{50}$ of the modified polymer and the unmodified PAA backbone (Table 29). The different hydrophobic groups had only a slight impact on the IC$_{50}$ values. The IC$_{50}$ of the unmodified PAA backbone was 23.3 µgmL^{-1} and the presence of the hydrophobic pendants did not significantly change the IC$_{50}$ value of the backbone. Ch$_5$ had a higher IC$_{50}$ value (37.4 µgmL^{-1}) indicating that the presence of the cholesteryl group improved the safety profile of the polymer. The presence of Dansyl had the adverse effect reducing the IC$_{50}$ to 17.4 µgmL^{-1} (Dansyl$_5$).

Table 29. IC_{50} values for Caco-2 cells treated with modified PAA polymers ($1 \times 10^{-4} - 0.5$ mgmL^{-1}) for 24 h n=3, ave (SD).

Polymer	IC_{50} value on Caco-2 cells (μgmL^{-1})	Number fold more cytotoxic compared to IC_{50} of PAA
PAA	23.3 (20.1)	-
Ch$_5$	37.4 (3.7)	-1.61
QCh$_5$	55.8 (13.9)	-2.39
Fmoc$_5$	22.9 (3.61)	0.98
QFmoc$_5$	28.1 (2.0)	-1.21
Fmoc$_{10}$	27.9 (9.62)	-1.19
QFmoc$_{10}$	18.4 (4.23)	1.26
Dansyl$_5$	17.4 (3.5)	1.39
QDansyl$_5$	51.3 (5.1)	-2.20
Dansyl$_{10}$	24.6 (0.9)	-1.06
QDansyl$_{10}$	34.3 (1.2)	-1.47

The addition of hydrophilic groups to the polymer backbone in general increase the IC_{50} value. The IC_{50} of Ch$_5$ (37.4 μgmL^{-1}) was increased to 55.8 μgmL^{-1} upon quaternization (Fig. 99). This can be attributed to the conversion of the primary amines on the polymer backbone to their less toxic quaternary ammonium status [317]. Furthermore this trend was exhibited by all quaternized polymers with the exception to Fmoc$_{10}$. Upon quaternization the IC_{50} of Fmoc$_{10}$ reduced from 27.9 μgmL^{-1} to 18.4 μgmL^{-1} (QFmoc$_{10}$), the reason for this observation is unknown (Table 29).

The degree of grafting also had an impact on the cytotoxicity of the polymers. At higher levels of grafting a decrease in cytotoxicity was observed (Fig. 100 & 101). Fmoc$_{10}$ and Dansyl$_{10}$ appeared safer than their 5 % counterparts (27.9 and 24.6 μgmL^{-1} respectively), this perhaps was due to the reduced number of primary amine groups present, thus reducing the cytotoxicity of the polymer.
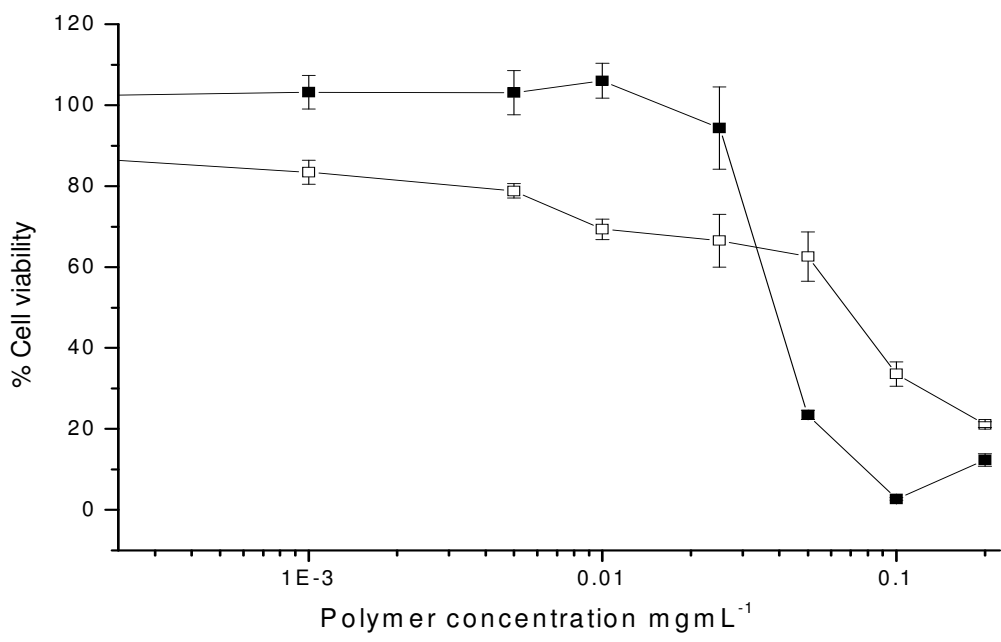
Figure 99. MTT results for % cell viability of Caco-2 cells exposed to ■ Ch_5 □ and QCh$_5$ (1.0 – 1.0 x 10^{-4} mgmL^{-1}) (n=3, ave ± SD).
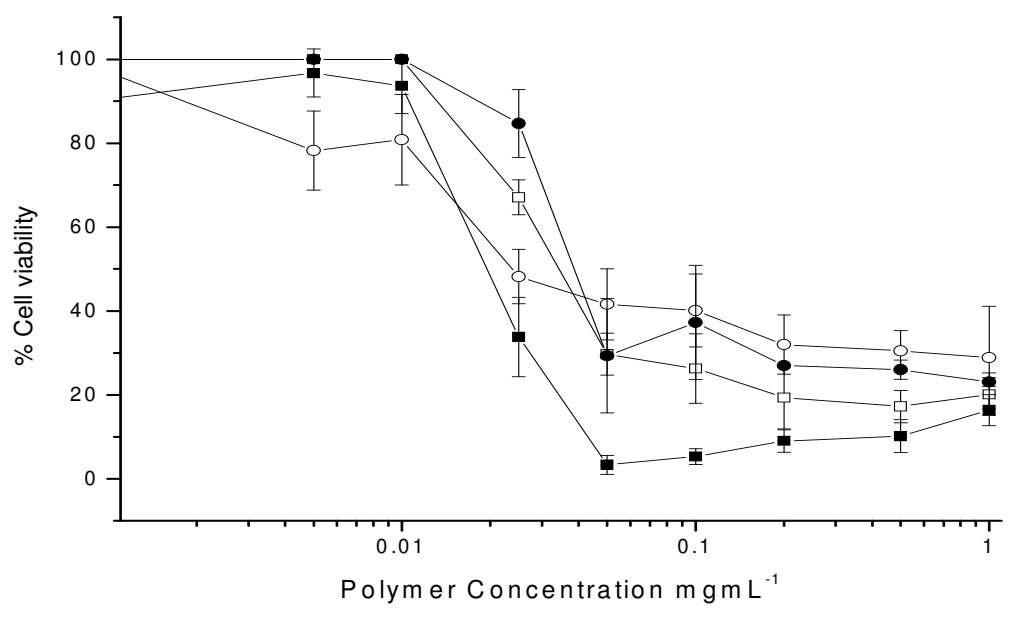
Figure 100. MTT results for % cell viability of Caco-2 cells exposed to ■ Fmoc, □ QFmoc$_5$, ● Fmoc$_{10}$ and ○ QFmoc$_{10}$ (1.0 – 1.0 x 10^{-4} mgmL^{-1}) (n=3, ave ± SD).
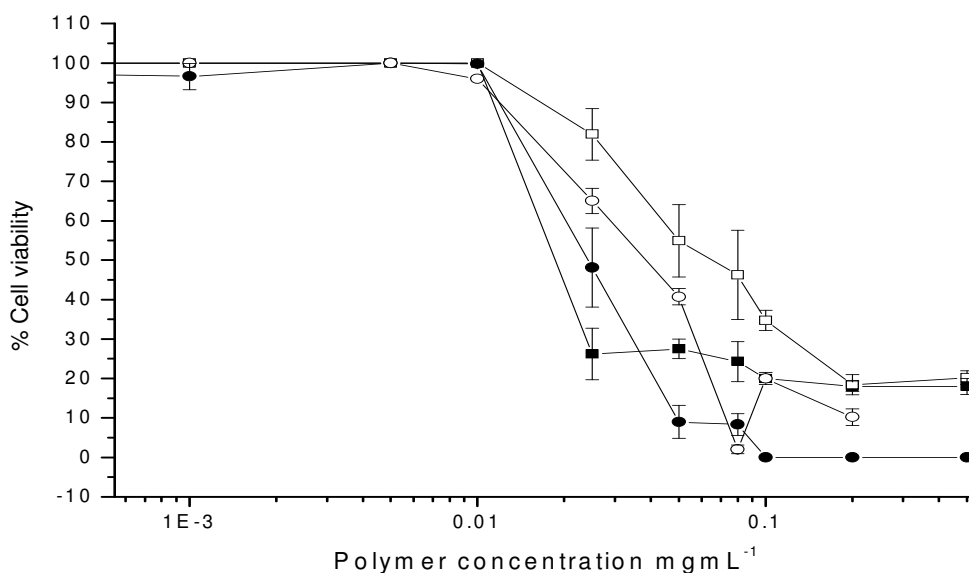
Figure 101. MTT results for % cell viability of Caco-2 cells exposed to ■ Dansyl$_5$, □ QDansyl$_5$, ● Dansyl$_{10}$ and ○ QDansyl$_{10}$ (1.0 – 1.0 x 10^{-4} mgmL^{-1}) (n=3, ave ± SD).

5.3.2.2. *Cytotoxicity of anticancer formulations*

MTT assays were carried out on Ch$_5$ and Dansyl$_{10}$ formulations of etoposide and BNIPDaoct to determine whether the polymeric self-assemblies were capable of delivering cytotoxic drugs into the cells and enhancing the therapeutic effect of the drugs.

In order for an anticancer agent to be successful, it requires a cytotoxic effect when in contact with cancer cells. This requires a low IC$_{50}$ value. To determine whether our formulation enhanced the therapeutic effect of the anticancer agent, they were formulated at the polymer IC$_{90}$ concentration (the concentration at which 90 % of cells where viable determined via MTT assay). Since the polymers were tested using their IC$_{90}$ values, it is assumed that they have negligible cytotoxic effect on cells, and any change in IC$_{50}$ value when treated with anticancer formulations when compared to the free drug is as a result of increased uptake of the drug or due to the enhanced therapeutic effect.

When Caco-2 and HEK293 cells were treated with etoposide, it appeared that the HEK293 cells had a much lower IC$_{50}$ values than the Caco-2 cells, 2.5 µgmL^{-1} and 189.9 µgmL^{-1} respectively, indicating etoposide is more cytotoxic on HEK cells (Table 30). Perhaps the slower rate of proliferation on healthy HEK cells compared to the carcinoma Caco-2 cells made them more susceptible to the cytotoxic effect *in vitro*.

Table 30. MTT assay of polymers and formulations on HEK 293 cells.

Polymer/Drug/Formulation	IC$_{50}$ value on Caco-2 cells (μgmL^{-1})	Increase in cytotoxicity	IC$_{50}$ value on HEK cells (μgmL^{-1})	Increase in cytotoxicity
Ch$_5$	37.4	-	51.4	-
Dansyl$_{10}$	24.6	-	19.3	-
Etoposide	189.9	-	2.5	-
Ch$_5$, etoposide	86.3	2.2 fold	1.4	1.8 fold
Dansyl$_{10,}$ etoposide	13.6	14 fold	0.2	10 fold
BNIPDaoct	6.4	-	5.0	-
Ch$_5$, BNIPDaoct	5.1	1.3 fold	0.2	30 fold
Dansyl$_{10,}$ BNIPDaoct	0.4	16 fold	0.2	30 fold

IC$_{90}$ of the polymer was used in the formulations (5 μgmL^{-1}).

When Ch$_5$, etoposide formulation was exposed to the two cell lines, an equal increase in cytotoxicity was experienced by both cell lines (Table 30). This indicates that Ch$_5$ was able to enhance the therapeutic effect of the drug compared with the free etoposide. A similar effect was observed for the Dansyl$_{10}$, etoposide formulation. However the Dansyl$_{10,}$ etoposide formulation achieved the largest decrease in IC$_{50}$ values for both cell lines (14-fold and 10-fold respectively), suggesting that the Dansyl$_{10}$ was a more effective delivery vehicle for the delivery of etoposide to Caco-2 and HEK cells.

When both cell lines were exposed to BNIPDaoct, the IC$_{50}$ value with the HEK cells was slightly lower than Caco-2 cells (Table 30). The presence of the Ch$_5$, BNIPDaoct formulation have similar cytotoxic effect as the free drug on Caco-2 cells, with only 1.3-fold increase in cytotoxicity experienced. However, when the formulation was exposed to the HEK293 cells, a larger increase in cytotoxicity was observed (30-fold). Again the Dansyl$_{10,}$ BNIPDaoct formulation increased the cytotoxic effect on both cell lines with higher cytotoxic properties on HEK293 than that of Caco-2 cells.

5.3.3. *Cellular localisation of BNIPDaoct formulations*

Cellular localisation studies of the Ch$_5$, BNIPDaoct formulation in Caco-2 and HEK293 cell lines. Both the polymer and drug were formulated at the non toxic concentrations, their IC$_{90}$ values were used which were previously determined from the MTT assay (5.3.2.2.). The Ch$_5$ polymer was tagged with rhodamine as a fluorophore to allow intracellular

visualisation. Rhodamine is a commonly used tag and exhibits red emission fluorescence. Dansyl$_{10}$ possessed its own inherent fluorescence and hence a tag was not required. The dansyl moiety on the polymer emits a green flourescence. The BNIPDaoct drug also possessed its own inherent fluorescence and appears as a blue colour on the confocal microscope when inside the cells. It is important to note that if no polymer or drug entered the cells, the images from the confocal microscope would appear black as no fluorescent moieties are present.

Fig. 102 (A4) shows the confocal images for the Ch$_5$, BNIPDaoct formulation on Caco-2 cells over 4 h. It was observed that polymer alone, free drug and formulation only appeared within the cells after 4 h. The polymer and the drug appear to co-localise within the cell cytoplasm. The polymer does not appear to enhance the uptake of the drug. This observation correlates well with the cytotoxicity assay. The small bright dots on A4 are due to cell debris remaining from dead cells stained with Ch$_5$. The cells also appear to be clustered, however, this might not be a true representation of the *in vitro* condition after sample treatment. Cells were 90 % confluent before cell fixation, and during this process some of the less adherent cells have been removed during the washing steps.
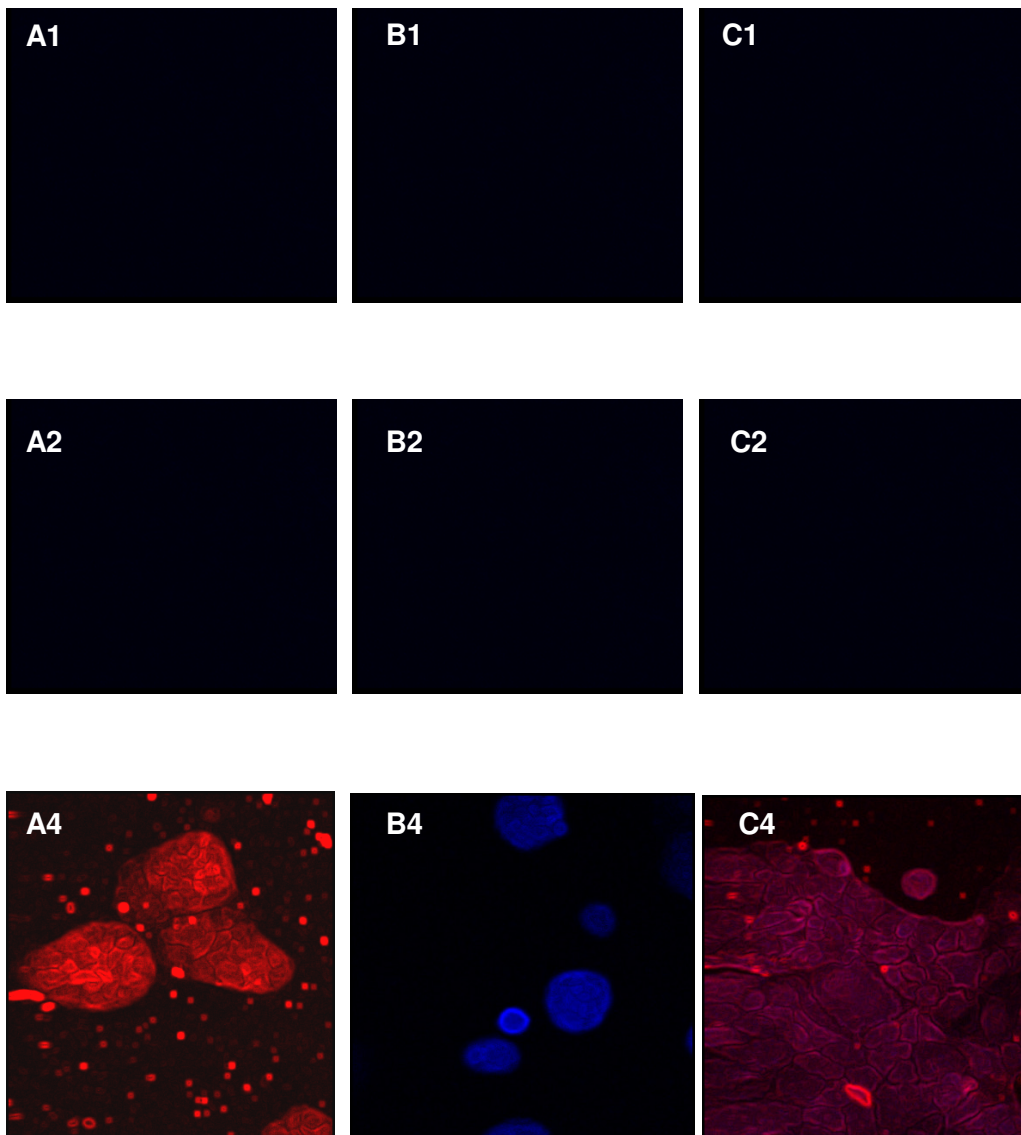
Figure 102. Confocal images (X 400 magnification) of A) Ch$_5$, B) BNIPDaoct and C) Ch$_5$, BNIPDaoct formulation at 1) 1 h, 2) 2 h and 4) 4h on Caco-2 cells. Red- polymer, blue-BNIPDaoct.

The confocal images showed the Ch_5 formulation also did not enhance the cellular uptake in HEK cells (Fig. 103). The free drug, polymer alone and formulation were co-localised in the cytoplasm after 4 h. This result does not correlate with the cytotoxicty assay as a 30-fold increase in cytotoxicty was observed with the presence of Ch_5.
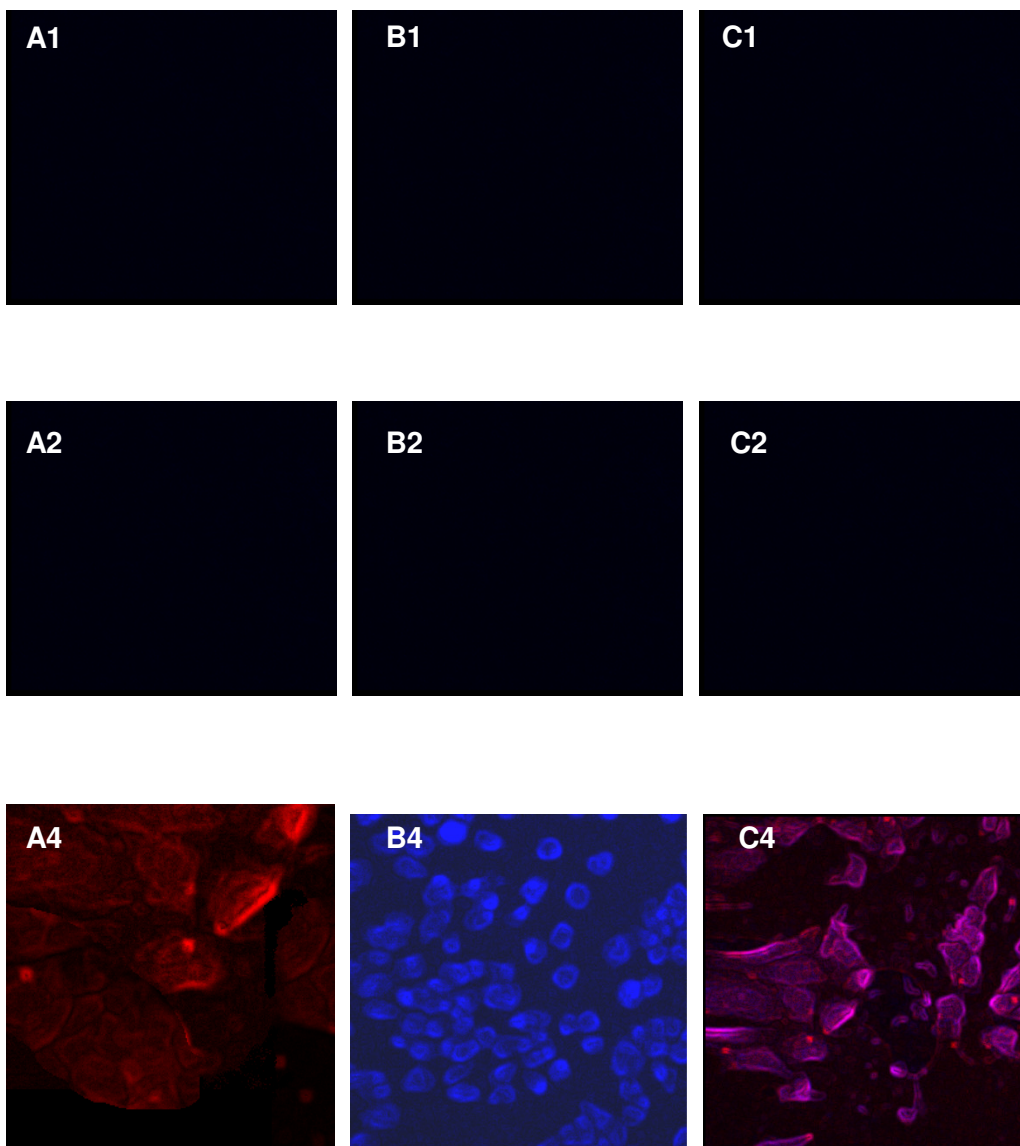
Figure 103. Confocal images (x 400 magnification) of A) Ch_5, B) BNIPDaoct and C) Ch_5, BNIPDaoct formulation at 1) 1 h, 2) 2 h and 4) 4h on HEK cells. Red- polymer, blue-BNIPDaoct.

The Dansyl$_{10}$ formulations showed similar uptake in both Caco-2 and HEK cell lines (Fig. 104 & 105). The drug and polymer separately were taken up by the cells after 4 h, however when formulated together they appeared to be co-localised within the cellular cytoplasm after 2 h. This suggests that the Dansyl$_{10}$ formulations (green) appeared to have a synergistic effect on the HEK cell and Caco-2 cell lines. This result correlates well with the cytotoxicty assay (Table 30). The Caco-2 cells treated with the formulation, the drug fluorescence was more evident as a deeper blue colour was observed, however in the HEK cells the green fluorescence of the polymer was predominant. This observation correlates well with the cytotoxicity assay, whereby the formulation achieved a 30-fold increase in cytotoxicty on the HEK cells but only a 16-fold increase on the Caco-2 cells.
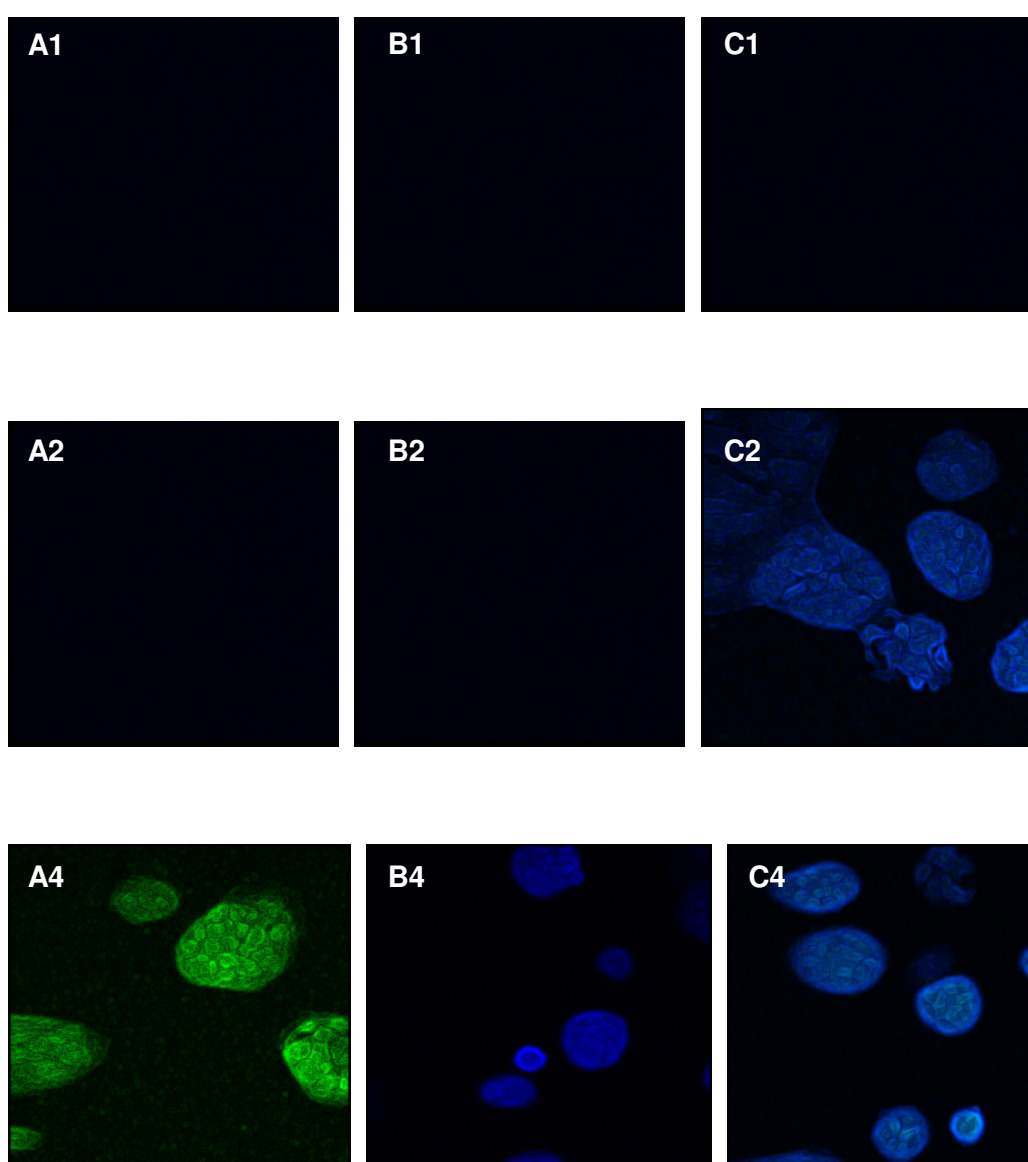
Figure 104. Confocal images (x 400 magnification) of A) Dansyl$_{10}$, B) BNIPDaoct and C) Dansyl$_{10}$, BNIPDaoct formulation at 1) 1 h, 2) 2 h and 4) 4h on Caco-2 cells. Green-polymer, blue- BNIPDaoct.
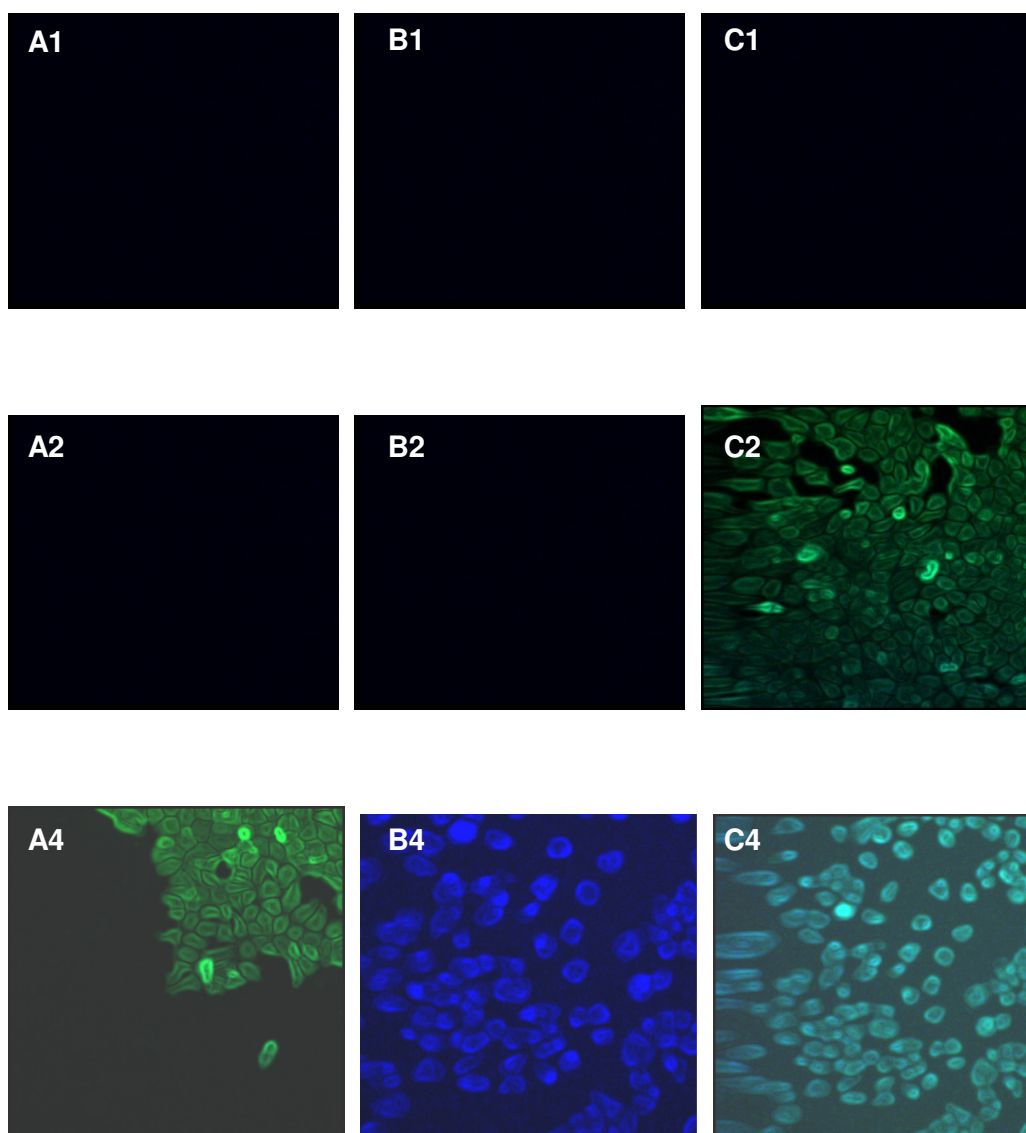
Figure 105. Confocal images (x 400 magnification) of A) Dansyl$_{10}$, B) BNIPDaoct and C) Dansyl$_{10}$, BNIPDaoct formulation at 1) 1 h, 2) 2 h and 4) 4h on HEK cells. Green- polymer, blue- BNIPDaoct.

5.3.4. *In vivo oral absorption of griseofulvin*

Griseofulvin in water and two griseofulvin formulations (using Ch$_5$ and Dansyl$_{10}$) were administered to male Sprague dawley rats via oral gavage. The rats were constantly monitored visually to ensure that no gross toxicity was experienced, causing pain or discomfort to the animals. The rats were fully alert and appeared comfortable after the dosing with the exception to one. After administration of the formulation, one of the Ch$_5$, griseofulvin group had to be euthanised due to suspected oesophageal puncture, a known possible adverse event of oral gavage. The level of griseofulvin present in plasma

samples of the rats was determined by HPLC analysis. The griseofulvin peak had a retention time of approximately 3 min (Fig. 106).
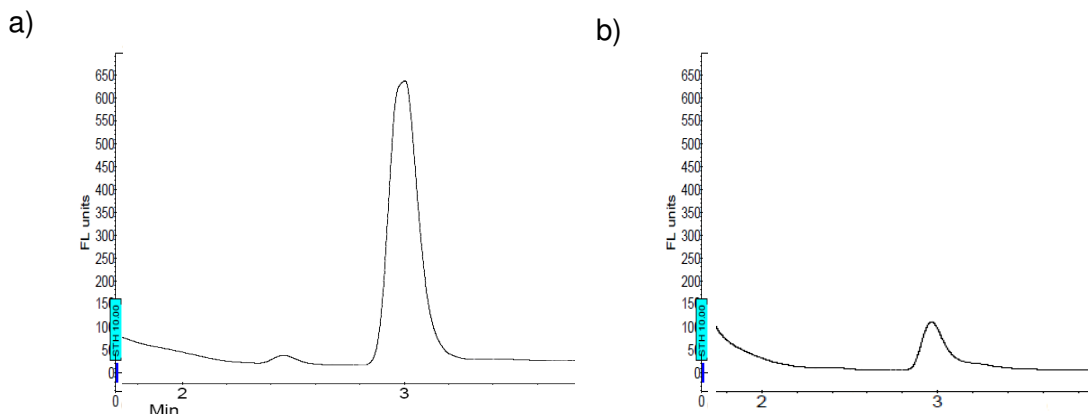
Figure 106. Reverse phase HPLC chromatogram of griseofulvin detected in plasma at 260 nm (excitation) and 239 nm (emission) of a) Ch_5, griseofulvin after 4 h and b) Ch_5, griseofulvin after 7 h.

The plasma concentration level was determined at 1, 4, 7 and 24 h time points, a graph of griseofulvin concentration vs. time was plotted (Fig. 107).
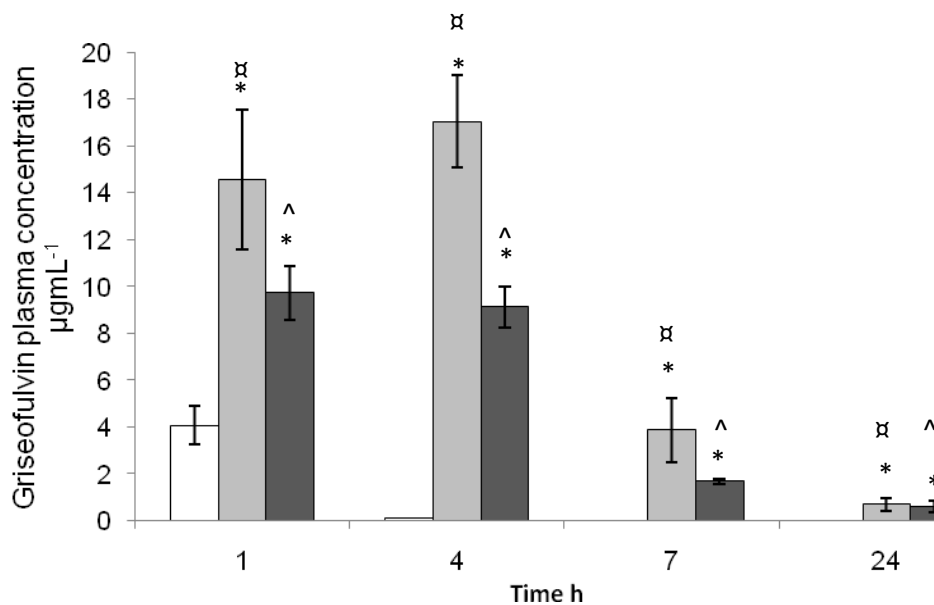
Figure 107. Mean plasma griseofulvin concentration (μgmL^{-1}) following administration of griseofulvin by oral gavage to male Sprague dalwey rats under fasted conditions over 24 h, □ griseofulvin in water (n=4), ▨ Ch_5, griseofulvin (n=3, ave) and ■ $Dansyl_{10}$, griseofulvin (n=4). Error bars = SD. * $p < 0.001$ formulations vs. griseofulvin in water, ¤ p,0.001 $Dansyl_{10}$, griseofulvin vs. Ch_5, griseofulvin, and ^ p,0.001 Ch_5, griseofulvin vs. $Dansyl_{10}$, griseofulvin.

At all time points the griseofulvin formulation appeared to have higher plasma drug levels than the griseofulvin in water. The griseofulvin concentration at each time point was found to be significantly higher than the griseofulvin in water control ($p<0.001$).The C_{Max} (concentration at which the maximum level of drug was absorbed) of the griseofulvin in water was at 1 h, after this time no more drug was absorbed. The Ch_5, griseofulvin showed the greatest absorption, with as much as 17.059 μgmL^{-1} found in the plasma. The t_{Max} (time at which the maximum concentration was observed) occurred at 4 h for this formulation. This indicated that the formulation was stable within the stomach enabling absorption possibly in the small intestine and into the blood plasma. In contrast, the t_{Max} of $Dansyl_{10}$, griseofulvin formulation was after 1 h with a C_{Max} of 9.752 μgmL^{-1}. The lower absorption of the $Dansyl_{10}$ formulation could be due to the dilution carried out in the preparation stages resulting in lower polymer concentration leading to instability within the stomach, whereby, the formulation prematurely released its payload hindering efficient absorption across the GI tract over sustained periods of time. This observation correlates well with the larger critical association concentration (CAC) of $Dansyl_{10}$ (0.25 $mgmL^{-1}$) compared to Ch_5 (0.093 $mgmL^{-1}$) (Table 11, pg 75).

5.3.5. *In vivo therapeutic effect of BNIPDaoct*

A Ch_5, BNIPDaoct formulation was administered weekly to tumour bearing nude mice and the effect on tumour volume was measured over a 4 week period. After 4 weeks the mice were sacrificed and the final tumour volume was determined (Fig. 108).
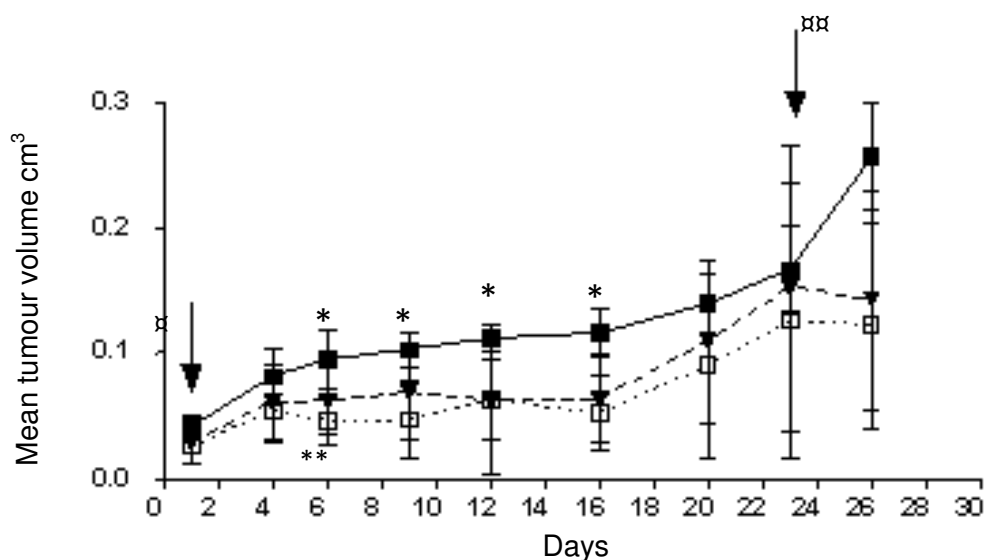
Figure 108. Mean tumour volume in mice implanted with BxPC3 cell line and treated with ■ CH₅, ▫ CH₅, BNIPDaoct formulation, and ▼ gemcitabine. Treatment was started after two weeks when tumour was palpable. Error bars are SD. (* $P < 0.05$, CH₅,BNIPDaoct formulation *vs.* CH₅; ** $P < 0.05$, CH₅, BNIPDaoct formulation *vs.* gemcitabine). Arrow indicate the first (¤) and the last injection (¤¤).

166

The tumour volume after treatment with Ch_5 alone grew from 0.03 cm^3 on day 0 up to 0.25 cm^3 on day 26. The tumour volume after administration with the Ch_5, BNIPDaoct formulation was quite remarkable, the growth of the tumour was significantly reduced with the tumour volume on day 26 being only 0.1 cm^3 (after 6,9,12,16 days, p values= 0.028,0.01, 0.003, 0.028 respectively when compared to the Ch_5 alone). The decrease in tumour size was similar with the gemcitabine formulation with the tumour volume being 0.125 cm^3 after the 26 days. When compared to gemcitabine there is a slight decrease in size, however this was only significant after the third injection (p=0.006). The results strongly suggested that the Ch_5, BNIPDaoct was as efficient as gemcitabine as an anticancer therapeutic agent.

Fig. 109 shows photographs of tumours extracted from the nude tumour bearing mice after 4 weeks. The tumour treated with Ch_5 is the largest in size at 10 mm, as expected since Ch_5 was the control. The tumour treated using the Ch_5, BNIPDaoct formulation, the tumour size is notably smaller at approximately 6 mm in comparison with the Ch_5 control. The tumour treated with commercially available anticancer drug gemcitabine which appears to have been impeded the tumour growth resulting in a final tumour size of approximately 8 mm. These images highlight the potential of Ch_5, BNIPDaoct formulations in anticancer therapeutics.
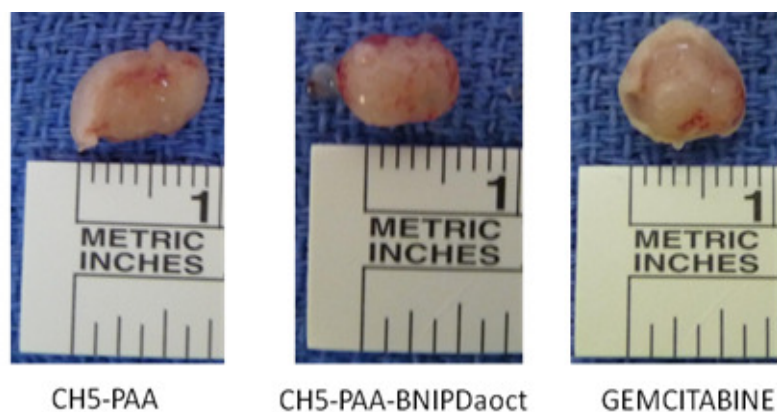
Figure 109. Representative example of each tumour recovered at the end of each drug treatment.

5.4. Discussion

Haemocompatibility is an essential characteristic of any drug or formulation being administered intravenously into the body. We observed that most of the modified PAA polymers had no notable haemolytic effect over the concentration range tested (0.005 - 1 mgmL^{-1}) with less than 10 % haemolytic activity observed (Fig. 93). Hydrophobic modification of the parent PAA backbone resulted in increased haemolytic activity. This finding was not consistent with other reports of cationic polymers [317]. Aravindan and colleagues reported that acyl grafting of poly(ethylenimne) (PEI) decreased the haemolytic effect as the positive charge density on the cationic polymer was reduced hence reducing interactions with negatively charged red blood cell membranes [317]. However, we found that higher grafting levels of hydrophobic modification generally reduced the haemolytic effect.

On the other hand, it has also been hypothesised that hydrophobic alkyl pendant groups are able to anchor into the phospholipid bilayer of the red blood cells and hence disrupting their structure and forming polymer-lipid aggregates [318]. Our study suggests that the aromatic pendant groups also possess the ability to disrupt the lipid bilayer causing rupture of the cell, however this phenomenon only occurs at high polymer concentrations.

Numerous research groups have published work on addition of hydrophilic moieties onto polymer backbones such as quaternization [3,76,125,319]. It has been reported that quaternization results in an increase in haemocompatibility [122]. We found that upon quaternization of the PAA amphiphiles, a decrease in haemolytic activity was observed consistent with the previous findings. The decrease in haemocompatibility can be attributed to the reduced number of 1º amine groups on the polymer, as 1º amines are known to exert haemolytic effects on erythrocyte membranes, while tertiary amines reduce the haemolytic effect [316,320]. It was observed however, that the presence of the permanent positive charge resulted in the formation of heamagglutination, whereby the cells had not deviated from their original shape, but had aggregated together into groups, possibly due to electrostatic interactions [321]. This phenomenon was not observed for the corresponding unquaternized amphiphile counterparts.

Hydrophobic modification of the PAA backbone had little impact on the cytotoxicity of the polymer. The hydrophobic pendant group had an impact on the cytotoxicity experienced by the cells, with Ch$_5$ having the highest IC$_{50}$ value (37.4 µgmL^{-1}) and Dansyl$_{10}$ having the lowest (17.4 µgmL^{-1}) on Caco-2 cells (Table 29). Addition of hydrophobic groups to the backbone resulted in slight decrease in cytotoxicity. Higher grafting levels and quaternization of the polymer resulted in a lower 1º amine levels in the polymer. It has previously been reported that 1º amines are highly cytotoxic and by reducing their

presence on a polymer will result in an increased safety profile of that polymer [317]. These findings are in agreement with both the haemolysis and cytotoxic assay results.

The IC_{50} values for the polymers were lower than the CMC values (Table 11, pg 75). However it is important to remember that *in vitro* conditions are not exactly the same as the conditions found *in vivo*. For example the cell line is only a representative of one or two cell types in the body, the cells were seeded onto a flat surface and therefore have lost their 3D geometry, they are also treated with a high concentration/cell number which would not happen *in vivo*. All these conditions need to be taken into consideration when analysing the cells as they may not be affected by much higher dosages than suggested *in vivo*.

Polymeric self-assemblies have been previously shown to enhance the *in vitro* cellular uptake of therapeutic agents such as anticancer drugs [70,98]. Danhier and colleagues loaded poly(ethyleneglycol)$_{750}$-block-poly(ε-caprolactone-co-trimethylenecarbonate) with anticancer paclitaxel and exposed the formulation to human cervix epithelial carcinoma cells [98]. They reported that the polymer loaded paclitaxel had a lower IC_{50} (12.5 µgmL^{-1}) than the free drug (17.6 µgmL^{-1}) after only 24 h exposure [98]. The polymer concentration was fixed at 82 % cell viability and therefore the decrease in IC_{50} value could be solely attributed to the cytotoxic effect of the paclitaxel [98]. These results do not show a notable difference between the cytotoxic effect of the free drug and the formulation. In comparison the Ch$_5$ and Dansyl$_{10}$ formulations achieved much larger increment of increased cytotoxicity.

Consistent with these results we observed that in both Caco-2 and HEK cell lines the cytotoxic effect of both etoposide and BNIPDaoct was enhanced as much as 2.2-fold and 14-fold on Caco-2 cells (Ch$_5$, etoposide and Dansyl$_{10}$, etoposide respectively) and 30-fold on HEK cells (Ch$_5$, BNIPDaoct and Dansyl$_{10}$, BNIPDaoct respectively) (Table 30). The Dansyl$_{10}$ appeared to be the more effective anticancer drug carrier as it showed the highest reduction of IC_{50} value. These findings could be attributed to the synergistic effect observed by confocal imaging of the BNIPDaoct formulations over time. The synergistic effect experienced with the Dansyl$_{10}$ formulation resulted in the polymer, drug formulations becoming co-localised in the cytoplasm after only 2 h whereas, separately they were only apparent after a 4 h period.

Oral absorption of griseofulvin through the gastrointestinal (GI) tract is very low and commonly varied amongst individual patients [265,271]. To achieve the desired therapeutic effect various formulations have been attempted *in vivo* including aqueous suspensions, emulsions etc. [270,271]. The absorption of griseofulvin *in vivo* is affected by a number of factors such as low aqueous solubility of drug, patients stomach and the type of formulation [270]. In clinics, patients who are prescribed with griseofulvin are advised to

eat a high fat content meal immediately following oral administration of the drug in order to increase drug solubility and to aid absorption across the GI tract [271].

Fujioka and colleagues administered griseofulvin orally in a gelatine capsule to male Wistar rats (20 mgKg^{-1}). They analysed the plasma drug levels over a 10 h period achieving a C_{Max} of 1.37 µgmL^{-1} after 7 h with the bioavailability of 1.04 [270]. However, the results from the study widely varied with inter-patient variation being evident [270]. Ahmed and colleagues have recently formulated griseofulvin in fast dissolving freeze dried emulsion tablets [271]. The tablets were administered in a single dose (125 mg) to healthy human volunteers. The maximum concentration of griseofulvin reported in the blood plasma was 2.42 µgmL^{-1} which occurred after 1 h [271]. They compared their formulation to the commercially available Fulvin which only resulted in a C_{max} of 1.10 µgmL^{-1} and with a much longer t_{Max} of 6 h [271]. This indicated that the current marketed formulation of griseofulvin was inefficient, taking a longer time to achieve C_{max} concentration.

Using our formulations we have demonstrated oral absorption of griseofulvin as high as 17.059 µgmL^{-1} for Ch_5, griseofulvin, this was a 8.89-fold increase compared to the aqueous griseofulvin formulation (for total concentration absorbed over 24 h period). $Dansyl_{10}$ achieved its t_{max} after only 1 h, whereas Ch_5 achieved t_{max} after 4 h. Perhaps the earlier t_{max} experienced by the $Dansyl_{10}$ formulation and reduced absorption can be attributed to destabilisation of the self-assemblies in the stomach, prematurely releasing their payload and thus hindering efficient absorption and sustained release of the drug. The shorter t_{max} of $Dansyl_{10}$ would suggest that C_{max} was observed after griseofulvin had been absorbed through the stomach wall, whereas, the longer t_{max} of the Ch_5, suggests that after 4 h the griseofulvin should have been absorbed through the intestine. The Ch_5 appears to be more efficient for oral delivery of the drug than $Dansyl_{10}$ (8.89-fold increase compared with 5.20-fold increase in total griseofulvin absorption respectively).

When compared with previous studies by other groups both the Ch_5 and $Dansyl_{10}$ formulations resulted in excellent drug absorption *in vivo*. A 50-fold (Ch_5, griseofulvin) and 28-fold ($Dansyl_{10}$, griseofulvin) increase of griseofulvin absorption compared to previously reported figures by Ahmed when comparing the C_{Max}, these were a 110-fold and 63-fold increase compared to the Fulvin formulation [271]. The effects of inter-individual variation did not appear evident using the $Dansyl_{10}$ formulation as all the subjects had drug plasma levels with a small standard deviation. This would suggest that the nano carriers were less susceptible to factors affecting the drug absorption among patients. The large concentrations of drugs absorbed together with the small standard deviations observed indicated that the PAA amphiphiles were capable of significantly enhancing the absorption of griseofulvin *in vivo* (p<0.0001 when compared to griseofulvin in water). The large increase in drug plasma levels experienced after oral administration of Ch_5 and $Dansyl_{10}$ griseofulvin formulations compared to others work. However this could be due to two

factors. Firstly, the increased aqueous solubility of griseofulvin experienced when in formulation could aid in greater absorption through the stomach wall and into the blood stream. However, the polymeric nano-carriers may also facilitate transport across the GI tract enabling a higher concentration of drug to become absorbed. The later of which could possibly explain the reduced inter-subject variations which have been previously reported [271].

In vivo delivery of anticancer drugs using polymeric self-assemblies has been reported not only facilitate the uptake of the drugs but also to enhance the therapeutic effect observed [322]. Le Garrec and colleague loaded anticancer agent paclitaxel into novel polymeric poly(N-vinyl pyrrolidone)-block-poly(D,L-lactide) (PVP-b-PDLLA) self-assemblies [97]. Female Balb/C mice with C26 colon adenocarcinoma were treated intravenously with the formulation over 20 days.They observed a 13-fold decrease in relative tumour size over 20 days of treatment, this was 2-fold better than Taxol[®] [97]. However, they concluded that this could be improved by the manipulation of polymer structure [97].

Recently, Xu and colleagues loaded methoxypolyethylene glycol –poly (D,L-lactic acid) with anti tumour drug triptolide with 66.7 % encapsulation efficiency [322]. They administered the drug (0.15 mgKg^{-1}) intravenously to S-180 tumour bearing mice and observed reduction in tumour weight from 2.58 g using free drug to 1.23 g using polymer formulation [322]. The rational for such activity is the tendency of the nano sized aggregates to accumulate within the tumour vasculature due to the enhanced permeability and retention effect [70].

A Ch_5, BNIPDaoct formulation (1 mgmL^{-1}, 0.3 mgmL^{-1}) was administered to nude tumour bearing mice over a 4 week period. The study found that the Ch_5, BNIPDaoct formulation was capable of reducing tumour growth rate when compared to Ch_5 alone. The reduction in tumour growth was comparable to the current commercially available drug gemcitabine for anticancer treatment. When compared with other studies, the reduction in tumour size is not as large. This could be due to the anticancer drug BNIPDaoct not being as effective or due to the polymer delivery system being less efficient. Nevertheless, this study indicates the reduction in tumour size was significant ($p < 0.05$) compared to the polymer alone control.

5.5. Conclusion

The polymers showed no haemolytic effect on red blood cells over the concentrations tested. The Ch_5 and $Dansyl_{10}$ polymeric self-assemblies were capable of increasing cytotoxic effect of etoposide and BNIPDaoct in two cell lines. The Dansyl10 exhibited a synergistic effect on the drugs enhancing their uptake into cells after only 2 h (compared with 4 h for the free drug and polymer alone). Both polymers increased oral absorption of griseofulvin *in vivo* without gross toxicity observed in rats. Ch_5 was shown to decreased

tumour size when encapsulating BNIPDaoct. In general the Ch_5 and $Dansyl_{10}$ show excellent potential as hydrophobic drug solubilisers.

Chapter Six

General Conclusions and Future Work

6.1 General conclusions

Homopolymer poly(allylamine) (PAA) has been successfully modified to produce novel PAA polymers different levels of hydrophobic (cholesteryl, fmoc, dansyl and naphthalene) modification and some amphiphilic PAA's were further modified with hydrophilic (quaternary ammonium) groups. Fourteen novel comb shaped amphiphilic PAA polymers were synthesised with high yield and good reproducibility.

In the aqueous environment all the PAA amphiphiles were capable of forming spontaneous nano self-assemblies comprising of a hydrophobic inner core. At 25 °C the PAA amphiphiles formed self-assemblies which were shown to have a hydrodynamic diameter of 120 – 199 nm. At low concentrations they all formed clear aqueous solutions upon sonication, the solutions formed were cloudy at higher concentrations. The 5 % grafted hydrophobic modified polymers formed intermolecular aggregates in solution. At higher concentration of fmoc and naphthalene modified polymers, excimer formation was observed whereby, the planar aromatic pendant groups began stacking in an ordered arrangement resulting in a second point of inflection on the surface tension measurements. The Ch_5 polymer had the lowest CAC with the aromatic pendant groups resulting in relatively larger CAC values. At higher levels of hydrophobic grafting (10 %) and upon hydrophilic modification some of the polymers formed intramolecular aggregates. It is thought that the presence of the permanent positive charge encouraged aggregation of the polymer at lower concentrations resulting in this self-aggregation.

The hydrodynamic size was shown to decrease at higher levels of hydrophobic grafting due to greater hydrophobic interactions occurring in the aqueous phase resulting in more compact self-assemblies. Upon quaternization of the polymers, the self-assemblies increased in hydrodynamic radius, probably due to the permanent positive charge causing weaker hydrophobic interactions to occur resulting in less compact aggregates. The PAA amphiphiles were loaded with five model hydrophobic drugs (propofol, prednisolone griseofulvin, etoposide and novel anticancer agent BNIPDaoct). The ability of the self-assemblies to encapsulate the hydrophobic drugs varied with the types of hydrophobic pendant group and drug. We observed that the polymer with the aromatic planar fmoc pendant (which exhibited excimer stacking at higher concentration) showed low drug solubilisation capacities for both the propofol and prednisolone (0.45 and 2.98 mgmL^{-1} respectively) compared to the Ch_5 (7.82 and 7.05 mgmL^{-1} respectively) and Dansyl$_{10}$ (22.40 and 31.82 mgmL^{-1} respectively) polymers. This indicates that the stacking pendant groups hinder the drug incorporation into the self assembly (Fig. 110).
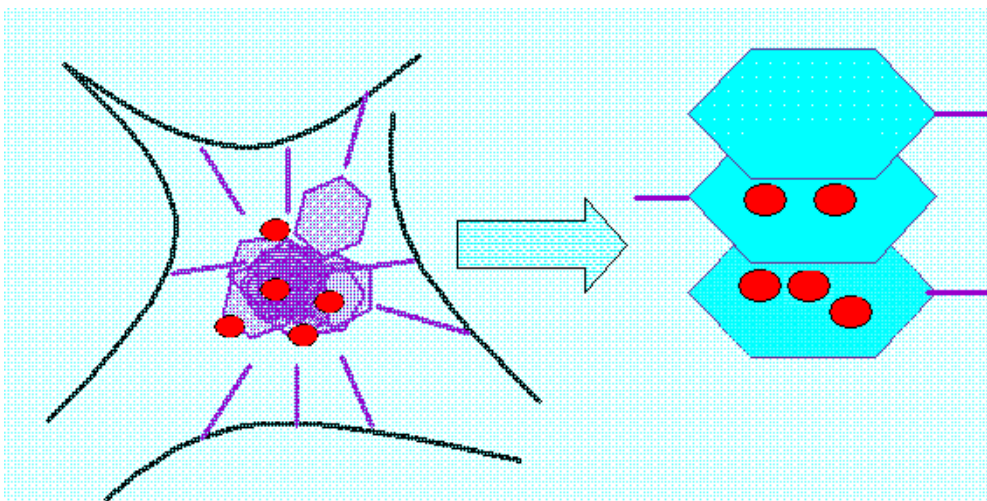
Figure 110. Drug incorporation into Fmoc-PAA self-assemblies.

The Ch_5 and $Dansyl_{10}$ were shown to be excellent universal drug solubilisers, with a 78–fold and 223–fold increase in aqueous propofol solubility observed respectively. The resultant formulations possessed extremely low excipient:drug ratios making them very efficient systems (as low as 0.77:1 for Ch_5, propofol and 0.19:1 for $Dansyl_{10}$, prednisolone). The Ch_5 and $Dansyl_{10}$ polymers did not form excimers due to steric hindrance of the pendant groups. The lack of excimer formation allowed for a degree of core expansion to occur upon drug encapsulation (Fig. 111). This expansion allowed for a greater drug solubilisation concentration. The sizes of the optimal formulations differed greatly for both formulations, possibly due to the varying architectures of both the drugs and the modified polymers and their ability to accommodate and shield each other from the 'hostile' aqueous environment. The formulations were shown to achieve sustained release of the drugs up to 48 – 96 h.
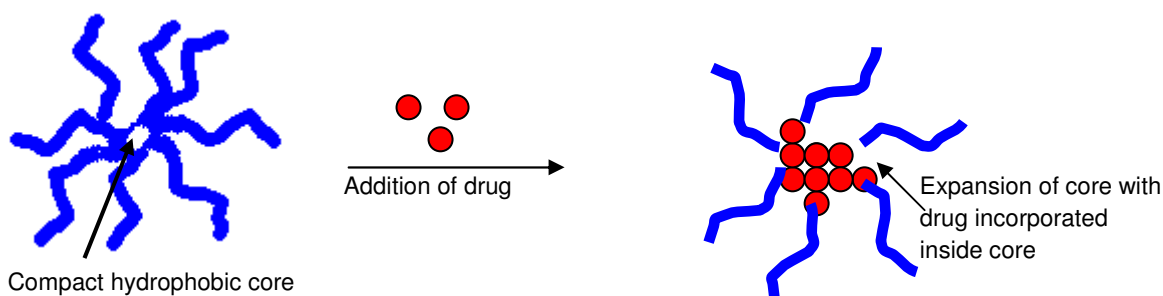
Figure 111. Expansion of hydrophobic core of Ch_5 and $Dansyl_{10}$ upon drug loading.

In vitro biocompatibility studies revealed that most of the polymers showed negligible haemolytic activity (< 10 %) on red blood cells (0.1 to 1 $mgmL^{-1}$). At higher hydrophobic grafting and upon quaternization the haemolytic effect was reduced, this possibly due to

the reduction of primary amines on the PAA backbone which contribute to the haemolytic effect. The quaternized polymers, however caused haemoguttenation of the cells. The low haemolytic effect of the unquaternized polymers supports the suitability for intravenous administration of drugs.

In vitro cytotoxicity assays using etoposide and BNIPDaoct formulations of Ch_5 and $Dansyl_{10}$ showed that when Caco-2 and HEK293 cells were exposed to the formulations, enhanced therapeutic effect was observed compared to the free drugs. The inherent fluorescent nature of the dansyl aromatic grafted polymers enabled ease of visualisation without the use of a secondary fluorescent marker tag. The Ch_5 polymer had to be tagged with a rhodamine tag to allow fluorescence analysis. Confocal microscopy was carried out using Ch_5, BNIPDaoct and $Dansyl_{10}$, BNIPDaoct formulations *in vitro* on Caco-2 and HEK293 cells. The study showed that Ch_5 formulations appeared co-localised within the cells after 4 h however the $Dansyl_{10}$ formulation appeared to have a synergistic effect on both the drug and polymer as they appeared co-localised after only 2 h whereas separately the drug or polymer alone took 4 h for cellular uptake to occur.

In vivo administration of Ch_5 and $Dansyl_{10}$ formulations of griseofulvin showed that both Ch_5 and $Dansyl_{10}$ significantly enhanced the absorption of griseofulvin in rats compared with griseofulvin in water and each other (p < 0.001) without any adverse side effects. The Ch_5 and $Dansyl_{10}$ formulations enhanced the C_{Max} for oral absorption of griseofulvin 4.18-fold and 1.16-fold and the increment increase of total griseofulvin absorbed over the 24 h study by 8.89-fold and 5.20-fold respectively. The $Dansyl_{10}$ was less effective for oral delivery of griseofulvin compared with Ch_5. The reason for this is perhaps the drug loaded self-assemblies experienced disruption upon dilution when they reached the stomach, prematurely releasing the drug and hindering its absorption across the stomach wall. This data correlates well with the CAC values obtained using surface tension measurements, whereby the $Dansyl_{10}$ had a much higher CAC value than the Ch_5 (0.25 and 0.093 mgmL^{-1}) indicating that the $Dansyl_{10}$ would experience decreased stability upon dilution when compared with Ch_5 (Fig. 112). *In vivo* administration of Ch_5, BNIPDaoct formulations was also shown to significantly decrease tumour growth when treated on nude tumour bearing mice over a 4 week period.
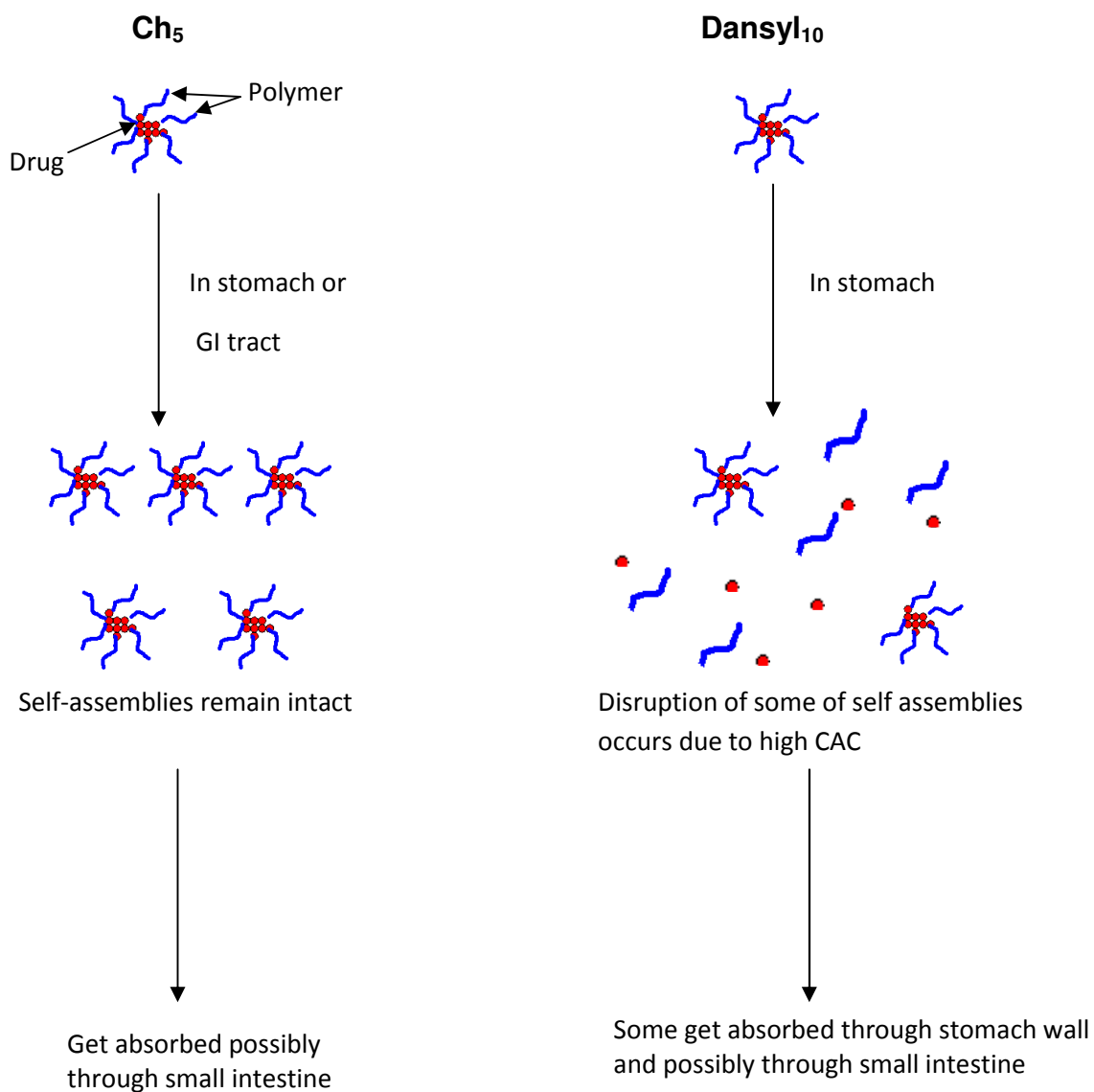
Figure 112. In vivo fate of orally administered Ch$_5$, griseofulvin and Dansyl$_{10}$, griseofulvin formulations.

In conclusion, this is the first time novel amphiphilic PAA polymers grafted with aromatic pendant groups have been shown to be capable of solubilising poorly soluble drugs such as propofol, prednisolone, griseofulvin, etoposide and BNIPDaoct and enhance absorption of drugs via oral route and intravenous administration. Overall Ch$_5$ and Dansyl$_{10}$ show great potential as future drug delivery systems.

6.2. Future Work

We carried out a short term stability test by storing liquid and freeze-dried preparations of the formulations. In the future it would be desirable to carry out further long term stability testing of the Ch$_5$ and Dansyl$_{10}$ formulations in order to determine their potential as pharmaceutical excipients.

We concluded that variation of the hydrophobic pendant group had a direct impact on the properties of the self-assemblies formed in aqueous solutions. Further modification of the PAA backbone including the attachment of poly(ethylene glycol) (PEG) could increase the biocompatibility and perhaps further influence the drug loading capabilities of the polymer. It would also be useful to investigate other aromatic and alkyl pendant group attachment to the polymer and test not only the drug solubilisation capacities but also the ability of complexation with proteins and genes. Further drug solubilisation studies of an increased number of drugs would also be necessary to back up the hypothesis that the Ch_5 and $Dansyl_{10}$ were universal solubilisers.

Cellular localisation studies enabled determination of time taken for cellular uptake of the formulations. It would It may be beneficial to repeat the confocal imaging of the formulations in cells, as the pictures could be improved upon. Perhaps it would also be valuable to carry out further *in vitro* intracellular trafficking to determine the mechanism of cellular uptake in the cell to visualise exactly where the drug and polymer reside [83,323]. This can be carried out by staining the organelles in the cell e.g. Nucleus, cell membrane, mitochondria etc. [83] It would also be advantageous to use a range of inhibitors such as sodium azide (metabolic inhibitor) or cytochalasin D (endocytosis inhibitor) to allow determination of the mechanism of cellular uptake e.g. endocytosis or active transport or a different type of transport [312, 323]. A Caco-2 transport study could also be carried out in order to determine if paracellular transport is involved. Further *in vivo* work is also necessary for both oral and intravenous delivery of hydrophobic drugs over longer time periods in order to elucidate the potential of these drug formulations for pharmaceutical therapies. All these studies must be carried out in order to bring the work forward before being considered for clinical investigation.

References

1. Wang.B, Siahaan.T and Soltero.R.A, Drug Delivery: Principles and Applications, Hoboken NJ, *John Wiley & Sons Inc.*, 2005
2. Florence.T.A and Atwood.D, Physiochemical Principles of Pharmacy 4th Edition, *London, Pharmaceutical Press,* 2006
3. Cheng.W.P, Gray.A.I, Tetley.L, Hang.T.L.B, Schätzlein.A.G and Uchegbu.I.F, 2006, Polyelectrolyte Nanoparticles with High Drug Loading Enhance the Oral Uptake of Hydrophobic Compounds, *Biomacromolecules, 7,* pp1509-1520
4. Spireas.S, Sadu.S, 1998, Enhancement of prednisolone dissolution properties using liquisolid compacts, *International Journal of Pharmaceutics*, 166, pp177-188
5. The Medicines and Healthcare products Regulatory Agency (MHRA), British Pharmacopoeia Volume I, *The Stationary Office*, 2005
6. de Rieux.A, Fievez.V, Garinot.M, Schneider.Y-J, Préat.V, 2006, Nanoparticles as potential oral delivery systems of proteins and vaccines: A mechanistic approach, *Journal of Controlled Release*, 116, pp1-27
7. Malmstein.M, Surfactants and Polymers in Drug Delivery, Basel NY, *Marcel Dekker,* 2002
8. Farías.T, de Ménorval.L.C, Zajac.J, Rivera.A, 2009, Solubilization of drugs by cationic surfactants micelles: Conductivity and 1H NMR experiments, *Colloids and Surfaces A: Physiochemical and Engineering Aspects*, 345, pp51-57
9. Jones.M.N,1999, Surfactants in membrane solubilisation, *International Journal of Pharmaceutics,* 177, pp137-159
10. *Ghosh.S, 2001,* Surface Chemical and Micellar Properties of Binary and Ternary Surfactant Mixtures (Cetyl Pyridinium Chloride, Tween-40, and Brij-56) in an Aqueous Medium, *Journal of Colloid and Interface Science*, 244, pp128-138
11. Materna.K, Schaadt.A, Bart.H.J, Szymanowski.J*, 2005,* Dynamics of surfactant-rich phase separation from solutions containing non-ionic and zwitterionic surfactants, *Colloids and Surfaces A: Physicochemical and Engineering Aspects*, 254, pp223-229
12. Kim.T.W, Kim.Y.J, Chung.H, Kwon.I.C, Sung.H.C, Jeong.S.Y, 2002, The role of non-ionic surfactants on cationic lipid mediated gene transfer, Journal of Controlled Release, 82, pp455-465
13. Acharya.D.P, Kunieda.H, 2006, Wormlike micelles in mixed surfactant solutions, *Advances in Colloid and Interface Science*, 123-126, pp401-413
14. Shah.D.O, Micelles, Microemulsions and Monolayers: Science and Technology, New York, *Marcel Dekker*, 1998
15. *Hargreaves.T, Chemistry World, Cambridge, London, Royal Society of Chemistry, 2007*
16. Uchegbu.I.F, Schätzlein.A.G, Polymers in Drug Delivery, Boca Raton *FA, Taylor & Francis,* 2006
17. Alam.M.S, Naqvi.A.Z and Din.K, 2006, Influence of Electrolytes / Non-electrolytes on the cloud point phenomenon of the aqueous promethazine hydrochloride drug solution, *Journal of Colloid and Interface Science,* 306, pp 161-165
18. Daintith.J, Oxford Dictionary of Chemistry, 5th Edition, *St. Ives*, *Oxford University Press,* 2004
19. Attwood.D, 1995, The mode of association of amphiphilic drugs in aqueous solution, *Advances in Colloid and Interface Science*, 55, pp271-303
20. Calhoun.A.R and King.A.D.Jnr, The solubility of ethane in aqueous solutions of sodium 1-pentanesulfonate, sodium 1-hexanesulfonate, sodium 1-heptanesulfonate, and sodium 1-octanesulfonate at 25°C. *Journal of Colloid and Interface Science*, received 15th September 2006.
21. Crothers.M, Zhou.Z, Ricardo.N.M.P.S, Yang.Z, Taboada.P, Chaibundit.C, Attwood.D and Booth.C, 2005, Solubilisation in aqueous micellar solutions of block copoly9oxyalkylene)s, *International Journal of Pharmaceutics*, 293, pp 91-100
22. Zhou.M, Rhue.R.D, 2000, Screening commercial surfactants suitable for remediating DNAPL source zones by solubilisation, *Environmental Science & Technology* , 34, pp1985-1990
23. Lawrence.M.J, 1994, Surfactant Systems: Their Use in Drug Delivery, *Chemical Society Reviews*, pp417-424
24. http://www2.basf.us/Pharma/pdf/Spec_CremophorELP.pdf (accessed 20/08/09)

25. Nehilla.B.J, Bergkvist.M, Popat.K.C, Desai.T.A, 2008, Purified and surfactant-free coenzyme Q10 loaded biodegradable nanoparticles, *International Journal of Pharmaceutics*, 348, pp 107-114

26. Kim.C-K, Hwang.Y-Y, Chang.J.Y, Choi.H-G, Lim.S-J, Lee.M-K, 2001, Develeopment of a novel dosage form for intramuscular injection of titrated extract of *Centella asiatica* in a mixed micellar system, *International Journal of Pharmaceutics*, 220, pp141-147

27. Zhu.W, Guo.C, Yu.A, Gao.Y, Cao.F, Zhai.G.X, 2009, Microemulsion-based hydrogel formulation of penciclovir for topical delivery, *International Journal of Pharmaceutics*, 378, pp152-158

28. Aulton.M.E, Pharmaceutics, The science of dosage form design, *China, Churchill Livingstone*, 1998

29. Hirunpanich.V, Sato.H, 2009, Improvement of cyclosporine A bioavailability by incorporating ethyl dosahexaenoate in the microemulsion as an oil excipient, *European Journal of Biopharmaceutics*, Article in press

30. Chakraborty.S, Shukla.D, Mishra.B, Singh.S, 2009, Lipid – An emerging platform for oral delivery of drugs with poor bioavailability, *European Journal of Pharmaceutics*, 73, pp 1-15

31. Sinko.P.J, Martin's Physical Pharmacy and Pharmaceutical Sciences 5th Edition, *Philadelphia, Lippincott Williams & Wilkins*, 2005

32. Ranade.V.V, Holliger.M.A, Drug Delivery Systems. *Boca Raton FA CRC,* 1996

33. Yamazaki.K, Imai.M, Suzuki.I, 2007, Water solubilization capacity and mean emulsion size of phospholipid-based isooctane-alcohol W/O microemulsion, *Colloids and Surfaces A: Physiochemical Engineering Aspects,* 293, pp241-246

34. Naoe.K, Noda.K, Kawagoe.M and Imai.M, 2004, Higher order structure of proteins solubilised in AOT reverse micelles, *Colloids and Surfaces B: Biointerfaces,* 38, pp 179-185

35. Ingelsten.H.H, Bagwe.R, Palmqvist.A, Skoglundh.N, Svanberg.C, Holmberg.K and Shah.D.O, 2001, Kinetics of the Formation of Nano-sized Platinum particles in Water-in-Oil Microemulsions, *Journal of Colloid and Interface Science,* 241, pp 104-111

36. Furusaki.S and Kishi.K, 1990, Extraction of amino acids by reverse micelles, *Journal of Chemical Engineering of Japan*, 23, pp 91-93

37. Pileni.M-P, Zemb.T, Petit.C, 1985, Solibilization by reverse micelles: Solute localization and structure perturbation, *Chemical Physics Letters,* 118, pp 414-420

38. Griffin.J.P, O'Grady.J, The Textbook of Pharmaceutical Medicine, 5th Edition, UK, BMJ Books, 2005

39. Porter.C.J.H, Pouton.C.W, Cuine.J.P, Charman.W.N, 2008, Enhancing intestinal drug solubilisation using lipid – based delivery systems, *Advanced Drug Delivery Reviews*, 60, pp673-691

40. Gregoriadis.G, 1973, Drug Entrapment in Liposomes, *Federation of European Biochemical Societies Letters,* 36, p292-296

41. Nii.T and Ishii.F, 2005, Encapsulation efficiency of water-soluble and insoluble drugs in liposomes prepared by the microencapsulation vesicle method, *International Journal of Pharmaceutics*, 298, pp 198-205

42. El-Ridy.M.S, Mostafa.D.M, Shehab.A, Nasr.E.A, El-Alim.S.A, 2007, Biological evaluation of pyrazinamide liposomnes for treatment of Mycobacterium tuberculosis, *International Journal of Pharmaceutics*, 330, 82-88

43. McNeil.S.E, Perrie.Y, 2006, Gene delivery using cationic liposomes, *Expert Opinion in Therapeutic Patents*, 16, pp 1371-1382

44. Mohammed.A.R, Coombes.A.G.A, Perrie.Y, 2007, Amino acids as cryoprotectants fro liposomal delivery systems, *European Journal of Pharmaceutical Sciences*, 30, pp406-413

45. Mohammed.A.R, Weston.N, Coombes.A.G.A, Fitzgerald.M, Perrie.Y, 2004, Liposome formulation of poorly water soluble drugs: optimisation of drug loading and SEM analysis of stability*, International Journal of Pharmaceutics*, 285, pp23-34

46. Perrie.Y, 2008, Gregory Gregoriadis: Introducing liposomes to drug delivery, *Journal of Drug Targeting*, 16, pp518-519

47. Gulati.M, Grover.M, Singh.S, Singh.M, 1998, Lipophilic drug derivatives in liposomes, *International journal of Pharmaceutics*, 165, pp129-168

48. Xu.Q, Tanaka.Y and Cznernuszka.J.T, 2007, Encapsulation and release of a hydrophobic drug from hydroxyapatite coated liposomes, *Biomaterials*, 16, pp2687-2694

49. Perrie.Y, Mohammed.A.R, Kirby.D.J, McNeil.S.E, Bramwell.V.W, 2008, Vaccine adjuvant systems: Enhancing the efficacy of sub-unit protein antigens, *International Journal of Pharmaceutics*, 364, pp272-280

50. Kirby.D.J, Rosenkrands.I, Agger.E.M, Anderson.P, Coombes.A.G.A, Perrie.Y, 2008, Liposomes act as stronger sub-unit vaccine adjuvants when compared to microspheres, *Journal of Drug Targeting*, 16, pp543-554

51. du Plessis.J, Ramachandran.C, Weiner.N, Muller.G, 1996, The influence of lipid composition and lamellarity of liposomes on the physical stability of liposomes upon storage, *International Journal of Pharmaceutics*, 127, pp273-278

52. Kersten.G.F.A, Crommelin.D.J.A, 1995, Liposomes and ISCOMS as vaccine formulations, *Biochemica et Biophysica Acta (BBS)*, 1241, pp117

53. Mohammed.A.R, Bramwell.V.W, Coombes.A.G.A, Perrie.Y, 2006, Lyophilisation and sterilisation of liposomal vaccines to produce stable and sterile products, *Methods*, 40, pp30-38

54. Du.Y-Z, Xu.J-G, Wang.L, Yuan.H, Hu.F-Q, 2009, Preparation and characteristics of hydroxypropyl-β-cyclodextrin polymeric nanocapsules loading nimodiprine, *European Polymer Journal*, 45, pp1397-1402

55. He.Y, Fu.P, Shen.X, Gao.H, 2008, Cyclodextrin-based aggregates and charaterization by microscopy, *Micron*, 39, pp495-516

56. Hatzi.P, Mourtas.S, Klepetsamis.P.V and Antimisiaris.S.G, 2007, Integrity of liposomes in presence of Cyclodextrins: Effect of liposome type and lipid composition, *International Journal of Pharmaceutics*, 333, pp 167-176

57. Li.J, Loh.X.J, 2009, Cyclodextrin-based supramolecular architectures: Synthesis, structures, and applications for drug and gene delivery, *Advanced Drug Delivery Reviews*, 60, pp1000-1017

58. Loftsson.T and Duchêne.D, 2007, Cyclodextrins and their pharmaceutical applications. *International Journal of Pharmaceutics* 329, pp1-11

59. Brewster.M.E, Loftsson.T, 2007, Cyclodextrins as pharmaceutical solubilizers, *Advanced Drug Delivery Reviews*, 59, pp645-666

60. http://portal.jindrich.org/projects/ReagentComplexation.gif accessed 18/08/09

61. Rasheed.A, Kumar.A.C.K, Sravanthi.V.V.N.S.S., 2008, Cyclodextrin as Drug Carrier Molecule: A Review, *Scientia Pharmaceutica*, 76, pp567-598

62. Yang.W, de Villiers.M.M, 2004, The solubilisation of the poorly water soluble drug nifedipine by water soluble 4-sulfonic calyx[n]arenes, *European Journal of Pharmaceutics and Biopharmaceutics*, 58, pp629-636

63. Sýkora.J, Himl.M, Stibor.I, Císarová.I and Lohták.P, 2007, Unique self-assembly patterns based on thiacalix[4]arene-silver interactions, *Tetrahedron*, 63, pp 2244-2248

64. Martin.O.M, Mecozzi.S, 2007, Synthesis and pH-dependant self-assembly of semifluorinated calyx[4]arenes, *Tetrahedron*, 63, pp 5539-554

65. Pochini.R, Ungaro.R, 1996, Comprehensive Supramolecular Chemistry, *Pergamon*, 2 , pp. 103–138.

66. http://www.rsc.org/ej/CP/2000/b004361n/b004361n-f2.gif accessed 18/08/09

67. Shin.D-M, Kim.T.H, Chung.G and Kim.K, 2001, Surface orientation and complex formation of new calixarene derivatives containing sulfur ligands, *Colloids and Surfaces A: Physiochemical Engineering Aspects*, 257-258, pp 461-465

68. Gualbert.J, Shahgaldian.P and Coleman.A.W, 2003, Interactions of amphiphilic calix[4]arene-based Solid Lipid Nanoparticles with bovine serum albumin, *International Journal of Pharmaceutics*, 257, pp 69-73

69. Millard.J.W, Alvarez-Núñez.F.A, Yalkowsky.S.H, 2002, Solubilization by cosolvents Establishing useful constants for the log-linear model, *International Journal of Pharmaceutics*, 245, pp 153-166

70. Bromberg.L, 2008, Polymeric micelles in oral chemotherapy, *Journal of Controlled Release*, 128, pp 99-112

71. Harada.A, Kataoka.K, 2006, Supramolecular assemblies of block copolymers in aqueous media as nanocarriers relevant to biological applications, *Progress in Polymer Science*, 31, pp949-982

72. Nishiyama,N.; Kataoka,K., 2006, Current state, achievements, and future prospects of polymeric micelles as nanocarriers for drug and gene delivery, *Pharmacology and Therapeutics,* , 112, 630-648

73. Kwon. G and Okano.T, 1996, Polymeric micelles as new drug carriers, *Advanced Drug Delivery Reviews* 21, pp107-116

74. Letchford.K, Burt.H, 2007, A Review of the formation and classification of amphiphilic block copolymer nanoparticulate structures: micelles, nanospheres, nanocapsules and polymersomes, *European Journal of Pharmaceutics and Biopharmaceutics*, 65, pp 259-269

75. Branco.M.C, Schneider.J.P, 2009, Self-assembling materials for therapeutic delivery, *Acta Biomaterialia*, 5, pp, 817-813

76. Thompson.C, Ding.C, Qu.X, Yang.Z, Uchegby.I.F, Tetley.L, Cheng.W.P, 2008, The effect of polymer architecture on the nano self-assemblies based on novel comb-shaped amphiphilic poly(allylamine), *Colloid Polymer Science*, 286, pp 1511-1526

77. Li.G, Zhuang.Y, Mu.Q, Wang.M, Fang.Y, 2008, Preparation, characterization and aggregation behaviour of amphiphilic chitosan derivative having poly (L-lactic acid) side chains, *Carbohydrate Polymers*, 72, pp60-66

78. Wang.W, Tetley.L, Uchegbu.I.F, 2001, The Level of Hydrophobic Substitution and the Molecular Weight of Amphiphilic Poly-L-lysine-Based Polymers Strongly Affects Their Assembly into Polymeric Bilayer Vesicles, Journal of Colloid and Polymer Science, 237, pp200-207

79. Prompruk.K, Govender.t, Zhang.S, Xiong.C.D and Stolnik.S, 2005, Synthesises of a novel PEG-block-poly(aspartic acid-stat-phenylalanine) copolymer shows potential for formation of a micellar drug carrier, *International Journal of Pharmaceutics* 297, pp242-253

80. Yamamoto.Y, Yasugi.K, Harada.A, Nagasaki.Y, Kataoka.K, 2002, Temperature-related change in the properties relevant to drug delivery of poly(ethylene glycol)-poly(D,L-lactide) block copolymer micelles in aqueous milieu, *Journal of Controlled Release*, 82, pp 359-371

81. La.S.B, Okano.T, Kataoka.K, 1996, Preparation and characterization of the micelle-forming polymeric drug: Indomethacin-incorporated poly(ethylene glycol)-poly(β-benzyl Laspartate) block copolymer micelles, *Journal of Pharmaceutical Science*, 85, pp 85-90

82. Kwon.G and Kataoka.K, 1995, Block Copolymer micelles as long-circulating drug vehicles, *Advanced Drug Delivery Reviews* 16, pp295-309

83. Savić.R, Luo.L, Eisenberg.A, Mayasinger.D, 2003, Micellar Nanocontainers Distribute to Defined Cytoplasmic Organelles, *Science*, 300, pp 615 – 618

84. Qui.L, Zheng.C, Jin.Y, Zhu.K, 2007, Polymeric micelles as nanocarriers for drug delivery, *Expert Opinion in Therapeutic Patents*, 17, pp 819-30

85. Torchilin.V.P, 2006, Multifunctional nanocarriers, *Advanced Drug Delivery Reviews*, 58, pp1532-1555

86. Uchegbu.I.F, 2006, Pharmaceutical nanotechnology: polymer vesicles for drug and gene delivery, *Expert Opinon in Drug Delivery*, 3, pp629-640

87. Lapienis.G, 2009, Star-shaped polymers having PEO arms, *Progress in Polymer Science*, 34, pp 852- 892

88. Ooya.T, Lee.J, Park.K, 2003, Effects of ethylene glycol-based graft, star-shaped, and dendritic polymers on solubilisation and controlled release of paclitaxel, *Journal of Controlled Release*, 93, pp121-127

89. Duncan.R, Izzo.L, 2005, Dendrimer biocompatability and toxicity, *Advanced Drug Delivery Reviews*, 57, pp2215-2237

90. Morgan.M, Nakanishi.Y, Kroll.D.J, Griset.A.P, Carnahan.M.A, Wathier.M, Oberlies.N.U, Manikumar.G, Wani.M.C, Grinstaff.M.W, 2006, Dendrimer-Encapsulated Camptothecincs: Increased Solubility, Cellular Uptake, and Cellular Retention Affords Enhanced Anticancer Activity In Vitro, *Cancer Research*, 66, pp11913-11921

91. Bae.Y, Kataoka.K, 2009, Intelligent polymeric micelles from functional poly(ethylene glycol)-poly(amino acid) block copolymers, *Advanced Drug Delivery Reviews*, 61, pp768-784

92. Kim.S, Kim.J-H, Jeon.O, Kwon.I.C, Park.K, 2009, Engineered polymers for advanced drug delivery, *European Journal of Pharmaceutics and Biopharmaceutics*, 71, pp 420-430

93. Chiapetta.D, Sosnik.A, 2007, Poly(ethylene oxide)-poly(propylene oxide) block copolymer micelles as drug delivery agents: Improved hydrosolubility, stability and bioavailability of drugs, *European Journal of Pharmaceutics and Biopharmaceutics*, 66, pp 303-317

94. Ravenelle.F, Gori.S, Le Garrec.D, Lessard.D, Luo.L, Palusova.D, Sneyd.J.R, Smith. D, 2008, Novel Lipid and Preservative-free Propofol Formulation: Properties and Pharmacodynamics, *Pharmaceutical Research*, 25, pp 313-319

95. Shuai.X, Ai.H, Nasongkla.N, Kim,S, Gao.J, 2004, Micellar carriers based on block copolymers of poly(ε-caprolactone) and poly(ethylene glycol) for doxorubicin delivery, *Journal of Controlled Release*, 98, pp415-426

96. Kwon.G, Polymeric drug delivery systems, Informa Healthcare, UK, 2005

97. Le Garrec.D, Gori.S, Luo.L, Lessard.D, Smith.D.C, Yessine.M-A, Ranger.M, Leroux.J-C, 2004, Poly(N-vinylpyrrolidone)-block-poly(D,L-lactide) as a new polymeric solubilizer for hydrophobic anticancer drugs: in vitro and in vivo evaluation, *Journal of Controlled Release*, 99, pp83-101

98. Danhier.F, Magotteaux.N, Ucakar.B, Lecouturier.N, Brewster.M, Préat.V, 2009, Novel self-assembling PEG-p-(CL-co-TMC) polymeric micelles as safe and effective delivery system for Paclitaxel, *European Journal of Pharmaceutics and Biopharmaceutics*, 73, pp 230-238

99. Matsumura.Y, 2008, Poly (amino acid) micelle nanocarriers in preclinical and clinical studies, *Advanced Drug Delivery Reviews*, 60, 899-914

100. Lee.S.C, Kim.C, Kwon.I.C, Chung.H and Jeong.S.Y, 2003, Polymeric micelles of poly(2-ethyl-2-oxazoline)-block-poly(ε-caprolactone) copolymer as a carrier for Paclitaxel, *Journal of Controlled Release* 89, pp437-446

101. Chang.Y-C, Chu.I-M, 2008, Methoxy poly(ethylene glycol)-b-poly(valerolactone) diblock polymeric micelles for enhanced encapsulation and protection of camptothecin, *European Polymer Journal*, 44, pp3922-3930

102. Kawano.K, Watanabe.M, Yamamoto.T, Yokoyama.M, Opanasopit.P, Okana.T, Maitania.Y, 2006, Enhanced antitumor effect of camptothecin loaded in long circulating polymeric micelles, *Journal of Controlled Release*, 112, pp329-332

103. Gaucher.G, Dufresne.M-H, Sant.V.P, King.N, Maysinger.D, Leroux. J-C, 2005, Block copolymer micelles: preparation, characterization and application in drug delivery, *Journal of Controlled Release*, 109, pp 169-188

104. Brigger.I, Dubernet.C, Couvreur.P, 2002, Nanoparticles in cancer therapy and diagnosis, *Advanced Drug Delivery Reviews*, 54, pp631-651

105. Riess.G, 2003, Micellization of block copolymers, *Progress in Polymer Science*, 28, pp1107-1170

106. Podhajeka.K, Prochazka.J and Hourdet.D, 2007, Synthesis and viscoelastic behaviour of water-soluble polymers modified with strong hydrophobic side chains, *Polymer*, 48, pp 1586-1595

107. Kim.J.S, Youk.J.H, 2009, Preparation of core cross-linked micelles using a photo-cross-linking agent, *Polymer*, 50, pp2204-2208

108. Zhang.J, Jiang.X, Zhang.Y, Li.Y, Liu.S, 2007, Facile Fabrication of Reversible Core Cross-linked Micelles Possessing Thermosensitive Swellability, *Macromolecules*, 40, pp9125-9132

109. Chang.K-Y, Lin.C-C, Ho.G-H, Huang.Y-P, Lee.Y-D, 2009, Synthesis and self assembly of comb-like amphiphilic Doxifluridine-poly(ε-caprolactone)-graft-poly(γ-glutamic acid) copolymer, *Polymer,* 50, pp1755-1763

110. Wu.Y, Zheng.Y, Yang.W, Wang.C, Hu.J, Fu.S, 2005, Synthesis and characterization of a novel amphiphilic chitosan-polylactide graft copolymer, *Carbohydrate polymers*, 59, pp165-171

111. Chui.H-C, Chern.C-S, Lee.C-K and Chang.H-F, 1998, Synthesis and characterization of amphiphilic poly(ethylene glycol) graft copolymers and their potential application as drug carriers, *Polymer,* 39, pp 1609-1616

112. Sugimoto.H, Nakanishi.E, Hanai.T, Yasumura.T and Inomata.K, 2004, Aggregate formation and release behaviour of hydrophobic drugs with graft copolypeptide-containing tryptophan, *Polymer International*, 53, pp 972-983

113. Lin.J, Zhang.S, Chen.T, Lin.S and Jin.H, 2007, Micelle formation and drug release behaviour of polypeptide graft copolymer and its mixture with polypeptide block copolymer, *International Journal of Pharmaceutics*, 336, pp 49-57

114. Xu. Y, Du. Y, Huang.R, Gao.L, 2003, Preparation and modification of N-(-2-hydroxyl) propyl-3-timethyl ammonium chitosan chloride nanoparticles as a protein carrier, *Biomaterials*, 24, pp 5015-5022

115. Zhu.S, Qian.F, Zhang.Y, Tang.C, Yin.C, 2007, Synthesis and characterization of PEG modified dimethylaminomethacrylate chitosan nanoparticles, *European Polymer Journal: Macromolecule Nanotechnology*, 43, pp2244-2253

116. Thompson.C.J, Tetley.L, Cheng.W.P, 2009, The influence of polymer architecture on the protective effect of novel comb shaped amphiphilic poly(allylamine) against in vitro enzymatic degradation of insulin – Towards oral insulin delivery, *International Journal of Pharmaceutics, Article in press*

117. Torchilin.V, 2001, Structure and design of polymeric surfactant-based drug delivery systems, *Journal of Controlled Release*, 73, pp137-172

118. Winnik.F.M, Davidson.A.R, Hamer.G.K, Kitano.H, 1992, Amphiphilic poly(N-isopropylacrylamide) prepared by using a lipophilic radical initiator: synthesis and solution properties in water, *Macromolecules*, 25, pp1876-1880

119. Gao.Z, Eisenburg.A, 1993, A model of micellization for block copolymers in solutions, *Macromolecules*, 26, pp7353-7360

120. Thompson.C.J, Tetley.L, Uchegbu.I.F, Cheng.W.P, 2009, The complexation between novel comb shaped amphiphilic polyallyamine and insulin – Towards insulin delivery, *International Journal of Pharmaceutics*, 376, pp 46-55

121. Perry.M, Cheng.W.P. 2006, New Polyamine Based Amphiphilic polymers for Drug Delivery, *Proceedings of the23rd Annual Meeting & Exposition of the controlled Release Society in Vienna*, 22-27 July

122. Brownlie.A, Uchengbu.I.F, Schätzlein.A.G, 2004, PEI-based vesicle-polymer hybrid gene delivery system with improved bocompatability, *International Journal of Pharmaceutics*, 274, pp41-52

123. Wang.W, Qu.X, Gray.A.I, Tetley.L, Uchegbu.I.F, 2004, Self-Assembly of Cetyl Linear Polyethlenimine To Give Micelles, Vesicles and Dense Nanoparticles, *Macromolecules*, 37, pp9114-9122

124. Brown.M.D, Gray.A.I, Tetley.L, Santovena.A, Rene.J, Schäzlein.A.G, Uchegbu.I.F, 2003, In vitro and in vivo gene transfer with poly (amino acid) vesicles,,,,, 93, pp193-211

125. Uchegbu.I.F, Sadiq.L, Arastoo.M, Gray.A.I, Wang.W, Waigh.R.D, Schäzleinä.A.G, 2001, Quaternary ammonium palmitoyl glycol chitosan – a new polysoap for drug delivery, *International Journal of Pharmaceutics*, 224, pp185-199

126. Uchegbu.I.F, Schältzen.A.G, Tetley.L, 1998, Polymeric chitosan based vesicles for drug delivery, *Journal of Pharmaceutical Pharmacology*, 50, pp 453-458

127. Wang.L-Q, Tu.K, Li.Y, Zhang.J, Jiang.L and Zhang.Z, 2002, Synthesis and characterisation of temperature responsive graft copolymers of dextran with poly(N-isopropylacrylamide), *Reactive and Functional Polymers*, 53, pp 19-27

128. Gao.Y, Li.H, Wang.X, 2007, Synthesis and characterization of syndiotactic polystyrene-*graft*-poly(glycidyl methcrylate) copolymer by atom transfer radical polymerization, *European Polymer Journal*, 43, pp1258-1266

129. Lai.R, Guo.H, Kamachi.M, 2009, Synthesis of a graft polymer PVAc-g-[P(AN-r-BE)-b-PCHO] in "one step" by radical/cationic transformation polymerization and coupling reaction, *Polymer*, 50, pp3582-3586

130. Liu.X-M, Pramoda.K.P, Yang.Y-Y, Chow.S.Y, He.C, 2004, Cholesteryl-grafted functional amphiphilic poly(N-isopropylacrylamide-co-N-hydroxymethylacrylamide): synthesis, temperature sensitivity, self-assembly and encapsulation of a hydrophobic agent, *Biomaterials*, 25, pp2619-2628

131.Qui.LY., Yan.M.Q, 2009, Constructing doxorubicin-loaded polymeric micelles through amphiphilic graft polyphosphazenes containing ethyl tryptophan and PEG segments, *Acta Biomaterialia*, 5, pp2132-2141

132.Li.H, Liu.J, Ding.S, Zhang.C, Shen.W, You.Q, 2009, Synthesis of novel pH-sensitive chitosan graft copolymers and micellier solubilisation on paclitaxel, International *Journal of Biological Macromolecules*, 44, pp249-256

133.Jeong.J.H, Kim.S.W, Park .T.G, 2007, Molecular design of functional polymers fro gene delivery, *Progress in Polymer Science*, 32, pp1239-1274

134.McPhail.D, Tetley.L, Dufes.C, Uchegbu.I.F, 2000, Liposomes encapsulation polymeric chitosan based vesicles – a vesicle in vesicle system for drug delivery, *International Journal of Pharmaceutics*, 200, pp73-86

135.Fazeli.N, Mohammadi.N, Afshar Taromi.F, 2004, Analysis Method: A relationship between hydrodynamic and static properties of star-shaped polymers*, Polymer Testing,* 23, pp431-435

136.Chen.W-Q, Wei.H, Li.S-L.Feng.J, Nie.J, Zhang.X-Z, Zhuo.R-X, 2008, Fabrication of star-shaped, thermo-sensitive poly(N-isopropylacrylamide)-cholic acid-poly(ε-caprolactone) copolymers and their self assembled micelles as drug carriers, *Polymer*, 49, pp3965-3972

137.Qiu.L.Y, Bae.Y.H, 2006, Polymer Architecture and Drug Delivery, *Pharmaceutical Research*, 23, pp1-30

138.Jie.P, Venkatraman.S.S, Min.F, Freddy.B.Y.C, Huat.G.L, 2005, Micelle-like nanoparticles of star-branched PEO-PLA copolymers as chemotherapeutic carrier, *Journal of Controlled Release*, 110, pp20-33

139.Peng.C-L, Shieh.M-J, Tsai.M-H, Chang.C-C, Lai.P-S, 2008, Self-assembled star-shaped chlorine-core poly(ε-caprolactone)-poly(ethylene glycol) diblock copolymer micelles for dual chemo-photodynamic therapies, *Biomaterials*, 29, pp3599-3608

140.Wei.H, Zhang.X, Cheng.C, Cheng.S-X, Zhuo.R-X, 2007, Self-assembled, thermosensitive micelles of star block copolymer based on PMMA and PNIPAAm for controlled drug release, *Biomaterials*, 28, pp99-107

141.Wei.H, Zhang.X.Z, Zhou.U, Cheng.S.X, Zhuo.R.X, 2006, Self-assembled thermoresponsive micelles of poly(N-isopropylacrylamide-b-methyl methacrylate), *Biomaterials*, 27, pp 2028-2034

142.Dufès.C, Uchegbu.I.F, Schätzlein.A.G, 2005, Dendrimers in gene delivery, *Advanced Drug Delivery Reviews*, 57, pp 2177-2202

143.Singh.B, Florence.A.T, 2005, Pharmaceutical Nanotechnology: Hydrophobic denderimer-derrived nanoparticles, *International Journal of Pharmaceutics*, 298, pp348-353

144.Malik.N, Witwattanapatapee.R, Klopsch.R, Lorenz.K, Frey.H, Weener.J.W, Meijer.E.W, Paulus.W, Duncan.R, 2000, Dendrimers: Relationship between struture and biocompatability in vitro, and preliminary stubies on the biodistribution of ^{125}I-labelled polyamidoamine dendrimers in vivo, *Journal of Controlled Release*, 65, pp133-148

145.Svenson.S, 2009, Dendrimers as versatile platform in drug delivery applications, *European Journal of Pharmaceutics and Biopharmaceutics*, 71, pp445-462

146.http://www.nanopharmaceuticals.org/Dendrimers.html accessed 18/08/09

147.Al-Jamal.K, Ramaswamy.C, Florence.A.F, 2005, Supramolecular structures from dendrons and dendrimers, *Advanced Drug Delivery Reviews*, 57, pp2238-2270

148.Biricova.V, Laznickova.A, 2009, Dendrimers: analytical characterization and applications, *Bioorganic Chemistry*, Article in Press

149.Cheng.Y, Xu.T, 2008, The effect of dendrimers on the pharmacodynamic and pharmacokinetic behaviours of non-covalently or covalently attached drugs, *European Journal of Medicinal Chemistry*, 43, pp2291-2297

150.Morgan.M, Carnahan.M.A, Finkelstein.S, Prata.C.A.H, Degoricija.L, Lee.S.J Grinstaff.M.W, 2005, Dendritic supramolecular assemblies for drug delivery, *Chemical Communication*, pp4309-4311

151.Boas.U, Heegaard.P.M.H, 2004, Dendrimers in drug research, *Chemical Society Reviews*, 33, pp43-63

152. Kohle.P, Khandare.J, Pillai.O, Kannan.S, Lieh-Lai.M, Kannan.R.M, 2006, Preparation, cellular transport, and activity of polyamidoamine-based dendritic nanodevices with a high drug payload, *Biomaterials*, 27, pp660-669

153. Ooga.T, Lee.J, Park.K, 2004, Hydrotropic Dendrmers of Generations 4 and 5: Synthesis, Characterization, and Hydrotropic Solubilization of Paclitaxel, *Bioconjugate Chemistry*, 15, pp1221-1229

154. Srinivas.V, Rodley.G.A, Ravikumar.K, Robinson.W.T, Turnbull.M.M, Balasubramanian.D, 1997, Molecular organization in hydrotrope assemblies, *Langmuir*, 13, pp 3235-3239

155. Wiradharma.N, Zhang.Y, Venkataraman.S, Hedrick.J.L, Yang.Y.Y, 2009, Self-assembled nanostructures for delivery of anticancer therapeutics, *Nano Today*, 4, pp302-317

156. Rapoport.N, 2007, Physical stimuli-responsive polymeric micelles for anti-cancer drug delivery, *Progress in Polymer Science*, 32, pp962-990

157. Gil.E.S, Hudson.S.M, 2004, Stimuli-responsive polymers and their bioconjugates, *Progress in Polymer Science*, 29, pp1173-1222

158. Wei.H, Cheng.S-X, Zhang.X-Z, Zhuto.R-X, 2009, Thermo-sensitive polymeric micelles based on poly(N-isopropylacrylamide) as drug carriers, *Progress in Polymer Science, Article in press*

159.[2] Li.J, Wang.B, Liu.P, 2008, Possibility of active targeting tumor by local hyperthermia with temperature sensitive nanoparticles, *Medical Hypotheses*, 71, pp249-251

160. San Miguel.V, Limer.A.J, Haddleton.D.M, Catalina.F, Peinado.C, 2008, Biodegradable and thermoresponsive micelles of triblock copolymers based on 2-(N,N-dimethylamino)ethyl methacrylate and ε-caprolactone for controlled drug delivery, *European Polymer Journal*, 44, pp3853-3863

161. Lo.C-L, Lin.S-J, Tsai.H.C, Chan.W-H, Tsai.C-H, Cheng.C-H.D, Hsiue.G-H, 2009, Mixed micelle systems formed from critical micelle concentration and temperature-sensitive diblock copolymer for doxorubicin delivery, *Biomaterials,* 30, pp3961-3970

162. Bae.Y, Fukushima.S, Harada.A, Kataoka.K, 2003, Design of Environment-Sensitive Supramolecular Assemblies for Intracellular Drug Delivery: Polymeric Micelles that are Responsive to Intracellular Ph Change, *Angewante Chemistry International Addition*,42, pp4640-4643

163. Nishiyama.N, Bae.Y, Miyata.K, Fukushima.S, Kataoka.K, 2005, Smart polymeric micelles for gene and drug delivery, *Drug Discovery Today: Technologies*, 2, pp21-26

164. Gu.J, Cheng.W.P, Liu.J, Lo.S-Y, Smith.D, Qu.X, Yang.Z, 2008, pH-Triggered Reversible "Stealth" Polycationic Micelles, *Biomacromolecules*, 9, pp 255-262

165. Lyer.A.K, Khaled.G, Fang.J, Maeda.H, 2006, Exploiting the enhanced permeability and retention effect for tumor targeting, *Drug Discovery Today*, 11, pp 812-818

166. Amiji.M.M, Nanotechnology for Cancer Therapy, *Boca Raton FA CRC,* 2006

167. Mikhail.A.S, Allen.C, 2009, Block copolymer micelles for delivery of cancer therapy: Transport at the whole body, tissue and cellular levels, *Journal of Controlled Release, Article in Press*

168. Bae.Y, Jang.W, Nishiyama.N, Fukushima.S, Kataoka.K, 2005, Multifunctional polymeric micelles with folate-mediated cancer cell targeting and pH-triggered drug releasing properties for active intracellular drug delivery, *Molecular Biosystems*, 1, pp 242-250

169. Lee.E, Na.K, Bae.y, 2003, Polymeric micelle for tumor pH and folate-mediated targeting, *Journal of Controlled Release*, 91, pp 103-113

170. Prabaharan.M, Grailer.J.J, Pilla.S, Steeber.D.A, Gong.S, 2009, Folate-conjugated amphiphilic hyperbranched block copolymers based on Boltorn® H40, polym(L-lactide) and poly(ethylene glycol) for tumor-targeted drug delivery, *Biomaterials*, 30, pp3009-3019

171. Lu.X, Gong.S, Meng.L, Li.C, Liang.F, Wu.Z, Zhang.L, 2007, Novel fluorescent amphiphilic block copolymers: Controllable morphologies and size by self-assembly, *European Polymer Journal*, 43, pp2891-2900

172. Laukkanen.A, Winnik.F.M, Tenhu.H, 2005, Pyrene-Labeled Graft Copolymers of N-Vinylcaprolactam: Synthesis and Solution Properties in Water, *Macromolecules*, 38, pp2439-2448

173. Ziang.H.L, Zhu.K.J, 2002, Bioadhesive fluorescent microspheres as visible carriers for local delivery of drugs. I: preparation and characterization of insulin-loaded PCEFB/PLGA microspheres, *Microencapsulation*, 19, p451-461

174. Suchao-in.N, Chirachanchai.S, Perrier.S, 2009, Ph- and thermo-multi-responsive fluorescent micelles from block copolymers via reversible addition fragmentation chain transfer (RAFT) polymerization, *Polymer*, 50, pp4151-4158

175. Grazuleviscius.J.V, Strohriegl.P, Pielichowski.J, Pielichowski.K, 2003, Carbazole-containing polymers: synthesis, properties and applications, *Progress in Polymer Science*, 28, pp1297-1353

176. Wu.D-Q, Lu.B, Chang.C, Chen.C-S, Wang.T, Zhang.Y-Y, Cheng.S-X, Jiang.X-J, Zhang.X-Z, Zhuo.R-X, 2009, Galactoylated fluorescent labelled micelles as a liver targeting drug carrier, *Biomaterials*, 30, pp1363-1371

177. Rapoport.N and Caldwell.K, 1994, Structural transitions in micellar solutions of Pluronic P-105 and their effect on the conformatiion of dissolved cytochrome C: and electron paramagnetic resonance investigation, *Colloids Surfaces B: Biointerfaces*, 3, pp 217-228

178. Munshi.N, Rapoport.N and Pitt.W.G, 1997, Ultrasonic activated drug delivery from Pluronic P-105 micelles, *Cancer Letters*, 118, pp 13-19

179. Shmolka.I.R, 1977, A review of block polymer surfactants, Journal *of American Oil Chemists' Society*, 54, pp 110-116

180. Husseini.G.A, Myrup.G.D, Pitt.W.G, Christensen.D.A and Rapoport.N.Y*,* 2000, Factors affecting accoustically triggered release of drugs from polymeric micelles, *Journal of Controlled Release*, 69, pp 43-52

181. Tachibana.K, Uchida.T, Ogawa.K, Yamashita.N, Tamura.K, 1999, Induction of cell-membrane porosity by ultrasound, *The Lancet*, 353, pp 1409

182. Liu.J, Lweis.T.N, Prausnitz.M.R, 1998, Non-invasive assessment and control of ultrasound-mediated membrane permabilization, *Pharmaceutical Research*, 15, pp 918-924

183. Thomas.H and Coley.H.M, 2003, Overcoming Multidrug resistance in cancer: an update on the clinical strategy of inhibiting P-glycoprotein, *Cancer Control*, 10, pp 159-165

184. Wang.Y, Yu.L, Han.L, Sha.X and Fang.X, 2007, Difunctional Pluronic copolymer micelles for Paclitaxel delivery: Synergistic effect of folate-mediated targeting and Pluronic-mediated overcoming multidrug resistance in tumour cells, *International Journal of Pharmaceutics*, 337, pp 63-73

185. Priutt.J.D, Husseine.G, Rapoport.N and Pitt.W.G, 2000, Stabilisation of Pluronic P-105 micelles with an interpenetrating network of *N,N*-diethylacrylamide, *Macromolecules*, 33, pp 9306-9309

186. Yang.T-F, Chen.C-N, Chen.M-C, Lai.C.H, Liang.H-F and Sung.H-W, 2007, Shell crosslinked Pluronic L121 micelles as a drug delivery vehicle, *Biomaterials*, 28, pp 725-734

187. Kabanov.A.V, Batrakova.E.V and Miller.D.W, 2003, Pluronic block copolymers as modulators of drug efflux transporters activity in the blood-brain barrier, *Advanced Drug Delivery Reviews*, 55, pp 151-164

188. Gromadzki,D.; Makuska,R.; Netopilik,M.; Holle,R.P.; Lokaj,J.; Janata,M.; Stepanek,P.; 2008**,** Comb copolymers of polystyrene-poly(ter-butyl (meth)acrylate) prepared by combination of nitroxide mediated polymerization and photoimduced imiferter technique, *European Polymer Journal*, ,44, 59-71

189. Westedt,U.; Kalinowski,M.; Wittmar,M.; Merdan,T.; Unger,F.; Fuchs,J.; Schäller,S.; Bakowsky,U.; Kissel,T., 2007**,** Poly(vinyl alcohol)-graft-poly(lactide-co-glycolide) nanoparticles for local delivery of paclitaxel for restenosis treatment, *Journal of Controlled Release*, , 119, 41-51

190. Nimesh.S, Kumar.R and Chandra.R, 2006, Novel polyallylamine-dextran sulfate-DNA nanoplexes: Highly efficient non-viral vector for gene delivery, *International Journal of Pharmaceutics* 320, pp143-149

191.Xu.J-P, Chen.W-D, Shen.J-C, 2005, Novel biomimetic polymersomes as polymer therapeutics for drug delivery, *Journal of controlled release*, 107, pp 502-512

192.Yusa.S, Mikiharu.K, Morishima.Y, 1998, Hydrophobic Self-Association of Cholesterol Moities Covalentyl linked to Polyelectrolytes: Effect of Spacer Bond, *Langmuir,* 14, pp 6059-6067

193.Robinson.J.W, Skelly Frame.E.M, Frame.G.M, Undergraduate Instrumental Analysis, 6th Edition, USA, CRC Press, 2005

194.Sibilia.J.P, A Guide to Materials Characterization and Chemical Analysis 2nd Edition, *USA, VCH,* 1996

195.McCarthy.A, Ratcliff. B, Methods of Analysis and Detection, *UK, Cambridge University Press,* 2001

196.Hore.P.J, Oxford Chemistry Primers: Nuclear Magnetic Resonance, UK, Oxford Science Publications, 1995

197.Holler.F.J, Skoog.D.A, Crouch.S.R, Principles of Instrumental Analysis, 6th Edition, Canada, Thomson Brooks/Cole, 2007

198.Banwell.C.N, McCash.E.M, Fundamentals of Molecular Spectroscopy, 4th Edition, UK, McGraw-Hill International, 1994

199.Williams.D.H, Fleming.I, Spectroscopic methods in organic chemistry, 4th Edition Revised, UK, McGraw-Hill Book Company, 1989

200.Schwedt.G, Haderlie.B, The Essential Guide to Analytical Chemistry, 2nd Edition, UK, John Wiley and Sons, 1997

201.Stuart.B, George.B, McIntyre.P, Modern Infrared Spectroscopy, UK, John Wiley and Sons,1996

202.Domard.A, Rinaudo.M*.,* 1986, New method for the quaternization of chitosan, *International Journal of Biological Macromolecules*, 8, pp 105-107

203.Qu.X, Khutoryanskiy.V.V, Stewart.A, Rahman.S, Papahadjopoulos-Sternberg.B, Dufes.C, McCarthy.D, Wilson.C.G, Lyons.R, Carter.K.C, Schätzlein.A, Uchegbu.I.F, 2006, Carbohydrate –Based Micelle Clusters Which Enhance Hydrophobic Drug Bioavaliability by up to 1 Order of Magnitude, *Biomacromolecules*, 7, pp 3452 – 3459

204.Zhang.Y, Huo.M, Zhou.J Yu.D and Wu.Y, 2009, Potential of amphiphilically modified low molecular weight chitosan as a novel carrier for hydrophobic anticancer drug: Synthesis characterization, micellization and cytotoxicity evaluation, Carbohydrate polymers, 77, pp231-238

205.Bian.F, Jia.L, Yu.W and Liu.,2009, Self assembled micelles of N-phthaloylchitosan-g-polyvinylpyrrolidone for drug delivery, Carbohydrate polymers, 76 pp454-459

206.Cai. G, Jiang.H, Chen.Z, Tu.K, Wang.L and Zhu.K, 2009, Synthesis, characterization and self assemble behaviour of chitosan-O-poly(ε-caprolactone), European polymer journal, 45, pp1674-1680

207.Streitweiser.A, Heathcock.C.H, Introduction to Organic Chemistry, 3rd Edition, UK, Collier Macmillan Publishers, 1985

208.Butun.V, Armes.S.P, Billingham.N.C, 2001, Selective quaternization of 2-(dimethylamino) ethyl methacrylate residues in tertiary amine methacyrlate di block copolymers, *Macromolecules*, 34, pp1148-1159

209.Luo.Y, Wang.A, Yuan.J, Gao.Q, 2009, Preparation, characterization and drug release behaviour of polyion complex micelles, International Journal of Pharmaceutics, 374, pp 139-144

210.Sperling.L.H, Introduction to physical polymer science, 4th edition, UK, John Wiley and sons, 2006

211.Mitra.S, Sample Preparation Techniques in Analytical Chemistry, USA, John Wiley and sons, 2003

212.Qu. A, Wang. A, Yuian.J, Shi.J, Gao.Q, 2009, Preparation and characterisation of thermo-responsive amphiphilic triblock copolymer and its self-assebled micelle for controlled drug release, Colloids and Surfaces B: Biointerfaces, 72, pp 94 – 100

213.Hyun. H, Lee .J.W, Cho. J.S, Kim. Y.H, Lee. C.R, Kim. M.S, Khang.G, Lee.H.B, 2008, Polymeric nano-micelles using poly(ethylene glycol) and poly(trimethylene carbonate) diblock copolymers as a drug carrier, Colloids and Surfaces A: Physiochemical Enginerering Aspects, 313-314, pp 131-135

214. Takamura.K, Urban. D, Polymer Dispersions and Their Industrial Applications, Germany, Wiley – VCH, 2002

215. Dutta.P, Dey.J, Ghosh.G, Nayak.R.R, 2009, Self-association and microenvironment of random amphiphilic copolymers of sodium N-acrylol-L-valinate and N-dodecylacrylamide in aqueous solution, *Polymer*, 50, 1516-1525

216. Smart.T, Lomas.H, Massignani.M, Flores-Merino.M.V, Perez.L.R, Battagalia.G, 2008, Block copolymer nanostructures, *Nano Today*, 3, pp38-45

217. Rapoport.N, Pitt.W.G, Sun.H, Nelson.J.L, 2003, Drug delivery in polymeric micelles: from in vitro to in vivo, *Journal of Controlled Release*, 91, pp85-95

218. Yu.B.G, Okano.T, Kataoka.K, Kwon.G, 1998, Polymeric micelles for drug delivery: solubilisation and haemolytic activeity of amphotericin B, *Journal of Controlled Release*, 53, pp131-136

219. Deeney.R.C, Sinclair.R, Ultraviolet and Visible Spectroscopy, 2nd Edition, Thomas.M UK, John Wiley and Sons, 1997

220. Zhang.X, Zhu.X, Ke.F, Ye.L, Chen.E-Q, Zhang.A-Y, Feng.Z.G, 2009, Preparation and self-assembly of amphiphilic triblock copolymers with polyrotaxane as a middle block and their application as carrier for the controlled release of Amphotericin B, *Polymer*, 50, pp 4343-4351

221. Li.X, Wu.Q, Chen.Z, Gong.X, Lin.X, 2008, Preparation, characterization and controlled release of liver-targeting nanoparticles from the amphiphilic random copolymer, *Polymer*, 49, pp 4769-4775

222. Liu.S et al., 2006, Microporous SiO2–TiO2 nanosols pillared montmorillonite for photocatalytic decomposition of methyl orange, *Journal of photochemistry and Photobiology A: Chemistry*, 179, pp780

223. Hurtubise.R.J, Phosphorimetry: Theory, instrumentation, and applications, USA, VCH, 1990

224. White.C.E, Argauer.R.J, Fluorescence Analysis: A Practical Approach, USA, Marcel Dekker Inc, 1970

225. Birks.J.B, 1975, Excimers, *Reports on Progress in* Physics, *38*, pp 903-974

226. Ruozi.B, Tosi.G, Forni.F, Fresta.M, Angela.M and Vandelli.M.A, 2005, Atomic force microscopy and photon correlation spectroscopy: Two techniques for rapid characterisation of liposomes, *European journal of pharmaceutical sciences*, 25, pp81-89

227. Sovanna.S, Suzuki.S, Kojima.M, Tachiyashiki.S, Kita.M, 2009, Surface tension reduction (STR) in aquoesu solution of anionic surfactants with cobalt (III) complexes, *Journal of Colloid and Interface Science*, 332, pp 194-200

228. Li.X, McGuffin.V.L, 2004, Selective fluorescence quenching of nitrogen-containing polycyclic aromatic hydrocarbons by aliphatic amines, *Analytica Chimica Acta*, 526 , pp 155–162

229. Suzuki.I, Kato.Y and Osa.T, 1997 Discrimination between deoxycholic acid epimers by fluorescence of excimer-forming 6A,6E-*O*-bis[2-(1-naphthyl)propanoyl]-ã-cyclodextrins, *Journal of the Chemical Society, Perkin Translation*. 2,pp 1061-1063

230. Lewis.F.D and Kurth.T.L, 2003, Intramolecular excimer fluorescence from folded ground state rotamers of *N,N'*dimethyl-*N,N'*-dipyrenylurea protophanes, *Canadian Journal Chemistry*, 81, pp 771-776

231. Jule.E, Yamaoto.Y, Thouvenin.M, Nagashi.Y, Kataoka.K, 2004, Thermal characterization of poly(ethylene glycol)-poly(D,L-lactide) black copolymer micelles based on pyrene excimer formation, *Journal of controlled release*, 97, pp 407- 419

232. Komorek.U and Wilk.K.A, 2004, Surface and micellar properties of new non-ionic Gemini aldoamide-type surfactants, *Journal of Collouid and Interface Science*, 271, pp206-211

233. Peltonen.L.J and Yliruusi.J, 2000, Surface Pressure, Hysteresis, Interfacial Tension and CMC of Four Sorbitan Monoesters at Water-Air, Water-Hexan, and Hexane-Air Interfaces, Journal of Colloid and Interface Science, 227, pp1-6

234. de la Maza.A, Coderch.L, Gonzalez.P and Parra.J.L, 1998, Subsolubilizing alterations caused by alkyl glucosides in phosphatidylcholine liposomes, Journal of Controlled Release, 52, pp159-168

235. Suzuki.O and Watanabe.K, Drugs and Poisons in Humans, A handbook of practical analysis, USA, *Springer* 2005

236. Rettig.W, Paeplow.B, Herbst.H, llen.I.M, Desvergne*e.J.P and* Bouas-Laurent.*H*, 1999, Intramolecular excimer formation in short- and long-chain length di(9-anthryl) bichromophoric compounds and relation to ground state properties, *New Journal of Chemistry,* 23, pp 453- 460

237. Mao. S, Shuai. X, Unger. F, Wittmar. M, Xie.X, Kissel. T, (2005), Synthesis, characterization and cytotoxicity of poly(ethylene glycol)-grafttrimethylchitosan block copolymers, *Biomaterials*, 26, pp6343–6356

238. Gouveia.L.M, Grassl.B and Müller.A.J, 2009, Sythesis and rheological properties of hydrophobically modified polyacrylamides with lateral chains of poly(propylene oxide) oligomers, Journal of Colloid and Interface Science, 333, pp 152-163

239. Candau.F and Selb.J, 1999, Hydrophobically-modified polyacrylamides prepared by micellar polymerization. Advances in Colloid and Interface Science, 79, pp 149-172

240. Volpert.E, Selb.j and Candau.F, 1996, Influence of the Hydrophobe Structure on Composition, Microstrucutre and Rheology in Association Polyacrylamides Prepared by Micellar Copolymerization, Macromolecules, 29, pp 1452-1463

241. Aryal.S, Prabaharan.M, Pilla.S, Gong.S, 2009, Biocompatible multi-arm star amphiphilic block copolymer as a carrier for hydrophobic drug delivery, *International Journal of Biological Macromolecules*, 44, pp346-352

242. Tian.Z, Wang.M, Zhang.A-Y, Feng.Z-G, 2007, Preparation and evaluation of novel amphiphilic glycopeptide block copolymers as carriers for controlled drug release, *Polymer*, 49, pp 446-454

243. Francis.M.F, Cristea.M, Winnik.M, 2004, Polymeric micelles for oral drug delivery: Why and how*, *Pure and Applied Chemistry*, 76, pp1321-1335

244. Okada.M, 2001, Molecular design and synthesis of glycopolymers, *Progress in Polymer Science*, 26, pp 67-104

245. Aliabadi.H.M, Elhasi.A.S, Mahmud.A, Gulamhusein.R, Mahdipoor.P, Lavasanifar.A, 2007, Encapsulation of hydrophobic drugs in polymeric micelles through co-solvent evaporation: The effect of solvent composition on micellar properties and drug loading, International *Journal of Pharmaceutics*, 329, pp 158-165

246. Lavasanifar.A, Samuel.J, Kwon.G.S, 2001, Micelles self-assembled from poly(ethylene oxide)-*block*-poly(*N*-hexyl stearate L-aspartamide) by a solvent evaporation method: effect on the solubilisation and haemolytic activity of amphotericin B, *Journal of Controlled Release*, 77, pp 155-160

247. Gong.J, Huo.M, Zhuo.J, Zhang.Y, Peng.X, Yu.D, Zhang.H, Li.J, 2009, Synthesis, characterization , drug-loading capacity and safety of novel octyl modified serum albumin micelles, *International Journal of Pharmaceutics*, 376, pp 161-168

248. Ibekwe.V.C, Fadda.H.M, Parsons.G.E, Basit.A.W, 2006, A comparative in vitro assessment of the drug release performance of pH-responsive polymers fro ileo-colonic delivery*, International Journal of aPharmaceutics*, 308, pp 52-60

249. Park.J.H, Lee.S, Kim.J-H, Park.K, Kim.K, Kwon.I.C,2008, Polymeric nanomedicine for cancer therapy, *Progress in Polymer Science*, 33, pp 113-137

250. Zhang.Y, Zhuo.R-x, 2005, Synthesis and in vitro drug release behavior of amphiphilic triblock copolymer nanoparticles based on poly(ethylene glycol) and polycaprolactone, *Biomaterials*, 26, pp 6736-6742

251. Brannon-Peppas.L, 1997, Polymers in Controlled Drug Delivery, *Medical device link*

252. Heurtault.B, Saulnier.P, Pech.B, Proust.J-E, Benoit.J-P, 2003, Physio-chemical stability of colloidal lipid particles, *Biomaterials*, 24, pp4283-4300

253. Abdelwahed.W, Degobert.G, Stainmesse.S, Fessi.H, 2006, Freeze-drying of nanoparticles: Formulation, process and storage considerations, *Advanced Drug Delivery Reviews*, 58, pp 1688-1713

254. Chacón.M, Molpeceres.J, Berges.L, Guzmán.M, Aberturas.M.R, 1999, Stability and freeze-drying of cyclosporine loaded poly(D,L lactide-glycolide) carriers, *European Journal of Pharmaceutical Sciences*, 8, pp 99-107

255.Vasileiou.I, Xanthos.T, Koudouna.E, Despoina.P, Klonaris.C, Katsargyris.A, Papadimitriou.L, 2009, Propofol: A review of its non-anaesthetic effects, *European Journal of Pharmacology*, 605, pp 1-8

256.Lundström.S, Zachrisson.U, Fürst.C.J, 2005, When Nothing Helps: Propofol as Sedative and Antiemetic in Palliative Cancer Care, Journal *of Pain and Symptom Management*, 30, pp 570-577

257.Trapani.A, Laquimtana.V, Lopedota.A, Franco.M, Latrofa.A, Talani.G, Sanna.E, Trapani.GN, Liso.G, 2004, Evaluation of new propofol aqueous solutions for intravenous anaesthesia, *International Journal of Pharmaceutics*, 278, pp 91-98

258.Trapani.G, Lopedota.A, Franco.M, Latrofa.A, Liso.G, 1996, Effect of 2-hydroxypropyl-β-cyclodextrin on aqueous solubility of the anaesthetic agent propofol (2,6-diisopropylphenol), *International Journal of Pharmaceutics*, 139, pp 215-218

259.Ravenelle.F, Vachon.P, Rigby-Jones.A.E, Sneyd.J.R, Le Garrec.D, Gori.S, Lessard.D, Smith.D.C, 2008, Anaesthetic effects of propofol polymeric micelle: a novel water soluble propofol formulation, *British Journal of Anaesthesia*, 101, pp186-193

260.Hui.Y, Raedschelders.K, Zhang.H, Ansley.D.M, Chen.D.D.Y, 2009, Quatitative analysis of propofol in whole blood capillary electrophoresis, *Journal of Chromatography B*, 877, pp 703-709

261.Wischke.C, Schwendeman.S.P, 2008, Priniciples of encapsulating hydrophobic drugs in PLA/PLGA, *International Journal of Pharmaceutics*, 364, pp 298-327

262.Kabasakalian.P, Britt.E, Yudis.M.D, 1996, Solubility of some steroids in water, *Journal of Pharmaceutical Science*, 55, pp642

263.Ahmed.M, Morrel.E.M, Clemente.E, 2001, Bioavaliability and Pharmacokinetics of a New Liquid Prednisolone Formulation in Comparison with Two Commercially Avaliable Liquid Prednisolone Products, *Current Therapeutic Research*, 62, pp 548-556

264.Teshima.M, Fumoto.S, Nishida.K, Nakamura.J, Ohyama.K, Nakamura.T, Ichikawa.N, Nakashima.M, Sasaki.H, 2006, Prolonged blood concentration of prednisolone after intravenous injection of liposomal palmitoyl prednisolone, *Journal of Controlled Release*, 112, pp320-328

265.Dahan.A, Hoffman.A, 2007, The effect of different lipid based formulations on the oral adsorption of lipophilic drugs: The ability of in vitro lipolysis and consecutive ex vivo intestinal permeability data to predict in vivo bioavailability, *European Journal of Pharmaceutics and Biopharmaceutics*, 67, pp 96-105

266.Zili.Z, Sfar.S , Fessi.H, 2005, Preparation and characterization of poly-ε-caprolactone Nanoparticles containing griseofulvin, *Pharmaceutical Nanotechnology*, 294, pp261-267

267.Trotta.M, Gallarate.M, Carlotti.M.E, Morel.S, 2003, Preparation of griseofulvin Nanoparticles from water-dilutable microemulsions, *International Journal of Pharmaceutics*, 254, pp 235-242

268.Tur.K.M, Ch'ng.H-S, Baie.S, 1997, Use of bioadhesive polymer to improve the bioavailability of griseofulvin, *International Journal of Pharmaceutics*, 148, pp63-71

269.Finkelstein.E, Amichai.B, Grunwald.M.H, 1996, Griseofulvin and its uses, *International Journal of Antimicrobial Agents*, 6, pp189-194

270.Fujioka.Y, Metsugi.Y, Ogawara.K-I, Higaki.K, Kimura.T, 2008, Evaluation of *in vivo* dissolution behaviour and GI transit of griseofulvin, a BSC class II drug, *International Journal of Pharmaceutics*, 352, pp 36-43

271.Ahmed.I.S, Aboul-Einien.M.H, Mohamed.O.H, Farid.S.F, 2008, Relative bioavailability of griseofulvin lyophilized dry emulsion tablet vs. immediate release tablet: A single-dose, randomized, open-label, six-period, crossover study in healthy adult volunteers in the fasted and fed states, *European Journal of Pharmaceutical Sciences*, 35, pp 219-225

272.Nielsen.P.B, Müllertz.A, Norling.T, Kristensen.H.G, 2001, The effect of α-tocopherol on the in vitro solubilisation of lipophilic drugs, *International Journal Of Pharmaceutics*, 222, pp217-224

273.You.B, Tranchand.B, Girard.P, Falandry.C, Ribba.B, Chabaud.S, Souquet.P-J, Court-Fortune.I, Trillet-Lenoir.V, Fournel.C, Tod.M, Freyer.G, 2008, Etoposide

pharmacokinetics and survival in patients with small cell lung cancer: A multicentre study, *Lung Cancer*, 62, pp261-272

274. Hande.K.R, 1998, Etoposide: Four Decades of Development of a Topoisomerase II Inhibitor, *European Journal of Cancer*, 34, pp 1514-1521

275. Jasti.B.R, Du.J, Vasavanda.R.C, 1995, Characterization of thermal behaviour of etoposide, *International Journal of Pharmaceutics*, 118, pp 161-167

276. Shah.J.C, Chen.J.R, Chow. D, 1995, Preformulation study of etoposide: II. Increased solubility and dissolution rate by solid-solid dispersions, *International Journal of Pharmaceutics*, 113, pp 103-111

277. Reddy .P.B, Paul.D.V, Agrawal.S.K, Saxena.A.K, Kumar.H.M.S, Qazi.G.N, 2008, Design, Synthesis, and Biological Testing of 4β-[(4-Substituted)-1,2,3-triazol-1-yl]podophyllotoxin Analogues as Antitumor Agents, Archives of Pharmacy, *Chemistry and Life Sciences*, 341, pp126-121

278. Oliveira.J, Ralton.L, Tavares.J, Codeiro-da-Silva.A, Bestwick.C, McPherson.A, Kong Thoo Lin.P, 2007, The synthesis and the in vitro cytotoxicity studies of bisnaphthalimidoproply polyamine derivatives against colon cancer cells and parasite *Leishmania infantum*, *Bioorganic & Medicinal Chemistry*, 15, pp541-545

279. Braña.M.F, Cacho.M, Gradillas.A, de Pascual-Teresa.B, Ramos.A, 2007, Intercalators as Anticancer Drugs, *Current Pharmaceutical Design*, 7, pp1754-1780

280. Dance.A-M, Ralton.L, Fuller.Z, Milne.L, Duthie.S, Bestwick.C, Kong Thoo Lin.P, 2005, Synthesis and biological activities of bisnaphthalimido polyamines derivatives: cytotoxicity, DNA binding, DNA damage and drug localization in bnreast cancer MCF 7 cells, *Biochemical Pharmacology*, 69, pp19-27

281. Kong Thoo Lin.P, Pavlov.V.A, 2000, The synthesis and In Vitro Cytotoxic Studies of Novel Bis-naphthalimidopropyl Polyamine Derivatives, *Bioorganic & Medicinal Chemistry Letters*, 10, pp1609-1612

282. Braña.M.F, Castellano.J.M, Morán.M, Pérez de Vega.M.J, Qian.X.D, Romerdahl.C.A, Keilhauer.G, 1995, Bis-naphthalimides. 2. Synthesis and biological activity of 5,6-acenaphthalimidoalkyl-1,8-naphthalimidoalkyl amines, *European Journal of Medicinal Chemistry*, 30, pp235-239

283. Kazakevich.Y and LoBrutto.R, HPLC for Pharmaceutical Scientists, John Wiley and Sons Inc., 2007, USA

284. Trimaille.T, Mondon.K, Gurny.R and Möller.M, 2006, Novel polymeric micelles for hydrophobic drug delivery based on biodegradable poly(hexyl-substituted lactides), *International Journal of Pharmaceutics*, 319, pp 147-154

285. Dandamudi.S, Campbell.R.B, 2007, The drug loading, cytotoxicity and tumor vascular targeting characteristics of magnetite in magnetic drug tareting, *Biomaterials*, 28, pp4673-4683

286. Lee.J, Cho.E.C and Cho.K, 2004, Incorporation and Release behaviour of hydrophobic drug in functionalized poly(D,L-lactide)-block-poly_ethylene oxide) micelles, *Journal of Controlled Release*, 94, pp 323-332

287. Xu.Q and Czernuszka.J.T, 2008, Controlled release of amoxicillin by hydroxyapatite coated poly(lactic-co-glycolic acid) microspheres, *Journal of Controlled Release*, 127, pp146-153

288. Lamprecht.A, Torres.H.R, Schäfer.U and Lehr. C.M, 2000, Biodegradable microparticles as a two-drug controlled release formulation: a potential treatment of inflammatory bowel disease, *Journal of Controlled Release*, 69, pp445-454

289. Franks.F, 1998, Freeze-drying of bioproducts: putting principles into practice, *European Journal of Pharmaceutics and Biopharmaceutics*, 45, pp 221-229

290. Husseini.G.A, Pitt.W.G, 2008, Micelles and nanoparticles for ultrasonic drug and gene delivery, *Advanced Drug Delivery Reviews*, 60, pp 1137-1152

291. Sezgin.Z, Yüksel.N, Baykara.T, 2006, Preparation and characterization of polymeric micelles for solubilization of poorly soluble anticancer drugs, *European Journal of Pharmaceutics and Biopharmaceutics*, 64, pp 261-268

292. Zhang.X, Jackson.J.K, Burt. H.M, 1996, Development of amphiphilic diblock copolymers as micellar carriers of Taxol, *International Journal of Pharmaceutics*, 132, pp195-206

293. Yao.Z, Zhang.C, Ping.Q, Yu.L (2007) A series of novel chitosan derivatives: synthesis, characterization and micellar solubilisation of paclitaxel, *Carbohydrate Polymers*, 68, pp781–792

294. Du.Y-Z, Wang.L, Yuan.H, Wei.X-H, Hu.F-Q, 2009, Preparation and characterisitics of linoleic acid-grafted chistosan oligosaccharide micelles as a carrier for doxorubicin, *Colloids and Surfaces B: Biointerfaces*, 69, pp257-263

295. Zhang.J, Li.S, Li.X, Li.X, Zhu.K, 2009, Morphology modulation of polymeric assemblies by guest drug molecules: TEM study and compatibility evaluation, *Polymer*, 50, pp1778-1789

296. Lui.R, Water-Insoluble Drug Formulation, 2nd Edition, CRC Press, 2008

297. Pop.E, Anderson.W, Prokai-Tatrai.K, Vlasak.J, Brewster.M.E, Bodor.N, 1992, Syhtesis and preliminary pharmacological evaluation of some chemical delivery systems of 2,6-diisopropylphenol (propofol), *Medicinal Chemistry Research*, 2, pp 16-21

298. Brewster.M, Estes.K, Bodor.N, 1990, An intravenous toxicity study of 2-hydroxypropyl-β-cyclodextrin, a useful drug solubilizer, in rats and monkeys, *International Journal of Pharmaceutics*, 59, pp231-243

299. Hendler.SS, Sanchez.R.A, Zielinski.J, 1999, Water-soluble prodrugs of propofol, PCT International Applications, WO 99127082

300. Sagara.Y, Hendler.S, Khon-Reiter.S, Gillenwater.G, Carlo.D, Schubert.D, Chang.J, 1999, Propofol hemisuccinate protects neuronal cells from oxidative injury, *Journal of Neurochemistry*, 73, pp 2524-2530

301. Stella.V.J, Zygmunt.JJ, Geog.I.G, Safadi.M.S, 2000, Water soluble prodrugs of hindered alchohols or phenols. PCT International Applications, WO 0008033

302. Seedher.N, Sharma.P, 2007, Solubility and Stability Enhancement of Poorly-Soluble Drugs Clarithromycin and Prednisolone by Combination with other drugs, *International Journal of Biological Chemistry*, 4, pp229-236

303. Balakrishnan.A, Rege.S.D, Amidon.G.L, Polli.J.E, 2004, Surfactant-Mediated Dissolution: Contributions of Solubility Enhancement and Relatively Low Micelle Diffusivity, *Journal of Pharmaceutical Sciences*, 93, pp 2064-2075

304. Shin.H-C, Alani.A.W.G, Rao.D.A, Rockich.N.C, Kwon.G.S, 2009, Multi-drug loaded polymeric micelles for simultaneous delivery of poorly soluble anticancer drugs, *Journal of Controlled Release*, Article In Press

305. Reddy.L.H, Sharma.R.K, Chuttani.K, Mishra.A.K, Murthy.R.S.R, 2005, Influence of administration route on tumour uptake and biodistribution of etoposide loaded solid lipid Nanoparticles in Dalton's lymphoma tumor bearing mice, *Journal of Controlled Release*, 105, pp 185-198

306. Kranz.G, Gutsche.S, 2009, Evaluation of the drug release patterns and log term stability of aqueous and organic coated pellets by using blends of enteric and gastroinstetinal insoluble polymers, *International Journal of Pharmaceutics*, 380, pp 112-119

307. [1]Lui.G-Y, Zhai.Y-L, Wang.X-L, Wang.W-T, Pan.Y-B, Dong.X-T, Wang.Y-Z, 2008, Preparation, charaterization, and in vitro drug release behaviour of biodegradable chitosan-graft-poly(1,4-dioxan-2-one) copolymer, *Carbohydrate Polymers*, 74, pp862-867

308. Wang.X, Wang.Y, Wei.K, Zhao.N, Zhang.S, Chen.J, 2009, Drug distribution within poly(ε-caprolactone) microspheres and in vitro release, *Journal of Materials Processing Technology*, 209, pp 348-354

309. Saez.A, Guzmán.M, Molpeceres.J, Aberturas.M.R, 2000, Freeze-drying of polycaprolactone and poly(D,L-lactic-glycolic) nanoparticles induce minor particle size changes affecting the oral pharmacokinetics of loaded drugs, *European Journal of Pharmaceutics and Biopharmaceutics*, 50, pp379-387

310. Freshney.R.I, Culture of Animal Cells A Manual of Basic Technique,5th Edition, Hoboken NJ, *John Wiley & Sons Inc.*, 2005

311. Kibbe.A.H, Handbook of Pharmaceutical excipients, 3rd Edition, *American Pharmaceutical Association*, Washington, USA., 2000

312. Maysinger.D, Lovrić.J, Eisenberg.A, Savić.R, 2007, Fate of micelles and quantum dots in cells, *European Journal of Pharmaceutics and Biopharmaceutics*, 65, pp 270-281

313. Savíc.R, Eisenberg.A, Maysinger.D, 2006, Block copolymer micelles as delivery vehicles of hydrophobic drugs: Micelle–cell interactions, *Journal of Drug Targeting*, 14, pp 343 - 355

314. Kimura.K, Buddington.K.K, Buddington.R.K, 2004, The Influence of Estradiol and Diet on Small Intestinal Gluscose Transport in Ovariectomized Rats, *Experts in Biological Medicine*, 229, pp227-234

315. Geng.L, Osusky.K, Konjeti.S, Fu.A, Hallahan.D, 2004, Radiation-guided drug delivery to tumor blood vessels in improved tumor growth delay, *Journal of Controlled Release,* 99, pp369-381

316. Aubert.M, Panicot.L, Crotte.C, Gibier.P, Lombardo.D, Sadoulet.M-O, Mas.E, 2000, Restoration of α(1,2) Fucosyltransferase Activity Decreases Adhesive and Metastatic Properties of Human Pancreatic Cancer Cells, Cancer Research, 60, 1449-1456

317. Aravindan.L, Bicknell.K.A, Brooks.G, Khutoryanskiy.V.V, Williams.A.C, 2009, Effect of acyl chain length on transfection efficiency and toxicity of polyethylenime, *International Journal of Pharmaceutics*, 378, pp201-210

318. Ladavière.C, Toustou.M, Gulik-Krzywicki.T, Tribet.C, 2001, Slow Reorganization of Small Phosphatodylcholine Vesicles upon adsorption of Amphiphilic Polymers, *Journal of Colloid and Interface Science*, 241, pp 178-187

319. Stepnova.E.A, Tikhonov.V.E, Babushkina.T.A, Klimova.T.P, Vorontsov.E.V, Babak.V.G, Lopatin.S.A, Yamskov.I.A, 2007, New approach to the quaternization of chitosan and its amphiphilic derivatives, *European Polymer Journal*, 43, pp 2414-2421

320. Fischer, D., Li, Y.X., Ahlemeyer, B., Krieglstein, J., Kissel, T., 2003. In vitro cytotoxicity testing of polycations: influence of polymer structure on cell viability and haemolysis, *Biomaterials,* 24, pp 1121–1131.

321. Moreau.E, Ferrari.I, Drochon.A, Chapon.P, Vert.M, Domurado.D, 2000, Interactions between red blood cells and a lethal, partly quaternized tertiary polyamine, *Journal of Controlled Release*, 64, pp 115-128

322. Xu.L, Chen.H, Xu.H, Yang.X, 2008, Anti-tumour and immune-modulation effects of triptolide-loaded polymeric micelles, *European Journal of Pharmaceutics and Biopharmaceutics*, 70, pp 741-748

323. Mahot.F, des Rieux.A, Ariën.A, Schneider.Y-J, Brewster.M, Préat.V, 2007, Transport mechanism of mmePEG750P(CL-co-TMC) polymeric micells across the intestinal barrier, *Journal of Controlled Release*, 124, 134-143

Appendix

1.0 NMR spectra of modified polymers

a)

b)

c)
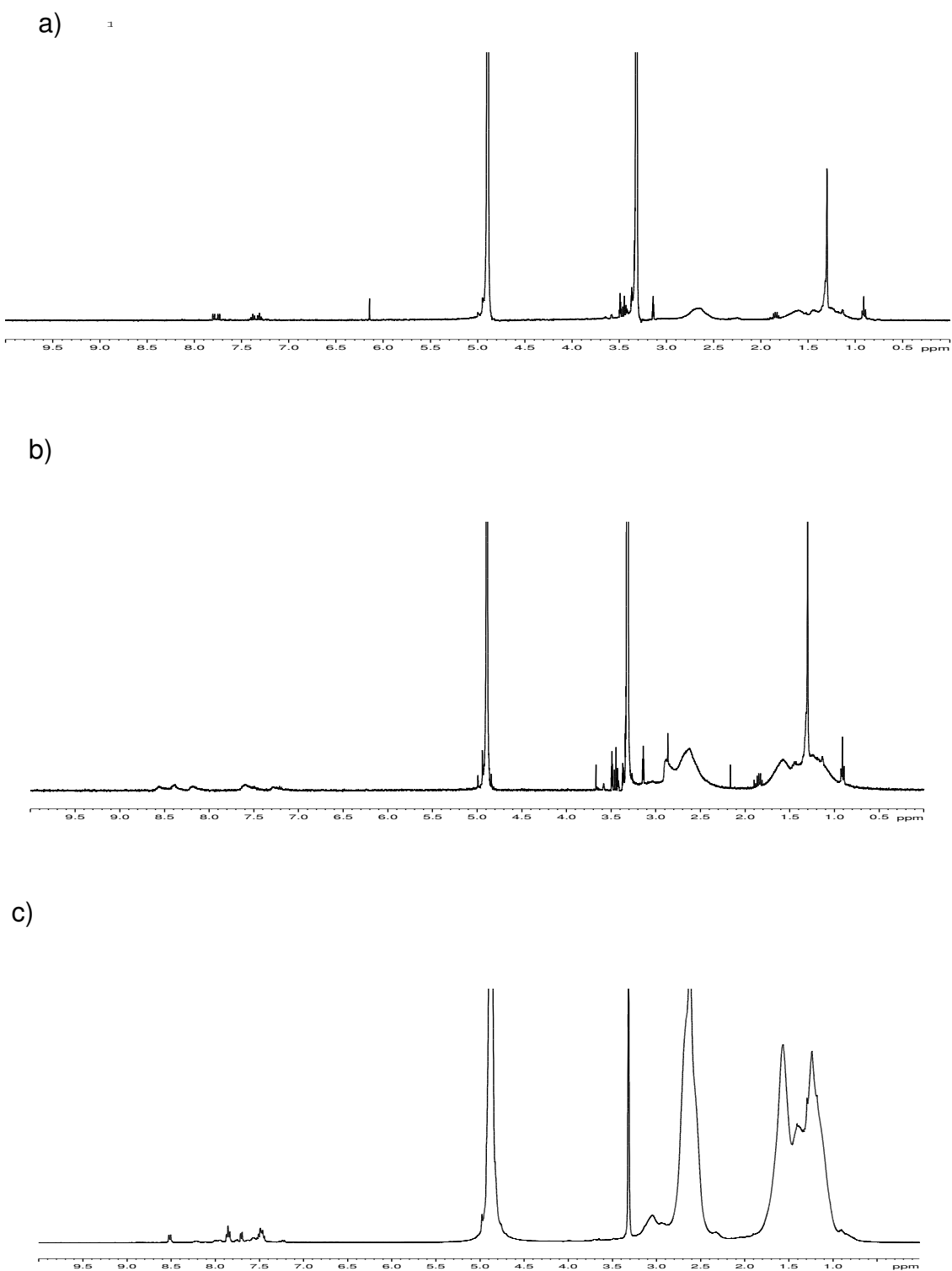
Figure 1. ^{1}H NMR spectra of a) Fmoc$_{10}$, b) Dansyl$_{10}$, c)Naphth$_{10}$ carried out in MEOD on 400Hz NMR @ 25°C
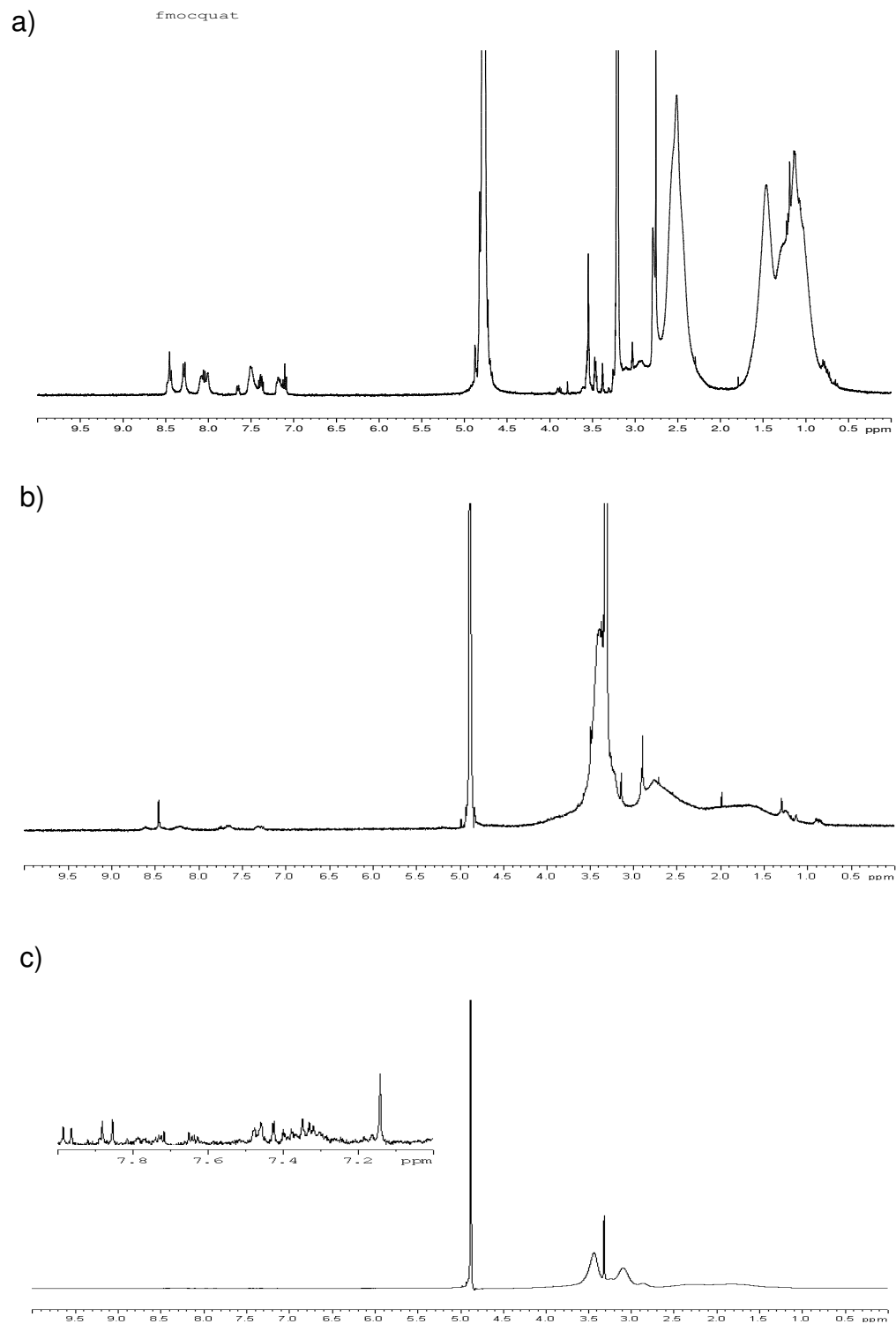
Figure 2. ^{1}H NMR spectra of a) QFmoc$_5$, b) QDansyl$_5$ and c) QNaphth$_5$ carried out in MEOD on 400Hz NMR @ 25°C
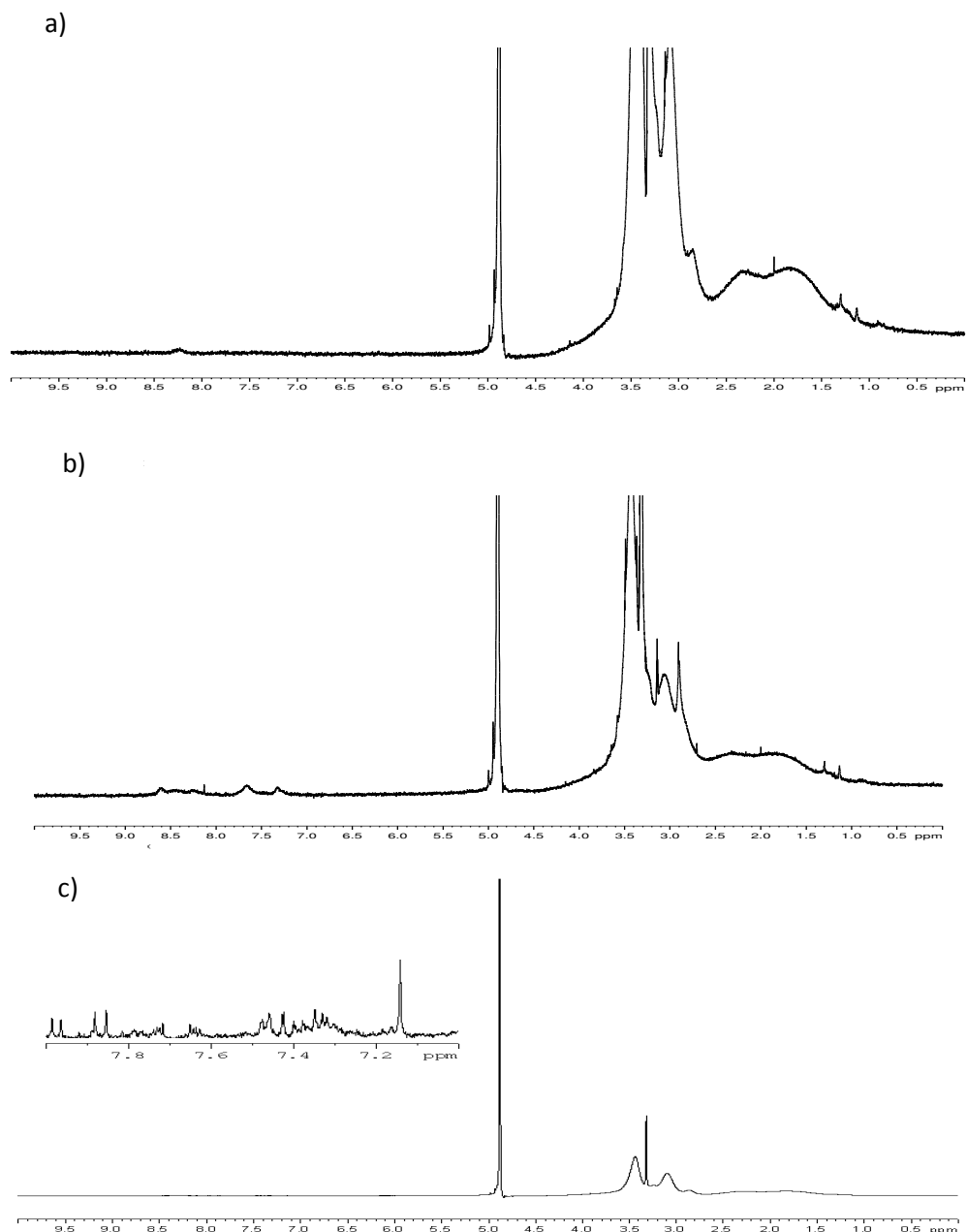
Figure 3. ^{1}H NMR spectra of a) qFmoc$_{10}$, and b) QDansyl$_{10}$ c) QNaphth$_{10}$ carried out in MEOD on 400Hz NMR @ 25°C

2.0 FTIR spectra of modified polymers
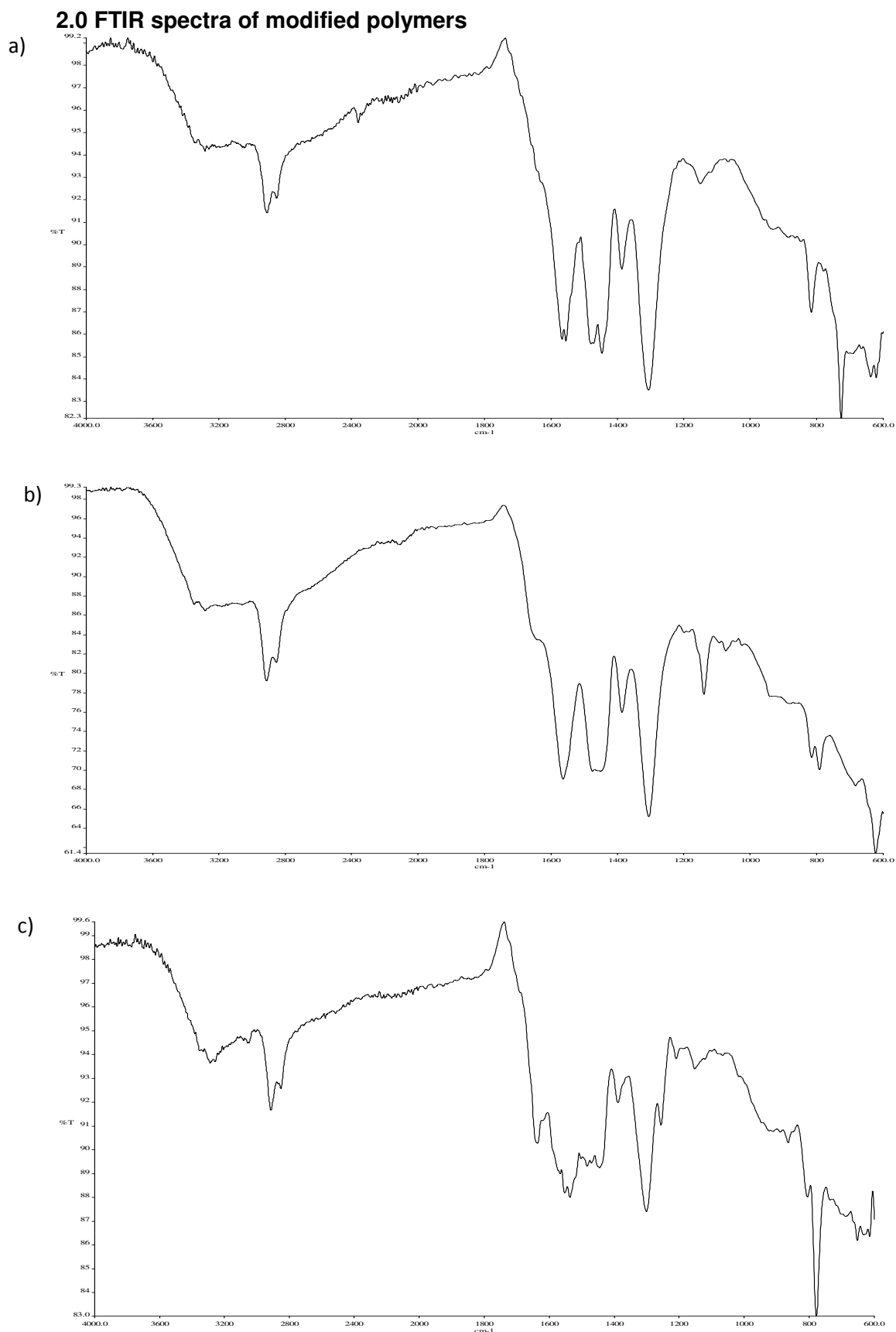
Figure 4. FTIR spectra for a) Fmoc$_{10}$,b) Dansyl$_{10}$ and c) Naphth$_{10}$ carried out using a diamond powder tip – 20 scans
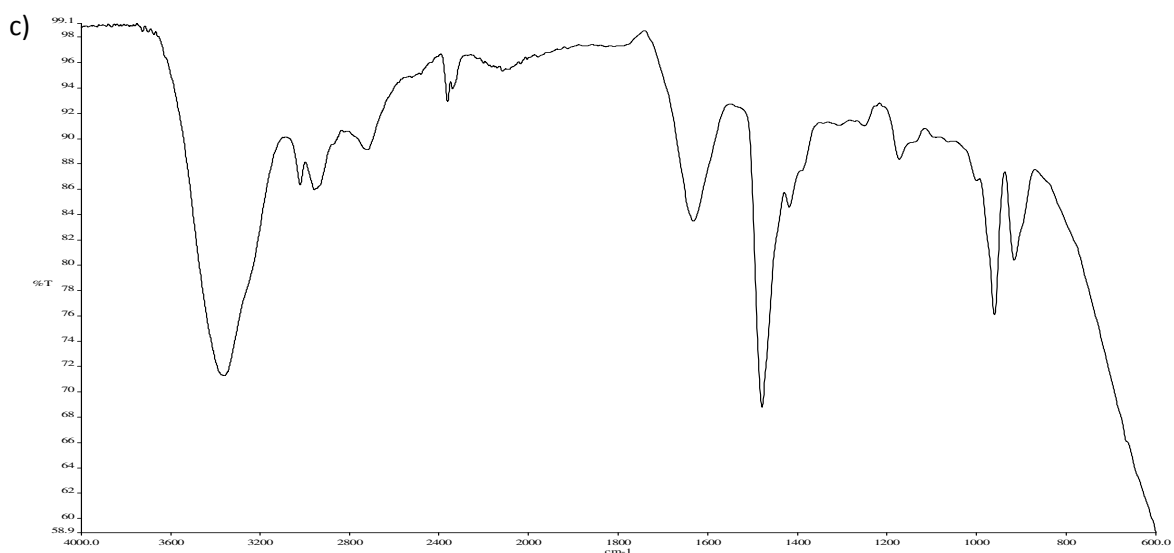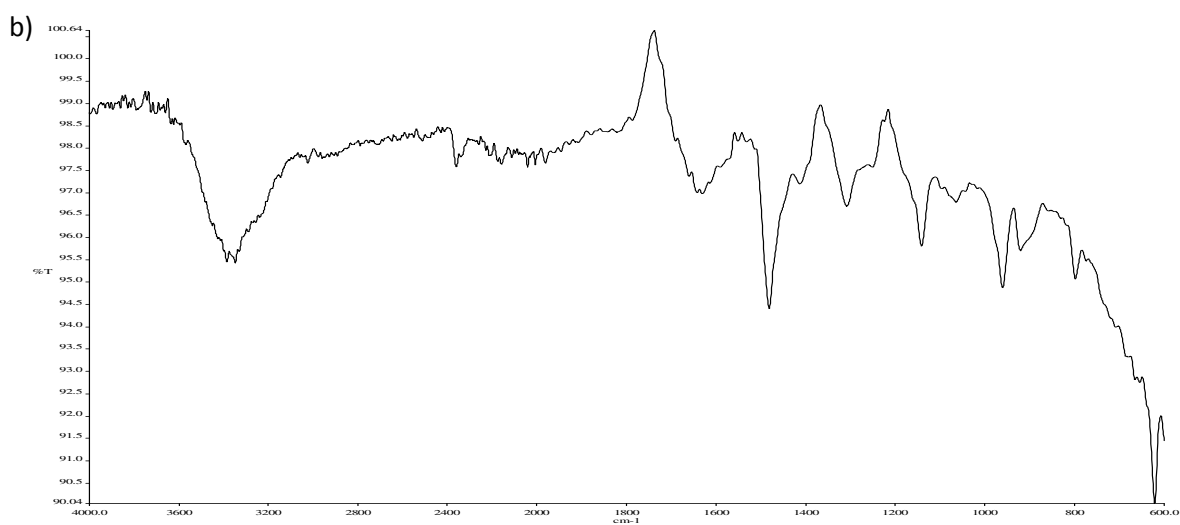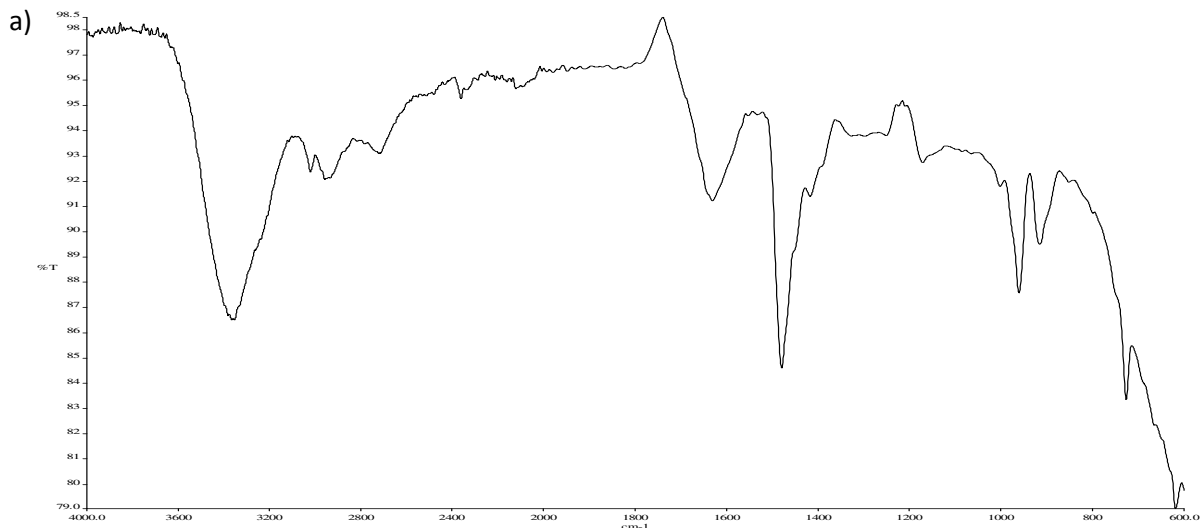
Figure 5. FTIR spectra for a) QFmoc$_{10}$,b) QDansyl$_{10}$ and c) QNaphth$_{10}$ carried out using a diamond powder tip – 20 scans

3.0 Photon correlation spectroscopy of self-assemblies
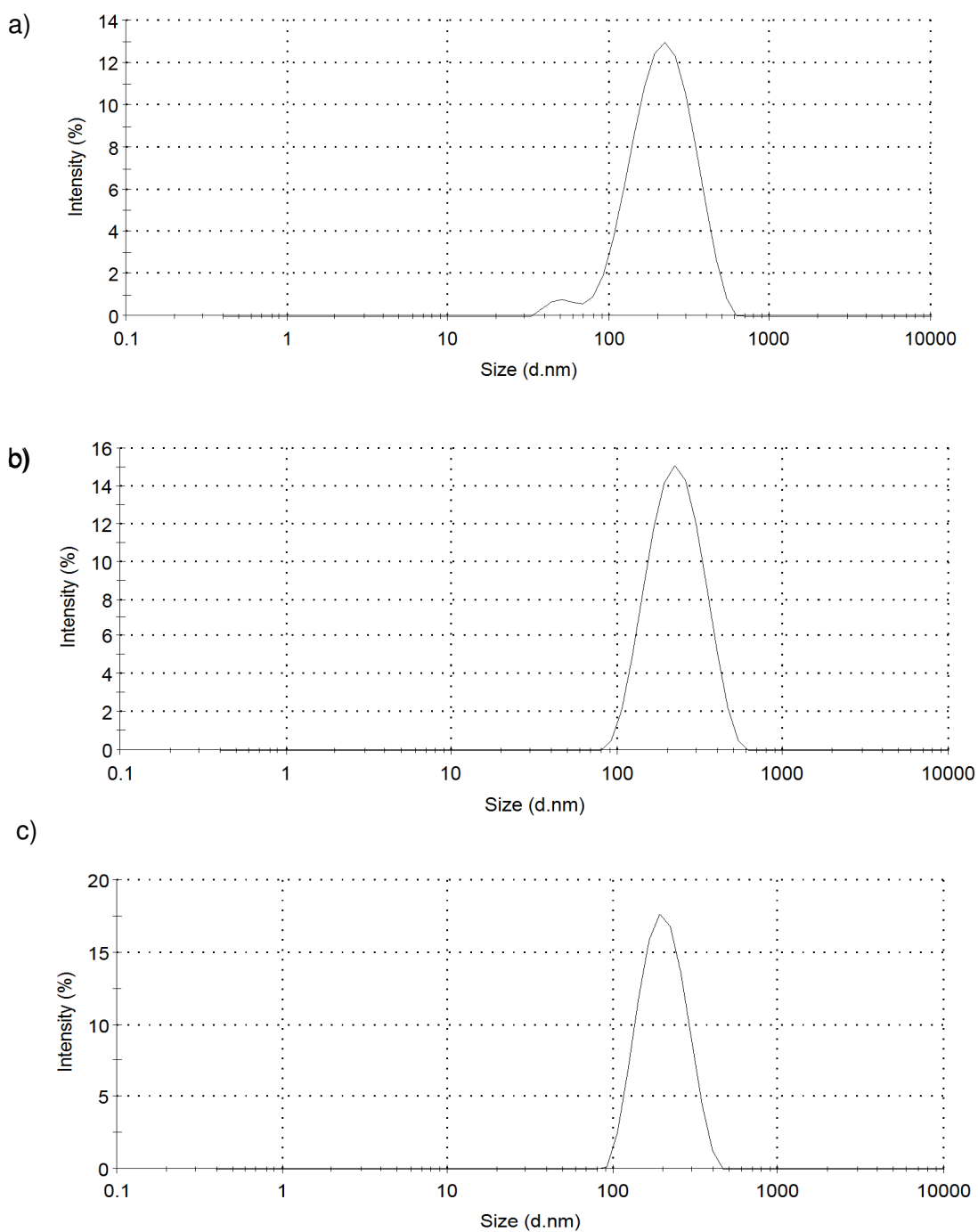
Figure 6. Photon correlation spectroscopy size correlation chart for 1mgmL^{-1} a) QCh$_5$, b) QFmoc$_5$, and c) QNaphth$_5$ in water
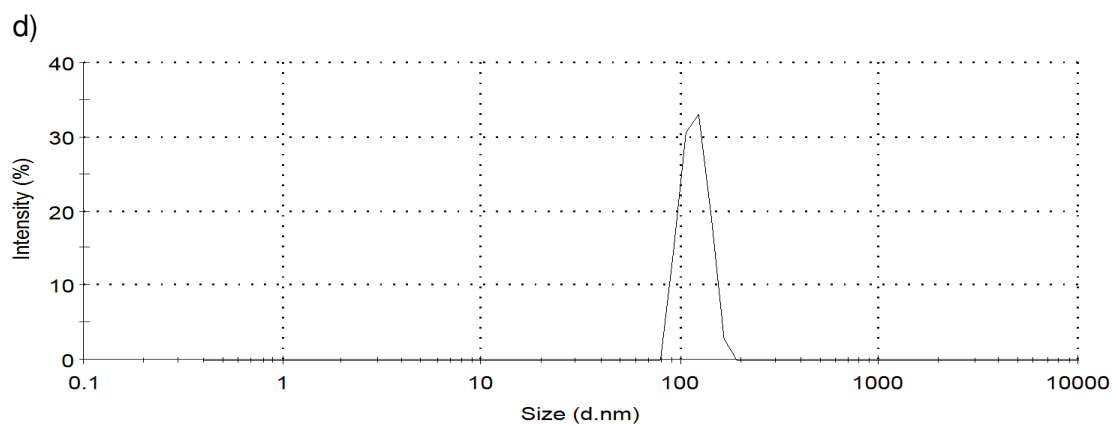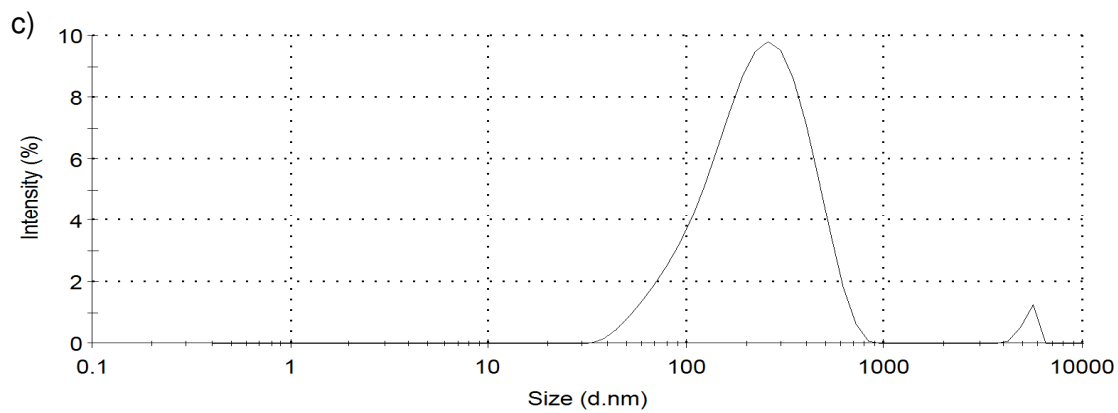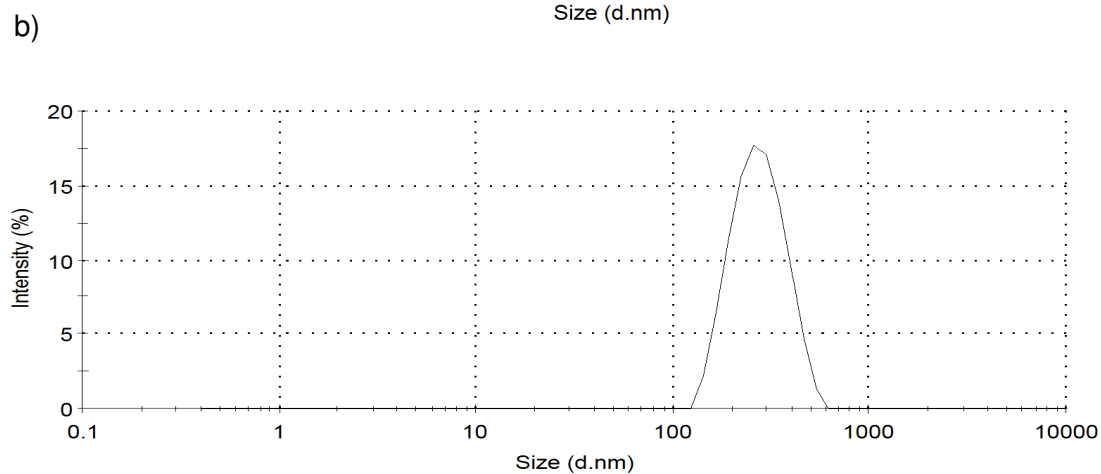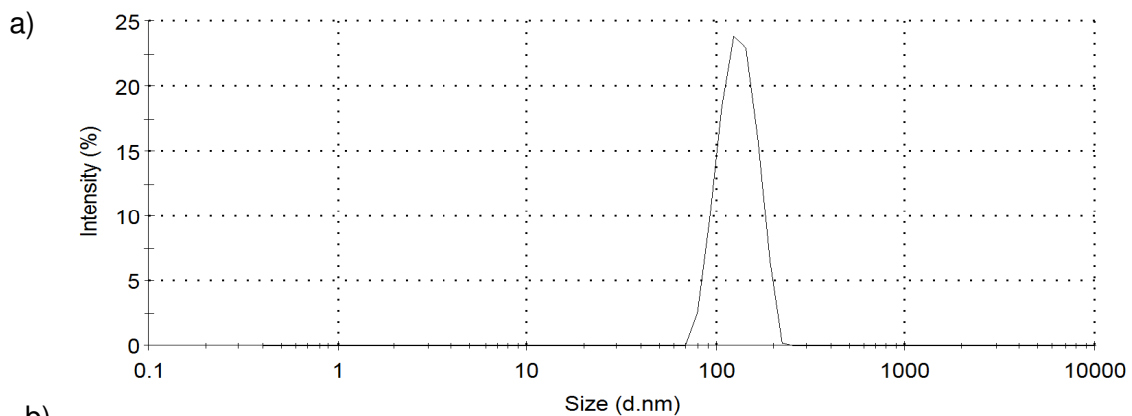
Figure 7. Photon correlation spectroscopy size correlation chart for 1mgmL^{-1} a) QCh$_5$, b) QFmoc$_5$, c) QDansyl$_5$ and d) QNaphth$_5$ in water.

a)

b)
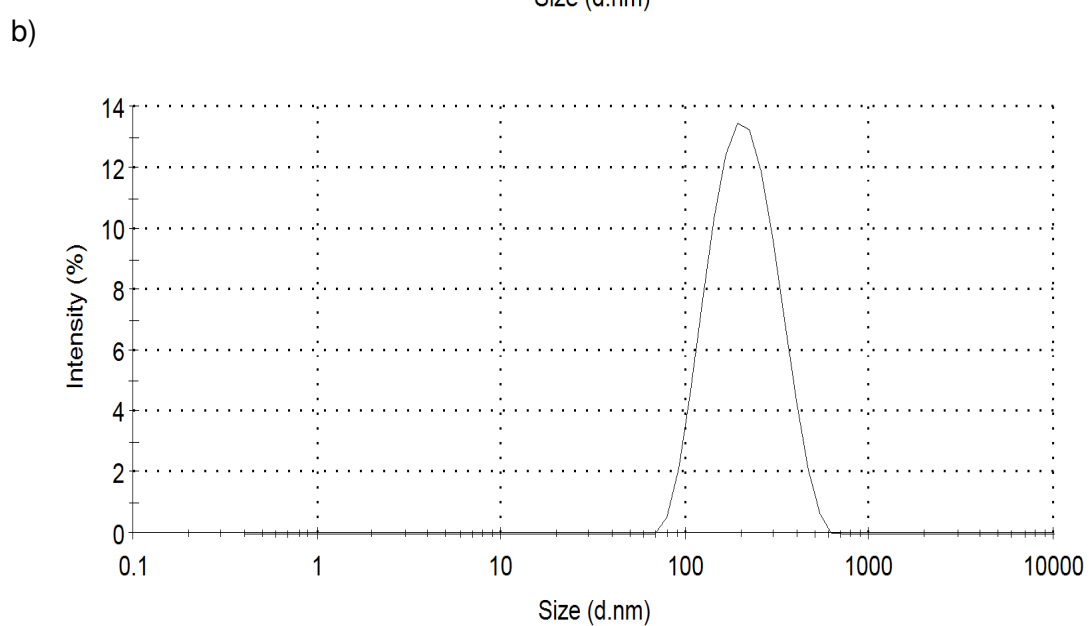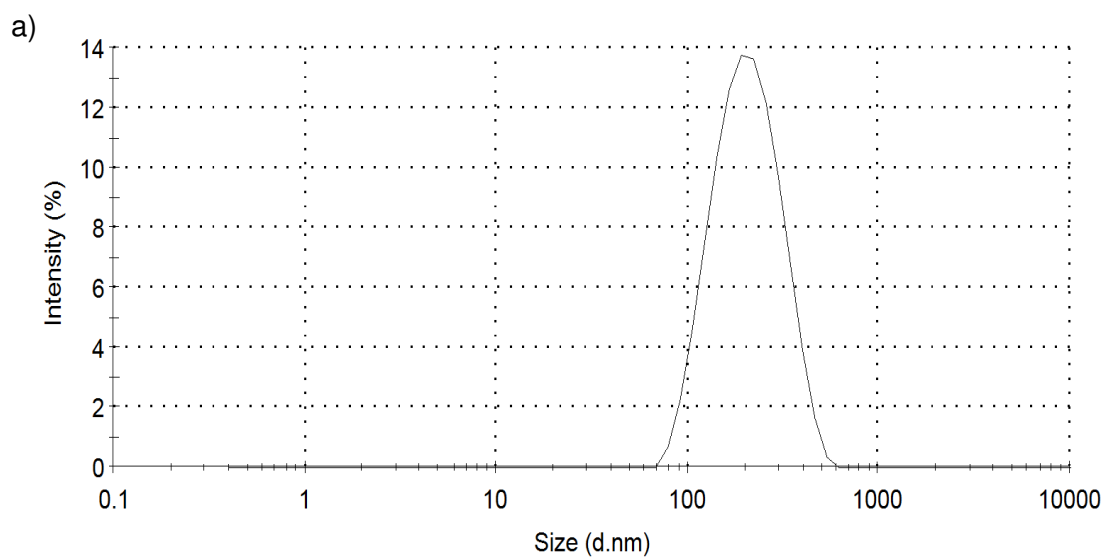
Figure 8. Photon correlation spectroscopy size correlation chart for 1mgmL^{-1} a) Fmoc$_{10}$ and b) Naphth$_{10}$ in water.
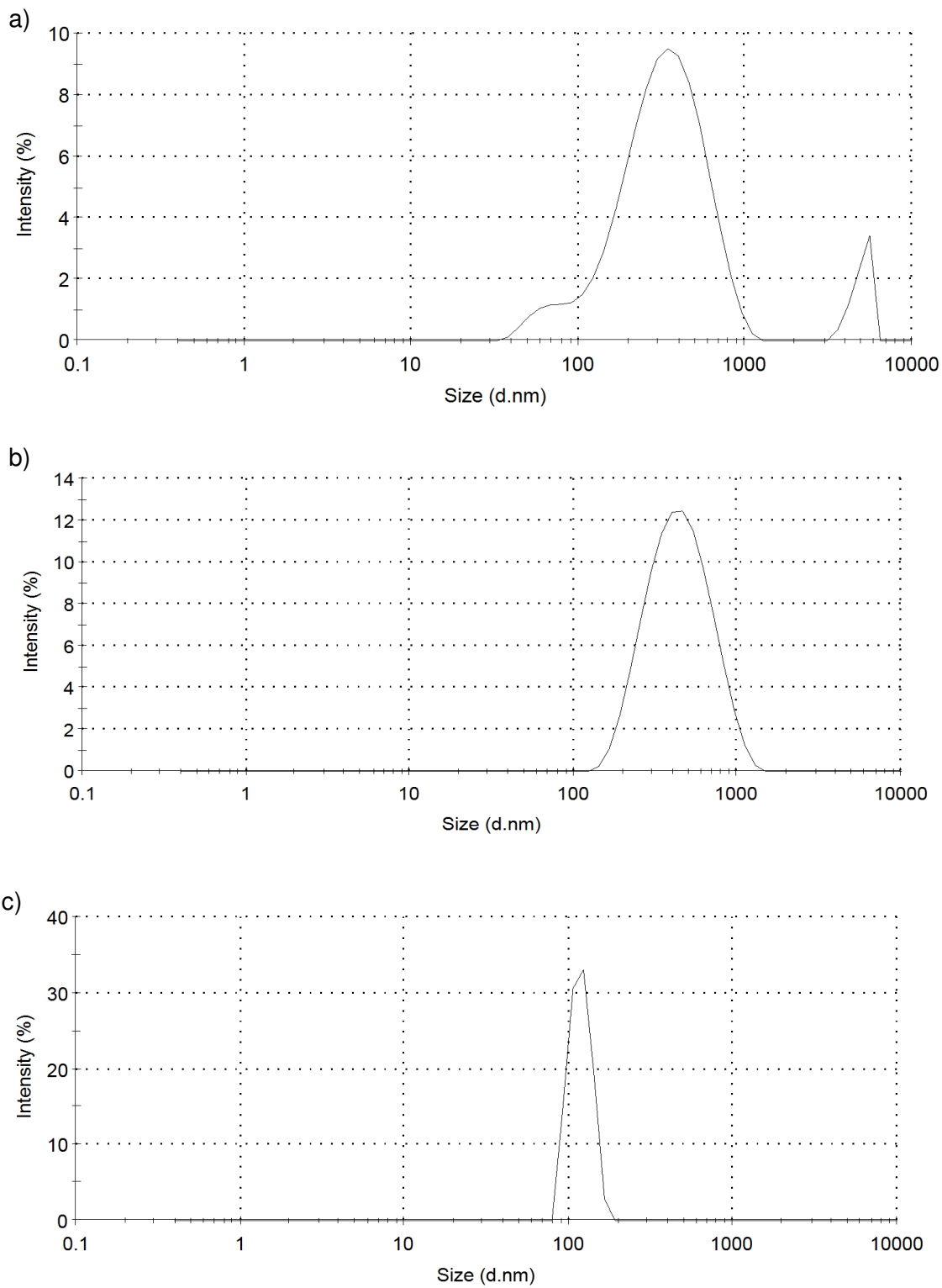
Figure 9. Photon correlation spectroscopy size correlation chart for 1mgmL^{-1} a) QFmoc$_{10}$, b) QDansyl$_{10}$ and c) QNaphth$_{10}$ in water.

4.0 Surface tension of self-assemblies
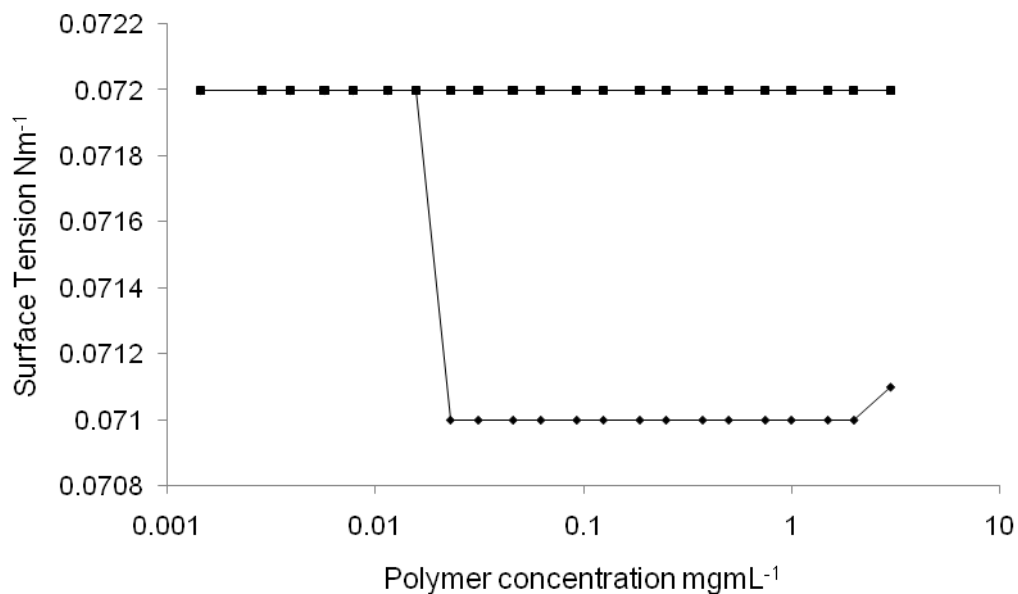
Figure 10. Surface Tension results for ◆ QCh_5 and ■ $QNaphth_5$ carried out on a torsion balance at 25°C (n=3, ave±SD).
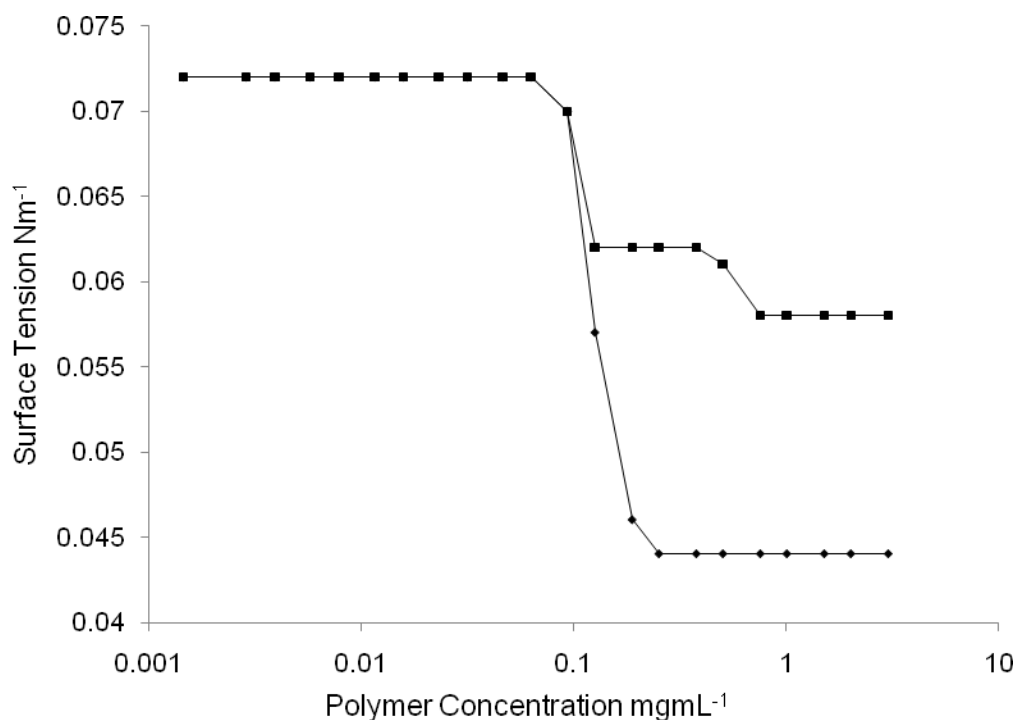
Figure 11. Surface Tension results for ◆ $Dansyl_{10}$ and ■ $Naphth_{10}$ carried out on a torsion balance at 25°C, (n=3, ave±SD).
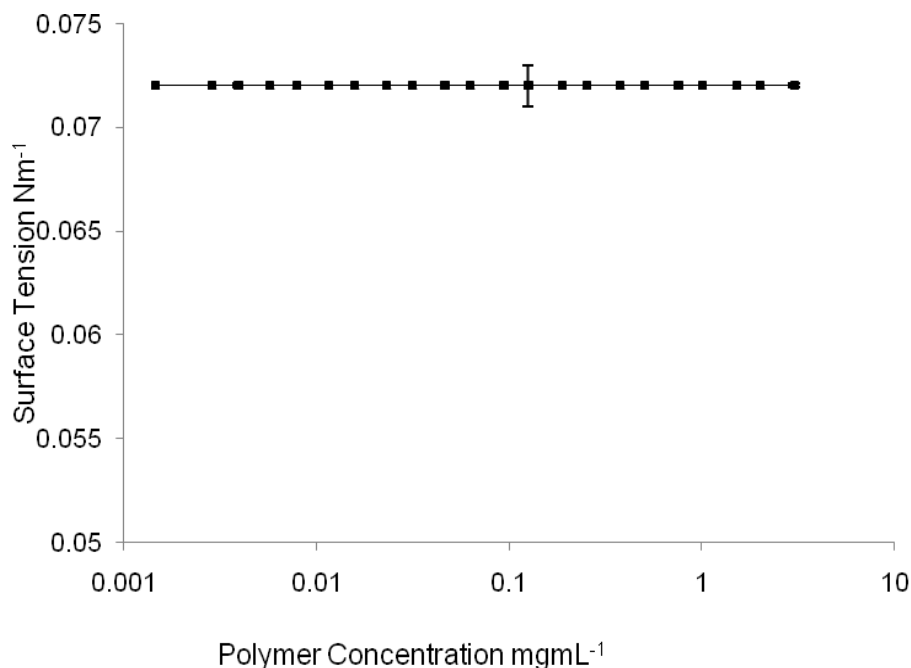
Figure 12. Surface Tension results for ◆ QFmoc$_{10}$, ■ QDansyl$_{10}$ and ▲ QNaphth$_{10}$ carried out on a torsion balance at 25ºC (n=3, ave ±SD).

5.0 Synthesis and characterisation of BNIPDaoct

5.1 Method

5.1.1. N-Acylation of Naphthalic Acid

Naphthalic anhydride (6.46 g) was dissolved in Dimethyl formaldehyde (DMF) (70 ml) in a round bottomed flask. The solution was stirred and slowly heated in an oil bath until homogeneous. 3-Amino 1- propanol (2.45 g) was added to solution forming a dark liquid. 1,8-diazabicycloundec-7-ene (DBU) (7.45 ml, 1 gmL^{-1}) was added and the solution was stirred at 85 ºC for 2 h. After cooling the solution was added slowly with stirring to icy water (200 ml) forming a precipitate. The resultant precipitate was filtered using a sintered glass funnel under pressure before being dried in a vacuum oven overnight. The product was recrystallised using ethanol and dried further. Thin layer chromatography (TLC) and ^{1}H NMR were run to determine the purity of the compound.

5.1.2. Tosylation of Naphthalimidoalkylpropanol

Naphthalimidoalkyklpropanol (5.10 g) was added to dry Pyridine (80 ml) and stirred at 0 ºC for 10 mins. Tosyl chloride (5.27 g) was added to the solution over 0.5 h and the resultant solution was refrigerated overnight at 0 – 5 ºC. The refrigerated mixture was poured slowly with forceful stirring into icy water (200 ml) producing a visocous liquid which solidified on cooling. The solid was filtered using a buchner funnel and washed with

deionised water. The solid was recrystallised with ethanol and dried in a vacuum oven overnight. NMR spectra were run to enable identification of the compound.

5.1.3. Protection and activation of polyamine

1,8- Diaminooctane (4.00 g) was dissolved in Pyridine (70 ml) with stirring. Mesitylenesulphonyl chloride (12.73 g) was added and the solution was stirred at room temperature for 4 h. The pyridine was removed using a rotary film evaporator (RFE) and the remaining solution was poured into icy water (200 ml) with stirring. The resultant precipitate was filtered and washed with hydrochloric acid (0.2 M) and deionised water. The purity of the compound was checked using TLC. The product was dried in a vacuum oven overnight before running ^{13}C and Dept NMR spectra.

5.1.4. Alkylation

Bimesitylene–1,8-diaminooctane (2 g) was dissolved in DMF (30 ml) with stirring. O-Tosylpropylnaphthalimide (3.38 g) was added to solution followed immediately by Caesium carbonate (7.04 g) and the mixture was stirred overnight at room temperature. The solution was poured into icy water (200 ml) and stirred with a glass rod. A few drops of Hydrochloric acid (2 M) were added to ensure any excess caesium carbonate was dissolved in the aqueous phase. The solution was filtered using a Buchner funnel and the solid precipitate was dried in a vacuum oven overnight. A TLC was run to determine the purity of the compound. The solid was recrystallised using ethanol before [13] C and Dept NMR spectra were run on the dried product.

5.1.6. Deprotection of BNIPDaoct

Bisnaphthalimidobismesitylene-1,8-diaminooctane (2 g) was dissolved in dry dichloromethane (47 ml) with stirring. Hydrogen bromide / methanoic acid solution (7.71 ml) was added and the mixture was left at room temperature overnight. The precipitate was filtered using a sintered glass funnel and washed with dry dichloromethane. The solid was dried I a vacuum oven overnight. 13C and Dept NMR were run to ensure the structure and purity of the final product.

5.2. Results

5.2.1.N-Acylation of Naphthalic anhydride
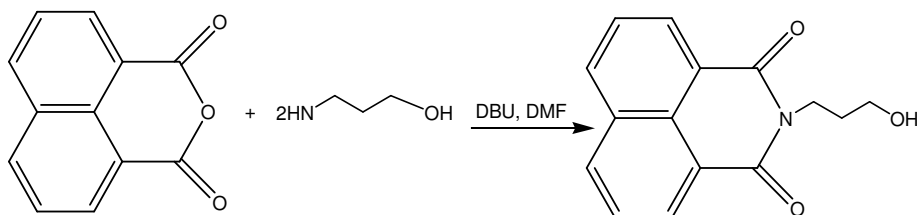
Figure 13. Reaction schematic for N-acylation of Naphthalic anhydride.

Amount of product before recrystallisation = 10.17 g

Amount of product after recrystallisation = 9.99 g (0.0389 moles)

% Yield = (Moles starting material / Moles product) x100 = (0.0389 / 0.0505) x100

$\qquad$ = 77 %
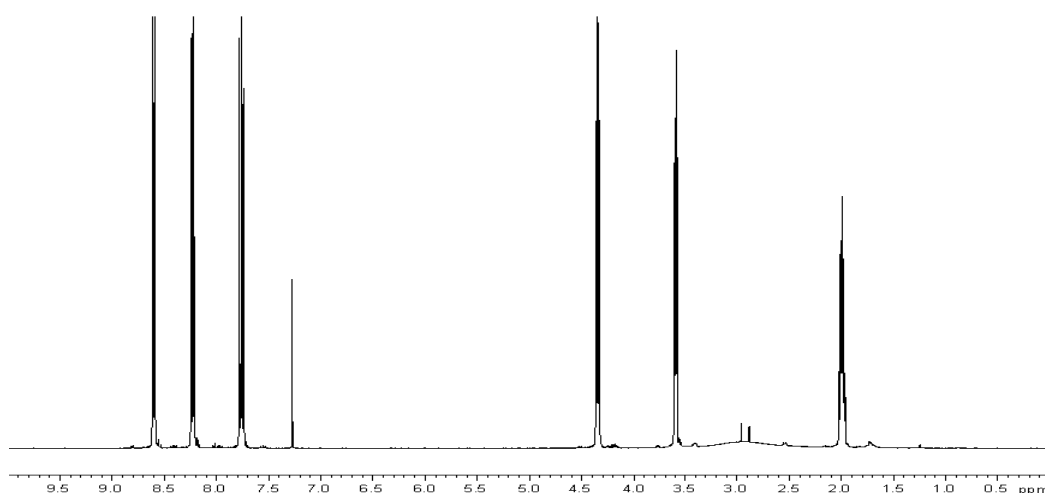
Figure 14.^{1}H NMR spectra with peak assignment of namphthalimidoalcohol product carried out using in CDCl$_3$ carried out using 400MHz NMR at 25 ºC.

Peak assignments on the ^{1}H NMR spectra for Naphthalimido alcohol product (Fig. 14) were as follows: δ_2 = CH$_2$ on alkyl chain, $\delta_{3.5}$ = CH$_2$ on alkyl chain beside O atom and O-H, $\delta_{4.4}$ = CH$_2$ on alkyl chain beside N atom and $\delta_{7.8 - 8.6}$ = CH's on aromatic rings.

5.2.2.Tosylation of Naphthalimidoalkylpropanol
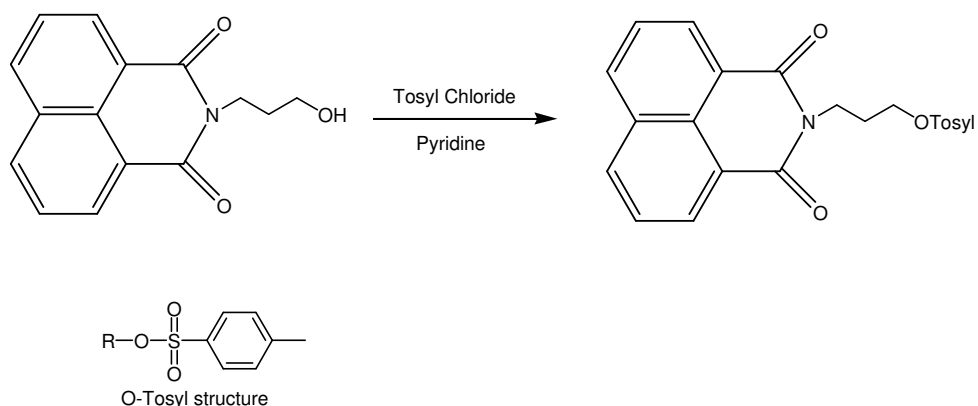
Figure 15. Reaction schematic for tosylation of naphthalimidoalkylpropanol.

Amount of product = 5.67 g (0.0138 moles)

% Yield = (Moles product / Moles starting material) x100 = (0.0138 / 0.020) x100

= 69 %

Peak assignments for ^{1}H NMR spectra of OTosyl product are as follows (Fig. 16): $\delta_{2.2}$ = CH$_2$ on alkyl chain, $\delta_{2.5}$ = CH$_3$ attached to aromatic ring, $\delta_{4.3}$ = CH$_2$'s on alkyl chain beside O and N atoms and $\delta_{7.3 - 8.5}$ = CH of aromatic rings.
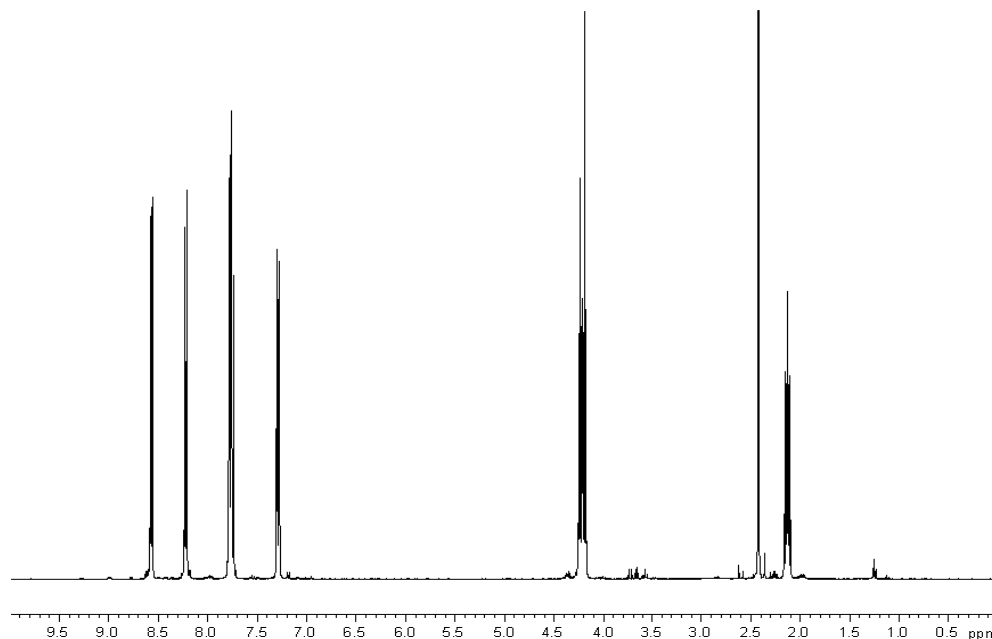
Figure 16.^{1}H NMR spectra with peak assignment of Otosyl product carried out using in CDCl$_3$ carried out using 400MHz NMR at 25 °C.
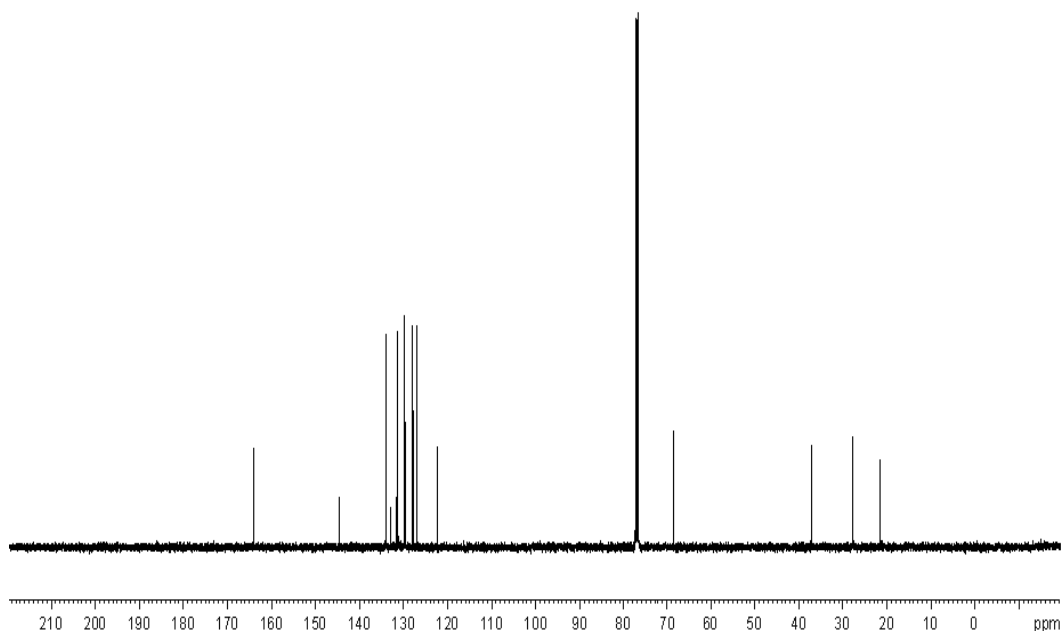

Figure 17.^{13}C NMR spectra with peak assignment of Otosyl product carried out using in CDCl$_3$ carried out using 400MHz NMR at 25 °C.

The carbon assignments for the ^{13}C NMR spectra of the OTosyl product as as follows (Fig. 17): C$_{20}$ = CH$_3$ group attached to aromatic ring, C$_{29}$ = CH$_2$ on alkyl chain, C$_{39}$ = CH$_2$ on alkyl chain next to N atom, C$_{69}$ = CH$_2$ on alkyl chain next to O atom, C$_{122-167}$ = C in aromatic rings.

211

Fig. 18 shows the dept NMR spectra for the OTosyl product. The dept is used to distinguish between CH, CH_2 and CH_3 groups in the atom. The peaks assignments for the spectra are as follows. The peak at 19 ppm = CH_3 on aromatic ring, 20 ppm CH_2 on alkyl chain, 35 ppm = CH_2 on alkyl chain beside N atom, 70 ppm = CH_2 on alkyl chain next to O atom and the peak occurring 120 – 140 ppm are due to the CH's of the aromatic rings.
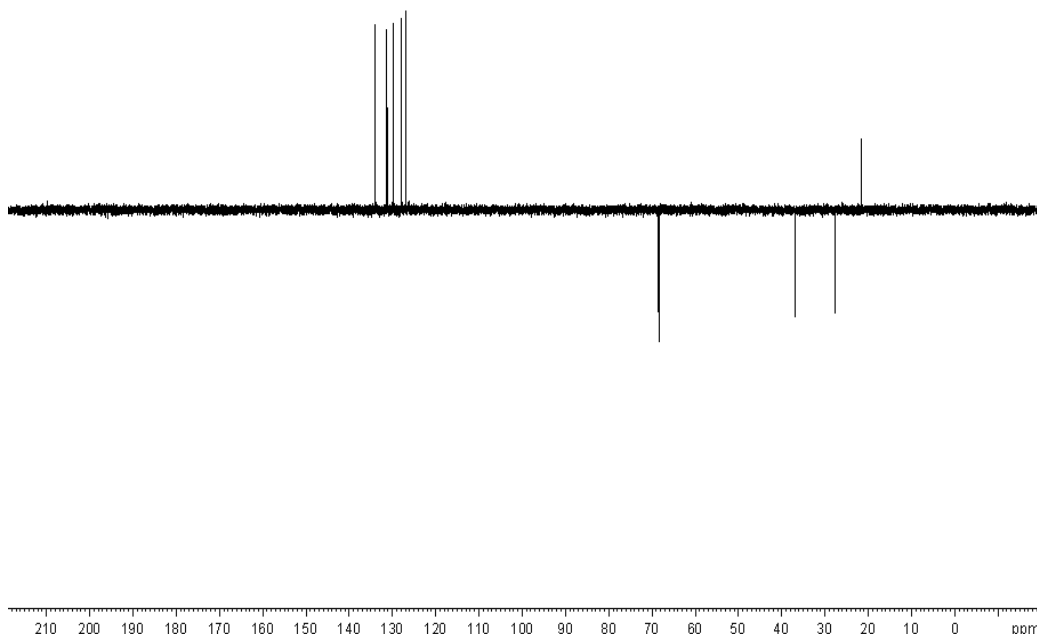
Figure 18.DEPT NMR spectra with peak assignment of Otosyl product carried out using in $CDCl_3$ carried out using 400MHz NMR at 25 ºC.

5.2.3.Protection and activation of polyamine
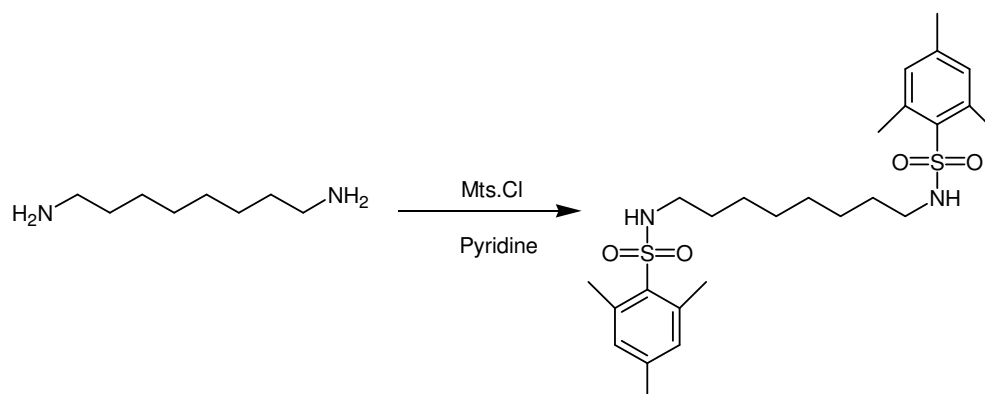
Figure 19. Reaction schematic for protection and activation of polyamine.

Amount of product = 9.10 g (0.018 moles)

% Yield = (Moles product / Moles starting material) x100 = (0.018 / 0.027) x100

= 67 %
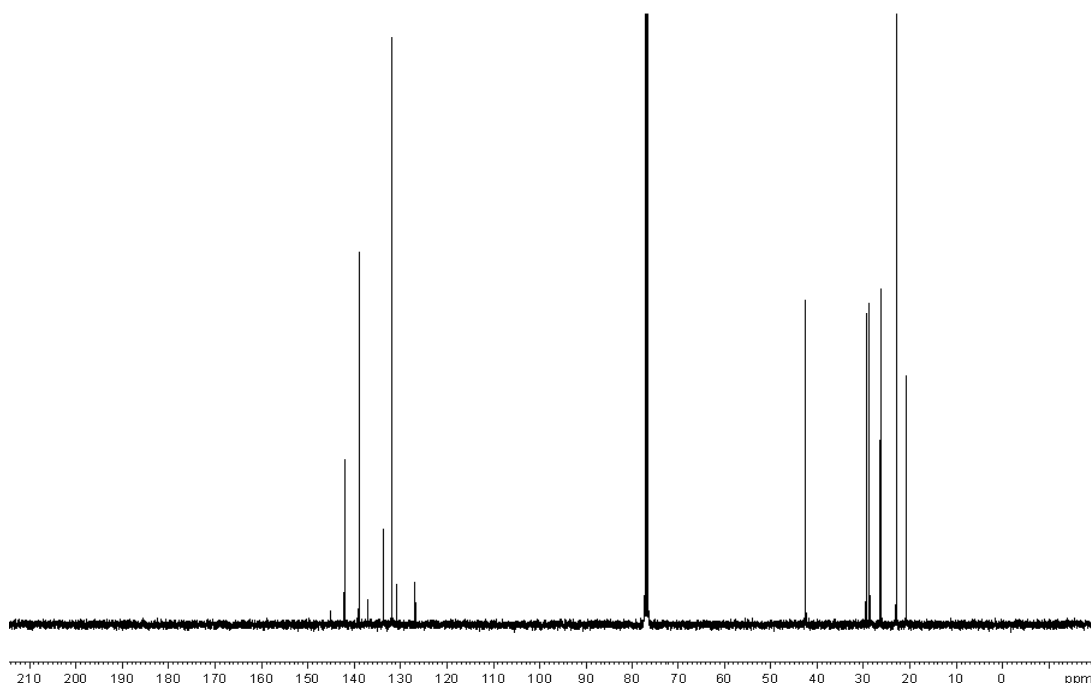
Figure 20.^{13}C NMR spectra and peak assignment of Mts-protected diaminooctane product carried out using in CDCl$_3$ carried out using 400MHz NMR at 25 ºC.

The peak assignment for ^{13}C NMR spectra of Mts-diaminooctane is as follows (Fig. 20): C$_{20}$ = CH$_3$'s on aromatic group, C$_{23}$ = CH$_3$'s on aromatic group in proximity to O atoms, C$_{27}$ = CH$_2$'s on alkyl chain, C$_{30}$ = CH$_2$'s on alkyl chain closer to N atom, C$_{41}$ = CH$_2$'s on alkyl chain next to N atom and C$_{130 - 143}$ = CH's on aromatic groups.

The dept NMR spectra for the Mts-diaminooctane (Fig. 21) showed peaks at 22 and 24 ppm, these were due to the CH$_3$ groups on the aromatic rings. Four CH$_2$ peaks were present at 27, 29, 30 and 43 ppm. CH$_2$'s were present in four different environments on the molecule and hence these correlated with the presence of the four peaks (Fig. 21). The peaks between 128 – 145 ppm were present due to the CH's in the aromatic rings.

213
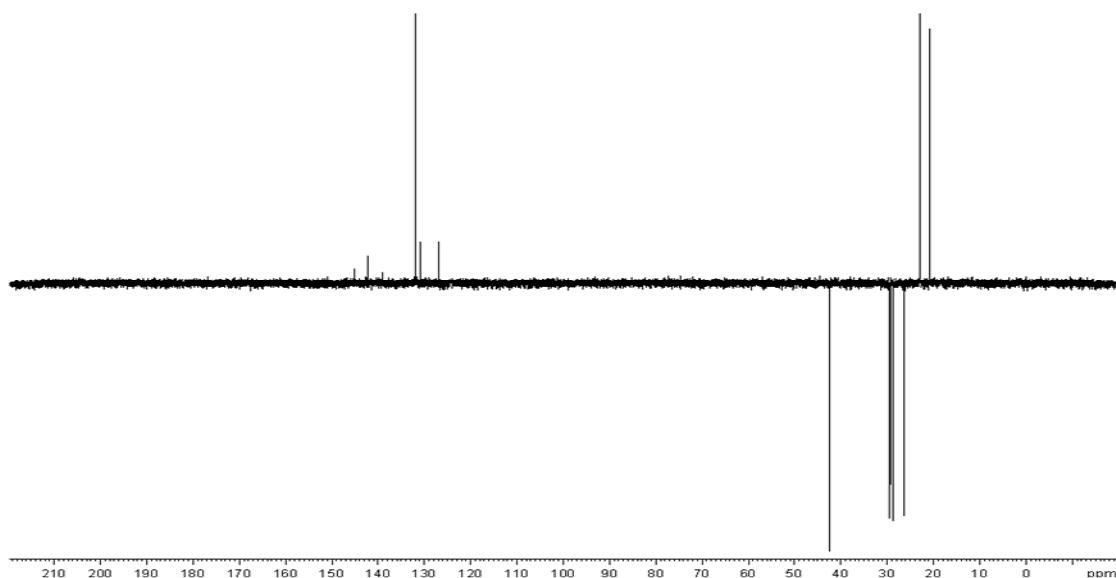
Figure 21. DEPT NMR spectra with peak assignment of Mts-protected diaminooctane product carried out using in CDCl$_3$ carried out using 400MHz NMR at 25 ºC.
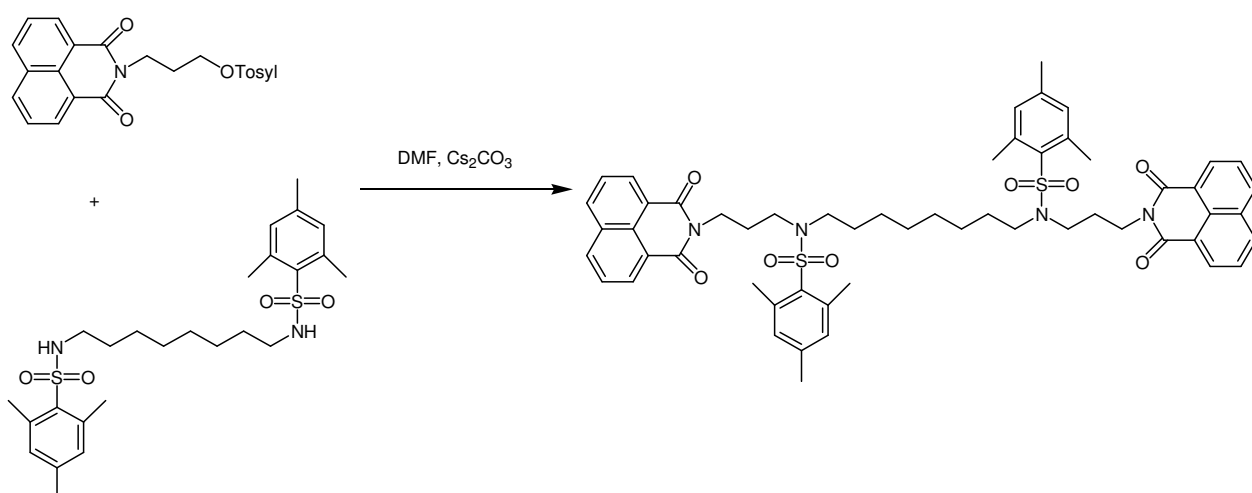
5.2.4.Alkylation

Figure 22. Reaction schematic for alkylation.

Amount of product before recrystallisation = 3.78 g

Amount of product after recrystallisation = 3.23 g (0.003248 moles)

% Yield = (Moles product / Moles starting material) x100 = (0.00328 / 0.0039) x100= 84%
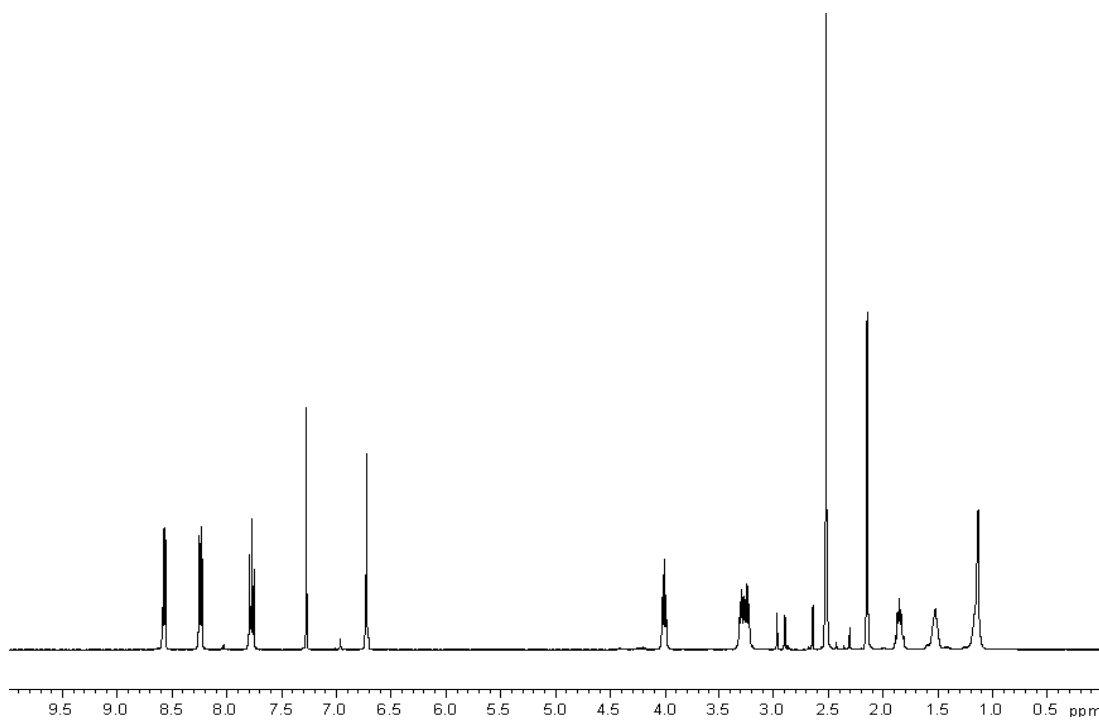
Figure 23. ^{1}H NMR spectra with peak assignment of alkylated product carried out using in CDCl$_3$ carried out using 400MHz NMR at 25 ºC.
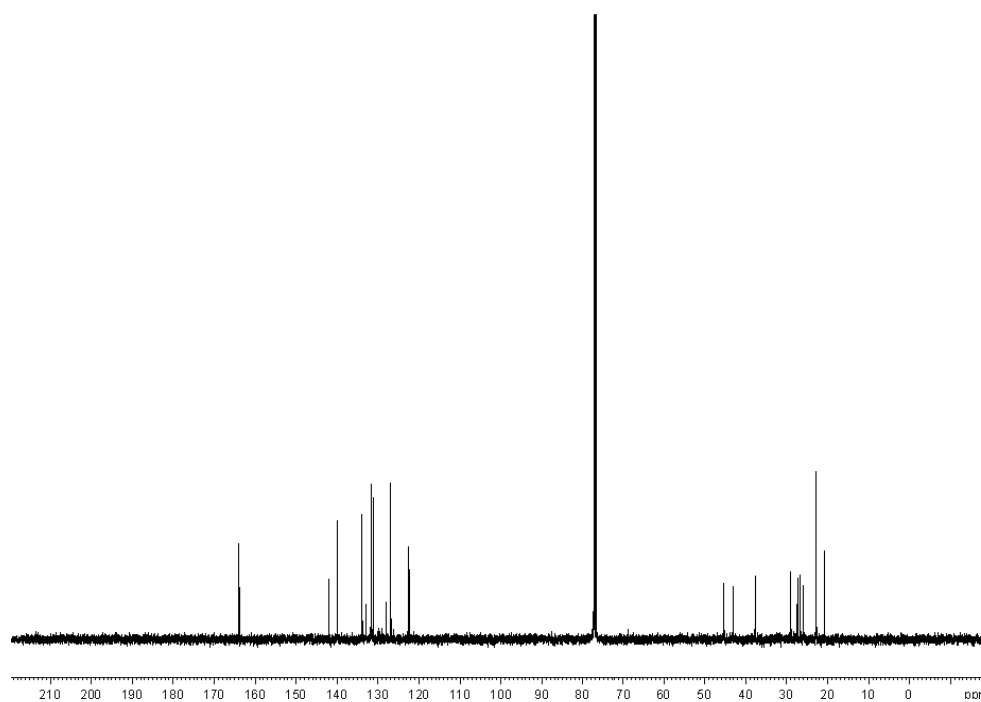
Figure 24. ^{13}C NMR spectra with peak assignment of alkylated product carried out using in CDCl$_3$ carried out using 400MHz NMR at 25 ºC.
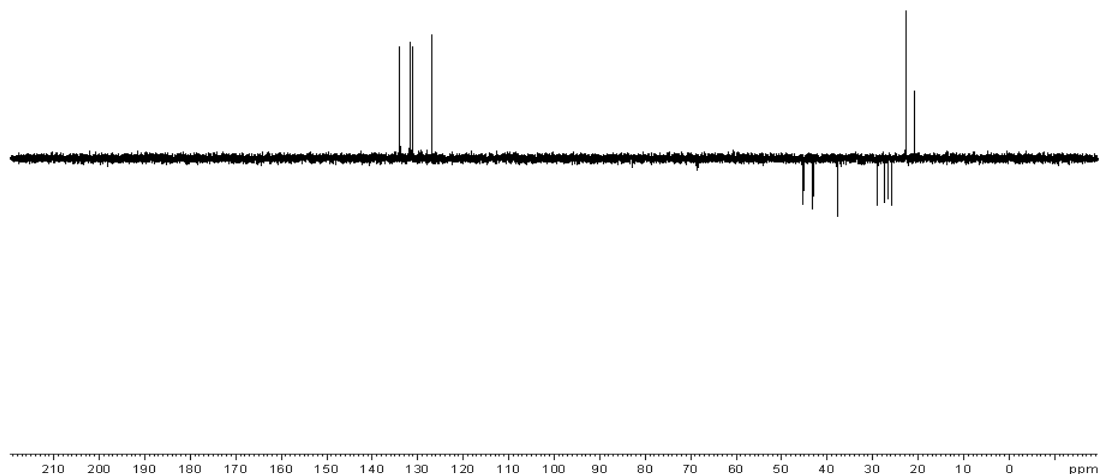
**Figure 25.**DEPT NMR spectra with peak assignment of alkylated product carried out using in CDCl$_3$ carried out using 400MHz NMR at 25 ºC.

5.2.5.Deprotection of BNIPDaoct
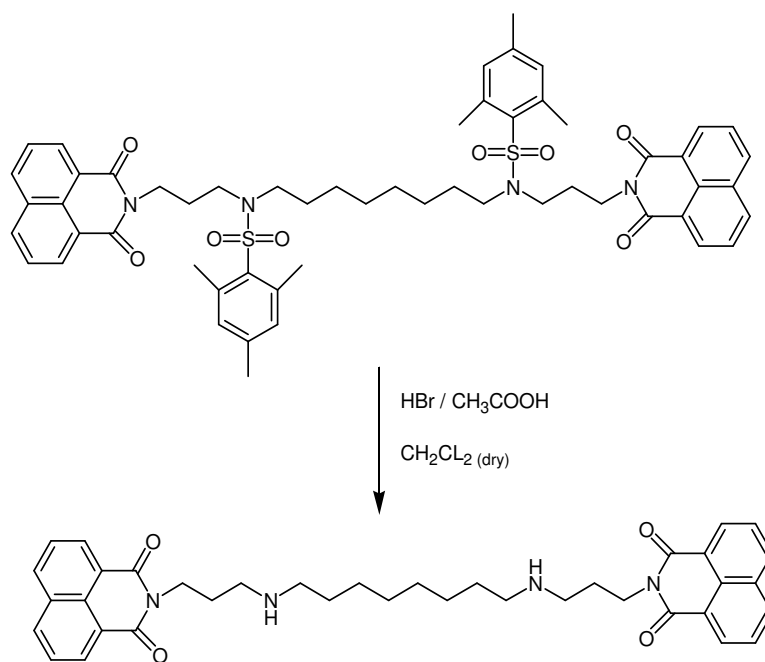
Figure 26. Reaction schematic for deprotection of BNIPDaoct.

Amount of product = 1.92 g (0.0025 moles)

% Yield = (Moles product / Moles starting material) x100 = (0.0025 / 0.002034) x100 = 123 %
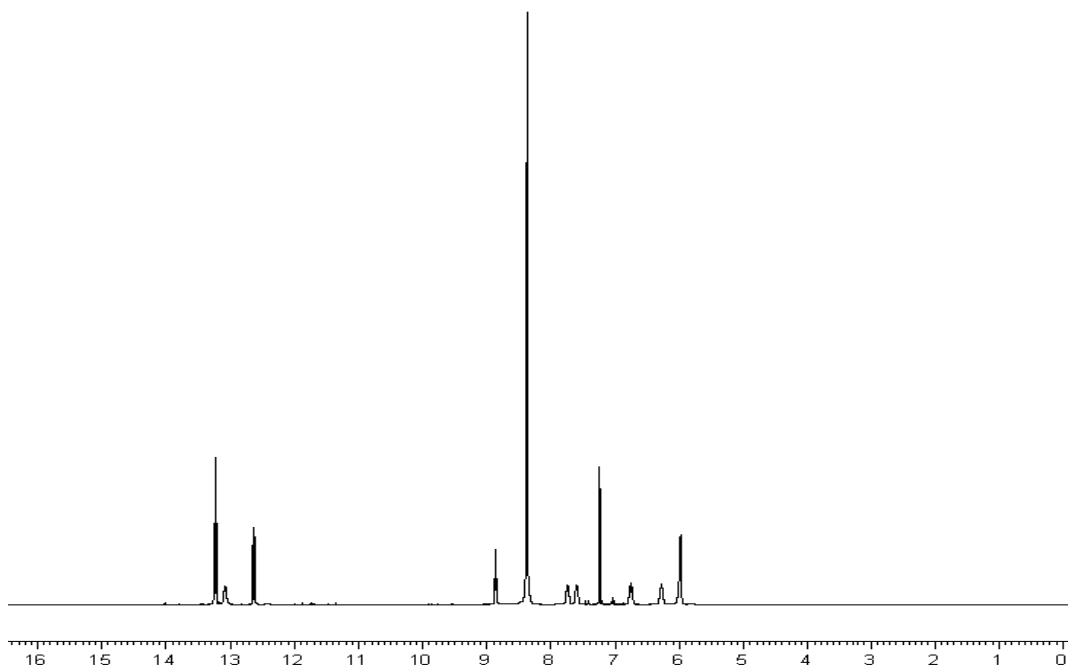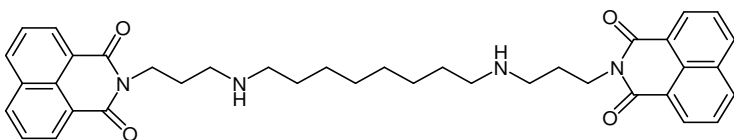
**Figure 27.**^{1}H NMR spectra of BNIPDaoct carried out using in CDCl$_3$ carried out using 400MHz NMR at 25 ºC.
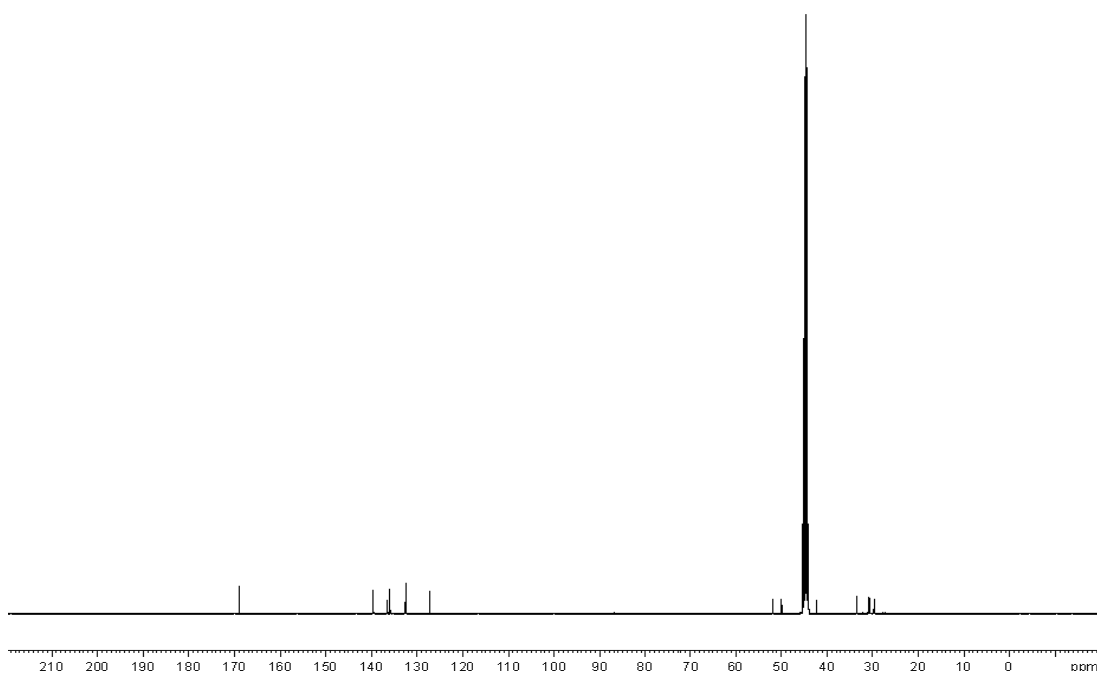
Figure 28.^{13}C NMR spectra of BNIPDaoct carried out using in CDCl$_3$ carried out using 400MHz NMR at 25 ºC.
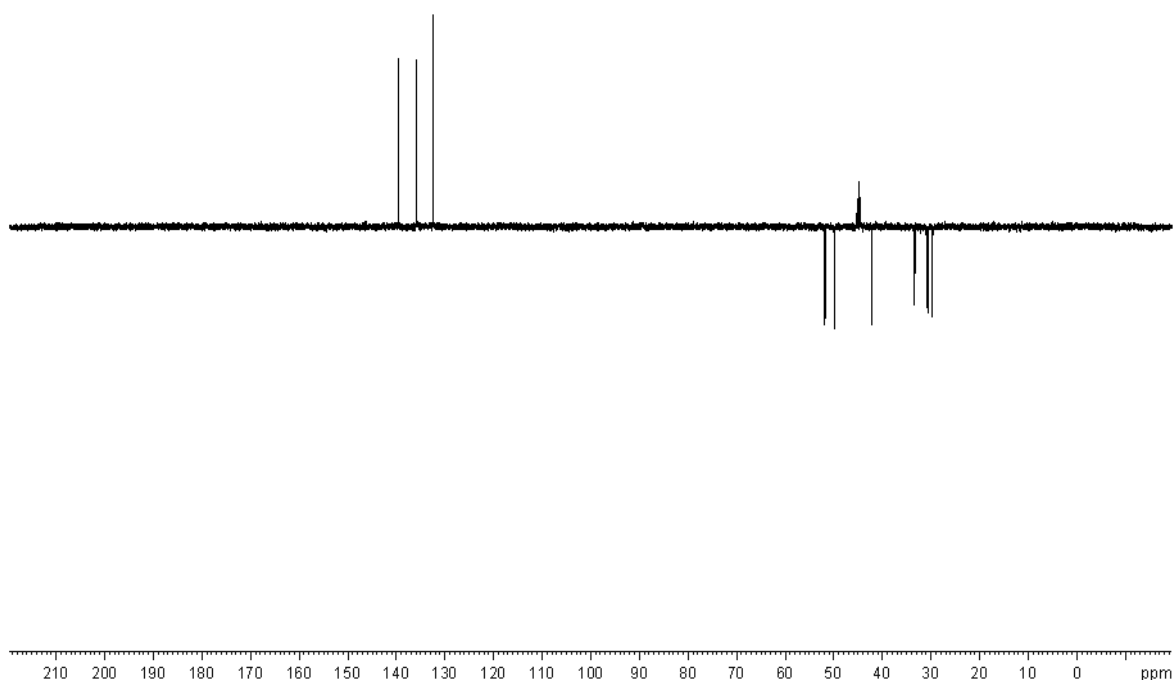
Figure 29. DEPT NMR spectra of BNIPDaoct carried out using in CDCl$_3$ carried out using 400MHz NMR at 25 °C.